Queen Mary
University of London

The role of FOXM1 in oral squamous cell carcinoma

Gemenetzidis, Emilios

The copyright of this thesis rests with the author and no quotation from it or information derived from it may be published without the prior written consent of the author

For additional information about this publication click this link.
https://qmro.qmul.ac.uk/jspui/handle/123456789/492

Information about this research object was correct at the time of download; we occasionally make corrections to records, please therefore check the published record when citing. For more information contact scholarlycommunications@qmul.ac.uk

The Role of FOXM1 in Oral Squamous Cell Carcinoma

A thesis submitted in accordance with regulations for the degree of Doctor of Philosophy

April 2010

Emilios Gemenetzidis

Centre for Clinical and Diagnostic Oral Sciences
Institute of Densistry
Barts and the Royal London School of Medicine and Dentistry
Queen Mary, University of London

ACKNOWLEDGMENTS

I would like to express my deepest gratitude to my PhD supervisor Dr. Muy- Teck Teh for his invaluable support, without which this thesis would not have materialised. I am greatly indebted by his constant enthusiasm to provide scientific and technical assistance whenever I needed it.

I also want to thank Dr. Ahmad Waseem and Dr. Hong Wan for their kind help and advice on immunostaining and confocal imaging. I am deeply grateful to Prof. Ken Parkinson for being always available to offer expert advice, and also to Prof. Farida Fortune for providing me with the opportuntiny of undertaking this exciting research project at the Institute of Dentistry.

I could not have been more grateful to my partner, Eleni Pantazi, for her deep understanding and support, not only during this thesis' writing period, but since the first day of my PhD.

Last, but not least, I am indebted to my family, that showed me the deepest love and encouragement during this period.

In remembrance of my father, Dr. Evangelos Gemenetzidis

DECLARATION

I hereby declare that all the work contained in this thesis is the result of my own independent investigation unless otherwise stated.

This work has not already been accepted for any degree, and is not being concurrently submitted for any other degree.

Emilios Gemenetzidis

_____

ABSTRACT

FOXM1 transcription factor regulates the expression of a multitude of genes, which are important for cell proliferation, mitosis, and differentiation. Although it is abundantly expressed in majority of human solid tumours, its role in early stages of human neoplasia remains unclear. Oral squamous cell carcinoma (OSCC) is characterized by sequential genomic alterations, which lead to invasive malignancy. In this study, it is shown that FOXM1 is significantly upregulated in early oral pre-malignant and OSCC tissues and cultured keratinocytes. Furthermore, the current study suggests that FOXM1B is the main isoform driving the cell cycle dependent expression of FOXM1, and that it is expressed mainly at the G2 phase of human epithelial keratinocytes. In an attempt to understand why FOXM1 precedes epithelial malignancy, the present study investigated 1) the genomic profile of FOXM1B overexpressing human epithelial keratinocytes, and 2) whether FOXM1B overexpression interferes with the innate program of keratinocyte differentiation, which is frequently reported as being the earliest oncogenic event in epithelial neoplasia. First, by using a high-resolution Affymetrix single nucleotide polymorphism (SNP) mapping technique, this study provides the first evidence that FOXM1B overexpression alone in primay human keratinocytes was sufficient to induce genomic instability, mainly in the form of copy number alterations. FOXM1B overexpression also cooperated with damaging agents relevant to human epidermal (UVB) and oral epithelial cancer (Nicotine), to promote genomic instability in human keratinocytes. Second, by using a 3D-organotypic culture model of oral mucosa, sustained overexpression of FOXM1 was found to induce a hyper-proliferative phenotype with suprabasal proliferation, exhibiting perturbed markers of epithelial differentiation such as cytokeratin 13 and filaggrin, resembling early oral dysplastic epithelium. Based on these observations it is hypothesised that aberrant upregulation of FOXM1B serves as a ‘first hit’ whereby cells acquire genomic instability, and an abnormal differentiation program. The latter event promotes epithelial proliferation at the expense of terminal differentiation, allowing sufficient time for the accumulation of additional genetic aberrations/mutations required for tumour promotion and expansion.

CONTENTS

List of Tables

List of Figures

CHAPTER 1

CHAPTER 2

CHAPTER 3

CHAPTER 4

CHAPTER 5

CHAPTER 6

ABBREVIATIONS

^{3}H-TdR	tritiated thymidine
5-FU	fluorouracil 5-fluoro-dUMP
AMVRT	avian myeloblastosis virus reverse transcriptase
BCC	basal cell carcinoma
CDK	cyclin dependent kinase
CDKI	cyclin dependent kinase inhibitor
CFE	colony forming efficiency
ChIP	chromatin immunoprecipitation
CIP	calf intestinal phosphatase
CIS	carcinoma *in situ*
CMV	cytomegalovirus
CNA	copy number alteration
DAPI	4',6-diamidino-2-phenylindole
DBD	DNA binding domain
DED	de-epidermalised dermis
DNA	deoxyribonucleic acid
ECM	extracellular matrix
EPU	epidermal proliferative unit
EVPOME	ex-vivo oral mucosa equivalent
FACS	fluorescence activated cell sorting
FBS	foetal bovine serum
FOXM1	Forkhead Box M1
HNSCC	head and neck squamous cell carcinoma
KHG	keratohyaline granule
LOH	loss of heterozygosity
LRC	label retaining cell
MCS	multiple cloning site (used as empty vector)
MEFs	mouse embryonic fibroblasts
miRNA	micro RNA
mRNA	messenger RNA
NHEK	normal human epidermal keratinocytes
NHOK	normal human oral keratinocytes
NOM	normal oral mucosa
OSCC	oral squamous cell carcinoma

PD	population doublings
pSIN	self-inactivating retroviral vector
qRT-PCR	quantitative real time PCR
RNA	ribonucleic acid
RNase	ribonuclease
RNasin	ribonuclease inhibitor
RS	random sorted
RT	reverse transcription
SB	stratum basale
SC	stratum corneum
SCC	squamous cell carcinoma
SD	stratum distendum
SF	stratum filamentosum
SG	stratum granulosum
shRNA	short hairpin RNA
siRNA	small interfering RNA
SNP	single nucleotide polymorphism
SS	stratum spinosum
SSE	stratified squamous epithelium
TA	transit amplifying
TAD	transactivation domain
TG	trans-glutaminase
TPA or PMA	12-0-tetradecanoyl phorbol-13-acetate
UVB	ultraviolet B
WHD	winged helix domain
WHO	World Health Organisation

Chapter 1

GENERAL INTRODUCTION

1 General Introduction

1.1 Oral Mucosa

Human epithelia are tissues composed of cells lining the cavities and surfaces of the body. They are classified into different groups, according to their structure and the amount of layers of which they are composed. The oral mucosa is made up of squamous (flat and thin) epithelial cells which are arranged in multiple layers, and is therefore classified as a stratified squamous epithelium (SSE). The stratification of such complex epithelia is the result of cell proliferation and sequential differentiation. The general consensus regarding SSE is that proliferation is the main property of cells located at the lowermost layers of the epithelium, and is gradually constricted as cells migrate upwards to the outermost epithelial layers. The differentiation of epithelial cells is initiated as soon as they start migrating to the upper layers of the SSE, to finally give rise to terminally differentiated squames that line the outer visible surfaces of the tissue.

The human oral mucosa can be subdivided into three functionally and structurally different types: **(a)** lining mucosa, **(b)** masticatory mucosa and **(c)** specialised mucosa (anatomical distribution of the oral epithelium is shown in **Figure 1.1**). Lining mucosa can be found in the lips, cheeks (buccal), soft palate, and the floor of the mouth. The masticatory mucosa is the rigid and tough protective cover of the hard palate and the gingiva. The third type of oral mucosa, the specialised mucosa, is located on the dorsum of the tongue and consists of more specialised structures such as the taste receptors. The average surface area of the oral epithelium is ~214 cm^2, of which lining mucosa seems to cover ~60%, while masticatory and specialised mucosal cover ~25% and ~15% respectively (Collins and Dawes, 1987; Squier and Kremer, 2001).

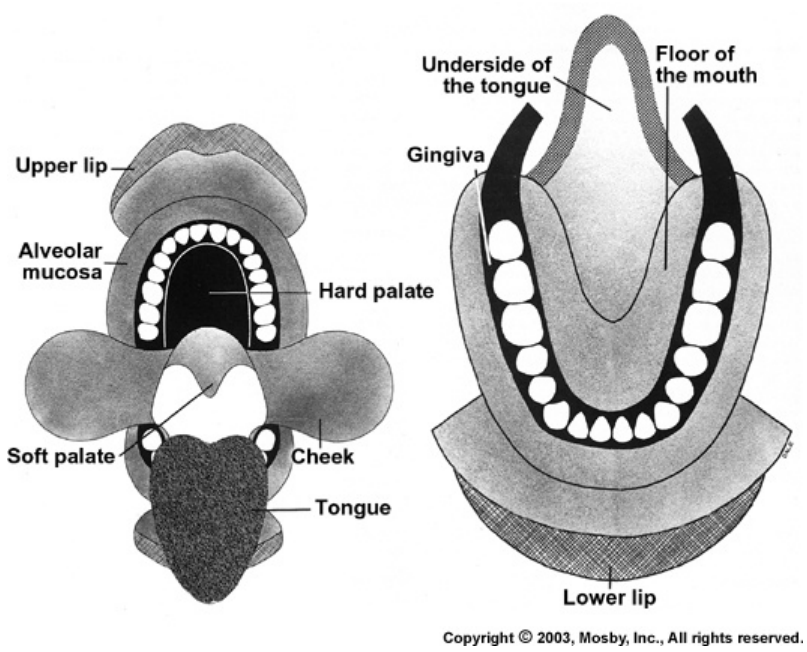

Figure 1.1: Anatomic locations of oral mucosal epithelium within the oral cavity

The diagram shows the anatomic locations and the extent of the lining, masticatory, and specialised mucosa. Masticatory mucosa is shown in black, lining mucosa is shown in grey, and specialised mucosa is shown in dark grey shading (Squier, 1989).

1.1.1 Epithelial differentiation

Arguably, the human oral epithelium shares many similarities with the human epidermis, and as such, oral epithelial differentiation is generally described and understood through the extensively studied epidermal model of epithelial renewal. However, contrarily to the epidermis, the differentiation processes in oral epithelia can show considerable site- and type-related variability.

Human stratified squamous epithelia generally contain four distinct cell layers. These include the basal layer (stratum basale; SB), spinal layer (stratum spinosum; SS), granular layer (stratum granulosum; SG), and the outermost cornified layer (stratum corneum; SC). There is however some site-related variability in the case of oral mucosa **(see Table 1.1 and Figure 1.2)**.

Table 1.1: The differentiation pattern of human oral epithelia according to their anatomical site

Type of Epithelium	Differentiation Pattern	Stratification
Epidermis	Cornified/(Ortho)-Keratinised	4-layered ; SB,SS,SG,SC
Hard Palate	Cornified/(Ortho)-Keratinised	4-layered ; SB,SS,SG,SC
Buccal Mucosa	Non Keratinised	3-layered; SB, SF,SD
Gingival Epithelium	(Para)-/(Ortho)-keratinised	4-layered; SB,SP,SG,SC
Dorsal Tongue	Mixed Cornified/Non-cornified	Papillae organisation
Lateral and Ventral Tongue	Non-keratinised	Papillae organisation
Floor of mouth	Non keratinised	3-layered; SB,SF,SD

SB=stratum basale, SS=stratum spinosum, SG=stratum granulosum, SC=stratum corneum, SF=stratum filamentosum, SD=stratum distendum (Gibbs and Ponec, 2000; Garant, 2003).

Within stratified squamous epithelia, including the oral mucosa and the epidermis, the keratinocytes of the basal layer retain the ability for DNA synthesis and mitosis. Cessation of cell proliferation is followed by the initiation of terminal epithelial differentiation as soon as basal cells start to migrate upwards and through the suprabasal layers, to reach the outermost epithelial tissue surfaces. The spinal layer forms the first suprabasal layer of the differentiation compartment, while the granular layer contains cells that have entered the stage of terminal keratinocyte differentiation. Keratinocytes finally reach the stratum corneum in the form of terminally differentiated dead squames, which are sloughed from the epithelial surfaces and are continuously being replaced by inner keratinocytes that are differentiating outward (Fuchs, 1993).

In oral mucosa epithelia, the outermost layers may contain either fully keratinized (ortho-keratinized), partially keratinized (para-keratinized), or non-keratinized squames, depending upon the type of oral mucosal epithelium. Although all epithelial cells mature to terminally differentiated squames, the differentiation path can vary between the types of oral mucosa (**Table 1.1**) The maturing cells of masticatory mucosa undergo a differentiation pattern known as para- (partial; palate and gingiva) or ortho- (full; hard palate and attached gingiva) keratinisation, whereas cells of the lining mucosa do not keratinise

(non-keratinised), while more specialised regions of the oral mucosa show mixed patterns (Dale et al., 1990). This process, so called epithelial turnover, commences with the mitotic division of basal keratinocytes and occurs continuously within the epithelial tissue.

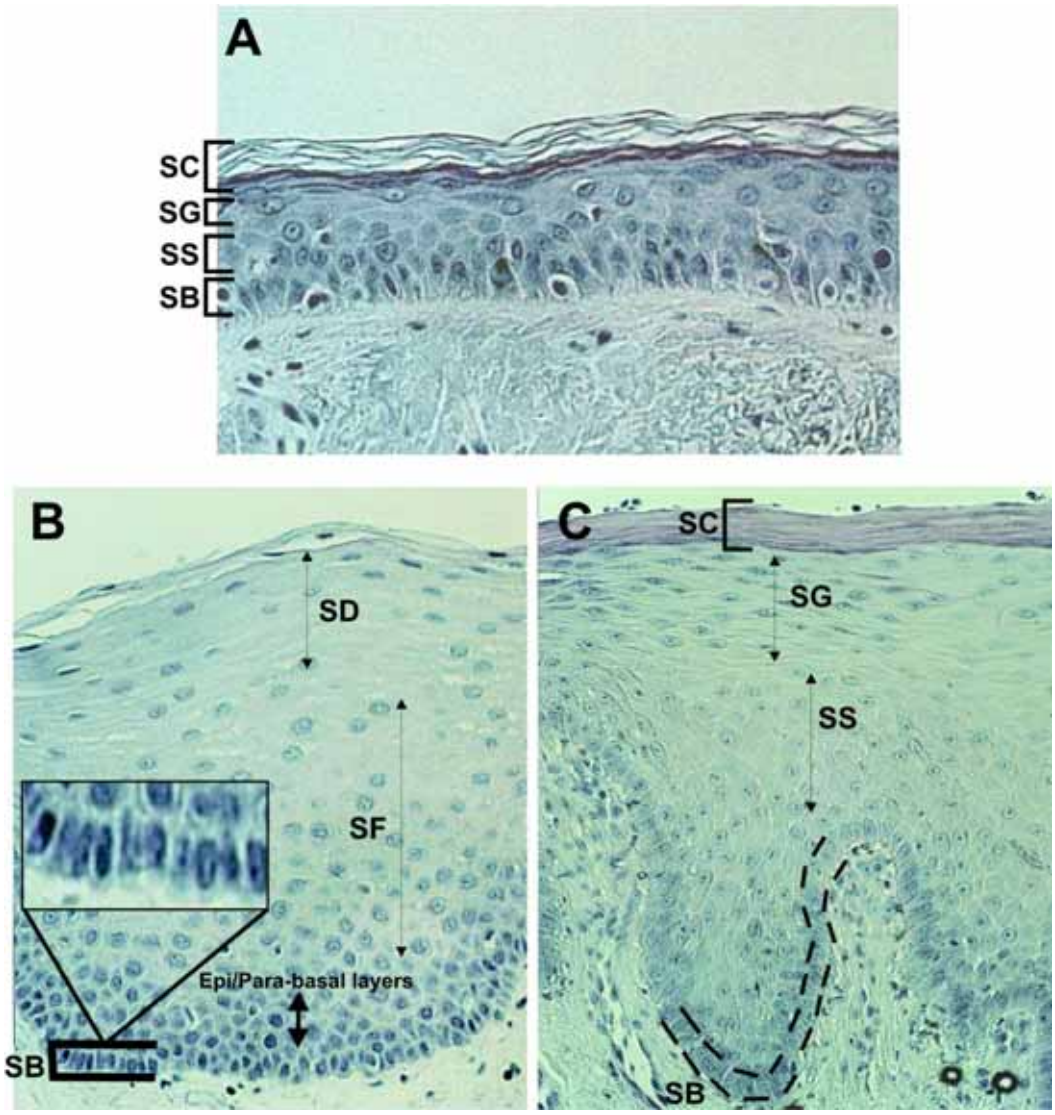

Figure 1.2: Differences in epithelial organisation

This figure depicts the clear morphological differences between human epidermis **(A)**, buccal mucosa **(B)**, and tissue of the hard palate **(C)**. Note the absence of the cornified epithelial layers in buccal mucosa. **SB**: stratum basale, **SS**: stratum spinosum, **SG**: stratum granulosum, **SC**: stratum corneum, **SF**: stratum filamentosum, **SD**: stratum distendum. (modified from Gibbs & Ponec, 2000).

1.1.2 Stratum basale

The cells that reside in the stratum basale (basal keratinocytes) have a cuboidal shape, with a high nuclear to cytoplasm ratio, and are positioned perpendicular to the basement membrane (**see Figure 1.2**). The basement membrane, which provides the support for basal keratinocytes, is a specialised extracellular network consisting of special collagen fibrils and the basal lamina, which is located just beneath all basal epithelial cells (Garant, 2003). Basal cells are anchored to the basal lamina by hemi-desmosomes, which are stable anchoring structures of the inner basal surface of keratinocytes and serve to attach the cell to the underlying basement membrane, by connecting the intermediate keratin filaments of keratinocytes with the extracellular matrix (ECM) (Burgeson and Christiano, 1997), as well as through focal adhesions which are formed by the clustering of integrins located at the basal surface of keratinocytes connecting the actin cytoskeleton with the ECM (De Strooper et al., 1989; Peltonen et al., 1989; Hynes, 1992; Jensen et al., 1999; van der Flier and Sonnenberg, 2001; Fuchs, 2008). Keratin filaments are the major component of epithelial keratinocytes and constitute as much as 85% of the cellular protein in cornified epidermal keratinocytes (Presland and Dale, 2000). The cells of the basal, and those of the spinous layer, are attached to each other by means of cadherin (calcium dependent adhesion molecules)-based adherens junctions, and of desmosomal glycoproteins (desmosomes) respectively (Fuchs, 1990; Fuchs, 1993; Garrod, 1993; Nievers et al., 1999; van der Flier and Sonnenberg, 2001; Blanpain and Fuchs, 2006; Blanpain et al., 2007; Fuchs, 2008). The former connect the actin filament cytoskeletons of adjacent cells by using different cadherin proteins, while the latter are membrane junctions that interconnect cells into three-dimensional lattices (Garrod, 1993), by connecting the keratin filament cytoskeletons of adjacent cells. A distinguishing attribute of basal keratinocytes is that their intracellular cytoskeleton is composed of two specialised keratin filaments, K5 and K14 (Dale et al., 1990; Fuchs, 1993). In addition to the latter, the basal keratinocytes of lining oral epithelia, such as buccal mucosa, also show expression of K19 filaments (Dale et al., 1990).

This compartment is responsible for the total proliferative output of the epithelial tissue. Although the basal layer is regarded as being the only proliferative layer within squamous stratified epithelia, some proliferative activity can be seen in the first suprabasal layers of the epidermis (Penneys et al., 1970; Lavker and Sun, 1982; van Neste et al., 1983; Watt, 1998) , while in the oral epithelial as well as in other tissues of the lining mucosa, proliferative activity is mainly present in a few layers above the basal, so called the epi- or para- basal layers (Liu et al., 1998; Gibbs and Ponec, 2000; Seery and Watt, 2000) **(see Figure 1.2)**. This demonstrates that the transition from the proliferative basal, to the differentiation compartment is not abrupt, but instead gradual, at least in terms of the cells' capability to divide. Early studies with tritiated (^{3}H-TdR) thymidine administration (thymidine analogue that is incorporated in the DNA of cells during DNA synthesis) have demonstrated that basal keratinocytes are capable of DNA synthesis, and that the actual rate of epithelial tissue renewal is proportional to the rate of basal keratinocyte division (reviewed in Adams, 1976). In general, non-keratinising tissues have a higher turnover rate compared to keratinised tissues. For example, the time needed for a basal dividing keratinocyte of the hard palate (ortho-keratinized tissue) of the mouse to reach the final stages of maturation is 6-7 days, while the same process takes only 3.5-5.5 days for the buccal mucosa (non-keratinized) (Hamilton and Blackwood, 1974). Similarly, the cornification of a basal epidermal keratinocyte is calculated to take approximately 10-14 days in mice, and 28-30 days in humans (Potten and Morris, 1988; Potten et al., 2002). However, this time may be rapidly reduced in the case of wound healing or pathologic hyperproliferative conditions. Based on these observations, it is estimated that basal keratinocyte mitotic divisions occur more frequently in non-keratinised epithelial tissues.

According to the epidermal model of epithelial homeostasis, a steady rate of epithelial renewal is achieved by the 'asymmetric' division of distinct immature basal keratinocytes (stem cells). This results in the generation of one stem cell, and one lineage-committed cell (transit amplifying; TA), which is destined to migrate upwards and terminally differentiate, after quick but limited rounds of cell division (Watt, 1998). The keratinocytes in transit divide

one to five times while undergoing the initial phases of differentiation, during which time they start migrating upward to the epithelial surface (Watt, 1998) (**Figure 1.3**).

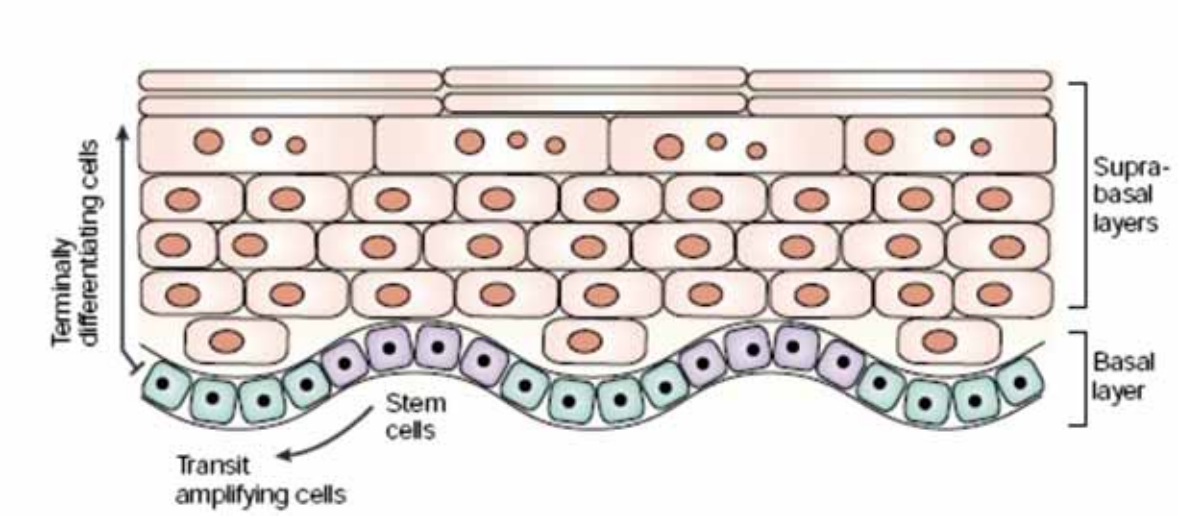

Figure 1.3: The organisation of the epidermis

Basal keratinocyte stem cells (pink) divide asymmetrically to give rise to one basal undifferentiated, and one differentiating transit amplifying daughter (green). The daughters of transit amplifying cells are committed to terminal differentiation and withdraw irreversibly from the cell cycle while moving upwards. Adapted from (Owens and Watt, 2003)

1.1.3 Stratum spinosum

The spinal layer (or prickle cell layer) consists of 4-8 layers and is the first layer of the differentiation compartment. The intracellular cytoskeleton of spinal keratinocytes of the oral ortho-keratinising epithelium is composed of K1, K10, and K6/16 filaments while the expression of K5 and K14 is gradually decreased as cell migrate further from the basal layer (Fuchs, 1993). The non-keratinising oral epithelial keratinocytes of the stratum filamentosum (the analogue of stratum spinosum in the non-keratinising oral tissues) have a unique keratin expression pattern as their intracellular cytoskeleton is composed of K4 and K13 (Dale et al., 1990; Presland and Dale, 2000). Spinal keratinocytes are strongly attached to each other by desmosomes, and although most keratinocytes within and above the spinal layer are normally post-mitotic, they still retain their metabolic activity. Much of their metabolic activity is devoted to the production of glutamine and lysine-rich envelope proteins like involucrin, which provides a scaffold for the cross-linking of

other envelope proteins (Fuchs, 1990; Candi et al., 2005). The envelope proteins are vital for the formation of the cornified envelope, which is an insoluble protein structure that is assembled by transglutaminases (TGs). The latter are calcium dependent enzymes which mediate the formation of a covalently linked network of proteins, to finally replace the plasma membrane of terminally differentiated keratinocytes, and to also act as a scaffold for lipid attachment (Steven and Steinert, 1994; Candi et al., 2005).

1.1.4 Stratum granulosum

This layer is named after the keratohyalin (keratin precursor) granules (KHGs) that are contained therein. As spinous keratinocytes reach the granular layer, they start synthesizing pro-filaggrin, a cationic precursor protein which is a major constituent of KHGs (Dale et al., 1990). Pro-filaggrin is converted to filaggrin during the transition of granular cells to cornified keratinocytes, which aggregates the keratin filaments into tight bundles, thereby promoting the collapse of keratinocytes into a flattened shape, which is a strong characteristic of surface corneocytes (Candi et al., 2005). In non-keratinising lining epithelia, filaggrin is almost undetectable in the stratum distendum (the analogue of stratum granulosum for the non keratinising epithelia), and hence KHGs are not normally present (Smith and Dale, 1986). Additionally, the keratin filaments of keratinocytes in the stratum distendum are composed of K4 and K13, which contrarily to keratinizing epithelia, are not bundled. Additional structural proteins of the cornified envelope including loricrin and involucrin are further produced by granular cells and are later cross-linked by several transglutaminases.

1.1.5 Stratum corneum

The outermost layer of cornified SSE, including the epidermis and the ortho-keratinized oral epithelia, consists of dead squames which are eventually shed of its surface. The organelles of such cells undergo autolysis through activation of distinct proteases (Candi et al., 2005), while intercellular contacts are lost, probably through a serine protease-mediated process (Sondell et al., 1994; Garant, 2003). Corneocytes are now composed entirely of keratin filaments which remain attached to the plasma membrane through the

previously assembled cornified envelope. Cells are tightly attached to each other by means of corneo-desmosomes (modified desmosomal structures), which are proteolytically degraded at the uppermost layers of the cornified layer to allow desquamation (shedding of corneocytes) (Candi et al., 2005). The outermost layer of lining oral mucosa (stratum distendum) contains non-cornified keratinocytes which retain their nuclei and intracellular organelles while in the stratum corneum of para-keratinized tissues, as are some parts of the gingiva, the corneocytes show incomplete/partial disintegration of the nucleus and cytoplasmic organelles. It is noteworthy that unlike rigid cornified epithelia, lining mucosa shows remarkable flexibility. This could be possibly attributed to the lack of filaggrin expression in granular keratinocytes, the shift of keratin expression pattern to K4 and K13 as previously mentioned, as well as the greater amount of elastin expression in the submucosal connective tissue (Garant, 2003). Although many of the cell envelope's components (loricrin, involucrin) are equally found in para- , ortho-, and non-keratinized oral epithelia, the resulting cell envelope of the latter is significantly thinner.

1.2 Epithelial Stem Cells

The formation and maintenance of epithelial tissues is owned to cells with distinct properties. Epithelial stem cells are suggested to be responsible for epithelial tissue renewal during normal homeostasis as well as during wound healing. A stem cell is defined as any cell being able to reproduce itself throughout the life-span of the host, while being able to give rise to differentiated cells (Lajtha, 1979; Slack, 2000). Consequently, a stem cell population should, by definition, be primarily undifferentiated. Although this holds true, adult tissue stem cells are thought to have a certain degree of commitment themselves, such that they can only form the differentiated cells of the tissue in which they reside (Slack, 2000).

1.2.1 Heterogeneity of the Basal Layer

As far as epithelial tissues are concerned, the stem cells of the epidermis are among the best studied. Epidermal stem cells are thought to reside in the basal layer, the hair follicle bulge, and the base of the sebaceous glands (Fuchs, 2008). The undifferentiated population of stem cells of the oral mucosa appear to be located within the basal layer of the epithelium. However, the exact location and organisation of epithelial stem cells within the basal layer is not yet clearly defined, mainly due to the lack of highly specific stem cell markers. According to the classical Epidermal Proliferative Unit model (EPU) introduced by Potten et al. (Potten, 1974), stem cells of the epidermis are arranged into 10-cell units, each of which contains a central self-renewing stem cell surrounded by transit amplifying cells, which consequently commit to terminal differentiation and migrate upwards to form cornified dead squames (Mackenzie, 1970; Potten, 1974; Mackenzie, 1997; Watt, 2002). A transit amplifying cell will further divide one to five times, thereby amplifying the effect of a single stem cell division. This amplifying effect significantly lowers the requirement for stem cell divisions within the epithelium. This has been suggested as a mechanism which allows infrequent divisions of stem cells, while at the same time leads to the production of sufficient numbers of terminally differentiated keratinocytes (Lajtha, 1979; Jones and Watt, 1993; Lavker and Sun, 2000; Potten and Booth, 2002). According to more recent

studies based on clone tracing in mouse basal epidermis however, it is suggested that only one type of progenitor is able to maintain mammalian epidermis through a combination of symmetric and asymmetric divisions that occur at rates that accustom the requirements of epithelial homeostasis, rather than through the more organised system predicted by the classical stem/TA model (Clayton et al., 2007; Jones et al., 2007).

It is expected that putative stem cells of the basal layer would exhibit longer cell cycle times, which would inevitably lead to a lower frequency of cell divisions. In continuously regenerating tissues such as the hemopoietic system and the intestinal epithelium, there appears to be a small number of stem cells which typically have a slow cell cycle, due to a prolonged G0 phase, and are the cells of origin for the rest of the proliferating cells (Lajtha, 1979; Bickenbach, 1981). In mouse epidermis, it is estimated that a stem cell will divide approximately every 8 days, which is twice the time needed for a transit amplifying cell to complete its cell cycle (Potten, 1974; Potten et al., 1982; Clausen et al., 1986; Loeffler et al., 1987; Potten and Morris, 1988; Kirkhus and Clausen, 1990; Potten and Booth, 2002). This heterogeneity within the basal layer was studied extensively by the use of tritiated thymidine (^{3}H-TdR), which if administered for prolonged periods of time, can effectively label most, if not all, basal epithelial cells. As ^{3}H-TdR is halved every time a cell divides, it was postulated that the slow cycling cells of the epidermis shall retain the thymidine label for longer times (Bickenbach, 1981; Potten and Morris, 1988; Clausen and Potten, 1990). These cells, so called label retaining cells, or LRCs, were found to reside towards the centre of columns in the epidermis at a very low frequency (1-4%), supporting the existence of the EPU (Potten, 1974; Bickenbach, 1981; Potten and Morris, 1988; Mackenzie, 1997; Potten and Booth, 2002), as well as in the hair follicle bulge, another suggested site for epidermal stem cells (Cotsarelis et al., 1990; Morris and Potten, 1994; Morris and Potten, 1999). Administration of ^{3}H-TdR in mice, also showed the presence of LRCs in the basal epithelial layers of oral mucosa, which accounted for ~0.02% - 0.1% in the palate, ~0% - 0.1% for the tongue epithelium, and ~0.06% - 0.1% for buccal epithelium (Bickenbach, 1981). Although studies on the presence of LRCs in human epithelia are lacking due to the inability of performing *in vivo* labelling

protocols, earlier studies on human embryonic and foetal epidermis grown *in vitro,* revealed the presence of 2% and 4% LRCs in the foetal and embryonic tissues respectively (Bickenbach and Holbrook, 1987). A more recent study aiming to identify LRCs in organotypic reconstructs of human epidermis (Muffler et al., 2008), showed that LRCs do appear at the basal layer at a frequency of <1%, which an estimation that is similar to what has been previously observed in mouse epidermis (Bickenbach, 1981; Schneider et al., 2003).

Apart from the heterogeneity in cell cycle times, the proliferative compartment of the epidermis was suggested to show significant functional heterogeneity as well, which is mainly shown through models of induced hyperplasia and epidermal destruction. TPA (12-0-tetradecanoyl phorbol-13-acetate or PMA) is a known tumour promoter, which exerts its effects by modulating the balance between proliferation and differentiation (Boutwell, 1974; Yuspa et al., 1976; Scribner and Suss, 1978). While the majority of epithelial cells respond to TPA with cell cycle arrest and terminal differentiation, LRCs are stimulated to proliferate while retaining their undifferentiated phenotype (Bickenbach, 1981; Morris et al., 1986; Cotsarelis et al., 1990). Further evidence for a functional heterogeneity in the basal epidermal populations came from the fact that only a 10% of the basal population is able to form new epidermis after irradiation of mouse skin, despite the fact that 60% of basal cells show proliferative activity (Withers, 1967; Potten and Hendry, 1973; Potten and Morris, 1988).

1.2.2 Evidence from Epithelial Keratinocyte Culture

Many studies have clearly provided a functional link between *in vivo* and *in vitro* observations regarding the heterogeneity of the basal epidermal population. When cultured in vitro, human keratinocytes show the presence of discrete populations that can be discriminated based on the speed with which they go through the cell cycle (Dover and Potten, 1983). Cultured keratinocytes with a high RNA content (i.e. larger volume) cycle faster than their smaller (i.e. lower RNA content) counterparts, which raised the possibility that the latter may represent a non-cycling quiescent basal population with stem cell properties (Eisinger et al., 1979; Barrandon and Green, 1985; Staiano-Coico et

al., 1986). A third, non-dividing, population comprised of large cells, was also described in human keratinocyte cultures and is thought to represent terminally differentiated keratinocytes (Barrandon and Green, 1985; Staiano-Coico et al., 1986). Resembling the *in vivo observations*, both human and mouse epidermal keratinocytes also show significant diversity in their responses to TPA treatment, since only a subpopulation is resistant to terminal differentiation upon treatment (Yuspa et al., 1980; Yuspa et al., 1982; Parkinson et al., 1983). This was estimated to be ~10% of human keratinocyte cultures, and due to its close approximation to the estimated percentage of basal cells that are able to re-constitute mouse epidermis, and the fact that they were refractory to induction of terminal differentiation, it was posited that the TPA-resistant population in culture could represent the *in vivo* basal stem cell population (Parkinson et al., 1983; Parkinson et al., 1987; Potten and Morris, 1988; Clausen and Potten, 1990).

The optimal culture of human keratinocytes *in vitro* requires the presence of various growth factors, many of which are supplied from lethally irradiated fibroblasts that are used as a feeder layer (Rheinwald, 1980). Under these conditions, human keratinocytes show clonal growth in culture, and early studies demonstrated the significant heterogeneity in terms of the colony forming ability of human keratinocytes. When grown at low density, epidermal keratinocytes can form large and actively growing colonies (holoclones), smaller irregular colonies composed of flat keratinocytes (paraclones), as well as colonies with intermediated features (meroclones) (Barrandon and Green, 1987; Jones and Watt, 1993). Following serial cultivation and grafting onto nude mice, it was suggested that holoclone derived cells were likely to represent the self-renewing clonogenic stem cells which are able to give rise to transit amplifying keratinocytes, while the remaining populations contained all the properties of transit amplifying and terminally differentiated keratinocytes (Barrandon and Green, 1987; Jones and Watt, 1993). A strong functional link between the *in vivo* and the *in vitro* observations was provided when LRCs derived from mouse epidermis were found to be clonogenic *in vitro*, and showed enhanced proliferative potential when compared to mature pulse-labelled keratinocytes (Morris and Potten, 1994). Further work showed that

LRCs of mouse epidermis are small, slow growing cells that are able to rapidly attach to extracellular matrix proteins such as those present in the basal membrane of the epidermis (Bickenbach and Chism, 1998; Li et al., 1998).

Although there is mounting evidence to support the heterogeneity of human keratinocyte cultures, two of the distinguishing attributes of stem cells, that is slow rate of cell cycle and extensive replicative potential, become less noticeable once they are expanded *in vitro*, and is also directly related to the donor age (Barrandon and Green, 1987). Although stem cells are expected to transiently maintain those features relative to their more mature counterparts, all cultured keratinocytes will inevitably undergo the differentiation path, a fact that makes the *in vitro* manipulation of keratinocyte stem cells a very difficult task.

1.2.3 Epithelial Stem Cell Markers

The molecular analysis and gene expression profiles of epithelial stem cells is cumbersome, due to the lack of reliable molecular stem cell markers that can readily distinguish stem cells from the larger pool of basal keratinocytes within the epithelium either *in vivo*, or *in vitro*.

Early studies in human epidermal keratinocytes showed that the population of cells that expresses the highest levels of β1 integrins (cell surface molecules mediating intercellular adhesion and attachment of basal cells to the basement membrane) show enhanced clonogenic capacity, and increased ability to attach rapidly to extracellular matrix proteins collagen type IV and fibronectin (Jones and Watt, 1993). Contrarily, cells with low levels of β1 integrins form abortive colonies, suggestive of transit amplifying and terminally differentiated keratinocytes (Jones and Watt, 1993).

The heterogeneity in the levels of expression of β1 integrins is also reflected *in vivo*. There are patches of highly expressing basal keratinocytes interspersed with patches of basal cells with lower levels of β1 integrins (Jones and Watt, 1993; Moles and Watt, 1997). The distribution of β1 integrins is different between various anatomical sites, with β1 integrin bright patches being present

at the tips of connective tissue papillae in foreskin and scalp epidermis, whereas in the palm epidermis, β1 integrins are more strongly expressed at the bottom of deep rete ridges (Jones et al., 1995). More importantly, the cells located in β1 integrin rich sites also show reduced frequency of S-phase activity, consistent with the concept that stem cells divide infrequently under normal homeostatic conditions (Potten and Morris, 1988; Cotsarelis et al., 1990; Jones et al., 1995).

Functional studies with mouse epidermal keratinocytes demonstrated that cells with high levels of integrin α6, but low levels of the proliferation associated surface molecule, transferrin receptor CD71, were enriched for quiescent cells with a high clonogenic and proliferative capacity *in vitro* (Li et al. 1998). Furthermore, this fraction of cells was highly enriched for LRCs which further strengthens the correlation between a slow cycling status and a strong proliferative potential (Li et al. 1998), both of which are suggested to be stem cell attributes. Interestingly, the putative epidermal stem cell marker, α6 integrin, was also shown to be heavily expressed in discrete regions at the tips of connective tissue papillae of normal oral buccal mucosa, while no functional evidence are shown to support that this molecular marker is relevant to the epithelial stem cells of the oral mucosa (Kose et al., 2007).

The relationship between quiescence and 'stemness' was further demonstrated by single-cell gene expression profiling of human keratinocytes, which provided evidence that the quiescent state of human keratinocyte stem cells is partly achieved by LRIG1 (leucine-rich repeats and immunoglobulin-like domains 1) which down-modulates the proliferative effects of c-MYC (Jensen and Watt, 2006). Consistent with its role in stem cell maintenance, LRIG1 was found to be primarily expressed in groups of basal cells at the top of rete ridges of human epidermis, while its expression is mutually exclusive with those of EGFR1 and Ki67, which is in keeping with the general consensus that epidermal stem cells are a slowly dividing population of basal keratinocytes (Jensen and Watt, 2006).

In the setting of the oral mucosa, there are considerably less reports as to the identification and isolation of epithelial stem cells. Recent reports suggested that the low affinity neurotrophin nerve growth factor receptor (p75NTR)

characterises populations of immature basal keratinocyte stem cells of the oral, as well as of the closely related, oesophageal epithelia (Okumura et al., 2003; Nakamura et al., 2007). Similar to what has been observed in the case of β1 integrins in human epidermis, the localisation of $p75NTR^+$ keratinocytes is different between the various anatomical sites of the oral mucosa. Basal cells expressing p75NTR were found primarily at the tips of connective tissue papillae in the buccal mucosa, while in oral gingival epithelium its expression was seen both at the tips and the bottom of rete ridges (Nakamura et al., 2007). The functional studies of oesophageal and oral $p75NTR^+$ keratinocytes *in vitro* suggested that these cells have a strong proliferative potential, are highly clonogenic and are able to support the artificial reconstruction of human oral mucosa *in vitro* (Okumura et al., 2003; Nakamura et al., 2007). Others have reported that successful isolation of human oral keratinocyte stem cells can be achieved by discriminating cells according to their size, with the smallest cells being the ones with the highest proliferative potential which were also able to successfully form a stratified ex-vivo oral mucosa equivalent (EVPOME) (Izumi et al., 2007). However, epithelial stem cell isolation based purely on cell size seems like an oversimplification if one considers that organotypic tissue reconstruction is not a definite proof of a stem cell identity, since stem and transit amplifying epidermal keratinocytes can equally support the re-epithelisation of organotypic tissues *in vitro* (Li et al., 2004a).

Within the oesophageal epithelium, which shares many similarities with the oral epithelium and especially the lining type (Squier and Kremer, 2001), stem cells have been suggested to lay in the basal layer, at the bottom of rete ridges (interpapillary zone; IBL), rather than at the tips of connective tissue papillae (PBL). The IBL contains cells which, by large, divide in an asymmetric fashion, giving rise to one basal and one suprabasal, differentiating daughter (Seery and Watt, 2000). The cells of the PBL as well as those of the epibasal (or parabasal; one to two layers above the basal) layers divide in high frequency and they do so symmetrically, and thus are thought to represent the transit amplifying compartment of the oesophageal epithelium (Seery and Watt, 2000). In stark contrast to human epidermis however, the cells of the IBL are generally

characterised by low levels of integrin β1, while being highly clonogenic *in vitro*.

1.2.4 Stem Cells: Hosts for Initiating Mutations

The two-stage carcinogenesis models in mice have provided evidence favouring the view that epithelial stem cells are the targets of initiating mutations. The period between exposure to known carcinogens and the development of tumours is regarded to be in the order of several months in mice, and even longer in humans (decades). Owing to their prolonged existence within the epithelial tissue, stem cells have been long proposed to be good candidates for hosting these initiating mutations (Potten and Morris, 1988).

The initiation events typically involve changes in genes that control cell proliferation. For example, 7,12 di-mehtylbenz[a]anthracene or DMBA induces an A to T transversion in codon 61 of c-Ha-ras, a common skin tumour initiator (Fujiki et al., 1989; DiGiovanni, 1992). Tumour promotion involves processes that allow the clonal expansion and sustained epithelial proliferation of initiated cells, leading to chronic hyperplasia and visible papillomas, which subsequently progress to form malignant tumours (DiGiovanni, 1992). This progression assumes that multiple genetic alterations are acquired along the way, to allow uncontrolled proliferation and malignant transformation (two to three events are estimated to be required for transformation of mouse cells, and five in human cells (Hahn et al., 1999; Hahn and Weinberg, 2002). In two stage carcinogenesis models, DMBA-initiated mouse skin can develop tumours whether promotion is begun one week or one year after initiation (Potten and Morris, 1988). This suggests that the initiated cells need to remain long enough in the epithelial tissue, firstly to be able to respond to tumour promotion after this latent period, and second to be able to accumulate all the genetic alterations needed for cancer initiation. Evidence have indeed shown that double labelling of epidermal cells with ^{3}H-TdR and 14-labelled benzo[a]pyrene (BP) carcinogen can detect the same slow cycling population of basal keratinocytes, suggesting that LRCs can retain carcinogens for long periods of time (Morris et al., 1986; Potten and Morris, 1988).Considering that LRCs display many of the attributes of putative

stem cells, it is postulated that epithelial stem cells preferentially retain initiating carcinogens, and presumably cancer initiating mutations.

One way to define whether the cells responsible for epithelial regeneration, and those responsible for the formation of tumour, are both slow cycling, is to efficiently eliminate all actively cycling cells. Selective killing of all rapidly dividing cells, but not quiescent cells, with DNA synthesis blocking agents, such as fluorouracil 5-fluoro-dUMP (5-FU) leads to extensive skin damage characterised by extensive reduction in the numbers of basal cells. However, complete hair follicle and epithelial regeneration can be seen after 30 days and 6 weeks respectively, suggesting the presence of a quiescent stem cell population responsible for replenishing the skin epithelium (Morris et al., 1997). More importantly, treatment of mouse epidermis with 5-FU before, or after, tumour initiation, alters neither the rate of papilloma nor carcinoma formation (Morris et al., 1997). These observations strongly suggest that the quiescent cells that were able to completely regenerate the epidermis of 5-FU treated mice (epidermal stem cells), are also responsible for the formation of epidermal tumours following tumour promotion (Morris, 2000).

This paradigm is also illustrated in the case of UVB-induced TP53 mutations in human epidermis. Although single TP53 mutated cells can be found in the transit amplifying and differentiating compartments, clusters of TP53 mutant cells are typically found in stem cell rich regions (Jonason et al., 1996; Owens and Watt, 2003). This suggested that stem cells have the capacity for clonal expansion that is necessary for the propagation of such insults, and can become increasingly pre-disposed to further genetic hits, which emphasizes that the response to an oncogenic insult will depend on the cell that sustains it. For example, targeted activation of Ras in proliferating cells of the hair follicle can lead to the development of malignant carcinomas in mice (Brown et al., 1998; Owens and Watt, 2003), as opposed to the development of regression prone benign papillomas when the same oncogene is driven by differentiation specific promoters (Bailleul et al., 1990; Greenhalgh et al., 1993; Brown et al., 1998). From these observations it is reasonable to assume that an oncogenic insult will

be successful if it is placed in an epithelial cell which has the ability of prolonged survival, and extensive proliferative output, and therefore a stem cell.

The understanding of stem cell fate in epithelial tissues is of vital importance in cancer biology, as mutational events in the differentiated cells will have little impact in tissue homeostasis since they will be rapidly lost as part of the tissue renewal process. Therefore, it is important to define the attributes of epithelial stem cells, in order to understand the molecular pathways that mediate their responses to various oncogenic stresses.

1.3 Oral Cancer

The epidemiology of oral cavity cancer, pharyngeal and laryngeal cancers are similar, so that they are often discussed in unity as head and neck squamous cell carcinomas (HNSCCs). HNSCC is the 6th most commonly diagnosed cancer with a global yearly incidence of 780,000 new cases (Parkin et al., 2005). Squamous cell carcinomas of the oral cavity, including larynx, hypopharynx (or laryngopharynx), oropharynx, and nasopharynx represent some of the most common malignancies encountered, with a high mortality rate (Ho et al., 2007). Patients in early stages of oral cancer show minimal symptoms, which significantly delays diagnosis and inevitably leads to poor survival rates (Califano et al., 1996). Although the use of surgery followed by adjuvant chemotherapy and radiotherapy has improved the 5-year survival rates of naso- , -oro, and hypopharynx carcinomas, there has been no improvement in the survival rates of HNSCCs involving the oral cavity (Carvalho et al., 2005). Some of the major risk factors include tobacco use and alcohol consumption in developed countries as well as betel quid chewing and bidi smoking in South Central and South East Asia (Parkin et al., 2005; Sturgis and Wei, 2007), while infection with human papillomavirus (HPV) has also been implicated in HNSCC development. (Munger and Howley, 2002; Perez-Ordonez et al., 2006).

1.3.1 Oral Pre-malignancy

A pre-cancerous oral lesion is generally defined as a morphologically altered tissue, which has a probability of malignant conversion that is higher than that of the surrounding normal tissue (Muller, 2007). The earliest detectable morphologic changes in the oral mucosa are the appearance of pre-malignant lesions, the most commonly described of which are leukoplakia and erythroplakia.

1.3.1.1 Leukoplakia

Oral leukoplakia is, according to the World Health Organisation (WHO), a clinical white patch that cannot be rubbed or scraped off, and cannot have any other diagnostic identity (Pindborg et al., 1997). The major risk factor for the appearance of leukoplakia is the use of tobacco since its clinical appearance is invariably associated with a tobacco smoking history (Mashberg et al., 1973),

and more importantly most leukoplakias regress, either temporarily or permanently, following smoking cessation (Muller, 2007). Leukoplakias can be generally divided into homogeneous and non-homogeneous, with the latter being rarer ~10% of leukoplakias (Pindborg et al., 1997), but with a higher risk of malignant conversion (Muller, 2007). A characteristic of oral leukoplakias is that they are hyperplastic exhibiting epithelial cell expansion with normal stratification and no cellular atypia (Warnakulasuriya et al., 2008) and present abnormal keratinisation patterns described as hyper-para-keratinisation or hyper-ortho-keratinisation. The former represents the incomplete keratinisation of corneocytes, while the latter is characterised by the abnormal expansion of the cornified orthokeratotic layers of the epithelium. Due to the incomplete keratinisation seen in hyper-para-keratotic leukoplakias, hyperplasia and acanthosis (expansion of spinal keratinocytes; see also **section 1.1.3** and **Figure 1.5**) can also be present, and it is generally regarded that this type of leukoplakia displays a higher mitotic index (Renstrup, 1963). A small minority of oral leukoplakias can also exhibit degrees of epithelial dysplasia, (more commonly seen in the non-homogeneous type) a condition which is defined as a precancerous lesion of stratified squamous epithelium displaying cellular atypia and loss of normal maturation and stratification (see also **Table 1.2** for the descriptive features of severe dysplasia, and **Figures 1.4, 1.5B, C, D** for morphologic appearance of dysplastic tissues) (Pindborg et al., 1997; Warnakulasuriya et al., 2008). The range of malignant transformation rates for oral leukoplakia vary greatly (0.4% -17.5%) (multi-source analysis from (Muller, 2007) and are subject to the length of follow-up, tobacco usage, and their anatomic location (Muller, 2007).

1.3.1.2 Erythroplakia

Erythroplakia, the red analogue of leukoplakia, is defined as being a red patch in the mouth that is not diagnosable clinically as any other disease (Pindborg et al., 1997). Erythroplasia is less commonly seen, but commonly displays features of epithelial dysplasia or even microscopic features of carcinoma in situ (CIS), and is thus regarded as having a high potential of invasive progression (Mashberg et al., 1973). It is estimated that more than 50% of erythroplakias will progress to form squamous cell carcinomas over the period of 10 years (Mashberg, 1977).

Table 1.2: Features of dysplastic epithelium

(Warnakulasuriya et al., 2008)

Architecture	*Cytology*
Irregular epithelial stratification	Abnormal variation in nuclear size (anisonucleosis)
Loss of polarity of basal cells	Abnormal variation in nuclear shape (nuclear pleomorphism)
Basel cell hyperplasia	Abnormal variation in cell size (anisocytosis)
Drop-shaped rete ridges	Abnormal variation in cell shape (cellular pleomorphism)
Increased number of mitotic figures	Increased nuclear–cytoplasmic ratio
Abnormally superficial mitoses	Increased nuclear size
Pre-mature keratinization in single cells (dyskeratosis)	Atypical mitotic figures
Keratin pearls within rete ridges	Increased number and size of nucleoli
	Hyperchromasia

The fact that erythroplakias are relatively rare, adds further limitations to early diagnosis, and although it is difficult to accurately predict which HNSCCs are preceded by oral dysplasias, a considerable amount of SCCs are surrounded by dysplastic areas (Bouquot et al., 1988; Hogewind et al., 1989; Hunter et al., 2005). However, the subjective nature of dysplasia assessment and doubtfulness over the relative importance of the discerning histological features (Warnakulasuriya et al., 2008), are limiting factors in providing an accurate prognosis (Hunter et al., 2005).

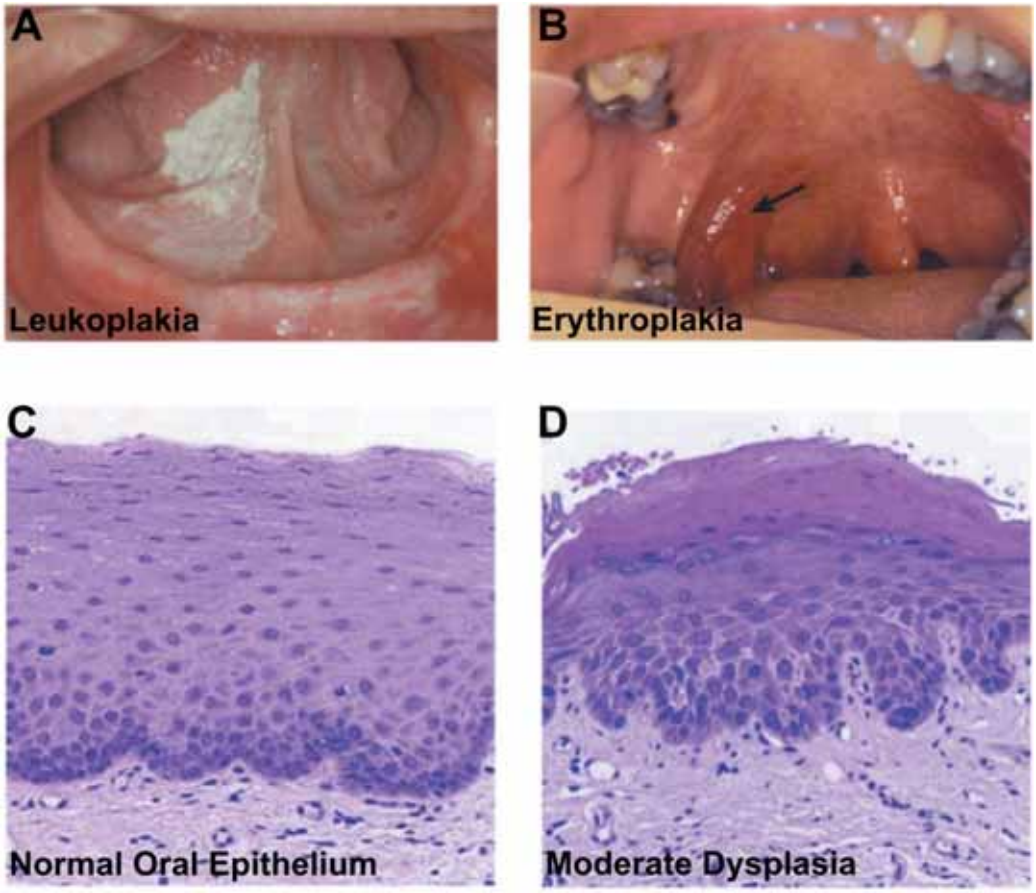

Figure 1.4: Pre-malignant lesions of the oral mucosa

(A) An area of leukoplakia on the floor of the mouth and verntral tongue. **(B)** An area of erythroplakia on the right tonsillar pillar. **(C)** Normal oral mucosa epithelium and **(D)** shows a moderately dysplastic epithelium within an area of leukoplakia on the floor of the mouth. Adapted from (Hunter et al., 2005).

1.3.2 Squamous Cell Carcinoma

Squamous cell carcinomas (SCCs) are invasive malignant epithelial tumours that show squamous cell differentiation. Although SCCs can originate from pre-existing dysplastic lesions, this is not always the case as many dysplasias do not progress to invasive malignancy (Sugerman and Savage, 1999), and it is estimated that 36-48% of oral cavity SCCs are surrounded by, or are adjacent to, dysplastic epithelium (Bouquot et al., 1988; Hogewind et al., 1989). The progression from a pre-malignant tissue to a CIS is a step of malignant transformation without the clinical appearance of stromal invasion (**Figure 1.5E**), albeit the distinctive histopathological features of malignant conversion require further consideration (Warnakulasuriya et al., 2008). The conversion of CIS to invasive cancer is generally defined by the break-down/degradation of

the protective basement membrane of the epithelium (**Figure 1.5**) (Kramer et al., 2005), which allows tumour cells to invade downwards in the connective tissue as tumour islands or individual cells (see **Figure 1.5 Fi, ii**). The neoplastic cells can invade further into deeper structures such as the adipose tissue, muscle, or bone, while less aggressive forms of SCC can also be seen, which are only locally destructive showing minimal invasion into the sub-epithelial tissues, also known as superficially invasive SCCs (Torske, 2007). The degree to which a SCC resembles the normal epithelium is referred to as grade (Grades 1-3). A low-grade (Grade 1), well differentiated tumour will mostly mimic the normal epithelium in that it has well defined basal, spinal and keratinised epithelial cells while most of the typical characteristics of tumour cells (high mitotic index, enlarged nuclei, cellular atypia, and necrosis) are at a very low frequency (Torske, 2007). On the other hand, poorly differentiated SCCs (Grade 3) display little resemblance to normal epithelium showing a very low, if any, degree of epithelial differentiation, while moderately differentiated tumours display intermediate features (Pindborg et al., 1997). Although prognosis is more favourable for cases of well and moderately differentiated oral SCCs, the subjective nature of histological grading of tumours itself can be problematic (Torske, 2007), and underscores the need for more accurate prognostic tools.

1.3.3 The Genetic 'Progression' of HNSCC

The fact that HNSCC progresses through a series of defined histopathological changes has fuelled attempts to correlate these changes to a model of genetic progression for HNSCC which, if true, would be expected to reveal genetic targets that are key to the progression of pre-malignant lesions and ultimately, malignant conversion to HNSCC. The accumulation of such events is thought to be driven by an underlying genomic instability (either chromosomal or microsatellite instability), which refers to the high rate of genomic alterations that take place over time (Negrini et al.), and is a widespread feature of all human malignancies (Lengauer et al., 1998).

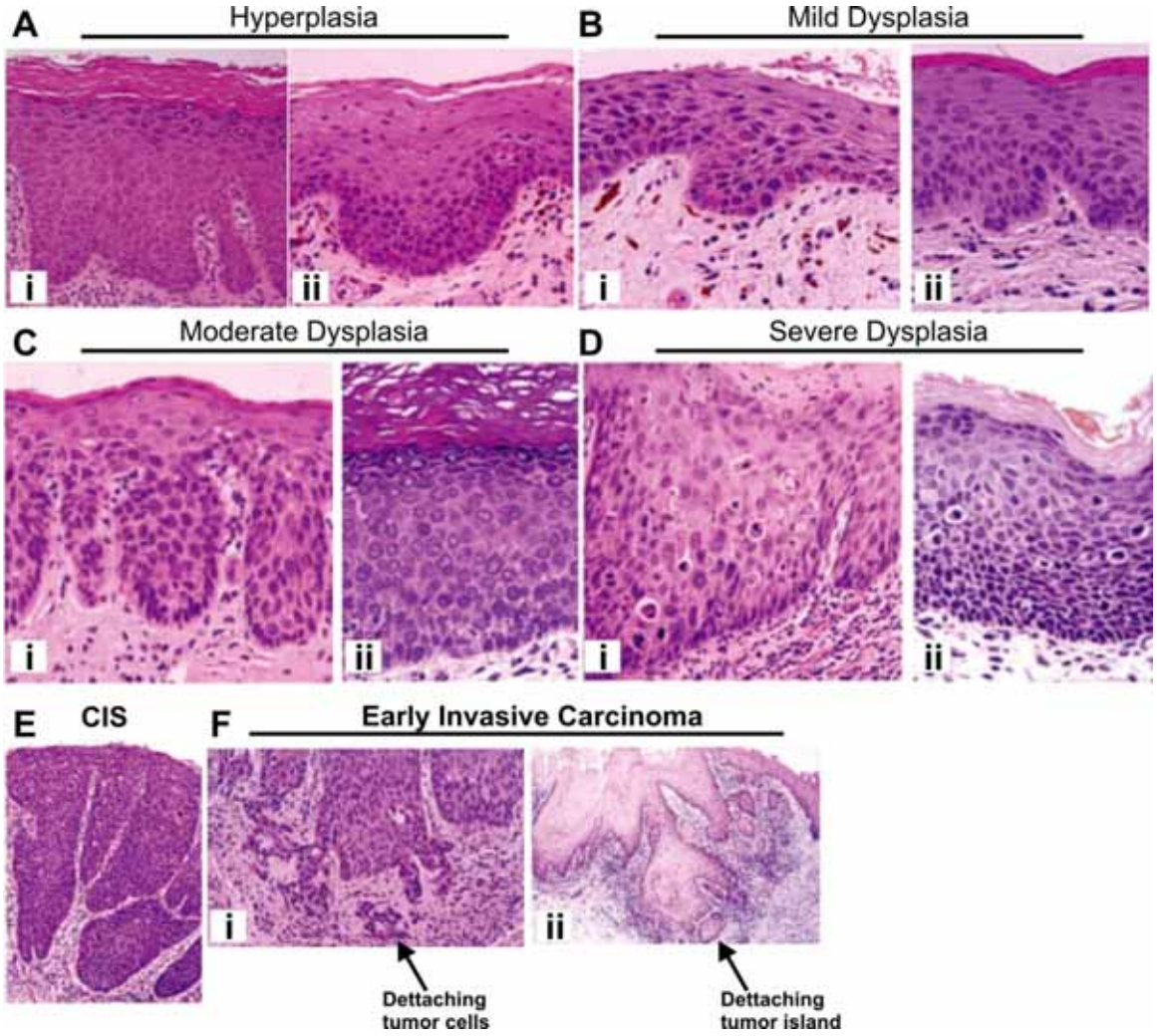

Figure 1.5: The histopathological progression of OSCC

(A) The hyperplastic epithelium shows **(i)** keratosis and abnormal expansion of the stratum spinosum and an increased maturation compartment, but without any changes in tissue architecture while **(ii)** shows expansion of the basal cell compartment (basal cell hyperplasia) again with no change in architecture. **(B)** Architectural changes can be noted in the lower third of the mildly dysplastic epithelium **(i, ii)** with the presence of some cellular atypia. **(C)** Tissue architectural changes now extend up to the middle third of the epithelium **(i, ii)** and cellular atypia is moderate. **(D)** Architectural changes are extending to the top third of the epithelium **(i, ii)** while cellular atypia is marked. **(E)** Architectural changes are widespread in the full thickness of the epithelium with marked cellular atypia. Cells are still contained within the epithelial basal membrane structure. **(F)** Irregular interface between the basal epithelium and the underlying connective tissue with some detaching tumour cells indicating early invasion **(i). (ii)** Epithelial tumour islands are separated from surface epithelium indicating early invasive behaviour of the oral carcinoma. Modified from (Warnakulasuriya et al., 2008)

Initial studies have shown that loss of heterozygosity (LOH) and allelic imbalances on chromosomes 9p and 3p were the most common alterations seen in benign oral hyperplasias and dysplasias (Califano et al., 1996; Roz et al.,

1996; Califano et al., 2000; Rosin et al., 2000) and have been characterized as the earliest detectable events in HNSCC progression. A more detailed analysis of the genetic material of microdissected pre-malignant and oral SCCs, showed that the loss of exon 1α (encodes p16INK4a) of the CDKN2A locus was lost at a frequency of 12% in oral pre-malignant lesions, while loss of either exon 1α or 2 was seen in the vast majority of oral SCCs (72%) (Shahnavaz et al., 2001). The CDKN2A locus on 9p21 encodes p16INK4A and p14ARF, which are important mediators of G1 cell cycle regulation, while chromosome region 3p21 contains FHIT and RSSF1A candidate tumour suppressor genes (Hogg et al., 2002; Dong et al., 2003; Perez-Ordonez et al., 2006). In support of its important role in the generation and maintenance of oral SCCs, it was demonstrated that p16INK4A inactivation is directly associated with the immortal phenotype of neoplastic oral keratinocytes *in vitro* (Munro et al., 1999). The importance of the above findings is further highlighted by the fact that in patients presenting with oral pre-malignant lesions (leukoplakias), 51% of them showed LOH in either 9p21 or 3p14 loci (Mao et al., 1996). More importantly, 37% of the lesions with LOH progressed to form SCCs, while only 6% of oral lesions without LOH occurrences progressed to form oral SCCs (Mao et al., 1996).

Epidermal growth factor receptor (EGFR) amplification has also been identified as an early event in HNSCC, largely as a result of trisomy in chromosome 7 which is present in oral dysplastic epithelium (Grandis and Tweardy, 1993; Ford and Grandis, 2003), a fraction of which progresses to HNSCC. Other common genetic alterations that occur in HNSCC involve tumour suppressor inactivation through p53 mutations (Somers et al., 1992)(LOH on chromosome 17p13). Mutations in p53 are also observed early in pre-invasive dysplastic epithelium (19% in non-invasive and 43% in invasive carcinomas; (Boyle et al., 1993), and the prevalence of these mutations is proportional to the stage of the disease (Shahnavaz et al., 2000). The amplification of cyclin D1 which is seen in 35-55% of HNSCCs (Meredith et al., 1995; Rousseau et al., 2001), clearly illustrates the progressive dependence of tumour cells on proliferative signals as CCND1 overexpression is detected in normal adjacent epithelium and continues throughout hyperplasia and early dysplasia (Izzo et al., 1998). Its overexpression is later followed by CCND1 whole gene amplification, which

becomes detectable in mildly dysplastic tissues and also in carcinoma *in situ* and invasive carcinomas (Izzo et al., 1998).

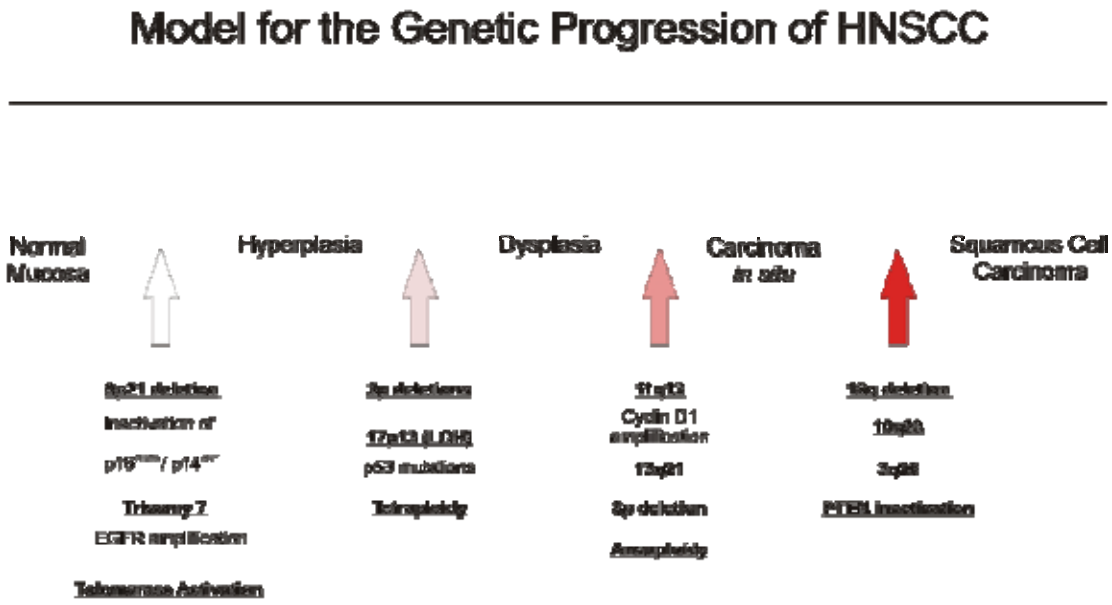

Figure 1.6**: Model for the genetic progression of HNSCC carcinogenesis**
(modified from Califano et al., 1996 and Perez-Ordonez et al., 2006).

The recapitulation of these *in vivo* findings was attempted *in vitro*, aiming to understand the effects of these molecular and genetic alterations in the creation of oral SCCs. Human oral epithelial keratinocytes could be immortalised by the combinatorial actions of only two of the aforementioned genetic alterations, that is CCND1 overexpression and inactivation of p53 (Opitz et al., 2001). However, the conversion of human oral keratinocytes to a fully malignant phenotype required the overexpression of EGFR, CCND1 and c-MYC (also amplified in HNSCC (Haughey et al., 1992), as well as tumour suppressor inactivation achieved by the introduction of a dominant negative form of p53 (Goessel et al., 2005). Although an exact model of genetic progression in respect to the specific genes involved cannot be accurately predicted for all OSCCs, either from *in vivo* or in *vitro studies*, it is strongly suggested that genomic instability is proportional to the severity of pre-malignant features and to the probability of conversion from pre-malignancy to oral SCC. Microsatellite analysis in oral premalignant lesions revealed that allelic imbalances are commonly seen (59%)

in pre-malignant lesions, albeit more often in those displaying features of epithelial dysplasia (77% dysplastic vs. 33% hyperplastic), while allelic losses were present in all pre-malignant lesions that progressed to form SCCs later on (Rosin et al., 2000). The fact that most, if not all, progressing lesions showed LOH on 9p and/or 3p (Rosin et al., 2000) further supports the notion that SCCs arise from a clonal outgrowth of genetically unstable populations that accumulate further genomic aberrations necessary for cancer initiation.

1.3.4 Field Cancerisation and Clonal Origin of HNSCC

It is now well accepted that the manifestation of a human tumour requires sequential genomic alterations (Vogelstein and Kinzler, 1998). Like most epithelial malignancies, HNSCC is thought to arise from a common premalignant progenitor, followed by the outgrowth of clonal populations, which are usually subjected to cumulative genetic alterations that lead to invasive malignancy (Perez-Ordonez et al., 2006).

Almost half a decade ago, Slaughter et al. (Slaughter et al., 1953) put forward the idea of field cancerisation when he observed that in all resected tumours, the benign epithelium that was surrounding them, was also abnormal. In the instances of small tumours, there were always adjacent abnormal foci, which were even suggested to 'merge' later on and culminate into the clinical appearance of recurrent HNSCCs (Slaughter et al., 1953). The multiple origins of oral SCCs can also partially explain **1)** the incidence of multiple individual tumours in distinct anatomical locations of the same individual and **2)** the high rate of local recurrence seen in the case of SCCs of the oral cavity (Slaughter et al., 1953), which is a significant clinical complication that occurs at a rate of 10-30% even with histopathologically tumour-free surgical margins after resection (Charles et al., 1994). The term of field cancerisation has been further adopted to describe epithelial neoplasms of the lung (Franklin et al., 1997), oesophagus (Prevo et al., 1999), vulva (Rosenthal et al., 2002), cervix (Chu et al., 1999), colon (Jothy et al., 1996), breast (Forsti et al., 2001), bladder (Takahashi et al., 1998), and skin (Stern et al., 2002).

A recent study has shown that in 36% of HNSCC cases, there are several tumour-associated genetic alterations found in macroscopically normal mucosa adjacent to the tumour (Tabor et al., 2001), supporting the earlier idea of field cancerisation. Since in 70% of cases these genetic alterations were present beyond the surgical margins (Tabor et al., 2001), at least some pre-neoplastic cells are spared after resection, and may be responsible for the recurrence of HNSCC tumours after a latent period. The fact that the 'cancerised' surrounding field lacks some of the alterations seen in the developing tumour (Tabor et al., 2001), further supported the idea that while oral SCCs are clonal in origin, their histopathological progression occurs parallel to the acquisition of further genetic alterations.

The theory of field cancerisation classically suggests that secondary tumours occur independently of one another due to the cancerisation of a field by sustained exposure to known carcinogens (Chung et al., 1993; van Oijen et al., 2000; Tabor et al., 2001). Based on the theory that tumours are clonal in origin, the multiple foci seen in HNSCC were also thought to arise from the separation of the tumour initiating clone into sub-clones, which have the ability to migrate within the local environment and get established into adjacent or remote sites with the oral cavity (Tabor et al., 2001; Tabor et al., 2002). Although the emerging sub-clones would be able to acquire further genetic alterations, independently of the originating clone, all should theoretically share the same early genetic hits that transformed them in the first place. The surrounding altered fields as well as secondary primary tumours (SPTs) have been examined in detail with various cytogenetic approaches, but evidence is still inconclusive as to whether multifocal or secondary HNSCCs share the same origin with primary tumours. By studying the patterns of allelic loss for 9p arm as an early marker in tumour progression, Bedi et al. 1996 found that 37% of HNSCC tumour pairs shared the same genetic alterations, while the remaining tumour pairs showed a different pattern of 9p loss, suggestive of different clonal origins (Bedi et al., 1996). Other studies have concluded that a only a small minority of secondary, or synchronous, oral carcinomas show evidence of a common clonal origin (Scholes et al., 1998; Califano et al., 1999). By comparing the allelotypes of numerous pre-malignant lesions and invasive carcinomas, a more recent

study suggested that while multiple pre-malignant lesions may arise independently, the probability of the mucosal spread of neoplastic cells is increased with malignant progression (Jang et al., 2001), possibly explaining the emergence of at least some clonally related secondary tumours found in other studies.

However, tumour cells are under a constant selection pressure, and their survival and progression depends on the rate by which they can beneficially alter their genetic material (Cahill et al., 1999). If one considers that multifocal or second primary HNSCCs could have the same origin, then their heterogeneity in terms of the pattern of allelic losses, as was observed from cytogenetic analyses, can also be an indication of the intra-tumoural genetic heterogeneity that is a hallmark of many, if not most, types of human malignancies (Mirchandani et al., 1995; Fujii et al., 1996; Heim et al., 1997; Gorunova et al., 1998; Macintosh et al., 1998; Pandis et al., 1998). It is known that most malignant tumours show considerable genetic heterogeneity, and as such, collective analysis of tumour samples can mask the presence of a certain genotype if the population that bears it is not the dominant one. The failure to detect common patterns of allelic loss and chromosome breaks is not therefore definitive evidence of the absence of such clones in the total pool of neoplastic cells. As both chromosomal instability, which results from multiple mitotic defects, and microsatellite instability, are consistently seen in human tumour evolution (Weaver and Cleveland, 2006; Storchova and Kuffer, 2008), it is possible that the clones of SPTs and anatomically remote malignant foci of the oral cavity, are indeed related and their genomic alterations can be explained by the genetic drift of a single pre-malignant progenitor.

While the jury is still out, it is becoming clear from all these studies that the complexity of human oral carcinogenesis is owned to multiple events that take place in earlier as well as in later stages of the disease. Even at the level of gene expression, large scale microarray analysis shows that most transcriptional alterations in HNSCC occur during the transition of normal oral mucosa to pre-malignant epithelium, rather than from a pre-malignant lesion to invasive carcinoma (Ha et al., 2003). Thus, there is a broad range of early molecular and

genetic events, the identification of which could provide significant prognostic and diagnostic benefit to HNSCC.

1.4 FOXM1 Transcription Factor

1.4.1 Forkhead Box Proteins

Forkhead box (FOX) proteins are a family of transcription factors that share a common DNA binding domain (DBD), termed the forkhead box or winged helix domain (WHD), are a highly conserved family of transcriptional regulators, with at least 43 genes being identified in humans, presenting a large functional diversity (reviewed in Myat & Lam, 2007). They regulate cell growth, proliferation, apoptosis, differentiation, longevity, and transformation and exhibit a diverse range of functions during embryonic development and adult tissue homeostasis (Katoh and Katoh, 2004). According to the Human Gene Nomenclature Committee (HGNC) (Wain et al., 2002), human gene symbols (including DNA, mRNA and protein) should be in upper case, therefore "FOXM1" is used throughout this thesis to indicate its human origin and "Foxm1" for mouse and rat.

1.4.2 Foxm1 Knock-Out Mouse Models

Foxm1 is also known in the literature as Trident (mouse), *HFH11* (human), *WIN* or *INS-1* (rat), MPP2 (human cDNA), or *FKHL-16* (Laoukili et al., 2007). Foxm1 knock out mouse models have provided evidence for the important role of this protein, in organogenesis, tissue proliferation, and differentiation. Homozygous *Foxm1* knock-out (*Foxm1*$^{-/-}$) leads to peri-natal lethality and/or to post-term death just after birth, due to heart defects in mice (Korver et al., 1998). Further analysis revealed ploidy abnormalities in both liver and the hearts of *Foxm1*$^{-/-}$ mice, with markedly increased DNA content present in both tissues (polyploidy) (Korver et al., 1998), while targeted deletion of *Foxm1* DBD and transactivation domains (TAD) in transgenic mice results in the same phenotype (Krupczak-Hollis et al., 2004). Additionally, hepatoblasts of Foxm1$^{-/-}$ mice show defective proliferation and incomplete differentiation of the biliary epithelial cell lineages of the liver (Krupczak-Hollis et al., 2004). Foxm1$^{-/-}$ mice also exhibit gross lung pulmonary defects, including hypertrophic arterioral smooth muscle cells, and defective peripheral pulmonary arteries (Kim et al., 2005), while *Foxm1*$^{-/-}$ lungs are significantly affected by reduced levels of Platelet endothelial

adhesion molecule-1 (Pecam-1), VEGF receptor type 1 (*Flt1*), and *FoxF1* (Kim et al., 2005). More recently, it was also shown that targeted pancreatic inactivation of Foxm1 in mice resulted in the steady reduction of β-cell proliferation and mass with age (Zhang et al., 2006). Collectively, Foxm1 knock-out mouse model established multiple roles of Foxm1 ranging from mitosis, embryonic tissue development to ageing.

1.4.3 Human FOXM1 Gene

The human *FOXM1* gene is located at the 12p13.3 chromosome band and is comprised of 10 exons, two of which (exons A1 and A2) are alternatively spliced (Korver et al., 1997b). The first exon and part of the last exon contain 3' and 5' untranslated sequences, respectively. The three FOXM1 isoforms, FOXM1A, FOXM1B, and FOXM1C, are created by alternative splicing of A1 and A2 exons, with FOXM1B being the only one isoform containing none of these exons (Ye et al., 1997) (**Figure 1.7**).

Although all three protein isoforms of FOXM1 can bind to DNA *in vitro* through the consensus site TAAACA (Korver et al., 1997b), only FOXM1B and FOXM1C have trans-activating ability (Korver et al., 1997a; Ye et al., 1997; Luscher-Firzlaff et al., 1999; Leung et al., 2001; Major et al., 2004; Wierstra and Alves, 2006c). FOXM1A is shown to be transcriptionally inactive due to the presence of the inhibitory A2 exon in the C-terminal of its transactivation domain (Ye et al., 1997), and is suggested to act as a regulator of FOXM1 gene activity by competing with FOXM1B and FOXM1C for DNA binding and gene transactivation (Laoukili et al., 2007).

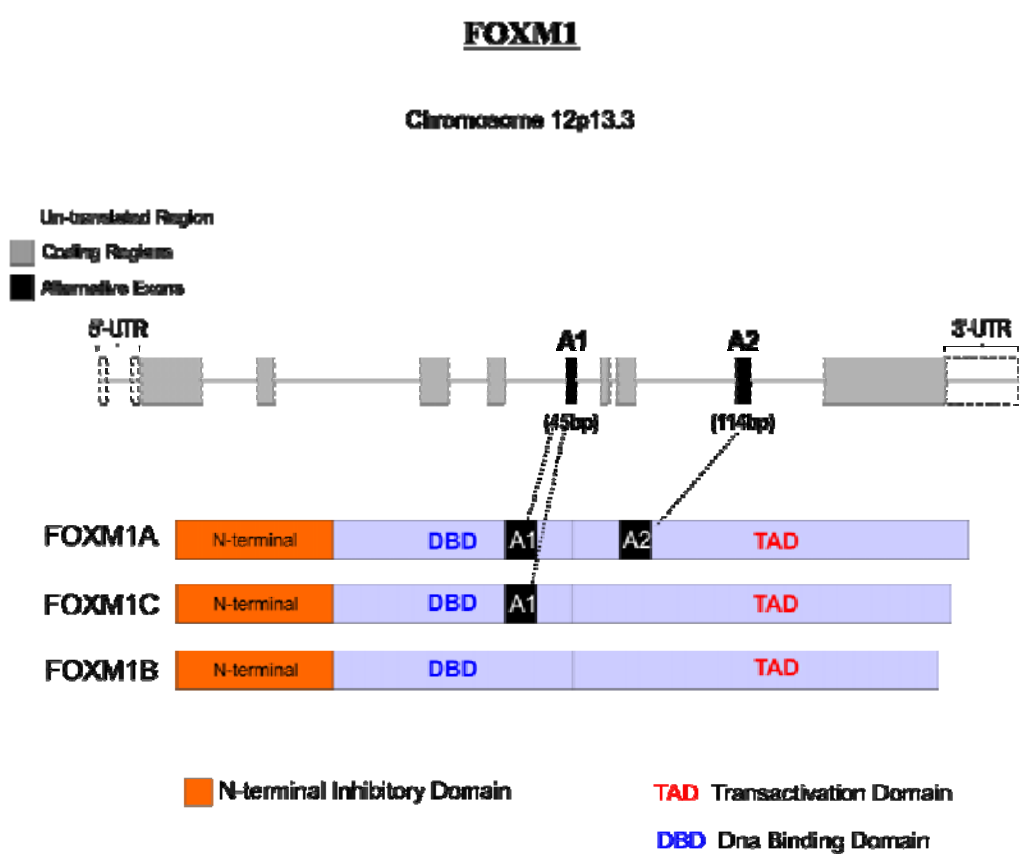

Figure 1.7: Human *FOXM1* gene

FOXM1 gene is located at chromosome 12p3.3 and encodes 10 exons. The first exon and part of the last exon contain 3' and 5' untranslated sequences, respectively. Exons A1 and A2 area alternatively spliced to give rise to three distinct isoforms. FOXM1A contains both exons. Exon A2 is located at the C-terminal of its transactivation domain (TAD) and abolishes its transactivation potential (Ye et al., 1997). FOXM1C possesses only A1 exon, while FOXM1B has none of the alternatively spliced exons. All three isoforms contain the conserved DNA binding domain and the N-terminal inhibitory domain that restricts the activation potential of FOXM1 (modified from Laoukili et al., 2007)

1.4.4 The Biological Function of FOXM1

FOXM1 is widely accepted as being a proliferation specific transcription factor, as it is mainly expressed in dividing cells, while its expression is almost absent in quiescent and terminally differentiated cells (Laoukili et al., 2007). Its expression is detected in tissues with a high proliferative index such as the thymus, testis, lung and the intestine (Korver et al., 1997b), as well as in various immortalized and cancer-derived cell lines (Korver et al., 1997a; Ye et al., 1997; Wonsey and Follettie, 2005; Kalin et al., 2006; Kim et al., 2006; Liu et al., 2006). In line with the fact that FOXM1 expression is strictly associated to cellular proliferation, it was shown that serum stimulation can activate its

expression (Korver et al., 1997b), possibly through activation by c-MYC which occupies its promoter *in vivo* (Fernandez et al., 2003).

FOXM1B was shown to have strong proliferative effects when over-expressed in the livers on transgenic mice, following partial hepatectomy (a strong mitotic inducer), since its overexpression could markedly increase the rate of hepatocyte DNA replication and subsequent mitosis (Ye et al., 1999; Wang et al., 2002b). More strikingly, overexpression of FOXM1B was sufficient to restore the regenerative potential and young phenotype in the livers of aged mice by inducing the expression of many G1/S as well as G2/M specific, growth promoting, genes including Cyclin D1, Cyclin F, Cyclin B1 and B2, Cyclin A2, and Cdc25B (Wang et al., 2001). This proliferative effect was also attributed to the fact that FOXM1B overexpression could significantly suppress the protein levels of $p21^{cip1/waf-1}$ and $p27^{Kip1}$ (Wang et al., 2002a; Wang et al., 2002b), which are able to halt the cell cycle at G1 phase by blocking the formation cyclin/Cdk complexes, which are required for S and M-phase progression by phosphorylating protein substrates, essential for mitosis (Pines, 1995; Harbour and Dean, 2000; Ishida et al., 2001). On the contrary, hepatic deletion of endogenous *Foxm1* in mice is associated with reduced proliferation rate and the upregulation of cdk inhibitor $p21^{waf1/cip1}$ (Wang et al., 2002a), thus highlighting its instrumental role in cell cycle regulation.

In addition to its proposed role in regulating the early phases of cell cycle progression, FOXM1 was also found to be implicated in the regulation of G2/M phase of the cell cycle. Accurate, but controlled activation of FOXM1 protein is required to ensure successful execution of the mitotic programme and the maintenance of chromosome stability (Laoukili et al., 2005). In line with this, *Foxm1*$^{-/-}$ mouse embryonic fibroblasts (MEFs) and endogenous *FOXM1* knock-down in U2OS cells (human osteosarcoma cell line), display gross chromosomal abnormalities characterized by spindle assembly defects, chromosome missegregation, and polyploidization (Laoukili et al., 2005), which is consistent with the phenotypes observed in knock-out mouse studies (see **section 1.4.2**). In a separate study, it was found that depletion of FOXM1

by RNAi in human breast cancer cell lines was also sufficient to inhibit cell proliferation and cause cell death due to mitotic catastrophe (Wonsey and Follettie, 2005). The biological function of FOXM1 can also be illustrated in the case of $Foxm1^{-/-}$ mouse derived embryonic fibroblasts (MEFs) and FOXM1-depleted human U2OS cells, which show DNA breaks parallel to persistent cell cycle arrest and activation of p53 and $p21^{cip1/waf1}$ proteins (Tan et al., 2007). Further to that, FOXM1 deficiency is also accompanied by reduced expression of DNA repair genes (Tan et al., 2007), while FOXM1 overexpression leads to stimulation of their expression both *in vitro* and *in vivo* (Ye et al., 1999; Tan et al., 2007). It is therefore becoming increasingly clear that the functions of FOXM1 extend to a broad range of biological processes.

1.4.5 FOXM1 in the Regulation of the Cell Cycle

1.4.5.1 The multi-step activation of FOXM1 throughout the cell cycle

Studies from transgenic mouse models provided evidence that FOXM1 has a strong regulatory role in cell cycle progression. In addition, its cell cycle specific pattern of expression (Korver et al., 1997a) suggests that FOXM1 is itself regulated by cell cycle events.

In line with this notion, FOXM1 protein was reported to contain a cyclin/cdk binding sequence (LXL motif) which serves for its phosphorylation and activation by Cdk2/CyclinE complex during G1/S, and by Cdk2/CyclinB complex during G2/M (Major et al., 2004). In addition to the latter, further work has demonstrated that FOXM1 is phosphorylated, and subsequently activated, also by CyclinD1/Cdk and CyclinA/Cdk complexes during G1 and S phases respectively (Wierstra and Alves, 2006b; Laoukili et al., 2008b), therefore proposing a multi-step model of FOXM1 activation throughout the cell cycle. The finding that FOXM1 can suppress the protein levels of important Cdk inhibitors, $p21^{CIP1/WAF1}$ and $p27^{KIP1}$ (Wang et al., 2002a; Wang et al., 2002b; Wang et al., 2005), further proposed a mechanism by which FOXM1 augments its own activation throughout cell cycle progression. The phosphorylation of FOXM1 protein is necessary for the transactivation

potential of FOXM1 transcription factor. First, because it allows the recruitment of p300/CBP co-activator proteins which increase the transactivation potential of FOXM1 transcription factor (Major et al., 2004), and second because it ablates the repressive function of FOXM1 N-terminus, therefore allowing full activation and FOXM1 dependent transcription (Wierstra and Alves, 2006a; Wierstra and Alves, 2006b; Laoukili et al., 2008b).

The clusters of genes that are activated as a result of FOXM1 transactivation depend on the phase of the cell cycle that this event takes place. The transcriptional network of genes induced by FOXM1 during G1/S transition includes Skp2 and Cks1, both of which are subunits of the SCF ubiquitin ligase complex that targets $p27^{KIP1}$ and $p21^{CIP1/WAF-1}$ for degradation (Wang et al., 2005). The growth promoting effect of FOXM1 was further highlighted by the finding that it can directly bind to, and activate the transcription of *c-MYC*, an early response transcription factor that stimulates cell cycle progression (Amati et al., 1998). However, most of FOXM1 target genes are induced upon entry into mitosis, where FOXM1 is though to have an instrumental role. FOXM1 transcriptional targets comprise a variety of important G2/M regulatory proteins, including Plk1, Aurora B kinase, cyclin B1, cyclin B2, Cdc25B, Nek2, CENP-A, CENP-B, and CENP-F (Leung et al., 2001; Laoukili et al., 2005; Wang et al., 2005) (see also **Figure 1.8**). All these proteins are directly associated to important mitotic processes including the activation of CyclinB/cdk complexes during mitotic entry, chromosome segregation, the assembly of the mitotic spindle checkpoint, and centrosome maturation and separation during cell division (Nigg, 2001; Meraldi et al., 2004). In fact, the phenotype of FOXM1 depleted cells clearly reflects the defective regulation of these genes, since in the absence of FOXM1 protein there is chromosome misalignment, defective chromosome segregation, defective localization of the spindle assembly checkpoint (SAC) proteins on the kinetochore which leads to disruption of the SAC, all of which lead either to cell death, or to the generation of genetically unstable progenies (Laoukili et al., 2005; Wonsey and Follettie, 2005).

Whether FOXM1 activation and subsequent transactivation of downstream targets occurs as early as in G1 phase, or later, and whether this is regulated by nuclear-cytoplasmic shuttling of the protein, remains unclear. For example, in the presence of Raf/MeK/MAPK signalling, FOXM1 was shown to translocate from the cytoplasm to the nucleus at S/G2 boundary, where it activates the expression of its downstream target genes, including Cyclin B1 (Leung et al., 2001; Ma et al., 2005). Others have also proposed that phosphorylation and activation of FOXM1 occurs mainly from late S phase onwards, with its activity being highest at the G2 and mitosis (Leung et al., 2001; Laoukili et al., 2005; Ma et al., 2005; Laoukili et al., 2008b). In support of this, most of the established downstream targets of FOXM1 are induced mainly at the G2/M phase of the cell cycle (Leung et al., 2001; Laoukili et al., 2005; Laoukili et al., 2008b). Despite these apparent discrepancies it is clear that, in addition to its cell cycle dependent expression at the mRNA level (Korver et al., 1997a), FOXM1 is subjected to numerous post-translational modifications that determine the level of its activation, and therefore that of its target genes, throughout a normal cell cycle.

1.4.5.2 Repression of FOXM1 activity

The repression of growth promoting transcription factors is important for the maintenance of a normal cell cycle, and as such, FOXM1 is held in check by various mechanisms that limit its transactivation ability. The first demonstration that FOXM1 is indeed a target of tumour suppressor proteins came from the finding that $p19^{ARF}$ tumour suppressor, a member of the INK4 family of Cdk inhibitor proteins, can associate with FOXM1 protein *in vivo* in transgenic mice while it was later found that $p19^{ARF}$ derived peptides can inhibit the transcriptional activity of FOXM1 in U2OS human osteosarcoma cells (Kalinichenko et al., 2004; Gusarova et al., 2007). It was further demonstrated that the activation of FOXM1 is restricted at G1 phase through its association with retinoblastoma tumour suppressor (Rb) which specifically binds to, and represses the TAD of FOXM1 protein (Major et al., 2004; Wierstra and Alves, 2006d). Rb normally constrains cellular proliferation by blocking the transactivation ability of growth promoting transcription factors, such as E2F1 (Harbour and Dean, 2000), and presumably the same applies for

FOXM1 since abrogation of Rb by high risk HPV type E7 oncoprotein results in activation of FOXM1 protein (Major et al., 2004). This can also account for the low levels of FOXM1 transcriptional activity in quiescent cells.

A very potent inhibitory mechanism of FOXM1 activity is that of auto-repression, which is imposed by the N-terminal of FOXM1 protein (Wierstra and Alves, 2006a; Park et al., 2007; Laoukili et al., 2008b). It is suggested that the N-terminal domain of FOXM1 is able to interact with its C-terminal activation domain, therefore limiting the overall transactivation potential of FOXM1 protein. Further analysis in U2OS cells provided evidence showing that FOXM1 protein is capable of binding to the its target genes' promoters as early as in G1 phase, but is unable to activate gene expression due to repression by the N-terminal domain (Laoukili et al., 2008b). Following entry into G2 phase, CyclinA/cdk complexes are required for efficient phosphorylation of FOXM1 which both relieves N-terminal repression, as well as it increases the transactivation potential of the TAD (Laoukili et al., 2008b). In support of these findings, deletion of the N-terminus can give rise to a truncated FOXM1 mutant protein that is insensitive to growth stimulation, and is constitutively active throughout the cell cycle without the requirement for Cyclin/cdk mediated phosphorylation (Park et al., 2007; Laoukili et al., 2008b). Cells that express ΔN-FOXM1 show greatly enhanced transactivation potential in luciferase reporter systems, as well as significantly enhanced activation of downstream target genes, irrespectively of cell cycle status (Park et al., 2007; Laoukili et al., 2008b).

The hyperphosphorylated forms of FOXM1 protein present throughout mitosis, are then rapidly extinguished from the cell during mitotic exit, serving as a mechanism to prevent the existence of active FOXM1 in G1 phase (Laoukili et al., 2008a; Park et al., 2008). This is achieved by the ubiquitin ligase complex APC (anaphase promoting complex)/Cdh1 (activating regulatory protein) (Laoukili et al., 2008a; Park et al., 2008), which recognizes target mitotic proteins for degradation (Sudo et al., 2001; Li and Zhang, 2009). In fact, some of its substrates include mitotic cyclins, Aurora A and Aurora B kinases, and Plk1, the degradation of which is necessary for the maintenance

of genomic integrity following exit from mitosis (Sudo et al., 2001; Engelbert et al., 2008; Li and Zhang, 2009). In a similar manner, FOXM1 protein is targeted for degradation at anaphase, and until the early stages of G1 phase (Laoukili et al., 2008a; Park et al., 2008) by APC/cdh1, which recognizes FOXM1 target sequences at the protein's N-terminal (Laoukili et al., 2008a; Park et al., 2008).Although there is currently no evidence to suggest that an N-terminal deleted variant of FOXM1 exists physiologically, these studies provide invaluable insight into the mechanisms that control FOXM1 activity throughout cell cycle progression.

Despite the fact that FOXM1 can induce the expression of a multitude of genes with roles that range from the stimulation of DNA synthesis to proper chromosome segregation, the mechanisms that repress its activity ensure the timely transcriptional activation of its targets, and the maintenance of a stable cell cycle.

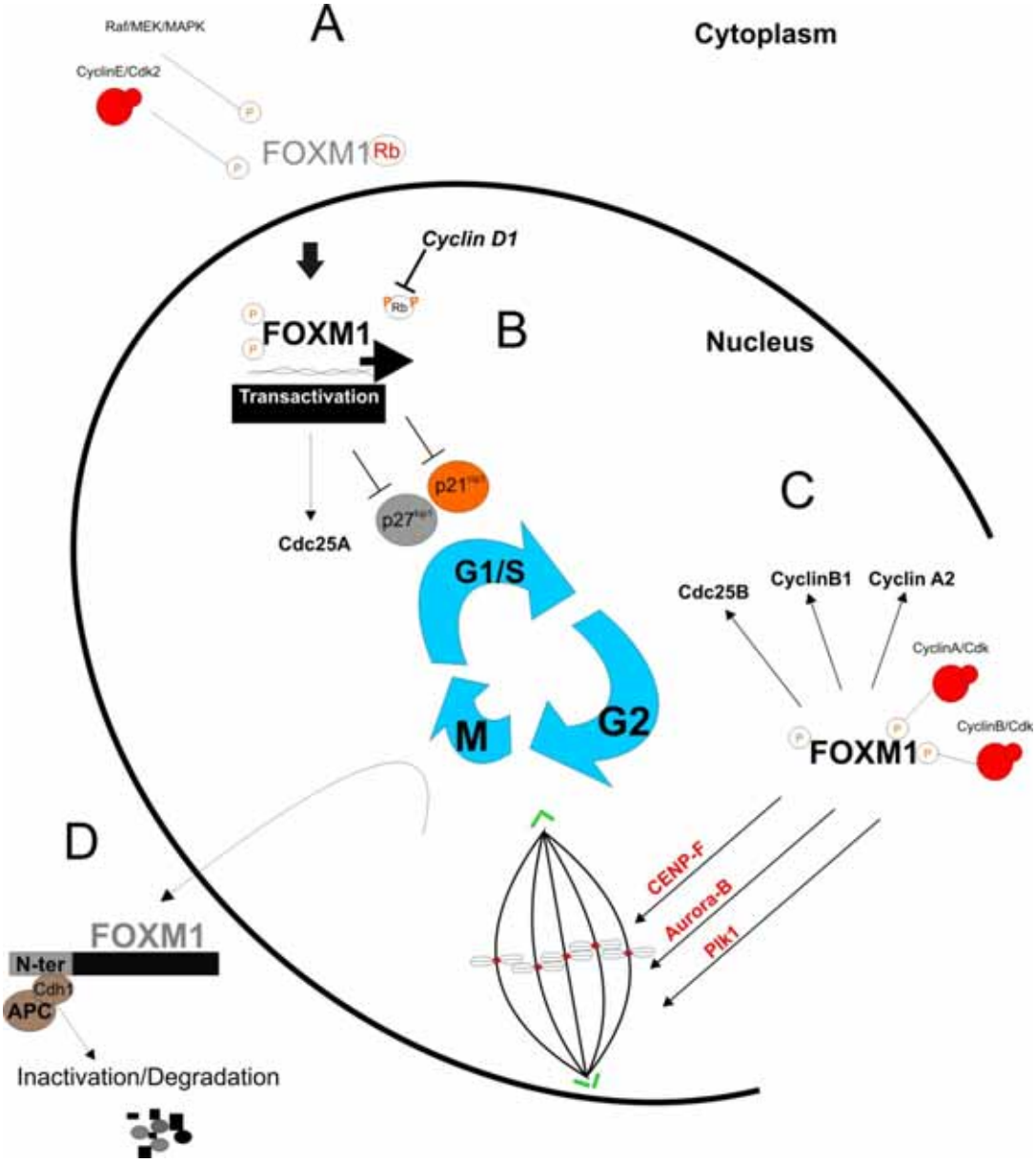

Figure 1.8: FOXM1 in cell cycle regulation.

(A) Phosphorylation of FOXM1 by Raf/MEK/MAPK and CyclinE/Cdk2 complexes leads to the nuclear accumulation of FOXM1. **(B)** Phosphorylation and subsequent inactivation of Rb by Cyclin D1 allows full activation of FOXM1, which initiates transactivation of downstream targets by binding to DNA. During G1/S phase progression, FOXM1 promotes the degradation of $p21^{CIP1/WAF-1}$ and $p27^{KIP1}$ while it activates Cdc25A. **(C)** At G2 phase FOXM1 is further activated by phosphorylation of CyclinA/Cdk and CyclinB/cdk complexes, and induces the expression of Cdc25B, cyclin B1 and cyclin A2, while it directly upregulates important mitotic spindle assembly proteins like CENP-F, Aurora B and Plk-1 that ensure normal chromosome segregation and genomic stability. **(D)** During late mitosis (anaphase), FOXM1 is sequestered to the cytoplasm where it gets inactivated by binding to Rb and followed by APC/Cdh1 mediated protein degradation.

1.4.6 The Role of FOXM1 in Carcinogenesis

FOXM1 gene was found to encode a protein identified by MPM-2 monoclonal antibody, which binds specifically to epitopes on mitotic proteins that are phosphorylated during the cell cycle (Westendorf et al., 1994). Initial observations led to the identification of MPM2 as an interaction partner of high risk human papillomavirus type 16 (HPV-16) E7 protein, a common cause of human malignancies, which could enhance the transformation potential of rat embryo fibroblasts (Luscher-Firzlaff et al., 1999). The first study to directly implicate FOXM1 in human cancer was performed by Teh et al. (2002) demonstrating that FOXM1B is the main isoform abundantly expressed in human basal cell carcinomas and further identified this gene as a downstream target of oncogenic transcription factor GLI1 (Teh et al., 2002).

Given the multiple roles of FOXM1 during cell division, it is not surprising that this transcription factor has since been listed amid the most common differentially expressed genes in majority of solid human tumours including prostate, skin, liver, breast, lung, ovary, colon, pancreas, stomach, bladder and kidney (van den Boom et al., 2003; Pilarsky et al., 2004). The chromosomal band where human FOXM1 gene is located (12p13) is also found to be amplified in breast adenocarcinomas (Spirin et al., 1996), nasopharyngeal carcinomas (Rodriguez et al., 2005) and HNSCC derived cell lines (Singh et al., 2001). This suggests that FOXM1 gain of function provides a selective advantage for the clonal expansion of tumourigenic progenies, therefore promoting tumour development.

1.4.6.1 Evidence from *in vivo* Models of Carcinogenesis

The oncogenic ability of FOXM1 was further confirmed in carcinogenesis models *in vivo*, clearly demonstrating that not only this transcription factor has a strong tumourigenic potential, but in some cases is essential for the progression of tumours in transgenic mice.

Sustained expression of human FOXM1 increases the proliferation rates of chemically induced (via the DNA damaging diethyl-nitrosamine; DEN; liver carcinogen) premalignant hepatocellular lesions, and its overexpression can

increase the size of the resultant liver tumours following promotion with phenobarbital (PB), without however altering the frequency by which they occur (Kalinina et al., 2003) . This apparent paradox was partially attributed to the fact that while FOXM1 could induce the expression of proliferation associated genes thereby promoting neoplastic cell proliferation, it could also concomitantly induce the expression of DNA repair associated genes which could potentially have anti-tumour activity (Ye et al., 1999; Kalinina et al., 2003). Due to this, and given that FOXM1B failed to show any proliferative effects on normal hepatocytes, treatment with FOXM1 was therefore suggested as a safe alternative to potential liver regeneration therapy (Kalinina et al., 2003). It was later found that endogenous levels of Foxm1 are essential for the growth and maintenance of hepatic tumours in transgenic mice following DEN/(PB), since **(a)** *Foxm1*$^{-/-}$ were almost completely protected from hepatocellular carcinogenesis (Kalinichenko et al., 2004), and **(b)** conditional knockout of *Foxm1* in pre-existing liver carcinomas could significantly reduce tumour size and proliferation (Gusarova et al., 2007). More importantly, the study by Gusarova et al. (2007) underscored the importance of FOXM1 in liver tumourigenesis by demonstrating that overexpression of FOXM1 in a p19^{ARF} null background induces rapidly growing hepatocellular carcinomas, compared to those of wild-type mice (Gusarova et al., 2007). The restoration of p19^{ARF} by treatment with p19^{ARF} derived peptides inhibited tumour cell proliferation and angiogenesis, and induced apoptosis of hepatocellular carcinomas in mice by reducing Foxm1 transcriptional activity as evidenced by downregulation of downstream Foxm1 targets such as Survivin, Aurora B, and Polo-like kinase 1 (Plk1) (Gusarova et al., 2007).

Targeted deletion of Foxm1 in the colonic epithelium of transgenic mice is also protective from chemically induced carcinogesis, whereas human FOXM1 transgenic overexpression results in increased numbers and size of colorectal carcinomas following tumour induction (Yoshida et al., 2007). These tumours also bared a typical FOXM1-dependent expression signature as evidenced d by the up-regulation of Cyclin A2, CyclinB1, and Survivin (Leung et al., 2001; Wang et al., 2005; Yoshida et al., 2007). Consistent with

previous observations (Kalinina et al., 2003), FOXM1 transgenic overexpression does not induce any phenotypic alterations in normal colonic mucosa (Yoshida et al., 2007), therefore suggesting again a role for this transcription factor in the selective expansion of pre-neoplastic and/or tumourigenic progenies. Transgenic expression of FOXM1 in mouse models of prostate cancer, can also significantly accelerate the development, proliferation, and subsequent growth of prostate tumours, while it was also observed that $p19^{ARF}$ tumour suppressor is continuously expressed in FOXM1-derived prostate carcinomas (Kalin et al., 2006), confirming the earlier prediction that sustained overexpression of FOXM1 is required to overcome the tumour suppressive effects of $p19^{ARF}$ (Kalinichenko et al., 2004; Kalin et al., 2006).

In a similar manner, conditional deletion of *Foxm1* in lung mouse cells, prior to lung tumour induction with urethane, resulted in significant reduction in both the number and size of lung adenomas of transgenic mice (Kim et al., 2006). Further analysis suggested that the developing tumours of $Foxm1^{-/-}$ mice were able to grow due to inefficient suppression of Foxm1 gene expression as judged by the fact that 84% of the lung adenomas that developed in $Foxm1^{-/-}$ mice, showed reactivation of the oncogene (Kim et al., 2006). The latest study to have looked into the role of FOXM1 in a mouse model of lung epithelial carcinogenesis, demonstrated that specific targeted deletion of endogenous Foxm1 from respiratory epithelial cells resulted in diminution of chemically induced lung tumour numbers and tumour cell proliferation (Wang et al., 2009). Interestingly, deletion of *Foxm1* prior to, or after tumour initiation (single with urethane, or two-stage with MCA initiation /BHT promotion) resulted in similar suppression in lung tumour growth. This suggests that the presence of Foxm1 during the initiation step is not critical. It is therefore suggested that Foxm1 is mostly required during the steps of tumour progression and expansion (Wang et al., 2009). As was expected, transgenic overexpression of FOXM1 in the lungs of mice also leads to significant increases in the numbers, size, and proliferation rates of lung adenomas induced by MCA (polycyclin aromatic hydrocarbon)/ BHT (butylated hydroxytoluene) treatment (Wang et al., 2008b).

1.4.6.2 Molecular Mechanisms of FOXM1-Induced Tumourigenesis

The transcriptional regulation of genes, such as *FOXM1*, which control multiple aspects of cell division, is of great interest in cancer biology, since it can provide significant insight into the mechanisms that mediate early as well as late events in the progression of human neoplasia. The contribution of FOXM1 during this process is well documented, and best illustrated through studies that investigate its function in the context of human tumour derived cell lines.

Large scale analysis of gene expression data has revealed that FOXM1 is significantly overexpressed in human infiltrating ductal breast carcinomas (Dahl et al., 2005; Wonsey and Follettie, 2005; Dahl et al., 2006). This observation was also confirmed in two separate studies showing increased expression of FOXM1 in breast carcinomas, and especially those with highly invasive properties (Bektas et al., 2008), while FOXM1 expression was also found to be associated with poor breast cancer prognosis (Martin et al., 2008). However, others have reported that there is no significant correlation between FOXM1 expression and breast tumour grade (Francis et al., 2009). In agreement with the *in vivo* observations, FOXM1 was also found overexpressed in transformed human breast cancer cell lines (Wonsey and Follettie, 2005; Bektas et al., 2008). It is noteworthy that FOXM1 overexpression is evident in breast cancer cell lines, even when compared to their un-transformed but spontaneously immortalised, and thus proliferatively active, counterparts (Wonsey and Follettie, 2005; Bektas et al., 2008). This strongly suggests that the effect of FOXM1 expression is directly associated with malignant transformation rather than just with the proliferative potential of immortalised cells *in vitro*. Expectedly, downregulation of FOXM1 by siRNA in human breast cancer cell line BT-20 leads to reduced proliferation, while chronic depletion of FOXM1 protein by shRNA leads to decreased viability followed by a phenotype that is highly reminiscent of that observed by Laoukili et al. (2005) , which is characterised by disruption of the mitotic spindle, centrosome amplification, and polyploidization, which leads to cell death (Laoukili et al., 2005; Wonsey and Follettie, 2005).

More insight into the potential mechanism by which FOXM1 may be implicated in human breast carcinogenesis, was provided by Madureira et al. (2006) who showed that in human breast cancer cell lines, there is a tight relationship between the expression pattern of FOXM1 and that of estrogen receptor α (ERα) (Madureira et al., 2006), the most common cause in the pathogenesis of human breast cancer (Sommer and Fuqua, 2001). Further to that, it was shown that FOXM1 can bind to the promoter of ERα gene, and directly induce its expression in human breast carcinoma derived cells (Madureira et al., 2006), suggesting a mechanism by FOXM1 may be regulating the abundance of ERα in human breast cancer. This relationship was shown to be reciprocal since the expression of FOXM1 itself can also be induced by estrogen receptor ligand treatment of estrogen responsive breast cancer cell lines, a mechanism that is mediated by ERα which directly binds to, and activates the promoter of FOXM1 (Millour et al.). Another link between FOXM1 and breast cancer pathogenesis was provided by evidence from breast carcinoma cell lines, showing that FOXM1 is a downstream target of epidermal growth factor receptor 2 (HER2) (Francis et al., 2009), which is amplified in 15% - 20% of invasive breast carcinomas and results in increased metastatic potential and a poor clinical outcome (Slamon et al., 1987; Slamon et al., 1989).

More importantly, it was shown that tamoxifen (OHT; estrogen receptor antagonist) was unable to repress the levels of FOXM1 in OHT resistant breast cancer clones, which maintained their proliferative capacity for longer times after treatment, as opposed to their OHT sensitive counterparts (Millour et al.). This implicated FOXM1 in the mechanism of acquired resistance to anti-estrogen treatment of breast cancer. In the same context, it was shown more recently that ectopic expression of the truncated ΔN-FOXM1 can also render MCF-7 breast cancer cells resistant to cisplatin treatment, presumably by potentiating DNA repair associated pathways as judged by the maintenance of cell viability and the reduction in the recruitment of γH2Ax at sites of DNA strand breaks following treatment (Kwok et al., 2010). Consistent with this potential role of FOXM1, its selective inhibition by thiostrepton (FOXM1

inhibitor (Bhat et al., 2009) was sufficient to abrogate acquired cisplatin resistance of MCF-7 breast cancer cells (Kwok et al., 2010).

Although the paradigm of breast carcinogenesis is among the most extensively studied *in vitro*, and provides several mechanisms by which FOXM1 exerts in tumourigenic potential, its over-expression has also been reported in a large variety of other human tumours and tumour-derived cell lines. Its overexpression has been reported in the majority of human lung adenocarcinomas (50% at mRNA and 78% at protein level) and lung squamous cell carcinomas (67% at mRNA and 68% at protein level). A more recent study, by examining 69 samples of lung SCCs, reported that intratumoural FOXM1 expression was not detected in more than 37% of SCCs (Yang et al., 2009). Despite the low frequency of FOXM1 immunoreactivity, it was shown that its presence is invariably associated with poor differentiation status, lymph node metastasis, and consequently poor patient survival (Yang et al., 2009). Furthermore, expression of FOXM1 in lung tumours is positively correlated with proliferation associated PCNA (proliferating cell nuclear antigen) and the expressions of cyclin A2 and cyclin B1 (Kim et al., 2006), both of which are established FOXM1 targets. Additionally, depletion of FOXM1 protein leads to significant reduction of the proliferative potential and anchorage independent growth rate of human lung cancer cell lines *in vitro* (Kim et al., 2006). Human prostate tumours also exhibit significantly elevated levels of FOXM1 protein that is even more evident in advanced tumour stages, and is related to proliferation and metastasis (Kalin et al., 2006; Chandran et al., 2007). In line with these observations, microarray gene expression analysis has also shown that FOXM1 is consistently overexpressed in metastatic prostate tumour samples (Chandran et al., 2007).

The cell cycle regulatory role of FOXM1B transcription factor is also a very important determinant of the tumourigenicity of glioma cells. Forced overexpression of FOXM1 in glioma cell lines was shown to enhance anchorage-independent growth and their ability to induce tumours when grafted in nude mice (Liu et al., 2006). In agreement with the expression pattern of FOXM1 observed in other human tumours, gliomas exhibit

increased FOXM1 protein and mRNA levels that show a positive relationship with more advanced states of the disease and decreased patient survival (Liu et al., 2006). In the same context, FOXM1 was shown to transcriptionally activate matrix metalloproteinalse-2 (MMP2) expression, thus enhancing the invasion of glioma cells (Dai et al., 2007), a process which is critical, and largely contributes to the poor prognosis generally associated with glioma tumours (Giese et al., 2003). Others have also reported that ability of FOXM1 to promote tumour cell invasion and migration is through the activation of JNK-1, which was found to be necessary for the upregulation of MMP-9 in U2OS human osteosarcoma cells (Wang et al., 2008a). In line with these observations, downregulation of FOXM1 by RNAi results in a rapid reduction of the metastatic potential of human glioma cells, and suppresses glioma growth in the brain of nude mice, resulting in increased overall survival time (Kim et al., 2006; Liu et al., 2006; Dai et al., 2007). Decreased levels of cyclin B1, cyclin A2, cyclin D1 as well as increased nuclear accumulation of $p27^{kip1}$ have been shown to mediate these growth suppressive effects following inhibition of FOXM1, in agreement with observation from *in vivo* mouse models (**see section 1.4.6.1**).

Another study points to a role for FOXM1 in the maintenance of the malignant properties of human pancreatic cancer cell lines. More specifically, FOXM1 depletion results in the activation of growth inhibitory proteins $p21^{cip1/waf1}$ and $p27^{KIP1}$ that mediate partial cell cycle arrest and reduced DNA replication, but also in the downregulation of matrix metalloproteinases MMP-2 and MMP-9 and vascular endothelial growth factor (VEGF) (Wang et al., 2008a). Collectively, these effects lead to significant reduction of the invasive and migratory activity of pancreatic cancer cells on Matrigel-coated membranes, and by using an *in vitro* assay of angiogenesis Wang et al. (2007) showed that treatment with cell culture medium secreted by FOXM1-depleted cells is sufficient to inhibit endothelial cell tube formation (*in vitro* measure of angiogenesis) of pancreatic cancer cell lines (Wang et al., 2007).

Taken together, these studies clearly demonstrate that apart from being a proliferation specific transcription factor, FOXM1 is necessary for the progression of human malignancies.

Aims and Hypothesis

Despite the fact that FOXM1 is overexpressed in the majority of human malignancies (Pilarsky et al., 2004), its expression has not yet been investigated in the case of human oral SCCs. This study will aim to investigate the regulation of FOXM1 expression in human oral squamous cell carcinomas *in vitro* and *in vivo*. Given the stepwise model of oral carcinogenesis, and the fact that FOXM1 has a tumour promoting function, it is hypothesised that FOXM1 also has a role in the progression of human oral squamous cell carcinoma. Therefore, this study will specifically aim to investigate the mechanism of FOXM1 in early pre-malignant lesions of human oral mucosa.

To date, studies of *FOXM1* as a cancer causing gene have been performed in the context of transformed and/or immortalized human cell lines, undoubtedly providing invaluable insight into the molecular mechanisms mediated by FOXM1. However, due to the aberrant molecular background already present in most cell line systems, the role of FOXM1 in the earliest stage of neoplasia could not be delineated and it is not fully understood. Therefore this study aims to understand the regulation of FOXM1 and the effect of its overexpression, in normal primary human epithelial keratinocytes as they represent the main target population of human malignancies. Due to the established role of FOXM1 in the maintenance of genomic integrity (Laoukili et al., 2005), this study will also follow the hypothesis that FOXM1 overexpression compromises the genomic integrity of primary human keratinocytes, possibly contributing to human cancer initiation. This study will specifically aim to understand whether FOXM1 overexpression in primary oral keratinocyte stem cells contributes to the generation of pre-malignant progenies, trying to provide an explanation to why FOXM1 is overexpressed in the majority of human epithelial malignancies.

Chapter 2

MATERIALS AND METHODS

2 Materials and Methods

2.1 Cell Culture

2.1.1 Primary Normal Human Keratinocyte Extraction and Establishment

Primary **n**ormal **h**uman **o**ral **k**eratinocyte (NHOK# 1, 2, 3, 4, 5, 376, 881, 355, and 113) and **n**ormal **h**uman **e**pidermal **k**eratinocyte strains (NHEK# 1, 2, and 3) were established from clinically normal oral buccal or gingival tissue and normal skin respectively. Donor tissues were collected in transport medium, consisting of DMEM (Lonza, Slough UK) with 3% (v/v) penicillin/streptomycin (Gibco Invitrogen, Paisley, UK). Tissues were minced using sterile scalpel and forceps, prior to digestion in Trypsin/EDTA solution (0.5 g/L of trypsin and 0.2 g/L of EDTA•4Na in Hanks' Balanced Salt Solution without $CaCl_{2)}$ (Gibco Invitrogen) for 4 hours at 37^{o}C under continuous shaking. The digested tissues were then passed through 75 μm cell strainers (BD Falcon Oxfordshire, UK) and keratinocytes were recovered underneath in DMEM medium (Lonza, Slough UK) with 10% FBS (FirstLink, Birmingham UK). Cells were spun at 140 x g for 5 minutes and finally resuspended in complete growth FAD medium with 3% (v/v) penicillin/streptomycin and 1% (v/v) antibiotic/antimycotic (PAA Laboratories, Somerset UK). FAD medium consisted of DMEM (4.5 g/L glutamine): F12 (Ham's F12 nutrient mixture; Gibco Invitrogen) in 3:1 ratio with 10% (v/v) FBS (FirstLink, Birmingham UK) and various mitogens (0.4 μg/ml hydrocortisone, 0.1 nM cholera toxin, 5 μg/ml transferrin, 20 pM lyothryonine, 0.18 mM adenine, 5μg/ml insulin and 10 ng/ml EGF; mitogens were either bought from Sigma Aldrich, Dorset UK, or were kindly provided by Prof. Mike Philpott from the Centre for Cutaneous Research at ICMS). All cells were plated in 6 cm dishes containing pre-plated 3T3 feeder layers (for feeder layer preparation see **section 2.2.1**). FAD medium was replaced 72 hours later with FAD medium containing only 1% penicillin/streptomycin and FAD medium was changed every other day thereafter. The first keratinocyte colonies became visible 4-6 days after

plating. Keratinocytes were let to grow to around 80% confluence prior to cryopreservation in freezing medium consisting of 10% (v/v) DMSO (Sigma Aldrich) 90% (v/v) FBS (FirstLink, Birmingham, UK). Keratinocyte population doublings were marked 0 at this point and all experiments were carried out with keratinocytes from the frozen stocks.

2.1.2 Primary Normal Human Keratinocyte Culture

Upon recovery from liquid nitrogen, keratinocytes were grown either in FAD medium in the presence of 3T3 feeders or in serum free media (K-SFM; Gibco Invitrogen) supplemented with 25 μg/ml of bovine pituitary extract (BPE) (Gibco Invitrogen), 0.2 ng/ml of epidermal growth factor (EGF) (Gibco Invitrogen) and either low or high concentrations of calcium (0.09 mM or 0.4 mM $CaCl_2$ respectively) (Rheinwald et al., 2002). Keratinocytes were passaged once they reached 60-70% confluence when grown in FAD + 3T3 feeder layer co-culture or at 40-50% confluence when grown in serum free conditions. All cells were grown at 37^{o}C in a humidified atmosphere of 10% (serum containing media) or 5% (serum-free media) CO_2/95% air. In order to obtain a pure keratinocyte population when growing keratinocytes in a 3T3 feeder co-culture system, the 3T3 feeder layer needs to be thoroughly removed. Cells were initially washed 1x in PBS and were then incubated at 37^{o}C for 10 minutes in the presence of versene (0.2 g/L EDTA-4Na in phosphate-buffered saline; Gibco Invitrogen). Next, versene solution containing any detached feeders was replaced with PBS. Any remaining feeders were removed by thorough and repeated pipetting, until only keratinocyte colonies were visible under the microscope. Then, keratinocytes were tyrpsinised in the presence of Trypsin/EDTA solution (0.5 g/L of trypsin and 0.2 g/L of EDTA•4Na in Hanks' Balanced Salt Solution without $CaCl_2$, $MgCl_2 \cdot 6H_2O$, and $MgSO_4 \cdot 7H_2O$) (Gibco Invitrogen) for at least 15 minutes, until a single cell suspension of keratinocytes was obtained. Cells were then recovered in serum containing media, spun at 140 x g for 5 minutes, and finally resuspended in FAD complete medium before plating. For keratinocytes growing in serum-free media, feeder layer free conditions, versene treatment and feeder removal steps were omitted. Keratinocytes were

typically plated at a density of $5x10^3/cm^2$ and were let to grow for an average of 5-6 days upon which time they have reached 60-80% confluence.

2.1.3 Cell Line Culture

N/TERT-1 (N/TERT) keratinocytes are derived from clinically normal foreskin tissue and are further immortalised by the addition of ectopic telomerase, followed by spontaneous downregulation/loss of p16INK4a (Dickson et al., 2000). N/TERT keratinocytes were cultured in K-SFM (Gibco Invitrogen) medium. SVpgC2a oral premalignant cell line is derived from normal oral keratinocytes that have been immortalised by ectopic expression of SV40-T antigen (Kulkarni et al., 1995). SVpgC2a keratinocytes were grown in serum free EpiLife medium (Cascade Biologics, Paisley UK) (0.04 mM $CaCl_2$) containing human keratinocyte growth supplements (HKGS; Cascade Biologics). Normal human telomerase-immortalised oral keratinocytes OKF6/T (Dickson et al., 2000) were grown in K-SFM medium. Oral premalignant cell lines POE9n-hTERT (Rheinwald et al., 2002), POE9n (Rheinwald et al., 2002), DOK (Chang et al., 1992; Munro et al., 1999), D19 (McGregor et al., 2002), D20 (McGregor et al., 2002) and primary head and neck cancer derived cell lines CA1 and UK1 (Harper et al., 2007), CaLH2 (Harper et al., 2007), CaLH3 (Harper et al., 2007), CaDec11, CaDec12, H357 (Prime et al., 1990), 5PT (Mackenzie, 2004), PE/CA-PJ15, and Vb6 (Harper et al., 2007), were kindly provided by Prof. Ian MacKenzie (ICMS, Centre of Cutaneous Research, Queen Mary University of London). BICR31 (Loughran et al., 1997), SCC4, SCC9, SCC15, and SCC25 (Rheinwald and Beckett, 1981) cell lines were kindly provided by Prof. Ken Parkinson (Clinical and Diagnostic Oral Sciences, Queen Mary University of London). Detailed information on the keratinocyte cell lines used herein, are displayed in **Table 2.1**. Normal human oral and NIH3T3 fibroblasts (kindly provided by Prof. Ken Parkinson), Phoenix amphotropic (PhxA) (human embryonic 293T derived; supplied by Nolan Lab (Medical Centre, Stanford University Medical School, CA), and HeLa cells were all grown in DMEM (Lonza) with 10% FBS (FirstLink) and 1% penicillin/streptomycin (Gibco Invitrogen). All cells were grown at 37 ^oC in a humidified atmosphere of 10% (serum containing media) or 5% (serum-free media) CO_2/95% air. All cell lines were cultured

and passaged according to the aforementioned conditions (see **section 2.1.2**) that apply for primary human keratinocytes, omitting the feeder preparation/removal steps, unless needed (SCC15).

Table 2.1: Cell lines origin and culture conditions

**N/A: Not Available *GF: Growth Factors*

Cell Line	Origin	Genetic Modification	Known Abnormalities	Culture Medium	Cell Line References
5PT	HNSCC	None	N/A	K-SFM	(Mackenzie, 2004)
BICR31	Advanced non metastasized HNSCC	None	CDKN2A locus deletion, p53 mutation	FAD	(Loughran et al., 1997)
CA1	HNSCC	None	N/A	K-SFM	(Harper et al., 2007)
CaDec11	HNSCC	None	N/A	FAD	-
CaDec12	HNSCC	None	N/A	FAD	-
CaLH2	HNSCC	None	N/A	FAD	(Harper et al., 2007)
CaLH3	HNSCC	None	N/A	FAD	(Harper et al., 2007)
D19	Erythroplakia derived keratinocytes from lateral tongue	None	p16INK4a downregulation	FAD	(McGregor et al., 2002)
D20	Severely dysplastic oral epithelium from lateral tongue	None	p16INK4a downregulation	K-SFM	(McGregor et al., 2002)
DOK	Dysplastic Oral Epithelium of the tongue	None	p16INK4a and p53 mutation, aneuploid	K-SFM	(Chang et al., 1992; Munro et al., 1999)
H357	HNSCC	None	N/A	K-SFM	(Prime et al., 1990)
N/TERT	Newborn foreskin	hTERT	p16INK4a downregulation	K-SFM	(Dickson et al., 2000)
PE/CA-PJ15	Human Tongue SCC	None	N/A	FAD	(Kulasekara et al., 2009)
OKF6/T	Normal buccal mucosa	hTERT	p16INK4a downregulation	K-SFM	(Rheinwald et al., 2002)

Cell Line	Origin	Genetic modification	Abnormalities (known)	Culture Medium	Cell Line References
POE9n	Pre-malignant dysplastic oral epithelial lesion	None	CDKN2A/INK4a deletion, p53 expression loss	K-SFM	(Rheinwald et al., 2002)
POE9n-hTERT	Premalignant dysplastic oral epithelial lesion	hTERT	CDKN2A/INK4a deletion, p53 expression loss	K-SFM	(Rheinwald et al., 2002)
SCC4	Tongue squamous cell carcinoma	None	N/A	FAD	(Rheinwald and Beckett, 1981)
SCC9	Tongue squamous cell carcinoma	None	N/A	FAD	(Rheinwald and Beckett, 1981)
SCC15	Tongue squamous cell carcinoma	None	p16 promoter methylation	FAD on 3T3 feeder layer	(Rheinwald and Beckett, 1981)
SCC25	Tongue squamous cell carcinoma	None	N/A	FAD	(Rheinwald and Beckett, 1981)
SVpgC2a	Normal buccal mucosa	SV40-T	Aneuploid, partially resistant to GF	EpiLife	(Kulkarni et al., 1995)
UK1	Head and Neck SCC	None	N/A	FAD	(Harper et al., 2007)
VB6	H357 derived subclone	Integrin $a_v\beta6$	N/A	FAD	(Harper et al., 2007)

2.2 Cell Treatments

2.2.1 Feeder Layer Preparations

Feeder layers were prepared by treating NIH3T3 fibroblasts with Mitomycin C to induce replication arrest. Although arrested, cells still retain the abilities of cell to matrix and cell-cell adhesion, and extracellular protein production, which are necessary for the initial growth phases of primary human keratinocytes when grown in high calcium, serum-containing media. NIH3T3 feeder layers were prepared by treating confluent NIH3T3 cultures in DMEM (Lonza) with 10% FBS (FirstLink) and 1% penicillin/streptomycin (Gibco Invitrogen) in the presence of 10 μg/ml mitomycin C (Sigma Aldrich) for 4 hours at 37^{o}C in a humidified atmosphere of 10%CO_2/90% air. Mitomycin C-treated NIH3T3 were plated at a density of $1.8x10^4/cm^2$, 24 hours prior to

keratinocyte plating. PhxA cells were also used as feeder layers for retroviral transduction experiments (see **section 2.3.3.2**). PhxA cells were prepared by treating confluent PhxA cultures in DMEM with 10% FBS and 1% penicillin/streptomycin in the presence of 2 μg/ml mitomycin C for 2 hours at 37^{o}C in a humidified atmosphere of 10%CO_2/90% air. Treated PhxA cells were then plated at a density of $1.1x10^5/cm^2$.

2.2.2 Cell Cycle Synchronization

To synchronize N/TERT and HeLa cells at G1/S phase by double thymidine block, $2x10^5$ cells were plated in 6 cm dishes. When cells reached 40-50% confluence, 2 mM thymidine (Sigma Aldrich) was added and cells were incubated for 16 hours. Cells were then washed twice with PBS and grown in complete medium for another 9 hours. Thereafter, cells were treated again with 2 mM thymidine (Sigma Aldrich) for another 12-16 hours. Release from the second thymidine block was performed by washing twice with PBS and replacing with complete growth medium, and cells were harvested at indicated time points.

2.2.3 Proteasome Inhibitor (MG132) Treatments

Semi-confluent cultures were treated with MG132 (Sigma Aldrich) (10^{-6}M for 24 hours), or vehicle control (0.001% DMSO; Sigma Aldrich), for 24 hours prior to harvesting.

2.2.4 Oral Carcinogens Treatment

Nicotine (Nicotine Hemisulfate salt; Sigma N-1019, Dorset UK) treatment of oral keratinocytes (NHOK or SVpgC2a) was performed by treating semi-confluent keratinocyte cultures in serum-free conditions with various concentrations of nicotine as mentioned. Nicotine dilutions were prepared in double-distilled sterile H_2O (ddH_2O) (Barnstead Nanopure, ThermoScientific, Cambridgeshire UK). Control treatments consisted of the same volume of double distilled sterile ddH_2O alone.

2.3 Retrovirus Mediated Gene Transfer

2.3.1 Retroviral Vectors

Retrovirus mediated gene transfer represents one of the most efficient methods (a minimum of 87% was achieved in this study) for inducing long-term, stable gene expression in human keratinocytes, since simple plasmid transfection methods are particularly ineffective in this cell type. Retroviral vectors are used to induce the expression of a specific protein in keratinocytes. In this study, replication incompetent retroviral vectors have been used to allow a one-time infection of target cells and to minimize safety hazards that may arise from continuous spreading of replication competent retroviruses. This is achieved by removal of viral packaging genes from the retroviral backbone, therefore incapacitating the self-replication machinery of retroviral vectors. The viral packaging proteins that are needed for retrovirus production are provided *in trans* by retrovirus packaging cell systems (e.g. Phoenix Cells) (**Figure 2.1**). In this study, p**SIN** (**S**elf **In**activating) vectors were employed (**Figure 2.1**) (Deng et al., 1997; Teh et al., 2002). These vectors were constructed by deleting the enhancer and the promoter in the U3 region of the 3' LTR (**L**ong **T**erminal **R**epeat) thereby abolishing any transcriptional activity driven by the LTR so that no full-length vector RNA is produced in transduced cells. After the first round of replication, the changes are copied into both the 5' and 3' ends of LTRs, and therefore gene expression is only driven by the internal CMV promoter.

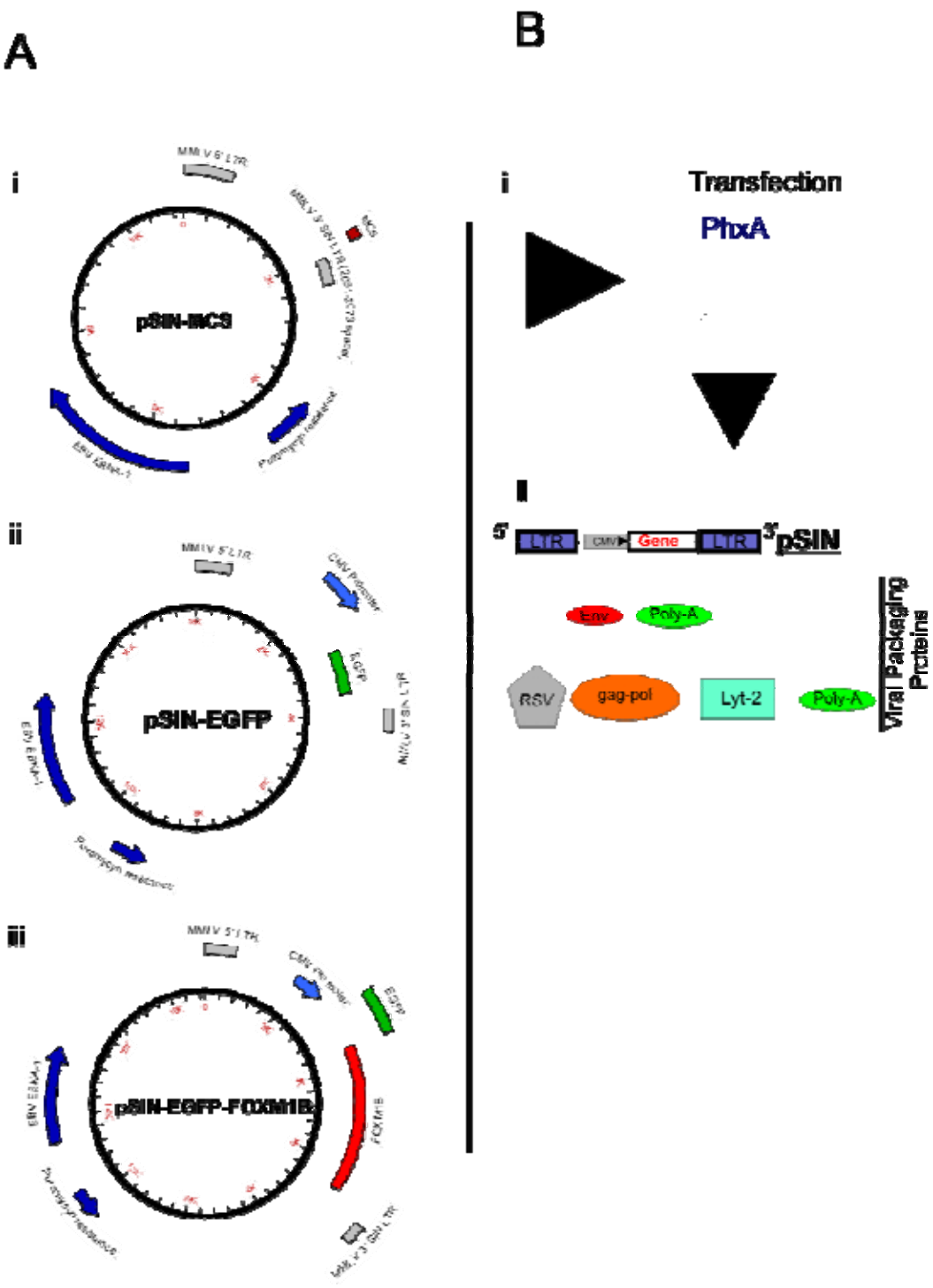

Figure 2.1: Retroviral Vectors, Packaging and Viral Particle Production.

(A) pSIN retroviral vector constructs are shown. pSIN-MCS **(i)** contains a multiple cloning site, but it lacks a promoter or a gene. pSIN-EGFP **(ii)** and pSIN-EGFP-FOXM1B **(iii)** contain genes driven by an internal CMV promoter. **(B)** Upon transfection of retroviral vectors **(i)** in PhxA packaging cells, retroviral packaging is initiated by the presence of retroviral packaging proteins **(ii)** that are stably expressed by PhxA cells.

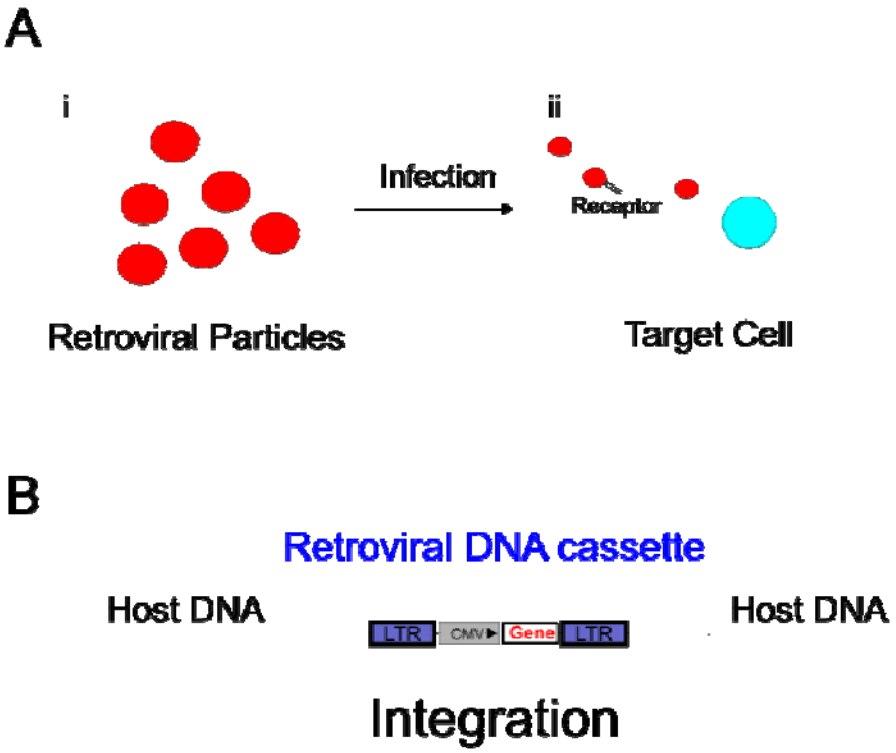

Figure 2.2: Retroviral Transduction

(A) Following viral packaging, retroviral particles are released from PhxA cells into the growth medium. Upon collection, retroviral particles are then used to infect target cells, which recognize the amphotropic cell surface molecules of the retroviruses. **(B)** Once the retrovirus enters the cell, it begins its life cycle. Retroviral integrase cleaves the host genomic DNA and integrates the retroviral DNA cassette into the host's genome. The expression of the gene of interest is thereafter being driven by the presence of the internal CMV promoter.

2.3.2 Retrovirus Production

For the production of retroviral particles containing the genes of interest, the retroviral producer cell line PhoenixA (PhxA) was used. PhxA cell line was created by stable trasfection of 293T cells with constructs expressing gag-pol, and envelope proteins for ecotropic and amphotropic viruses (supplied by Nolan Lab, Medical Centre, Stanford University Medical School, CA). PhxA (amphotropic) were used for the production of amphotropic retroviruses bearing the MCS (empty), CMV-EGFP or CMV-EGFP-FOXM1B transgene. For retrovirus production, PhxA packaging cells were plated in 10 cm dishes and were transfected with 10 µg of viral plasmid DNA using FuGENE 6 reagent (Roche, Hertfordshire UK) in a 1:2 DNA: FuGENE ratio. Transfected PhxA cells were incubated for 48 hours and then sub-cultured in selection

medium consisting of DMEM (Lonza) with 10% FBS (FirstLink) and puromycin (3μg/ml) (Sigma Aldrich). Cells were maintained in selection medium for 1 week, after which they were incubated overnight at 32^{o}C in complete normal growth medium without puromycin. Retroviral supernatants were collected the next day and were thereafter collected once daily for 2-3 days post-confluent. Upon collection, retroviral supernatants were spun at high speed centrifugation at 871 x g for 10 minutes to remove any non-adherent PhxA cells present in the medium. Retroviral supernatants were then snap-frozen in liquid nitrogen before being stored at -80^{o}C until use.

2.3.3 Retroviral Supernatant Quantification and Titration

The retroviral titre can vary significantly between retrovirus preparations, mainly depending upon the nature of the retroviral vector (i.e. gene of interest may be affecting the survival of PhxA cells), as well as on the culture and selection methods. Therefore, titration of the retroviral supernatant is important to achieve equal transduction efficiencies in target cells. Titration of the retroviral supernatant can be achieved by direct quantification of a retrovirus specific component present in the retroviral supernatant (detailed protocols below). Also, transduction efficiency can be directly assessed by absolute quantification of the incorporated transgene within the host genomic DNA (gDNA) (i.e. EGFP copy number) in the target cells immediately after transduction (shown in results **section 2.3.4**). Herein, both techniques were used to ensure that target cells receive equal number of the transgene.

2.3.3.1 Retrovirus Purification and Viral Titre Quantification

Retroviral supernatants (RVSN) containing pSIN-EGFP or pSIN-EGFP-FOXM1B were collected as described in **section 2.3.2**. The protocol used to quantify retroviral vector titres is a modified version of the protocol described in Sanburn and Cornetta, 1999 (Sanburn and Cornetta, 1999). A volume of 300 μl of RVSN was added in a mixture of 900 μl TriZol (Roche Diagnostics Ltd, England, UK) with 10 μg tRNA carrier (Sigma Aldrich) and 240 μl chloroform. The mixture was then vortexed for 30 seconds, incubated at room temperature for 10 minutes and then spun at 8,000 x g at room temperature in a table-top centrifuge. The aqueous layer was isolated and retroviral genome

RNA was precipitated with 600 µl isopropanol, followed by centrifugation at 8,000 xg for 10 minutes. The dried pellet was resuspended in reverse transcription mixture (Promega; detailed in s**ection 2**.**7**) containing only EGFP specific primers (1µM) and was incubated at 42^{o}C for 1 hour, followed by 5 minutes at 85^{o}C. Then, 2 µl of the resultant cDNA was used in SYBR 1 Master Mix (Roche) reaction (detailed in **section 2.8**) with 5 µM EGFP primers and reaction mix was run using a standard qRT-PCR protocol (see **section 2.8**).

2.3.4 Retroviral Transduction of Human Keratinocytes

2.3.4.1 Retroviral Transduction in Serum-Free Conditions

Cells to be infected were plated at a density of 7.5x10^{4}/cm^{2}. The next day, cells were incubated for 15 minutes in the presence of polybrene (hexadimethrine bromide) (5 µg/ml; Sigma Aldrich) prior to adding retroviral supernatant containing equal concentrations of polybrene. Cells were then spun at 14 x g for 1 hour at 32^{o}C, washed twice in PBS and finally incubated for 48-72 hours in normal growth medium prior to any experiments.

2.3.4.2 Retroviral Transduction in Feeder-Layer System

To infect NHOKs in a feeder layer system, keratinocytes were co-cultured with Mitomycin C-treated 3T3 and transfected/selected PhxA cells. Initially, mitomycin C-treated 3T3 feeder cells were plated at a density of 5x10^{3}/cm^{2}. The next day, NHOKs were seeded at a density of 1.9x10^{3}/cm^{2}. For flow sorted keratinocytes, a cell density of 54–1000 cells /cm^{2} was used instead. Two hours after keratinocyte plating, mitomycin C-treated PhxA cells were plated on top at a density of 1.1x10^{5}/cm^{2} and polybrene was added at a final concentration of 5 µg/ml (Day 0 of retroviral transduction). Normal growth medium (FAD), without polybrene, was replaced the next day (Day 2 of retroviral transduction). Next, (Day 3) PhxA-3T3 feeder layer was gently removed with PBS and freshly prepared mitomycin C-treated 3T3 feeders were added at a density of 1.8x10^{4}/cm^{2}.

2.3.5 Optimization of Retroviral Gene Delivery

Retrovirus-mediated gene transfer has proven to be an invaluable tool for fast and stable gene delivery on a wide range of mammalian cell types. However, there are certain factors to be considered when employing such a method. These include the determination of the retroviral titre and transduction efficiency, both of which are critical factors for successful gene integration and stable transgene expression.

Transgene incorporation is a random event whereby exogenous genes are integrated in arbitrary positions of the host genome. Depending upon the retroviral titre and transduction efficiency, multiple copies of the viral transgene may be introduced in each host cell genome. The ratio of viral particles to target cells is called multiplicity of infection (MOI), and can influence the extent of transgene expression and the genomic stability of the host. It has been reported that MOI of 15 in human keratinocytes is able to induce long-term gene delivery with strong transgene expression, without the need for further selection (Robbins et al., 2001; Lazarov et al., 2002).

In this study I used pSIN (**S**elf-**IN**activating) retroviral constructs bearing EGFP or EGFP-FOXM1B expression cassettes for stable gene delivery in human keratinocytes. Expression of both transgenes is driven by the CMV promoter. In order to achieve maximum transduction efficiency, N/TERT cells were subjected to low speed centrifugation in the presence of different concentrations of the retroviral supernatant, and were allowed to express the transgenes for 72 hours (**Figure 2.3 A**). Fluorescence microscopy showed that protein expression correlated with retrovirus concentration, indicated by both fluorescence intensity and the percentage of transduced cells (**Figure 2.3 B**). However, fluorescence intensity is not an accurate marker for the quantitation of transgene incorporation because the gene of interest may be subjected to post-transcriptional and post-translational modifications. In order to directly quantify the absolute copy number of transgenes incorporated in our target cells, qPCR was employed. Genomic DNA was extracted 72 hours post-transduction and the copy number of EGFP transgene was quantified by

qPCR, using primers that would detect either EGFP alone (control cells) or EGFP fused with FOXM1B (**Figure 2.3 A**).

Initial experiments showed that EGFP retroviral transduction was at least 10-fold more efficient when compared to EGFP-FOXM1B. Thus, EGFP retroviral supernatant preparation was further diluted before achieving comparable transduction levels for both transgenes. This could have been both a result of higher concentrations of retroviral particles in the EGFP supernatant, or due to favourable incorporation of a smaller sized transgene. Genomic EGFP copy number shows a dose-dependent relationship with increasing concentration of retrovirus in both EGFP and EGFP-FOXM1B transduced cells (**Figure 2.3 B, C**). Linear regression analysis showed a highly significant (R^2>0.96) positive correlation between retroviral concentration and genome EGFP copy number per 10ng of gDNA (**Figure 2.3 D**). In order to achieve equal transgene copy number incorporation of both EGFP and EGFP-FOXM1B into host cells, the appropriate volume of retroviral supernatant was calculated based on the respective regression analyses. Assuming that each cell contains ~6.5pg of DNA (Dole et al., 2003), and according to results shown in **Figure 2.3 C**, where a maximum of $2.5x10^4$ EGFP transgenes are detected in 10ng of gDNA (~1000 cells), is can be deduced that by using this retroviral transduction method each cells could receive up to ~16 copies of each transgene. All subsequent experiments were carried out using appropriate retroviral concentration to achieve an incorporation rate of ~10 copies/cell.

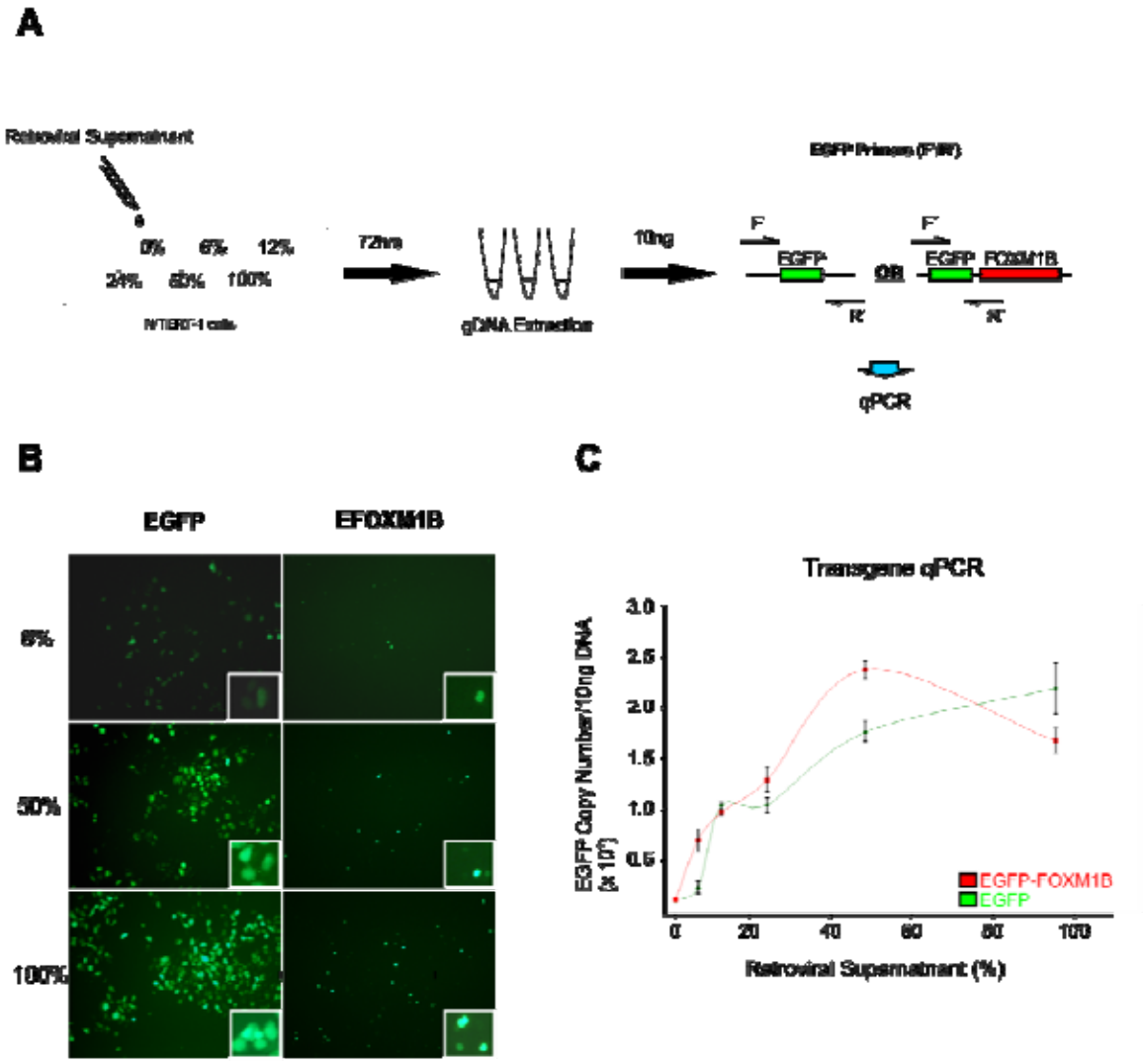

Figure 2.3: Optimization of retroviral gene delivery.

(A) N/TERT human keratinocytes were transduced with various concentrations of retroviral supernatant and gDNA was extracted after 72 hours. qPCR was performed on 10ng of DNA using EGFP specific primers. **(B)** Fluorescent microscopy indicated that transgene expression was directly related to retrovirus concentration. Inset images show the intracellular localization of EGFP and EGFP-FOXM1B protein distributions in transduced N/TERT keratinocytes. **(C)** Quantification of EGFP or EGFP-FOXM1B transgenes copy number in N/TERT human keratinocytes.

2.4 Cell Counting and Clonogenic Assays

Cell number and density were determined using CAsy® Cell Counter (Innovatis, Sittingbourne UK). Each sample was prepared three times in CAsyTon® (Innovatis) buffer and triplicate measurements of 200 µl sample volume were taken each time. Viable cells were measured by excluding cells smaller that 10 µm in size. Keratinocyte population doublings were calculated

as follows: **PD** = *3.32* * [$\log_{10}$ (N1) – $\log_{10}$ (N0)] where N1 = total yield and N0 = initial number of seeded keratinocytes. Clonogenicity percentages were determined by the percentage of initial keratinocytes plated that were able to form visible colonies after 12 days in culture. For colony forming assays, keratinocyte cultures were washed once with PBS and were fixed in 4% (v/v) formaldehyde (Sigma Aldrich) in PBS for 20 minutes at room temperature. Then, cells were washed 1x with PBS and stained with 1% Rhodamine B (Sigma) in PBS for 30 minutes at room temperature. Bright field images of Rhodamine B-stained dishes were digitally captured (AutoChemi imaging system (UVP, Upland, CA). Colony area coverage measurements were performed using Adobe Photoshop CS4 and CorelDraw X by using the quick selection tool with a constant hardness value among samples to acquire quantitative pixel counts. To measure the relative surface areas covered by each keratinocyte clone, a well of a 6-well plate was selected, and its pixel count was assigned as being representative of 35mm^2. Therefore, the actual surface area (mm^2) of each individual keratinocyte clone was deduced from its pixel count value relative to that of a 35mm^2 well (Zhu and Watt, 1999).

2.5 Organotypic Culture on De-Epidermalized Dermis (DED)

A three-dimension *in vitro* functional reconstruction of oral mucosa epithelum can be achieved by organotypic cultures of primary oral keratinocytes and fibroblasts on DED. This allows a better representation of the *in vivo* situation, compared to monolayer culture models. Organotypic cultures of oral mucosa show histological and immunohistochemical characteristics very close to that of normal oral mucosa (Ophof et al., 2002; Moharamzadeh et al., 2007). The procedure entails the culture of primary fibroblasts, preferentially derived from the tissue of interest (i.e. oral mucosal fibroblasts), within the reticular side of the DED. After fibroblasts are established and have migrated within the DED (usually within 24 hours), oral keratinocytes are placed on the papillary (epidermal) side of the DED which where then allowed to grow for an initial period of 24-48 hours. After this stage, the organotypic rafts are raised to the air-liquid interface to allow keratinocyte differentiation and the induction of

tissue keratinisation. This allows functional investigation of epithelial differentiation patterns, in the presence or absence of exogenous factors (i.e. forced expression or suppression of target genes of interest). Herein, primary human oral keratinocytes were genetically manipulated (pSIN-MCS, pSIN-EGFP, pSIN-EGFP-FOXM1B) as described above, and were cultured on DEDs, in the presence of primary normal human oral fibroblasts. (**Figure 2.4**)

2.5.1 Organotypic Culture Protocol

Glycerol preserved human donor skin (Euro Skin Bank, Beverwijk, the Netherlands) was initiated by thoroughly washing in PBS and incubated at 37^{o}C at 10%CO_2/90% air in PBS with 1% antibiotic-antimycotic Solution (PAA Laboratories, Somerset UK) for 14 days. The epidermis was then mechanically removed by using sterile forceps and scalpel, and the de-epidermalised dermis (DED) was cut in 1.5x1.5cm squares. At day 0, $5x10^5$ primary human oral fibroblasts were seeded in the reticular, and were allowed to grow for 24 hours. On day 1, $5x10^5$ primary human oral keratinocytes (pSINMCS, pSINEGFP, pSINEGFP_FOXM1B) were seeded on the papillary surface, and were allowed to grow for 48hrs. On day 3, the DEDs were washed once in PBS and were gently cut in half, across the centre of the ring shaped region where keratinocytes were initially seeded during day 1. The organotypic rafts were then raised at the air-liquid interface by placing them on top of 1 cm high stainless steel grids within wells of a 6-well plate. The organotypic rafts were allowed to grow for 2-4 weeks and were refed every 48 hours with FAD medium. Each of the identical pieces of the organotypic raft was then fixed in either 4% (vol/vol) formaldehyde (Sigma Aldrich) in PBS overnight at 4^{o}C for paraffin embedding processing, or was embedded in mounting medium (Thermo Fisher Scientific, Loughborogh, UK) for frozen sectioning. Paraffin embedding was carried out in the facilities of Centre for Cutaneous Research, ICMS by Dr. Wesley Harrison. Both paraffin and frozen processed tissue sections were cut at 4 μm thickness at the pathology core facility (Bart's and the London School of Medicine and Dentistry, ICMS).

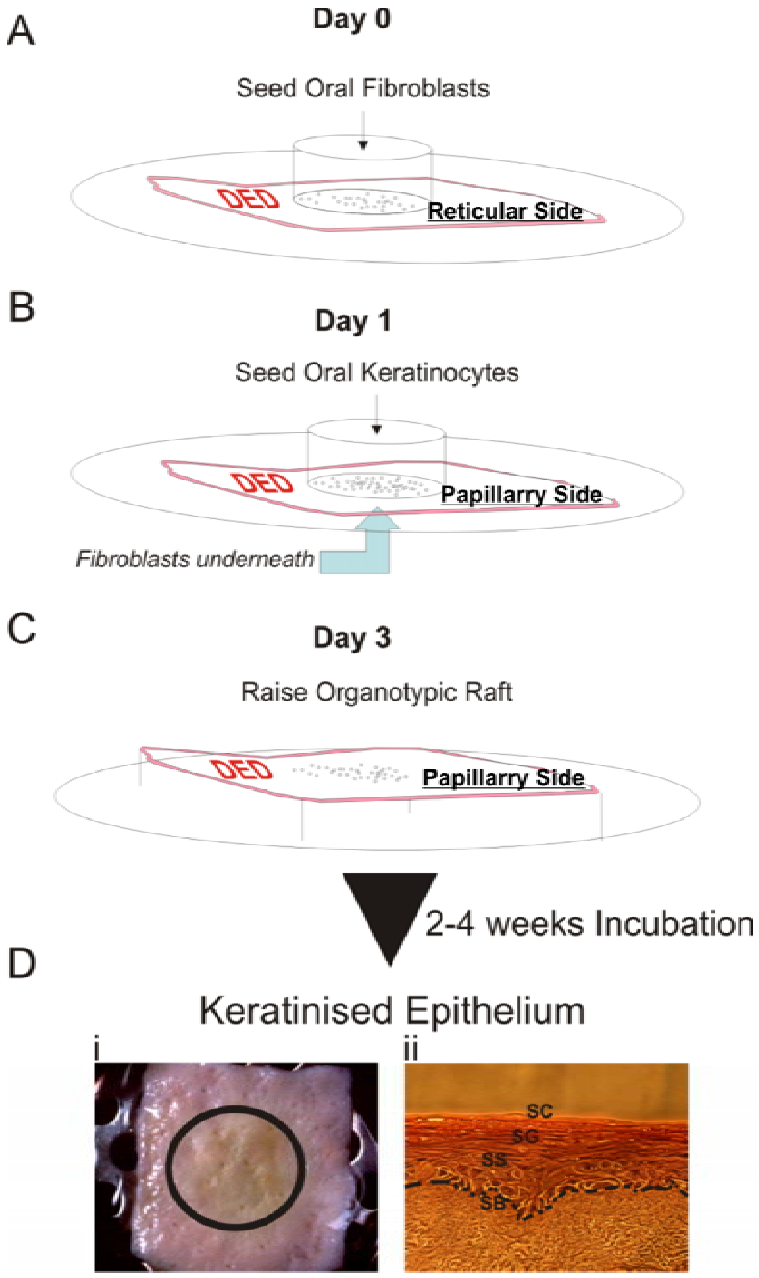

Figure 2.4: Organotypic Three Dimensional Reconstruction of Oral Mucosa

(A) De-epidermalised dermis (DED) is positioned with the papillary (dermal) surface facing up, and human primary oral fibroblasts are seeded within stainless steel rings placed onto the DED as shown in the diagram. **(B)** After 24 hours, the DED is reversed, to expose the reticular side (epidermal), where primary human keratinocytes are seeded. **(C)** Following 48 hours incubation, stainless steel rings are removed, and the DED is raised to air-liquid interface to allow epithelial keratinisation for the next 2-4 weeks. **(D)** A visible opaque cell layer **(i)** of keratinized epithelium is visible macroscopically. *Image source (Di)* (Moharamzadeh et al., 2007). Histological H&E staining shows that all epithelial layers are present the in organotypic tissue sections indicating a functional reconstruction of oral mucosa epithelium **(ii). SB**=stratum basale, **SS**=stratum spinosum, **SG**=stratum granulosum, **SC**=stratum corneum.

2.6 RNA extraction from cultured cells

2.6.1 Total RNA Extraction

Total RNA was extracted from cells using RNeasy Mini Kit (Qiagen, West Sussex UK). Semi-confluent cultures were harvested in 350 µl of RLT lysis buffer containing 10 µl/ml β-mercaptoethanol (β-ME) (Sigma Aldrich). Next, cell lysates were collected in eppendorf tubes before being snap frozen in dry ice. Cell lysates were either kept at -80^{o}C for long-term storage or processed immediately. cell lysates were homogenized by passing them through QIAshredder columns (Qiagen) and centrifuged at 14,000 x g for 2 minutes. Next, 70% ethanol was added to precipitation RNA. RNA was captured in RNA spin columns (Qiagen) by centrifugation for 15 seconds at 8,000 x g, and then columns were rinsed with RW1 buffer, and washed twice in RPE buffer. RNA was finally eluted in 20-30 µl of RNAse free water (Qiagen) and RNA concentration was measured with NanoDrop^{TM} ND-1000 (ThermoScientific, Cambridgeshire UK).

2.6.2 Direct mRNA Extraction

PolyA^{+} tail mRNA was extracted using Dynabeads$^{®}$Oligo(dT)$_{25}$ (Invitrogen, Paisley UK) according to manufacturer's instructions. Briefly, semi-confluent cultures were lysed in 0.5-1 ml of RNA Lysis/Binding Buffer (100 mM Tris-HCL, pH 7.5, 500mM LiCl, 10mM EDTA, 1% LiDS, 5mM dithiothreitol (DTT)) (Invitrogen) and stored at -80^{o}C or were processed immediately. Upon processing 30 µl of Dynabeads®Oligo(dT)$_{25}$ were added to RNA lysates and were rotated for 15 minutes at room temperature. RNA lysates were attached to Ambion® 6 Tube Magnetic Stand and Dynabeads®Oligo(dT)$_{25}$ magnetic beads were concentrated at the back of each eppendorf tube. Supernatant was removed, tubes were released from the magnetic stand and the beads were washed with 1 ml of Washing Buffer A (10mM Tris-HCl, pH 7.5, 0.15M LiCl, 1mM EDTA, 0.1% LiDS) (Invitrogen), then the procedure was repeated and beads were re-washed in 0.8 ml Washing Buffer B (10 mM Tris-HCl, pH 7.5, 0.15M LiCl, 1mM EDTA) (Invitrogen). Supernatant was again removed and beads were finally resuspended in 10 µl of 10 mM Tris-HCl, pH 7.5. Resuspended beads were incubated for 2 minutes at 80^{o}C to release mRNA, and tubes were immediately returned to the magnetic stand to minimize re-

annealing of mRNA to beads. mRNA in the supernatant was immediately used in reverse transcription reaction described below. (**section 2.2.7**)

2.7 Reverse Transcription

Purified RNA (1-2 µg of total RNA, as described in **section 2.6.1** or 10 µl mRNA in Tris-HCL, as described in **section 2.6.2**) was reverse transcribed into cDNA with the Reverse Transcription Kit (Promega, Hampshire UK) with slight modifications to manufacturer's protocol. A typical reverse transcription reaction to convert 1 µg of total RNA contained the following (all reagents were supplied with Reverse Transcription Kit from Promega, Hampshire UK):

$MgCl_2$	5 µl
10x Reverse Transcription Buffer	2.5 µl
10mM dNTPs	2.5 µl
Oligo(dT) Primers	0.5 µl
Random Primers	0.5 µl
RNAsin®	0.5 µl
AMVRT (10units/ul)	0.75 µl
RNA*	10 µl (1µg; 100 ng/µl RNA)
Total	**25 ± 0.25 µl**

**** For more than 1µg of RNA, the reaction volume was increased accordingly***

The mixture was incubated for 10 minutes at room temperature before incubating at 42°C for 30 minutes, followed by reverse transcriptase inactivation at 85°C for 5 minutes. Finally, RT mix was diluted (1:3) with 50 µl of molecular biology grade H_2O (Sigma Aldrich) before being used in downstream PCR applications.

2.8 Real-Time Absolute Quantitative PCR (qRT-PCR)

Real-time absolute quantitative Real Time-PCR (qRT-PCR) was performed using Light Cycler® 480 SYBR green I Master (Roche Diagnostics Ltd, England, UK) (hot-start Taq polymerase master mix) with a standard final concentration of 0.5 µM for each primer in the LightCycler® 480 qPCR system (Roche). SYBR green I Master contained $5x10^{-6}$ % Bromophenol blue (Sigma

Aldrich) to visually assist with sample loading in Roche qPCR 96-well white opaque plates (Roche).

2.8.1 Generation of Standard Curves

To acquire a standard curve for each gene, each primer pair was initially mixed with SYBR green I Master and a template cDNA (cocktail from a wide range of normal and HNSCC derived keratinocytes) in the following reaction mixture.

SYBRI	20 µl
H_2O	20 µl
Template cDNA	5 µl
5µM F/R Primer	7 µl
Total	**50 ± 2 µl**

The above qRT-PCR reactions were run in LightCycler 480 qPCR system on a typical amplification protocol that included denaturation at 95°C for 10 min, followed by 45 cycles of 95°C for 10 s, 60°C annealing for 6 s, and 72°C elongation (incubation time depends on the length of the product; 1 s/25 base pairs). Fluorescence readings were acquired at 75^{o}C following the elongation step. At the end of the 45 cycles, samples were subjected to a melting analysis to confirm amplification specificity of the PCR products. Single product amplification was also visualized on AutoChemi imaging system (UVP, Upland, CA) after separation of DNA products in 2% Agarose (Sigma Aldrich) gels stained with 0.5µg/ml Ethidium Bromide (Sigma Aldrich). Amplified templates were then purified using Qiagen PCR Purification kit (Qiagen) according to manufacturer's instructions. Amplified products were mixed with 5x volume (i.e. 50 µl PCR product + 250 µl) of PB buffer (Qiagen) and then placed in a Qiagen spin column and were spun at 14,000 x g on a table top centrifuge for 1 minute, and elute was discarded. Columns were washed once in 500 µl PE buffer (Qiagen) before centrifugation at 14,000 x g for 1 minute. Finally, Qiagen spin columns were spun at 14,000 x g to completely dry the filter. Purified PCR products were eluted in 20-30 µl of dH_2O, and concentrations were measured using NanoDrop (ThermoScientific, Wilmington USA). DNA concentrations were used to calculate the absolute copy number of amplified products, based on the Avogadro principle, as

follows: Total Copy number (x) = $6.02x10^{14}$ / basepair (nt) x (660) x DNA concentration. Serial 10-fold dilutions (10^2 – 10^7 cDNA copies) of the amplified products were prepared in tRNA carrier (5 µg/ml) (Sigma Aldrich). A qRT-PCR run was prepared, using a dilution series range of 10^2-10^7 for each gene. A single qRT-PCR reaction was prepared as follows:

SYBRI	4 µl
Template cDNA	2 µl
5µM F/R Primer	1 µl
H_2O	4.5µl
Total	**10 ± 1.5 µl**

Samples were run on a typical PCR amplification protocol as mentioned above. Standard curves for each given gene were thus calculated by the LightCycler® 480 qPCR software program, and were thereafter used for absolute copy number quantitative PCR.

2.8.2 Gene Amplification by qRT-PCR

A panel of 8 human reference genes (*HPRT1, UBC, GAPDH, RPLP0, ESD, 18SRNA, POLR2A and YAP1*) were initially tested on a panel of human oral tissues used in this study (including normal gingival mucosa, normal buccal mucosa, normal tongue, dysplasias and HNSCC tissues), and keratinocyte cell types (including both primary and cell lines). Using the GeNorm algorithm analysis method (Vandesompele et al., 2002) and the LightCycler 480 Relative Quantification Software (with built-in multiple reference genes normalisation algorithm, Roche Diagnostics Ltd, England, UK), of the 8 reference genes, two were identified as being most reliable and stable reference genes: polymerase (RNA) II (DNA directed) polypeptide A (*POLR2A*) and Yes-associated protein 1 (*YAP1*) across the aforementioned panel of human keratinocyte cells and tissues. POLR2A and YAP1 were used as reference genes for all subsequent qRT-PCR experiments to calculate target gene expression levels. Given that the LightCycler 480 software was fast, convenient and produces highly similar results to the GeNorm analysis method, all subsequent data analysis was performed using the LC480 software to expedite work flow. Samples were analyzed in triplicates and values of statistical significance were calculated using either Microsoft Excel student's

t-test or Graphpad Instat software (Graphpad) by using two-sided P values or using ANOVA analysis for multiple sample comparisons. All primer sequences are listed in primer table (**Table 2.2**).

Table 2.2: Primer Table:

Genes	Sequence (5'-3')	Product (bp)
CCNB1-F	CATGGTGCACTTTCCTCCTT	102
CCNB1-R	AGGTAATGTTGTAGAGTTGGTGTCC	
CENPA-F	GCACCCAGTGTTTCTGTCAGT	104
CENPA-R	CCAGACAGCATCGCAGAAT	
CENPF-F	GCTGCAAGAAGAACTCAGTGG	104
CENPF-R	GTGTGAGCTCCTTCAATTGATCT	
CEP55_P-F	GCGCTCGAGGCTGAGGCAAGACGATCG	154
CEP55_P-R	GCGAGATCTCCTGCCCTGGGACAACG	
CEP55-F	TGAAGAGAAAGACGTATTGAAACAA	112
CEP55-R	GCAGTTTGGAGCCACAGTCT	
CK4-F	TCCTGAAGGTCCTCTATGATGC	134
CK4-R	GTACTGGGCACGGACCTC	
EGFP-F	TGGCCGACAAGCAGAAGAAC	138
EGFP-R	CTTCTCGTTGGGGTCTTTGCTC	
FOXM1A-F	TGGGGAACAGGTGGTGTTTGG	120
FOXM1A-R	GCTAGCAGCACTGATAAACAAAG	
FOXM1B -F	CCAGGTGTTTAAGCAGCAGA	287
FOXM1B –R	TCCTCAGCTAGCAGCACCTTG	
FOXM1C-F	CAATTGCCCGAGCATTGGAATCA	279
FOXM1C-R	TCCTCAGCTAGCAGCACCTTG	
HELLS_P-F	ACTCCGCCTGGTCCATCACTTCT	167
HELLS_P-R	CGCGCGGCTCACATCTTAAGTG	
HELLS-F	GGATGGCTGAATTCAAAAGATT	113
HELLS-R	CAAAGTCCCTTTCCGTTTGT	
NEK2-F	CATTGGCACAGGCTCCTAC	90
NEK2-R	GAGCCATAGTCAAGTTCTTTCCA	
NESTIN-F	GAGGTGGCCACGTACAGG	86
NESTIN-R	AAGCTGAGGGAAGTCTTGGA	
NUMB-F	GTAAAGGGCACAGCCAAGAT	69
NUMB-R	AAAACTTTGCCGTAATTTGTTCA	
p75NTR-F	TCATCCCTGTCTATTGCTCCA	110
p75NTR-R	TGTTCTGCTTGCAGCTGTTC	

POLR2A-F	GCAAATTCACCAAGAGAGACG	72
POLR2A-R	CACGTCGACAGGAACATCAG	
YAP1-F	CCCAGATGAACGTCACAGC	82
YAP1-R	GATTCTCTGGTTCATGGCTGA	

2.9 Immunoblotting

2.9.1 Protein Extraction

Total cell proteins were extracted from cultured cells in 1x RIPA buffer [50 mM Tris 1 M, pH 7.3, 150 mM NaCl, 0.02% (w/v) SDS, 1% (v/v) Nonidet P-40, 10 mM sodium orthovanadate, 1x CM-EDTA complete mini EDTA-free cocktail tablets (Roche Diagnostics, Burgess Hill UK)]. Cell lysates were kept on ice for 20 minutes and then centrifuged at 20,000 x g at 4°C for 20 min, and the supernatant was snap frozen in dry ice before being stored at -80°C. Protein concentrations were measured using the Dc Protein Assay Kit (BioRad, Hertfordshire, UK).

2.9.2 Western Blotting

Extracted proteins were diluted in 5x SDS sample buffer (0.3 M Tris-HCL, 0.25 M DTT, 0.1 % Bromophenol Blue (v/v) , 50% Glycerol (v/v) , 10% SDS (w/v)) and briefly denatured for 5 min at 100°C before loading on either pre-cast 4-12% or 10% NuPAGE® (Invitrogen, Paisley UK) gels, or on standard 6% or 8% SDS-polyacrylamide gels. Gels were typically run in the presence of NuPAGE® MES-SDS running buffer (Invitrogen) for pre-cast gels, or standard 1x SDS based running buffer (3.0 g Trizma Base, 14.4 g Glycine, 1 g SDS, 1 L of dH_2O) at a constant rate of 90V until molecular weight marker (Precision Plus Protein All Blue Standards; Bio-Rad Laboratories, Hertfordshire UK) separation was evident, after which point voltage was increased to 120V. Proteins were then transferred to nitrocellulose membranes (Hybond C-extra; Amersham; GE Healthcare UK) in a Bio-Rad transfer tank containing 1x Transfer Buffer (25 mM Tris, 192 mM Glycine, 20% methanol) at a constant current of 300 mA for 90 minutes or at constant 25V for overnight transfer at 4°C. Membranes were then blocked in 5% non-fat dry milk in TBS (Tris buffered saline) containing 0.1% Tween-20 (Sigma Aldrich) (TBST) for 30 min at room temperature. Next, membranes were probed with primary antibodies in either 3% TBST milk or 5% BSA (bovine serum

albumin; Sigma, Dorset UK) –TBST. Secondary antibodies were diluted in 3% TBST non fat dry milk. Primary antibodies used are listed in antibody table (Table 2.2). Secondary antibodies used were polyclonal rabbit anti-mouse immunoglobulin/HRP (DakoCytomation, Cambridgeshire UK), polyclonal goat anti-rabbit immunoglobulin/HRP (DakoCytomation). Immunodetection was performed with enhanced chemiluminescence reagent ECL plus (Amersham, GE Healthcare UK). For protein dephosphorylation, cell lysates were incubated at 37°C for 1 hour in a mix containing 7.5 µg protein, 1x CM-EDTA complete mini EDTA-free protease inhibitors (Roche), 1x NEB buffer 3 and 1 unit/µg of protein of calf-intestinal alkaline phosphatase (CIP; New England Biolabs, UK). Samples were then denatured for 5 minutes at 100°C and were run on 6% SDS PAGE and immunoblotted with the corresponding antibody (See antibodies Table 2.2)

2.10 Immunocyto/histo-chemistry Paraffin (IHC-P)/Frozen (IHC-F)

Organotypic raft sections, cut at a thickness of 4 µm, were initially heated at 60^{o}C for eight minutes. Sections were then deparaffinised in Xylene (3x for 5 minutes) and then dehydrated in (95% ethanol, 90% ethanol, 70% ethanol for 5 minutes each) and finally rehydrated by incubating for 5 minutes in water. Antigen unmasking was performed by incubating sections in sub-boiling temperature for 20 minutes in high pH (9.0) antigen retrieval solution (DakoCytomation). The sections were allowed to cool down to room temperature for 30 minutes before washing 2x in TBST and were then permeabilised with TBS 0.2% Triton-X (Sigma) for 10 minutes at room temperature. Protein blocking was performed by 1 hour incubation in 10% Goat Serum (Sigma) in TBST at room temperature. Primary antibody probing was performed by overnight incubation at 4^{o}C in 1%BSA TBST. Sections were then washed 3x in TBST and probed with fluorescence conjugated secondary antibodies (diluted in 1% BSA in TBST) for 1 hour at room temperature. Finally sections were washed 3x in TBST and mounted with Shadon Immu-Mount^{TM} (Thermo Scientific) solution cotaining DAPI (DAPI dilactate; Sigma) at a final concentration of 300 ng/ml. For frozen section staining, the fixation protocols included 4% (v/v) formaldehyde in PBS for 20

minutes at room temperature or ice cold methanol: acetone (1:1) for 10 minutes at room temperature. The staining procedure was thereafter the same as mentioned above for paraffin embedded tissues. Similarly, cultured keratinocytes were fixed in either 4% (v/v) formaldehyde (Sigma) in PBS for 20 minutes at room temperature or in ice cold acetone methanol 1:1 for 10 minutes. When the latter fixation protocol was used, the permeabilisation step was omitted. The staining protocol was thereafter the same as described above.

Table 2.3: Table of Antibodies

Antigen	Antibody (Cat. No)	Species	Supplier	Dilution/Concentration
CD271 (p75NTR) – PE	557196	Mouse	BD Biosciences	20 µl / 10^6 cells / 100 µl (FC)
CD29 (β1 integrin) – FITC	Ab 23834	Rabbit	Abcam	10 µl / 10^6 cells / 100 µl (FC)
EGFP	Ab 2390	Rabbit	Abcam	1:2000 (WB) 1:100 (IHC-P, IHC-F)
Filaggrin	15CID	Mouse	Monosan	1:50 (IHC-P)
FOXM1	MPP2 (C:20) sc-502	Rabbit	Santa Cruz	1:1000 (WB) 1:100 (IHC-P, IHC-F)
GAPDH	9485	Rabbit	Abcam	1:20000 (WB)
Integin β1	sc-13590	Mouse	Santa Cruz	1:100 (IHC-F)
Involucrin	Ab68	Mouse	Abcam	1:40,000 (WB)
Involucrin	H120	Rabbit	Santa Cruz	1:250 (IHC-P)
Cytokeratin 13	Ab 48575	Mouse	Abcam	1:50 (IHC-F, IHC-P)

Cytokeratin 16	-	Mouse	CRUK	1:100 (IHC-P)
Ki-67	M7240 (clone MIB-1)	Mouse	Dako Cytomation	1:500 (IHC-P-IHC-F)
p16INK4a (CDKN2a)	551154	Mouse	BD Biosciences	1:2000 (WB)
p21 (CDKN1a)	sc-817	Mouse	Santa Cruz	1:500 (WB)
p63 (4A4)	sc-8431	Mouse	Santa Cruz	1:2000 (WB)
p75NTR	MAB365	Mouse	Millipore	1:100 (IHC-F)
PARP	9542	Rabbit	Cell Signalling	1:1000 (WB)
Phospho-p38 (Thr180/Tyr182)	9215	Rabbit	Cell Signalling	1:1000 (WB)
Phospho-p53 (Ser 15)	9284	Rabbit	Cell Signalling	1:1000 (WB)
Phospho-Rb (Ser 780)	9307	Rabbit	Cell Signalling	1:4000 (WB)
TGAse-1	Pab0061	Rabbit	Covalab-UK	1:250 (IHC-P)
β-catenin (CTTNB1)	C7082	Mouse	Sigma	1:5000 (WB)
β-tubulin	sc-9104	Rabbit	Santa Cruz	1:5000 (WB)

2.11 Time-Lapse Fluorescence Video microscopy and digital pixel densitometry

Time-lapse microscopy was performed at 20 minute intervals for 72 hours where fluorescence and brightfield images (n=6) were recorded from each test well at each time point using the Metamorph software linked to a fluorescence microscope (Nikon Eclipse TE200S) equipped with a temperature-controlled humidified chamber with 5% CO_2/95% atmospheric air. Live-cell EGFP fluorescence expression levels were quantified using Adobe Photoshop CS3 (Adobe Systems Incorporated, USA) utilizing the Colour Range tool for EGFP quantification or Lasso tool for manual selection of epidermal area and subsequent pixel area readout from the Histogram data chart. Whilst we have also used ImageJ program for pixel densitometry and obtained similar results, Photoshop was the preferred choice for its accuracy, reproducibility and ease of use.

2.12 Flow Cytometry

2.12.1 Cell Cycle Analysis

Flow Cytometry analytical runs were performed on a BDLSRII fitted with an Argon Laser 488 nm, violet diode 405 nm, red diode 633 nm and a UV laser 35036 nm (San Jose, California, USA) at the Flow Cytometry Core Facility, at the Institute of Cell and Molecular Sciences, Bart's and the London School of Medicine and Dentistry, by Dr. Gary Warnes. For flow cytometry – Hoechst-33342 (Sigma) analysis cells were trypsinised and centrifuged at 218 x g for 5 minutes. After washing with 1x PBS, cell pellets were resuspended in 2ml of Hoechst-33342 10 μg/ml in PBS. After 1h incubation at 37^{o}C/10%CO_2/90% air, cells were passed through a 75 μm cell strainer (BD Biosciences) and cellular DNA content was measured by flow cytometry where 30-50,000 events per sample were acquired. For flow cytometry - propidium iodide (PI; Sigma) analysis culture medium was centrifuged together with trypsinised cells to include detached cells in analysis. After washing once in PBS, cell pellets were resuspended in 1 ml of ice-cold 70% ethanol under light vortexing to avoid the formation of cell clumps. Cells were then incubated either for 2

hours or overnight at 4 ^{o}C. Cells were washed once in PBS, before resuspending in 500 µl of PI/RNaseA mix (500 µg/ml PI, 5 mg/ml RNaseA; Sigma), 100m M NaCitrate, PBS), incubated for 20 min in the dark at room temperature and cellular DNA content was measured by flow cytometry by collecting 25,000 events per sample.

2.12.2 Fluorescence Activated Cell Sorting (FACS)

Fluorescence activated cell sorting experiments were performed on BD FACSAria Cell-Sorter (BD Biosciences, Oxford UK) at the Flow Cytometry Core Facility, at the Institute of Cell and Molecular Sciences, Bart's and the London School of Medicine and Dentistry, by Dr. Gary Warnes and Dr. Sandra Martins. For FACS, keratinocytes were tyrpsinised, spun at low speed centrifugation at 140 x g for 5 minutes, and resuspended in cold PBS. Cells were then counted as described (see **section 2.2.4**). Cells were then spun again as above and finally resuspended in cold FACS buffer consisting of PBS with 5% FBS, and 1% penicillin/streptomycin at a concentration of 10^6 cells/100 µl.

2.12.3 Oral Keratinocyte Stem Cell Sorting

Keratinocytes were stained by direct immunofluorescence for 15 minutes on ice with either FIT-C conjugated anti-integrin β1 (CD29-FITC; Abcam, Cambridge UK), PE conjugated anti-p75NTR (CD271-PE; BD Biosciences, Oxford UK) or both at a concentration of 10 µl/10^6 cells in 100 µl of FACS buffer for anti-integrin β1 or with 20 µl/10^6 cells in 100 µl for anti-p75NTR. Cells were spun at low speed centrifugation at 140 x g for 3 minutes, washed once in cold PBS, spun again at 140 x g for 3 minutes, and finally resuspended in cold FACS buffer for live cell sorting, which essentially consisted of FAD medium that contained only 5% FBS. For dead cell exclusion 200 ng/ml DAPI (DAPI dilactate; Sigma) were finally added in FACS buffer. DAPI positive cells were gated out, and integrin β1 or p75NTR positive/negative fractions were sorted by selecting the highest/lowest 20% of stained cells respectively. Double-positive cells consisted of the combined percentage of positive fractions for both antibodies. Random sorted control populations were selected randomly from the total pool of DAPI negative cells. Keratinocytes were directly plated, through the automated cell dispenser, to achieve maximum

accuracy, on 6-well plates at concentrations ranging from of $5x10^2$ to $1x10^4$ keratinocytes per 35 mm well, which already contained a pre-plated (24 hours ago) mitomycin C treated 3T3 feeder layer (see **section 2.2.1** for feeder layer preparations).

2.13 DNA Extraction and Quantification

Genomic DNA (gDNA) was extracted from confluent keratinocyte cultures using Nucleon Genomic DNA Extraction kit BACC3 (RPN8512, Amersham Biosciences, Bucks, United Kingdom) according to the manufacturer's instructions. Confluent keratinocyte cultures were lysed in Buffer B (350 µl/100mm dish; Amersham Biosciences, Bucks, UK) and lysates were very gently scraped into eppendorf tubes. Proteins were precipitated by the addition of 5 M sodium perchlorate (100 µl, Amersham Biosciences) and gentle mixing, followed by addition of 700 µl chloroform (Sigma). Phase separation was followed by addition of nucleon resin (Amersham Biosciences) and tubes were spun at 1,000 x g for 2 minutes at 4^{o}C. Top aqueous layer was removed and DNA was precipitated by addition of room temperature 100% ethanol. DNA was pelleted at 20,000 x g for 10 minutes at 4^{o}C. DNA pellet was washed in 70% ethanol, before being spun at 20,000 x g at 4^{o}C for 5 minutes. Finally, DNA pellet was air dried before being dissolved in reduced EDTA-Tris buffer (0.5 mM EDTA,10 mM Tris pH 7.5). gDNA concentrations and purity were determined using the NanoDrop^{TM} ND-1000 (ThermoScientific, Cambridgeshire UK).

2.14 10K SNP Microarray Mapping Assay

2.14.1 GeneChip® Mapping Assay

The GeneChip® Mapping Assay (Affymetrix Inc., Santa Clara, CA) genotypes at least 10,000 human single nucleotide polymorphisms (SNPs), on a single array. Although this tool is classically used for the identification of genotypic regions that are linked, or associated to, a particular phenotype, it is also useful for the identification of regions of chromosomal abnormalities that may occur during the progression of human malignancies.

Allele discrimination and genotyping is achieved by allele specific hybridization (ASH). The array contains pairs of 25-mer DNA probes, each of which (sense and antisense) corresponds to both of the two possible alleles of a genomic region that contains one SNP. By hybridizing the target DNA on the arrays, it is possible to determine whether a given SNP is homozygous (i.e. AA or BB) or heterozygous (i.e. AB), by analyzing the resulting signal generated by hybridization. The 25-mer probes contain a sequence that is a perfect match to allele A (PMA) and B (PMB). Specificity of DNA hybridization is controlled by the addition of single base-pair mismatches at the centre of each 25-mer (MMA and MMB). An example of a hybridized SNP is shown on **Figure 2.5**

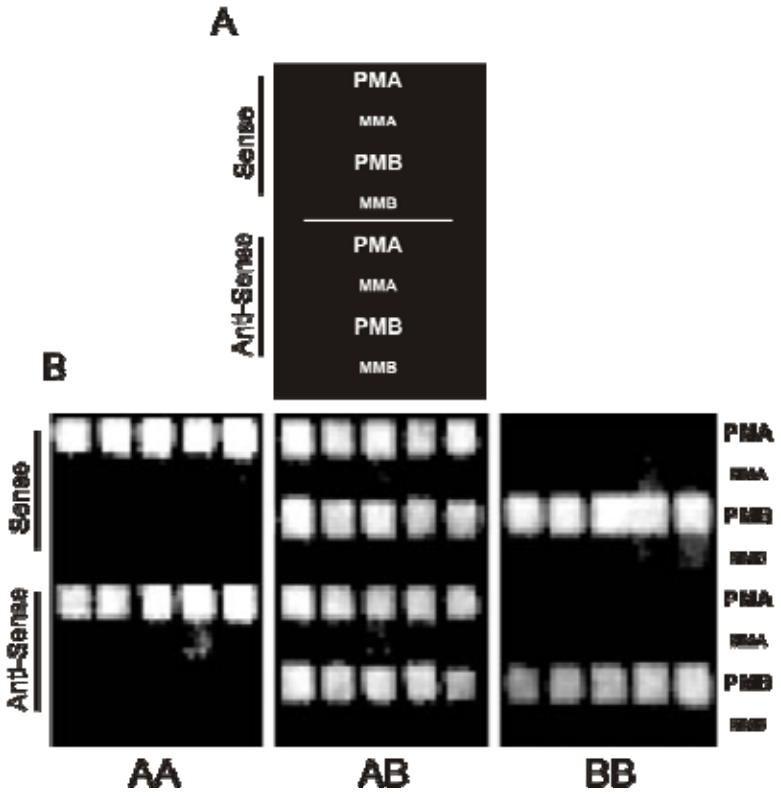

Figure 2.5 : Allele specific hybridization

(A) This probe contains sense and anti-sense 25-mer DNA sequences that correspond to both of the two possible alleles of a SNP (PMA and PMB). They also contain mismatch sequences for A and B (MMA and MMB). **(B)** If target DNA is AA or BB, then hybridization signal will be derived solely from either PMA or PMB. If target DNA is AB, then hybridization signal will come from both PMA and PMB. Image obtained from protocol provided by Affymetrix.

For DNA to hybridize on the array, it must first be biochemically prepared. Genomic DNA is first broken down in many pieces by restriction enzyme digestion, and is then ligated to adaptors that specifically recognize the base overhangs. A generic primer is thereafter used to recognize the sequence of the adaptor, and to amplify all ligated sequences resulting in the generation of 250-1000 bp genomic DNA fragments. The amplified DNA is finally fragmented, labeled and hybridized to GeneChip® arrays.

2.14.2 Genomic DNA Preparation and Data Analysis

Primary NHEK and N/TERT gDNA samples were processed as described previously (Kelsell et al., 2005; Teh et al., 2005; Blaydon et al., 2006) with slight modification to the standard GeneChip Mapping 10K (V2.0) Xba Assay protocol (Affymetrix Inc., Santa Clara, CA). An amount of 350-500 ng of DNA was digested with XbaI and ligation to the XbaI adaptor prior to PCR amplification using AmpliTaq Gold with Buffer II (Applied Biosystems, Foster City, CA). The PCR amplification profile on an MJ DNA Engine thermal cycler was: 95/180, 59/15, 72/60 (°C/sec) for 40 cycles followed by a termination step at 72°C for 7 minutes. PCR products were purified using Ultrafree-MC 30,000 NMWL filter columns (Cat#UFC-3LTK00; Amicon) and DNA concentrations determined using NanoDrop spectrophotometer. Hybridisation and scanning of the arrays were processed as described previously (Kelsell et al., 2005; Teh et al., 2005; Blaydon et al., 2006) and has been performed by Ms. Tracy Chaplin-Perkins at the Cancer Research UK Medical Oncology Laboratory, Institute of Dentistry, Barts & The London School of Medicine and Dentistry, Queen Mary University of London, United Kingdom. LOH and LOH likelihood were analyzed using Affymetrix GeneChip Genotyping Analysis software (GTYPE, version 4.1) where the threshold for statistical significance was $P \leq 10^{-6}$ as recommended by Affymetrix (Kennedy et al., 2003; Liu et al., 2003). The data were cross verified and genome ploidy ± standard deviation for Log 2 ratio values were obtained using an independent algorithm, Copy Number Analyzer for GeneChip (CNAG, version 2), which has been shown to improve signal-to-noise ratios in heterogeneous genomes (Nannya et al., 2005). The SNP call

rates for the control (mock transduced), EGFP and FOXM1B transduced primary NHEK cells were 98.45%, 98.24% and 97.27%, respectively. Putative genes within or adjacent to the LOH SNPs were identified using Affymetrix Integrated Genome Browser (IGB, version 4.56) using the NCBI Human Genome Assembly (version 36; March 2006). Data were also analyzed using Ideogram Browser v.0.20.4 from http://www.informatik.uni-ulm.de/ni/staff/HKestler/ideo/ (Muller et al., 2007) for easier visualization and illustration of the analyzed results.

Chapter 3

REGULATION OF FOXM1 IN ORAL SQUAMOUS CELL CARCINOMA

3 Regulation of FOXM1 in Oral Squamous Cell Carcinoma

3.1 Introduction

Despite the fact that the FOXM1 is overexpressed in the majority of human solid tumours, the regulation of its expression in oral epithelial malignancies has not been investigated. Oral squamous cell carcinomas (OSCCs) are highly aggressive and a major cause of mortality and morbidity worldwide. The link between tumour growth and overexpression of FOXM1 in certain tumours of epithelial origin, predicts an important role of this transcription factor in the initiation and progression of OSCCs. Therefore, this study initially aimed to understand how FOXM1 is regulated at both the transcription and protein levels in a variety of normal, pre-malignant, and OSCC tissues, and tissue derived cells.

Recent studies conducted in our group have shown that concomitant exposure to nicotine, a major constituent of tobacco (risk factor associated with the genesis of OSCCs), and overexpression of FOXM1B isoform, can mediate the transition of pre-malignant keratinocytes to a malignantly transformed cell line, as judged by its ability to form colonies in soft agar (Gemenetzidis et al., 2009). During the course of FOXM1B-induced malignant transformation, certain genomic loci, containing genes important in chromatin remodelling, gene expression regulation, and mitotic division, were frequently amplified (Gemenetzidis et al., 2009). Therefore, this study will also examine the potential effects of nicotine, in the expression of FOXM1, and further assess the possibility that FOXM1 can directly regulate the expression of genes that are important in the malignant conversion of oral keratinocytes.

3.2 Results

3.2.1 FOXM1 Protein Levels Correlate with Disease Progression

FOXM1 protein levels were investigated in a cohort of 25 patients' tissue samples containing normal oral mucosa, oral pre-malignant (dysplastic) lesions, OSCCs, and metastatic tumour tissue samples by means of immunohistochemistry (Sample

processing and IHC shown in **Figure 3.1** were performed by Dr. Ahmed Waseem, Centre for Clinical and Diagnostic Oral Sciences, Bart's and the London School of Medicine and Dentistry). In normal oral mucosa, FOXM1 appears to be present mainly in the parabasal layers of normal epithelium, with few cells staining positive at the basal layers **(Figure 3.1A)**. FOXM1 transcription factor is localized to the nucleus prior to, and during mitotic cell division. Consistent with the low index of proliferative activity of epithelial tissues under homeostatic conditions, the localisation of FOXM1 protein was mainly cytoplasmic in normal oral mucosa (**Figure 3.1A)**. However, it can be noted that many cells in the suprabasal, post-mitotic layers of the epithelium have been positively stained, possibly due to non-specific staining. FOXM1 protein levels in mild/moderately dysplastic tissues were not only markedly increased compared to normal tissue, but also became strictly nuclear, indicating increased FOXM1 protein activity **(Figure 3.1B)**. Further upregulation of FOXM1 protein can be noted in moderately/severely and severely dysplastic/carcinoma *in situ* (CIS) tissues of oral mucosa, where FOXM1 remains predominantly nuclear **(Figure 3.1 C, D)**. Protein levels remained high in tissues derived from both primary OSCC and lymph node metastases **(Figure 3.1 E, F)**. Quantitative immunohistochemistry analysis of stained tissues confirmed the findings, whereby FOXM1 protein displays a progressive upregulation during the transition from normal to dysplastic, OSCC, and tissues derived from local metastases.

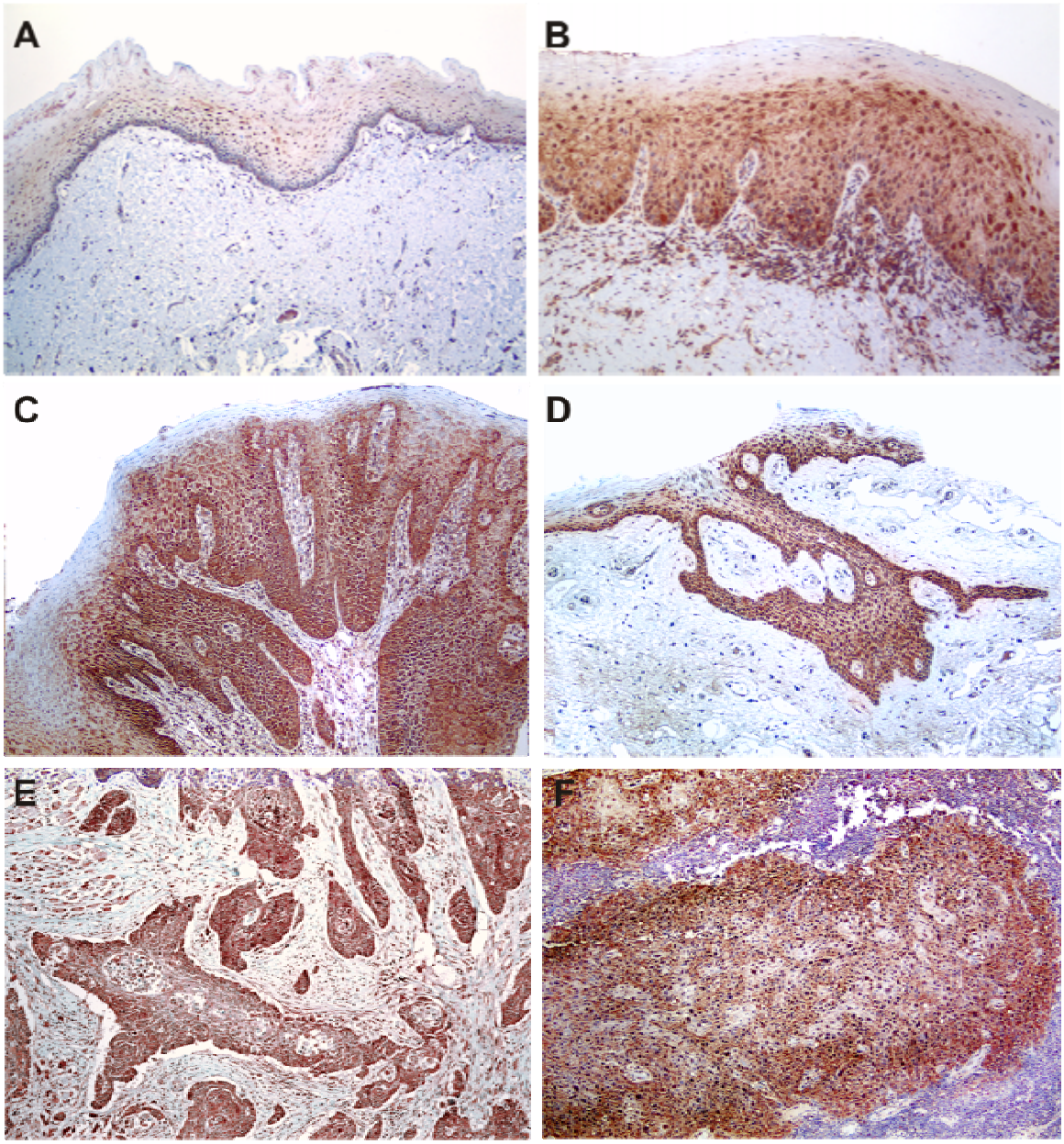

Figure 3.1: Upregulation of FOXM1 in pre-malignant and OSCC tissues

Immunohistochemistry of FOXM1 protein on a panel of formalin fixed, paraffin embedded **(A)** normal human oral mucosa, **(B)** mild/moderate dysplasia, **(C)** moderate/severe dysplasia, **(D)** severe dysplasia/carcinoma in situ, **(E)** primary OSCC, **(F)** and lymph node OSCC metastasis.

3.2.2 FOXM1 Expression in Pre-Malignant and OSCC-derived Cell Lines

A panel of different cell lines/primary cells derived either from clinically normal oral mucosa or diseased tissues was employed to investigate FOXM1 protein levels *in vitro*. Protein levels were first examined in all different cell types by means of immunofluorescence. Results clearly demonstrate that, in agreement to *in vivo*

observations, FOXM1 protein levels are increased in culture keratinocytes derived from early premalignant, as well as in keratinocytes derived from late-stage advanced OSCC tumours, compared to normal oral keratinocytes **(Figure 3.2)**. Notably, the nuclear presence of FOXM1 is enhanced in normal oral keratinocytes, compared to what was observed *in vivo*, possibly due to the increased proliferation rates of primary keratinocytes during *in vitro* culture expansion.

Next, protein lysates were prepared from keratinocytes derived from normal oral mucosa, dysplastic, and OSCC tissues, and FOXM1 protein levels were assessed by means of immunoblotting. Results show a clear upregulation of FOXM1 protein levels in all pre-malignant and OSCC derived cell lines compared to early passage normal oral primary keratinocytes **(Figure 3.3)**.

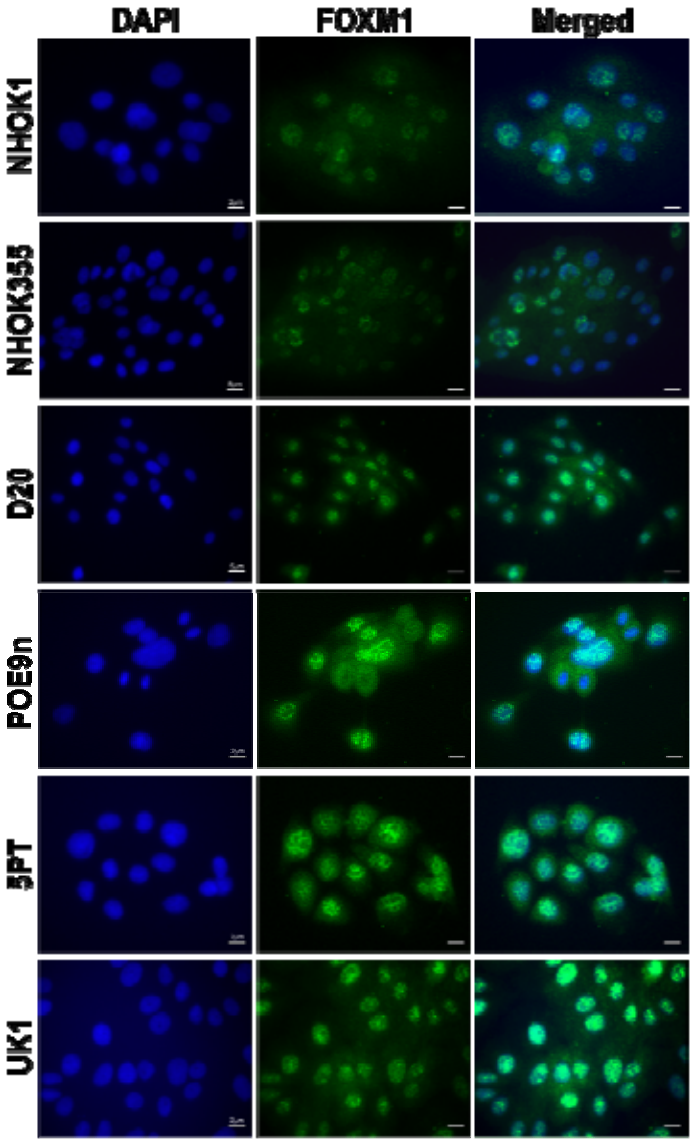

Figure 3.2: FOXM1 immunocytochemistry in pre-Malignant and OSCC cultured keratinocytes

Cultured primary human oral (NHOK1, NHOK355), oral pre-malignant (D20, POE9n) and OSCC derived (5PT, UK1) keratinocytes were examined for FOXM1 protein levels by immunofluorescence, using normal primary oral keratinocytes (NHOK1, NHOK355) as control cells. Nuclear DNA was counterstained with DAPI.

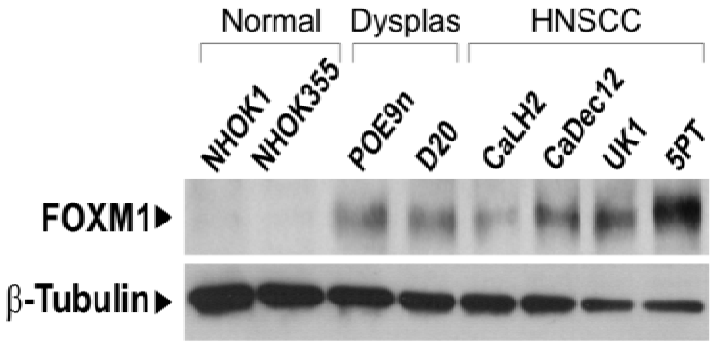

Figure 3.3: Elevated FOXM1 protein levels in OSCC keratinocytes

(A) Immunoblotting for endogenous FOXM1 protein in normal (NHOK1 and NHOK355), dysplasia (POE9n and D20) and OSCC (CaLH2, CaDec12, UK1 and 5PT) derived keratinocytes as indicated. β-Tubulin was used as a protein loading control in each sample.

3.2.3 Downstream Targets of FOXM1 are Overexpressed in OSCC

Although FOXM1 protein is required for binding to its downstream targets, its post-translational modification (mainly phosphorylation) is essential for subsequent activation of target gene expression (Wierstra and Alves, 2006b; Wierstra and Alves, 2007; Laoukili et al., 2008b). Therefore, FOXM1 protein activity was assessed in OSCC derived keratinocytes to understand whether overexpressed FOXM1 protein is also transcriptionally active. Protein separation on lower percentage SDS-PAGE, revealed the presence of a slow migrating band immunoreactive to anti-FOXM1 antibody. This form of FOXM1 protein was sensitive to treatment with calf intestinal phosphatase (CIP), suggesting that this slow migrating band corresponds to a post-translationally modified form of FOXM1. This could be either the phosphorylated, transcriptionally active form of FOXM1 (FOXM1pp), or the product of further protein modifications which can also lead to an increase in molecular size (e.g. glycosylation). It can be noted that in 5PT cells, which show the highest protein levels of FOXM1 among all cell lines (**Figures 3.2, 3.3**), FOXM1pp was less sensitive to CIP treatment, probably due to the presence of excessive post-translational protein modification, which could suggest that FOXM1 protein in 5PT cells is mainly modified by means other

than phosphorylation alone. This intense protein band shift of 5PT cells can also be observed in **Figure 3.4 A.**

To further confirm that FOXM1 remains transcriptionally active in OSCC cell lines, the mRNA expression levels of FOXM1 downstream targets CENP-F, CENP-A, NEK2, CCNB1 (Leung et al., 2001; Laoukili et al., 2005; Wang et al., 2005; Wonsey and Follettie, 2005) were examined. The mRNA expression levels of all aforementioned targets were significantly upregulated in OSCC derived cell line UK1 **(Figure 3.4 B)**.

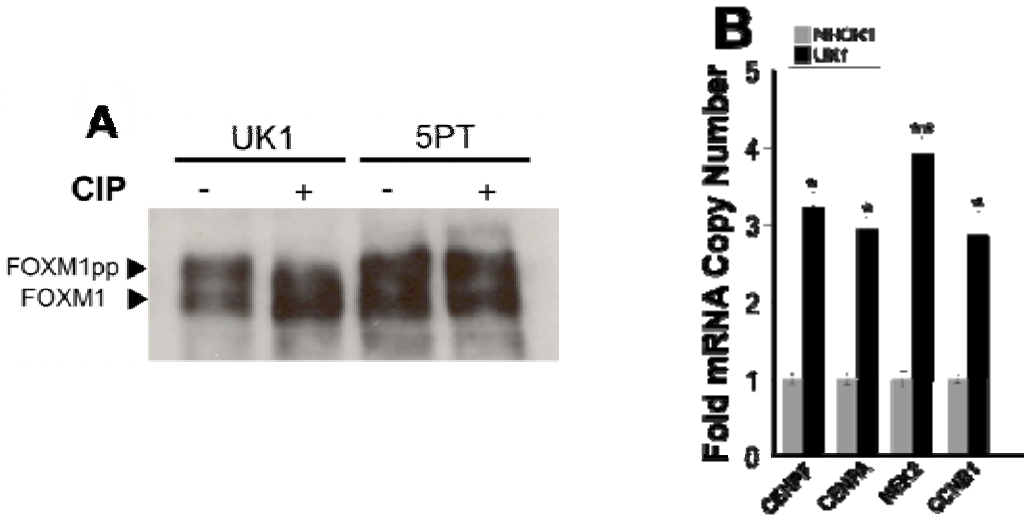

Figure 3.4: FOXM1 protein is active in OSCC derived keratinocytes

(A) UK1 and 5PT keratinocytes were lysed and CIP treated or untreated control protein extracts were immunoblotted against anti-FOXM1 antibody. **(B)** qPCR data showed that known FOXM1B target genes such as CENPF, CENPA, NEK2 and cyclin B1 are upregulated in UK1 compared to NHOK1 cells. Bars represent the mean fold difference from NHOK1 (arbitrary value of 1) normal control ±SEM for triplicate samples. **(P≤0.05), **(P≤0.01) and ***(P≤0.001)* indicate significant increase in FOXM1 protein levels when compared to NHOK1 cells.

3.2.4 FOXM1 Isoform Specific Expression in OSCC Cell Lines

Although the data presented here strongly support that FOXM1 protein levels are significantly and progressively upregulated in early premalignant and OSCC derived tissues, the transcriptional regulation of FOXM1, especially its three alternatively spliced isoforms, was unclear. Therefore, the mRNA expression levels of each of the three FOXM1 isoforms was investigated in a large panel comprising

NHOK control, pre-malignant, and OSCC derived keratinocytes, by the use of well-characterized and previously validated, FOXM1 isoform specific primers. FOXM1 isoforms are created upon alternative splicing of exons A1 and A2 (see **Figure 1.7**). FOXM1A has both A1 and A2 exons whilst FOXM1C possesses only A1 exon, and FOXM1B has neither of the alternatively spliced exons. Based on these molecular structures, isoform-specific primers have been designed (**Figure 3.5 A**) (primer design and specificity validation was performed by Dr. Muy-Teck Teh, Centre for Clinical and Diagnostic Oral Sciences, Barts and The London School of Medicine and Dentistry). The amplification specificity for each isoform is shown in **Figure 3.5 B**. Melting analysis showed the presence of single PCR products, indicated by a single peak for each isoform amplified (**Figure 3.5 C**). PCR products of each reaction were visualized on 2% Agarose gels confirming the presence of single products which rules out cross-amplification of other isoforms (**Figure 3.5 D**).

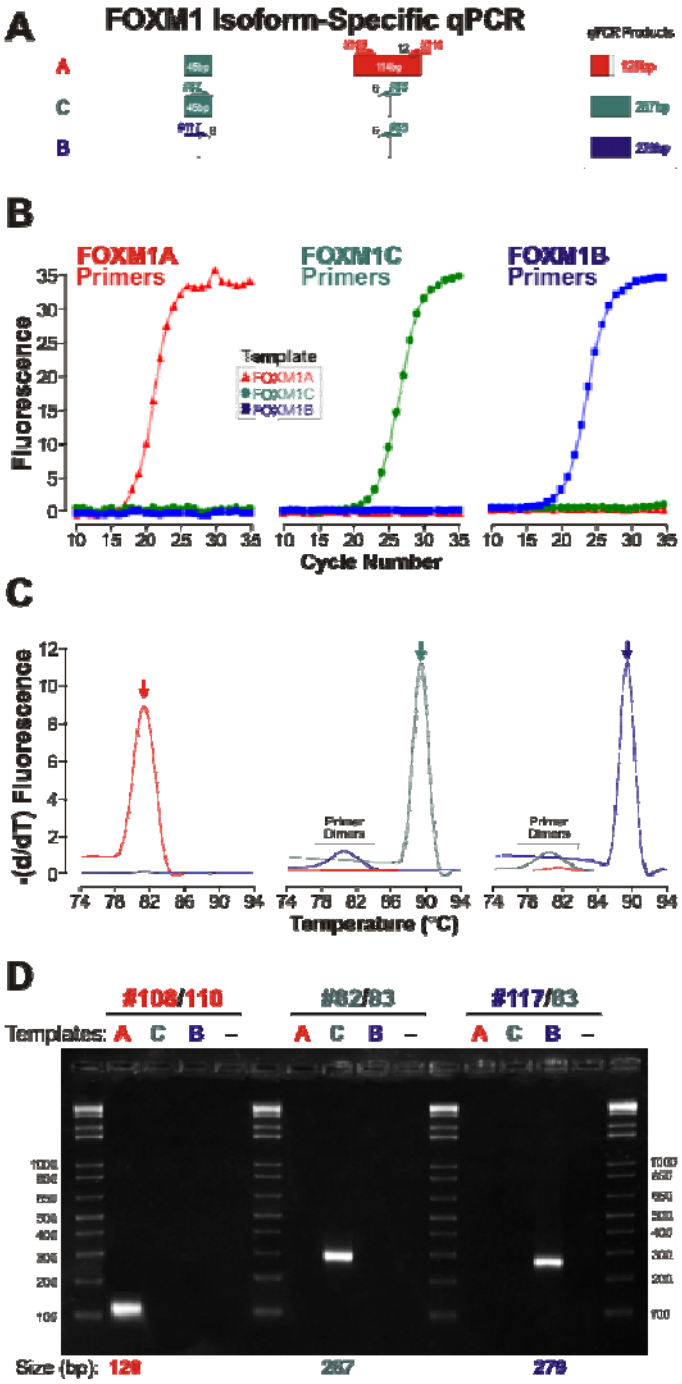

Figure 3.5: FOXM1 isoform-specific qPCR

(A) Primer design based on the gene structure of the three FOXM1 isoforms. Primers were designed to recognize alternative exons A1 and A2 (FOXM1A), or A1 only (FOXM1C), or none of the above (FOXM1B). qRT-PCR product amplification **(B)** and melting peak analysis **(C)** at the end of qPCR analysis showing single PCR product for each isoform validating amplification specificity. **(D)** Agarose gel electrophoresis confirmed the presence of single PCR product of the expected molecular size for each isoform.

Absolute qPCR was performed to compare the expression levels of all FOXM1 isoforms, between primary NHOK from clinically healthy tissues, to a variety of oral pre-malignant (moderate and severe dysplasias) and OSCC cell lines. It was found that all three FOXM1 isoforms (FOXM1A, FOXM1B, and FOXM1C) were upregulated in both premalignant and OSCC derived cell lines. FOXM1A levels were upregulated in OSCC cell lines by 2.3 to 2.5-fold over control normal cells, but were not significantly ($P>0.05$) increased in pre-malignant keratinocytes **(Figure 3.6)**. Both FOMX1B (2.3 to 4-fold) and FOXM1C (2.7 to 3.2-fold) isoform expressions were significantly increased in both pre-malignant and OSCC cell lines **(Figure 3.7 A, B)**.

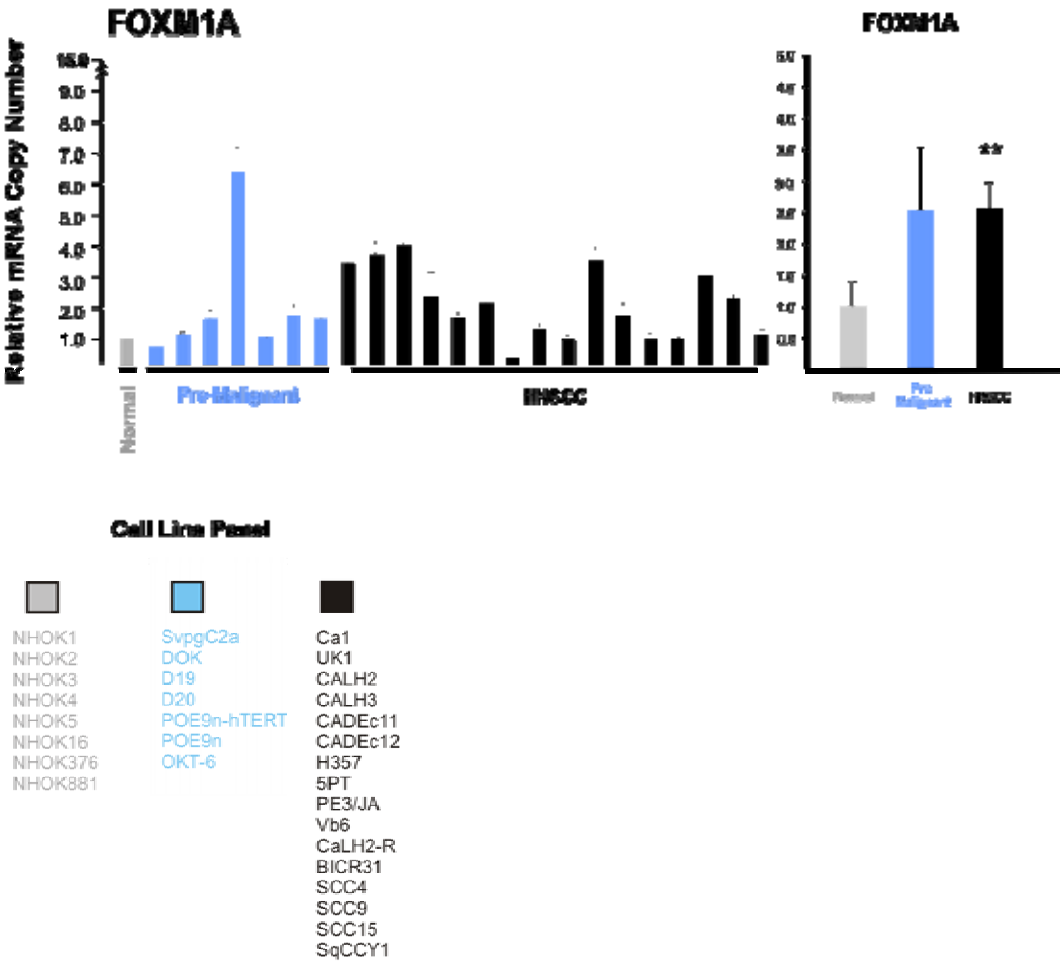

Figure 3.6: FOXM1A expression in oral cancer cell lines

FOXM1A isoform expression pattern in normal, premalignant and OSCC keratinocytes. Normal, pre-malignant, and OSCC keratinocytes were used to study the expression levels of FOXM1. mRNA was extracted and qPCR was used to detect expression levels of FOXM1A isoform. Relative fold mRNA copy numbers FOXM1A in premalignant and OSCC cells was calculated using the average mRNA copy number of a large array of normal oral keratinocytes. FOXM1A showed a non-significant ($P>0.05$) upregulation of expression in pre-malignant oral keratinocytes, whilst mRNA levels were 2.5 fold increased in OSCC derived cell lines ($**P\leq0.01$). Bars represent the relative fold difference of mRNA copy number compared to the average mRNA copy number value of eight different normal control samples (arbitrary value of 1) ±SEM for triplicate samples. The cell line panel that was used for expression analysis is shown at the bottom. Cell lines were used in the specified order from top to bottom for each group.

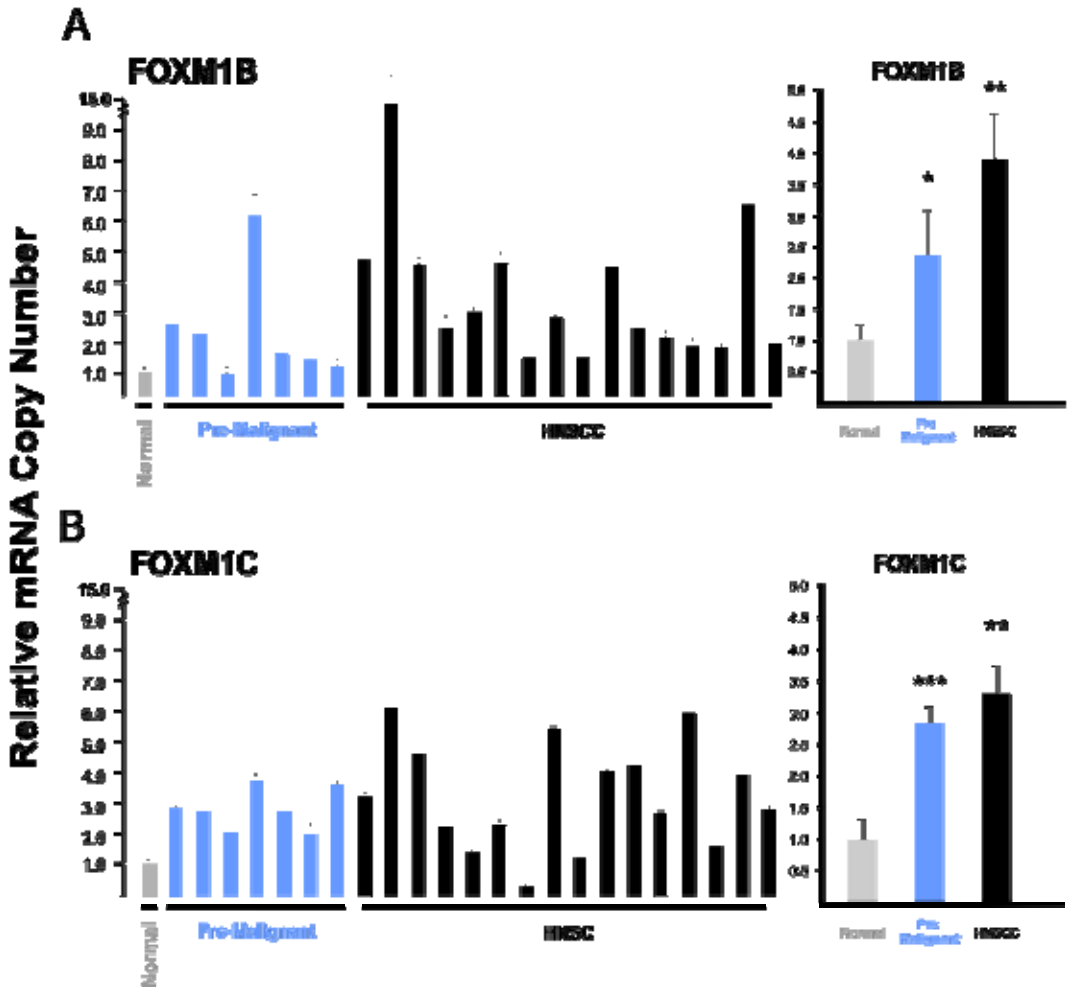

Figure 3.7 FOXM1B and FOXM1C expression in oral cancer cell lines

FOXM1B and FOXM1C isoforms expression pattern in normal, premalignant and OSCC keratinocytes. Normal, pre-malignant, and OSCC keratinocytes were used to study the expression levels of FOXM1. mRNA was extracted and qPCR was used to detect expression levels of FOXM1B **(A)** and FOXM1C **(B)** isoforms. FOXM1B expression **(A)** shows a gradual upregulation in pre-malignant cancer cell lines by 2.3 fold (*$P \leq 0.05$) and is significantly (**$P \leq 0.01$) increased by 4-fold in OSCC derived cell lines. **(B)** FOXM1C is significantly upregulated in oral pre-malignant (2.7-fold) (***$P \leq 0.001$) and OSCC derived cells (3.2-fold) (**$P \leq 0.01$). Bars represent the relative fold difference of mRNA copy number compared to the average mRNA copy number value of eight different normal control samples (arbitrary value of 1) ±SEM for triplicate samples.

3.2.5 Nicotine as a Causative Agent Contributing to FOXM1 Upregulation

The generation of OSCC is strongly associated with the exposure of the epithelium to known risk factors, such as tobacco and betel quid (Sturgis and Wei, 2007). A previous study in our group had identified that nicotine directly activated FOXM1 expression (Gemenetzidis et al., 2009).

To investigate how endogenous FOXM1 protein levels are regulated in response to nicotine exposure, oral keratinocytes were cultured in the presence of increasing nicotine concentrations, or vehicle control (DMSO), for 24 hours prior to preparing total protein extracts. FOXM1 protein levels showed a dramatic increase even in the presence of nicotine concentrations as low as 10^{-6}M (Figure **3.8 Ai**). This response was similar for both premalignant SVpgC2a and primary human oral keratinocytes. The lack of significant induction of FOXM1 at high doses of nicotine (10^{-3} M) in NHOK is possibly a result of increased cytotoxicity (**Figure 3.8 Ai**), which was clearly evident under routine microscopic examination. Protein lysates from treated keratinocytes were also run in lower percentage SDS-PAGE, which revealed the presence of a slow migrating band immunoreactive to anti-FOXM1 antibody (**Figure 3.8 Aii**). Again, this form of FOXM1 protein was sensitive to CIP treatment, indicating that FOXM1 protein is heavily phosphorylated in response to nicotine treatment, and therefore capable of downstream target transactivation, in both SVpgC2a and primary human oral keratinocytes (**Figure 3.8 Aii**).

To further confirm that FOXM1 protein retains transcriptional activity in response to nicotine treatment, a construct containing five repeats of the consensus DNA binding sequence of **FOXM1 (Ye et al., 1997) (5xBS)**, which upon binding of active FOXM1 protein can enhance transcription of luciferase gene (Ye et al., 1997), was used in SVpgC2a premalignant as well as two other malignant keratinocyte cell lines SqCC/Y1 and SCC25. Keratinocytes were transfected with 5BS and subsequently exposed to various concentrations of nicotine. FOXM1 protein activity was significantly increased in all types of keratinocytes (**Figure 3.8 B**). Maximum levels of protein activity were observed in premalignant SVpgC2a cell line, in a dose dependent manner, and FOXM1 protein reached its peak activity in the presence of 10^{-3} – 10^{-4} M nicotine (Gemenetzidis et al., 2009) (FOXM1 reporter assay in **Figure 3.8 B** was performed by Dr. Adeel Riaz).

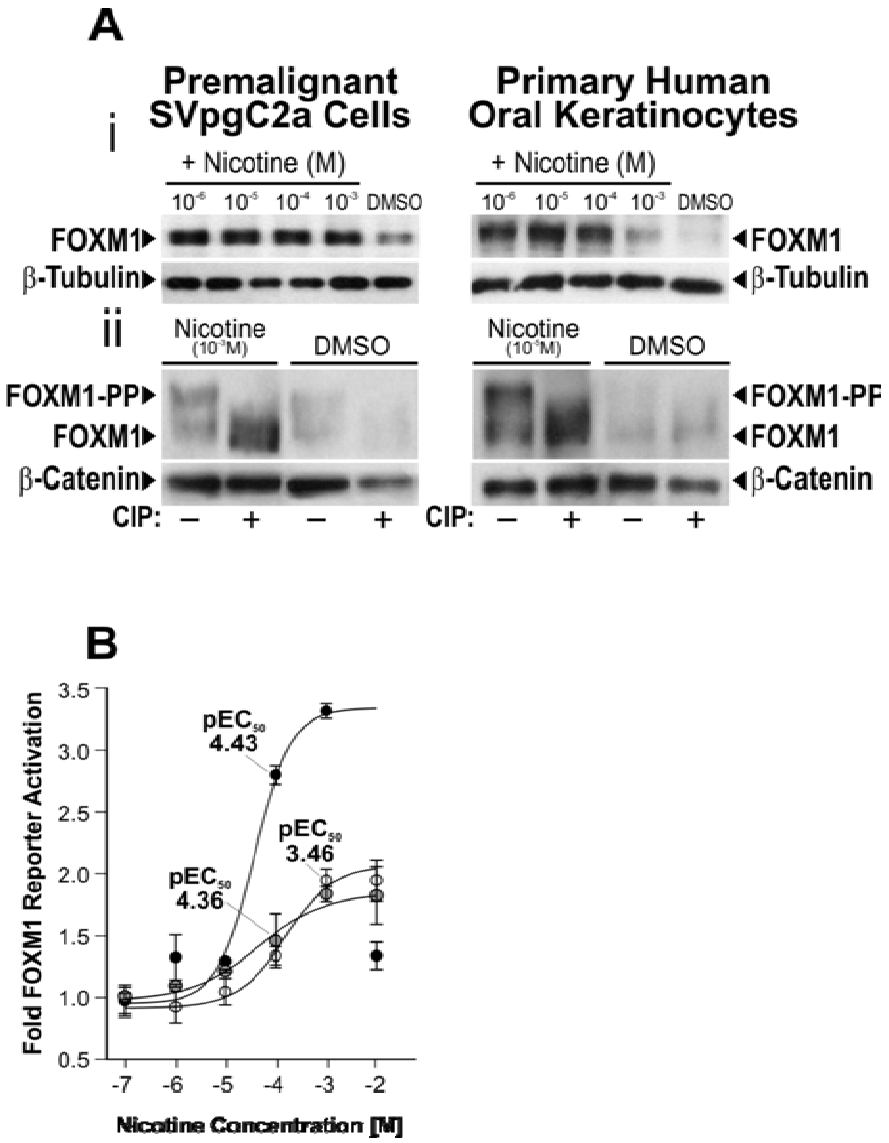

Figure 3.8: FOXM1 is expressed and activated in response to nicotine treatment

(A) Immunoblotting shows that nicotine dose-dependently activated endogenous FOXM1 protein in both the SVpgC2a (left panel) and primary normal human oral keratinocytes (right panel) as indicated. Bottom panels showed that protein lysates were either pretreated with or without calf-intestinal phosphatase (CIP) prior to immunoblotting. Nicotine at respective optimal doses for each cell type showed reduction of the phosphorylated FOXM1 (FOXM1-PP, top bands) in CIP-treated lysates. b-Tubulin and b-catenin were used as loading control. **(B)** Dose-response curves of nicotine on FOXM1 protein transcriptional activity SVpgC2a (closed black circles), SqCC/Y1 (grey shaded circles), and SCC25 (clear white circles) cells treated with the indicated doses of nicotine. Each data point indicates mean±SEM (n = 3). pEC_{50} = The potency of nicotine drug in relation to FOXM1 transactivation.

3.2.6 Identification of Novel FOXM1 Targets in Neoplastic Oral Keratinocytes

Studies conducted in our group have shown that concomitant exposure to nicotine and overexpression of FOXM1B isoform, can induce the transition of SVpC2a keratinocytes from a pre-malignant, to a malignantly transformed cell line, as judged by its ability to form colonies in soft agar (Gemenetzidis et al., 2009). By examining the genotype of eight transformed clones, using 10K SNP array analysis, several loci were identified as being among the most commonly amplified regions. Two of the putative loci contained centrosomal protein 55 (CEP55 ; also known in the literature as FLJ10540) and lymphoid-specific helicase (HELLS ; also known in the literature as LSH, PASG) genes (Gemenetzidis et al., 2009).

Therefore, further investigation took place to understand whether the expression of CEP55 and HELLS, were physiologically relevant to OSCC biology. The mRNA expression levels of both genes were investigated in a large panel comprising NHOK control, pre-malignant, and OSCC derived keratinocytes (details on the cell lines used can be found in **Chapter 2, section 2.1.3**). Both genes were significantly and consistently overexpressed in both pre-malignant and OSCC derived keratinocytes, compared to a series of 8 individually derived keratinocytes from clinical normal oral mucosa (**Figure 3.9**).

Although CEP55 and HELLS were overexpressed in a variety of human pre-malignant and OSCC derived keratinocytes, this did not constitute definite evidence that FOXM1 is the major regulator of either gene in neoplastic keratinocytes. To investigate whether FOXM1 may be regulating the expression of either gene, primary human oral keratinocytes were retrovirally transduced with pSIN-MCS (empty vector), pSIN-EGFP, or pSIN-EGFP-FOXM1B retroviral vectors. For retroviral vector information and an experimental approach for the optimization of retroviral gene delivery methods in human keratinocytes, see **Chapter 2, section 2.3.5.** Ectopic overexpression of FOXM1B strongly induced the expression of both CEP55 and HELLS in primary human oral keratinocytes (**Figure 3.10**). This evidence

shows that in addition to previously identified FOXM1 targets, two novel downstream targets, CEP55 and HELLS, are also significantly upregulated in oral neoplastic keratinocytes, further highlighting the importance of FOXM1 in the generation and progression of OSCC.

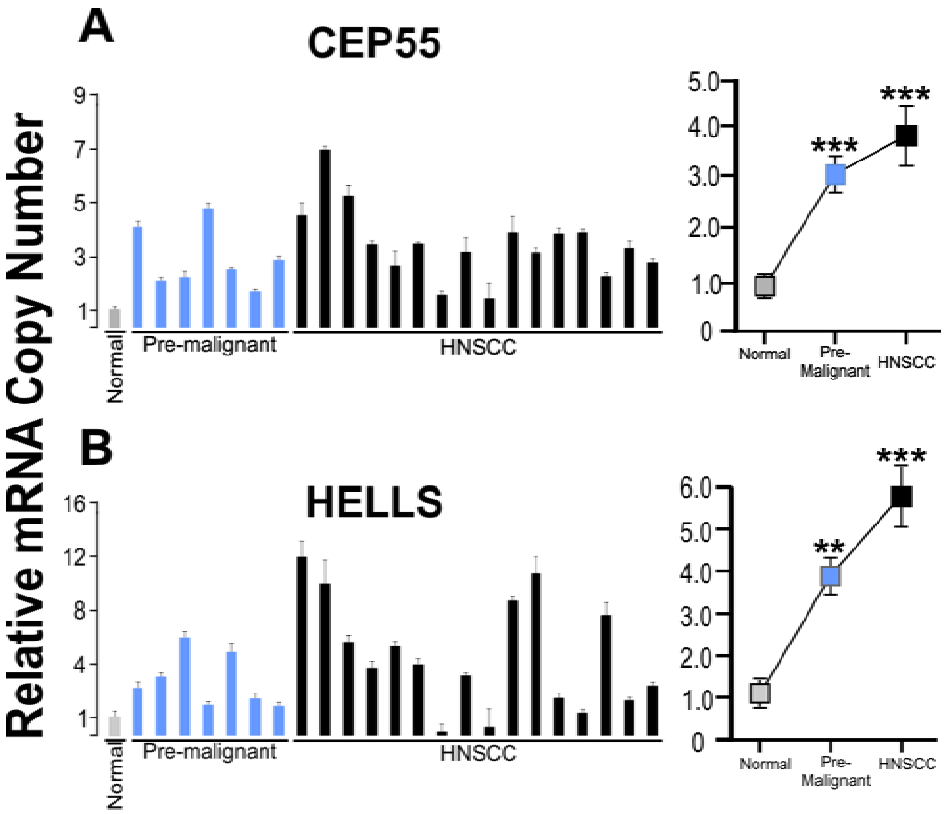

Figure 3.9: CEP55 and HELLS expression patterns in normal, premalignant and OSCC keratinocytes.

Normal, pre-malignant, and OSCC keratinocytes were used to study the expression levels of CEP55 and HELLS. mRNA was extracted and qPCR was used to detect expression levels of **(A)** CEP55 and **(B)** HELLS. CEP55 expression **(A)** shows a gradual upregulation in pre-malignant cancer cell lines by 3 fold (right hand panel) (****P≤0.001*) and is significantly (****P≤0.001*) increased by 4-fold in OSCC derived cell lines. **(B)** HELLS is significantly upregulated in oral pre-malignant (4-fold) (***P≤0.01*) and OSCC derived cells (6-fold) (****P≤0.001*). Bars represent the relative fold difference of mRNA copy number compared to the average mRNA copy number value of eight different normal control samples (arbitrary value of 1) ±SEM for triplicate samples.

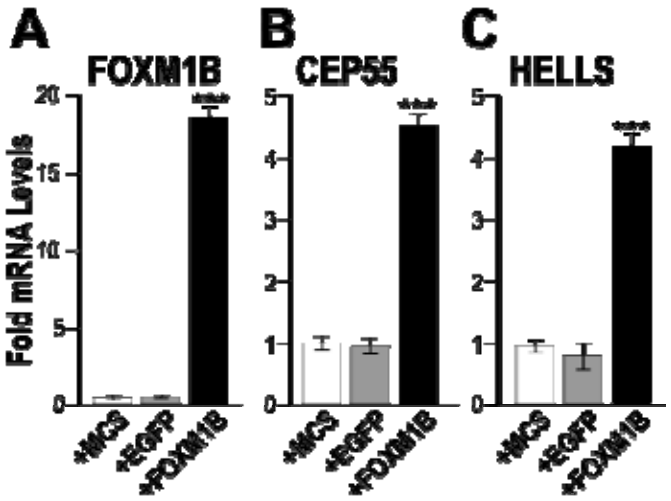

Figure 3.10: FOXM1B induces the expression of CEP55 and HELLS

(A) Exogenous overexpression of FOXM1B (determined using isoform-specific qPCR), but not MCS (empty vector) or EGFP, in primary human normal oral keratinocytes (NHOK1), showed significant (****P≤0.001*) induction of endogenous mRNA of **(B)** CEP55 and **(C)** HELLS, respectively. Bars represent the relative fold difference of mRNA copy number compared to the average mRNA copy number value of pSINMCS (arbitrary value of 1) ±SEM for triplicate samples.

The fact that FOXM1B overexpression resulted in strong induction of CEP55 (**Figure 3.10 B**), and the strong correlation between FOXM1B and CEP55 expression in OSCC derived keratinocytes (FOXM1B:CEP55 R^2=0.665; FOXM1B: HELLS R^2=0.205, **see Appendix 2**), suggested that CEP55 may be a direct transcriptional target of FOXM1. This also fits with the well-known function of FOXM1 at mitosis, where it directly transactivates the expression of many important mitotic proteins (Laoukili et al., 2007).

The possibility that FOXM1 transcription factor directly binds to, and activates the promoter of *CEP55*, was assessed by chromatin immuno-precipitation experiments. Putative FOXM1 DNA binding sites (TACGTTGTTATTTGTTTTTTTCG) (Ye et al., 1997) were identified within 1Kbp upstream (-570: -730 bp) of the CEP55 gene, using DsGene® Discovery Studio (Accelrys Inc.) ClustalW Alignment Tool, and specific qPCR primers were designed flanking the region of interest (**See Table 2.3 in Chapter 2, section 2.8)**. Primary human keratinocytes were either mock transduced (Mock; no virus), or retrovirally transduced with EGFP control, or EGFP-FOXM1B retroviral vector, and genomic DNA was extracted 48 hours later. Chromatin was immuno-precipitated (IP) with anti-FOXM1, anti-GAPDH (control),

or anti c-Myc (control) antibodies, to examine whether FOXM1 protein specifically binds to the putative promoter of *CEP55* gene. The resultant IP fractions were amplified using primers specific for the *CEP55* promoter region, which contained the DNA binding sites for FOXM1 protein (ChIP and qPCR amplification shown in **Figure 3.11** was performed by Dr. Muy-Teck Teh). Results clearly show that the IP fractions retrieved by anti-FOXM1 antibody contain significantly more copies of the *CEP55* promoter region, indicating preferential binding of FOXM1B protein, and providing evidence that *CEP55* is direct transcriptional target of FOXM1B.

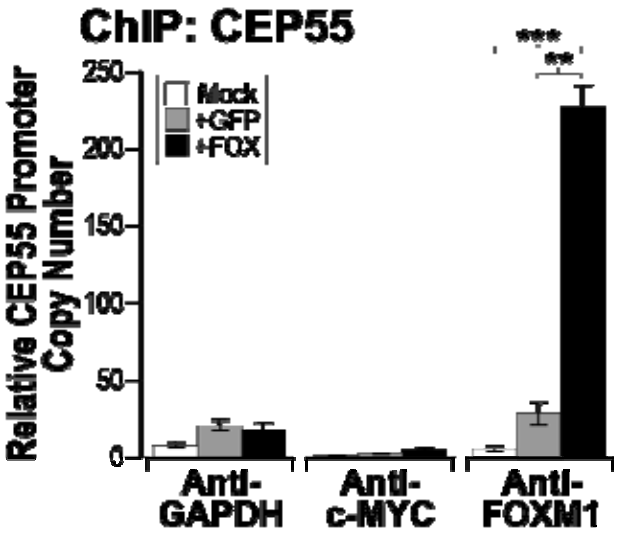

Figure 3.11: CEP55 is a direct transcriptional target of FOXM1B

ChIP-qPCR assays for CEP55 promoter in normal keratinocytes transduced with Mock (empty virus), EGFP or FOXM1B. Antibodies for GAPDH and cMYC were used as controls for immunoprecipitiation. ***P≤0.01, ***P≤0.001*

3.3 Discussion

3.3.1 FOXM1 Expression in Normal Oral Epithelium

The forkhead box transcription factor FOXM1 is abundantly expressed in actively proliferating cells and as a result its expression is often detected in tissues with high proliferative index such as the thymus and testis (Ye et al., 1997; Laoukili et al., 2007). Although Foxm1 is expressed at high levels in mice embryonic developing tissues, its expression is significantly reduced in adult tissues, which are under homeostatic conditions. In mouse epithelial adult tissues, Foxm1 expression is restricted to the most proliferative layers, but is absent from differentiated layers (Ye et al., 1997). These observations, along with the fact that it can be strongly induced during tissue regeneration in response to injury (Ye et al., 1997), suggested that Foxm1 functions to replenish the short lived population of differentiated epithelial cells.

The epithelial tissue undergoes continuous renewal, under a strictly organised system that is governed by a hierarchy of cells with differing capacities for proliferation. This process is believed to commence by the slow cycling stem cell (SC), which is thought to reside within the basal epithelial layer. The tissue undergoes expansion by rapid, but limited, rounds of cell division achieved by transit amplifying (TA) cells, to finally give rise to post-mitotic terminally differentiated cells (Slack, 2000). In human epidermis, which has a high degree of similarity with normal oral mucosa epithelium, FOXM1 is mainly localised in basal proliferative and immediate suprabasal keratinocytes (Teh et al., 2002). Similarly, FOXM1 is mainly expressed in basal and early suprabasal layers of human cervical epithelium (Chan et al., 2008), thereby confirming earlier predictions that this transcription factor may be involved in the overall proliferative output as well as in the continuous replenishment of the adult tissue.

Consistently with these observations, FOXM1 was detected in both the cytoplasm and the nucleus of basal and parabasal keratinocytes of the oral mucosal epithelium (**Figure 3.1**). However, it was absent from the uppermost differentiated layers of the epithelium, which contain post-mitotic terminally differentiated squames (**Figure 3.1**). The relative intensity and immunohistochemical positivity for FOXM1 in

human oral mucosa appeared to be higher compared to what was previously observed in normal human epidermis (Teh et al., 2002). This could be attributed to the fact that normal oral epithelium cell renewal occurs much faster than that of the epidermis (Garant, 2003). Consequently, FOXM1 protein levels could be elevated, either because it is required for, or as a result of increased proliferation of the oral epithelium compared to human epidermis. The localisation, regulation and relative expression of FOXM1 during human oral epithelial tissue renewal has been more extensively investigated and will be discussed later in **Chapter 5**.

3.3.2 FOXM1 Overexpression in OSCC Tissues and Cell Lines

In light of the fact that some FOX genes are active in the same developmental settings with sonic hedgehog signalling (Shh) in mice (Mahlapuu et al., 2001), FOXM1 was identified as downstream target of Shh effector, GLI1, during the generation of human basal cell carcinoma (Teh et al., 2002). This provided the first direct evidence for the involvement of FOXM1 in human carcinogenesis, and further studies have established that upregulation of FOXM1 is a common event in majority of human solid malignancies, strongly suggesting an important role for this transcription factor in the manifestation and/or the progression of human tumourigenesis. Several studies suggest that FOXM1 is directly associated to the transformation potential of human cells (van den Boom et al., 2003; Pilarsky et al., 2004; Wonsey and Follettie, 2005; Madureira et al., 2006). In the epithelial context, FOXM1 protein elevation has been detected in the cases of human breast, lung, cervical, and gastric carcinomas (Wonsey and Follettie, 2005; Bektas et al., 2008; Chan et al., 2008; Francis et al., 2009; Yang et al., 2009; Zeng et al., 2009). Importantly, FOXM1 expression shows a gradual elevation toward the generation of lesions of cervical intraepithelial neoplasia III (severe dysplasia), and further increases are detected in fully formed cervical SCCs (Chan et al., 2008), while a similar correlation between tumour grade and FOXM1 expression was recently shown in the case of human lung cancer (Yang et al., 2009).

In agreement with its anticipated role in carcinogenesis, FOXM1 protein levels were significantly upregulated even in very early lesions of mild oral dysplasias (**Figure 3.1**). FOXM1 protein levels progressively increased through moderate and severe oral dysplasias, to maximum levels of expression observed in established carcinoma

in situ (CIS) and lymph node metastases (**Figure 3.1** and **Appendix 1**). This expression pattern is consistent with evidence from numerous studies suggesting that FOXM1 has multiple roles in human tumour development and metastasis (see also **Chapter 1, section 1.4.6**)

The same expression pattern, in terms of intensity and intracellular localisation, was also observed in cultured oral keratinocytes, obtained from oral epithelial dysplasias and OSCC tumours. Although oral keratinocytes derived from clinically normal oral mucosa display FOXM1 protein levels lower than those observed in neoplastic cells, FOXM1 was still abundantly detected in majority of normal oral keratinocytes. Since FOXM1 expression is tightly linked to the cycling status of cells, young normal oral keratinocytes were grown for a maximum of 3-4 PD before detection of endogenous levels of FOXM1, to avoid any growth inhibitory effects that may arise from *in vitro* senescence of primary cells. Early passage normal human keratinocytes can undergo rapid cell division when initially expanded *in vitro*, which can possibly explain the fact that a large majority of keratinocytes was stained positive for FOXM1 in culture, compared to normal oral mucosa tissue *in vivo*. Nevertheless, in comparison to normal oral keratinocytes, the intensity of FOXM1 immunoreactivity was significantly elevated in neoplastic keratinocytes, which was also evidenced by elevated FOXM1 protein levels in total cell protein extracts.

Since FOXM1 is a proliferation associated transcription factor, it is possible to assume that the apparent increase of FOXM1 expression in neoplastic cells is an outcome of their increased proliferation rate. However, most of premalignant and OSCC cell lines examined here had similar, or even reduced, proliferation rates (personal observation) than young early passage normal oral keratinocytes grown under optimum conditions in serum free (feeder layer free) with low or high calcium, as well as in serum containing medium in the presence of NIH3T3 feeder layers. Similarly, upregulation of FOXM1 was also found in transformed human breast cancer cell lines when compared to their un-transformed, but proliferatively active counterparts (Wonsey and Follettie, 2005; Madureira et al., 2006). This strongly suggests that the effect of FOXM1 expression is also involved in processes other than cell proliferation, and could be directly associated with malignant

transformation of human cells. This is also consistent with the demonstration that FOXM1 and Ki67 proliferation marker, which show limited co-localisation in human basal cell carcinomas (Teh et al., 2002).

3.3.3 FOXM1 Isoform Specific Expression in OSCC Keratinocytes

The FOXM1 gene locus produces three separate isoforms; FOXM1A, FOXM1B, and FOXM1C, by alternative splicing of the A1 and A2 exons. Although FOXM1 protein elevation could be readily detected in pre-malignant and OSCC tissues (**Figure 3.1**), this method did not allow discrimination between individual isoform expression. By using isoform specific primers, it was found that although all the expression of all FOXM1 isoforms was elevated in OSCC derived keratinocytes, only FOXM1B and C were significantly and consistently upregulated in pre-malignant and OSCC keratinocytes (**Figure 3.7**). Since all isoforms are generated by a common FOXM1 gene locus, the relative differences in the abundance of mRNA of each isoform can be attributed to post transcriptional modifications, which may influence the stability of distinct FOXM1 isoform mRNAs. The inability of FOXM1A to transcativate downstream targets (Ye et al., 1997)may potentially render the expression of this isoform unnecessary for processes that are otherwise efficiently executed by the remaining functional FOXM1 isoforms. Consequently, there would be no selective advantage for neoplastic oral keratinocytes to enhance the stability of mRNA that encodes a transcriptionally inactive isoform. Gene expression and protein translation can be influenced by factors such as mRNA stability/decay (Ross, 1995; Guhaniyogi and Brewer, 2001) as well as by other regulatory mechanisms involving microRNA (miRNA) expression and miRNA/mRNA interactions which can lead to suppression of gene expression through mRNA degradation (Filipowicz et al., 2008). Although interesting and novel, further studies are required to delineate the post-transcriptional regulation of differential FOXM1 isoform mRNA abundance in human oral cancer cells.

3.3.4 Overexpression of FOXM1 Downstream Targets in Oral Cancer

FOXM1 protein localisation becomes increasingly nuclear in neoplastic cultured oral keratinocytes (**Figure 3.2**), which agrees with *in vivo* observations (**Figure 3.1**). Upon nuclear translocation, and protein phosphorylation, FOXM1 can efficiently bind to genomic DNA, to activate transcription of a multitude of genes,

most of which are involved in mitotic progression (Wang et al., 2005; Laoukili et al., 2007). The expression signature of OSCC derived keratinocytes (**Figure 3.4**), further suggests that OSCC derived keratinocytes retain elevated, active levels of FOXM1 protein, which activates important mitotic regulatory proteins including cyclin B1 (CCNB1), centromere protein A (CENP-A), centromere protein (CENP-F), and never in mitosis gene a-related kinase 2 (NEK2). CENP-A and CENP-F have vital roles in centromere formation and chromosome seggregation respectively (Howman et al., 2000; Wonsey and Follettie, 2005), while NEK2 kinase is an important regulator of centrosome disjunction (Faragher and Fry, 2003). Importantly, all of the above mitotic regulatory proteins have been found to be overexpressed and/or amplified (genomic locus amplification) in variety of human malignancies and tumour derived cell lines (Tomonaga et al., 2003; Perez de Castro et al., 2007).

Consistent with the observation that FOXM1 and its downstream targets are upregulated in OSCC tissues and cultured keratinocytes respectively, CENP-F protein levels are also elevated in oral leukoplakias and high degree dysplasias (Liu et al., 1998), while a subset of head and neck tumours exhibits CENP-F gene amplification and increased gene expression (de la Guardia et al., 2001). The expression of NEK2 has not yet been reported as being elevated in human oral carcinomas, but evidence suggests that its expression is highly de-regulated by overexpression of HPV type16 E6 and E7 (risk factor associated with a subset of OSCC) oncoproteins in human epidermal keratinocytes (Patel et al., 2004). The fact that FOXM1 acts as a downstream effector of E7 (Luscher-Firzlaff et al., 1999) protein raises the possibility FOXM1 may be mediating the upregulation of NEK2 in a proportion of OSCC that are associated with HPV infection.

3.3.5 CEP55 and HELLS are Novel Downstream Targets of FOXM1 in OSCC

The finding that FOXM1B-induced malignant transformation is accompanied by genomic amplification of CEP55 and HELLS (Gemenetzidis et al., 2009), raised two important possibilities. First, both genes are critical for malignant transformation of pre-malignant oral keratinocytes, and second FOXM1B may be the main regulator of both genes during that process.

The evidence presented here suggest that both CEP55 and HELLS are highly overexpressed in pre-malignant and OSCC derived keratinocytes (**Figure 3.9**), confirming the prediction that both genes might have an important role in the initiation and/or progression of head and neck cancer. CEP55 is strictly expressed at mitosis, during which it plays a crucial role in cytokenesis (Fabbro et al., 2005). Following the observation that CEP55 and FOXM1 tightly linked with OSCC initiation and progression (Gemenetzidis et al., 2009), a study further confirmed that CEP55 is correlated with aggressiveness of oral squamous cell carcinomas (OSCCs), and further suggested that CEP55 promotes cell migration and invasion through increased FOXM1 and matrix metalloproteinase-2 (MMP2) activity (Chen et al., 2009a). CEP55 overexpression has also been reported in hepatocellular (Chen et al., 2007), lung (Chen et al., 2009b), and breast (Martin et al., 2008) carcinomas. Most importantly, the latter study has also established that FOXM1 and CEP55 are amongst the signature prognostic markers which predicted breast cancer outcome (Martin et al., 2008). Lymphoid specific helicase (LSH or HELLS) belongs to the family of SNF2/helicases/chromatin remodelling proteins (Geiman et al., 1998), and has been shown to be a major regulator of DNA methylation (Dennis et al., 2001). A recent study demonstrated that overexpression of LSH is sufficient to delay *in vitro* senescence of human fibroblasts by silencing the expression of p16INK4a (Zhou et al., 2009). HELLS has been previously linked to human carcinogenesis, since its overexpression has been reported in leukaemia (Lee et al., 2000), non-small cell lung carcinomas (Yano et al., 2004), breast cancer (Einbond et al., 2007), and melanoma (Ryu et al., 2007).

It is demonstrated here, that FOXM1 is potentially having an important role in the regulation of CEP55 and HELLS since ectopic expression of FOXM1B alone was sufficient to induce the expression of both genes in primary human oral keratinocytes (**Figure 3.10**). This, along with the high correlation exhibited by FOXM1B and CEP55 expressions in neoplastic keratinocytes, prompted investigation into whether FOXM1B can directly induce the expression of CEP55. Putative DNA binding sites for FOXM1 protein were identified within the CEP55 promoter, and following ChIP-qPCR, it was confirmed that FOXM1B protein can directly bind to this specified region of the CEP55 promoter. This finding fits with the fact that FOXM1 is a critical regulator of mitotic proteins (Laoukili et al., 2007),

and is in line with the fact that depletion of FOXM1 mRNA (siRNA against FOXM1) from breast carcinoma cell lines, leads to dramatic down-regulation of CEP55 expression levels (Wonsey and Follettie, 2005) (Retrieved GEO Data Sets from Affymetrix Gene Expression Analysis; see **Appendix 3**). The finding that FOXM1B induced the expression of HELLS, is indeed an intriguing observation since, unlike most FOXM1 targets, HELLS is not directly linked to mitotic progression. This interaction seems to be indirect, since FOXM1 did not bind within the 1Kb putative promoter of HELLS (Gemenetzidis et al., 2009). However, the existence of a FOXM1 bindging site byond the 1Kbp promoter of HELLS remains to be investigated. Nevertheless, further investigation is needed to understand the mechanism by which FOXM1 enhances the transcription of HELLS, and whether through this interaction, FOXM1 may exert functions related to chromatin remodelling and regulation of gene transcription.

In addition to the upregulation of previously identified FOXM1 targets, this study identified two novel targets of FOXM1, and further showed that both are also significantly overexpressed in cells derived from pre-malignant lesions and OSCC tumours.

3.3.6 Potential Mechanisms Leading to FOXM1 Upregulation in OSCCs

Head and neck squamous cell carcinoma (OSCC), like many epithelial malignancies, arises from a common premalignant progenitor, followed by the outgrowth of clonal populations, which are usually subjected to cumulative genetic alterations that lead to invasive malignancy (Hunter et al., 2005). This multistep process involves the inactivation of tumour suppressor genes and activation of proto-oncogenes as a result of deletions, point mutations, promoter methylation and gene amplification (Perez-Ordonez et al., 2006). Which of these mechanisms contributes the most to FOXM1 upregulation is currently unknown. *FOXM1* gene locus (12p.13) was found to be amplified in keratinocytes derived from primary OSCCs. However, the very low frequency of gene amplification (only 1 out of 7 OSCC related studies has reported 12p13 amplification, which was found in MD886 OSCC keratinocytes) (Rao et al., 1994; Sreekantaiah et al., 1994; Mertens et al., 1997; Bockmuhl et al., 1998; Jin et al., 2000; Singh et al., 2001), suggests that this is probably a late event occurring in only a small subset of tumour cells, and thus

unlikely to be the sole explanation for the high-level overexpression of FOXM1 in majority of OSCCs.

Since FOXM1 is deregulated at both the transcription and protein levels in oral pre-malignant and OSCC tissues and cultured keratinocytes, the pathway, or pathways, leading to its upregulation may influence both FOXM1 protein expression and stability. In terms of gene transcription, FOXM1 is regulated by proliferative stimuli, some of which have also been implicated in the pathogenesis of oral squamous cell carcinoma. c-MYC transcription factor, and HIF-1α (the active HIF-1 subunit) transcription factor subunit, can both induce transcription of FOXM1 by direct binding to its promoter (Fernandez et al., 2003; Wierstra and Alves, 2007; Blanco-Bose et al., 2008; Xia et al., 2009), and more importantly, they have been reported to be either overexpressed or amplified in cases of OSCCs (Haughey et al., 1992; Eversole and Sapp, 1993; Porter et al., 1994; Aebersold et al., 2001; Beasley et al., 2002). Moreover, the upstream regulator of FOXM1, GLI1, has been found overexpressed in oesophageal tumours and tumour derived cell lines, suggesting a mechanism of FOXM1 upregulation similar to that observed in BCCs (Teh et al., 2002; Mori et al., 2006). The recent finding that GLI2, which can directly bind to, and activate the promoter of GLI1 in human epidermal keratinocytes (Regl et al., 2002), is amplified in OSCCs (Snijders et al., 2009), suggests a mechanism whereby FOXM1 increased expression may be the outcome of a regulatory pathway between oncogenic transcription factors GLI1, and GLI2. Recent studies showed that FOXM1 expression is negatively regulated by the tumour suppressor p53, in human cell lines (Barsotti and Prives, 2009; Pandit et al., 2009). Since inactivating mutations of the latter are frequently seen in pre-malignant lesions of the oral mucosa and HNSCCs (Somers et al., 1992; Boyle et al., 1993; Shahnavaz et al., 2000) as well as in HNSCC derived keratinocytes (see **Table 2.1**), it is possible to suggest that such a mechanism, alone or in combination with those suggested above, contributes to the apparent elevation of FOXM1 transcription levels. Although the information available in this study does not allow definitve correlations to be made, it is interesting that the expression levels of FOXM1 (isoforms B and C) are very similar between HNSCC derived keratinocytes with reported *TP53* mutations or expression loss (DOK, POE9n, POE9n-hTERT, BICR31; see Materials and

Methods **Table 2.1**; see **Figure 3.7**), suggesting that such an event may be an important determinant of FOXM1 gene transcription control.

Arguably, the abundance of information regarding FOXM1 protein stability and activation, provide much room for speculation, as to what may be a possible mechanism for the elevated levels of FOXM1 protein and its downstream transcriptional activity in OSCCs. The activity of FOXM1 can be increased by many important proliferative signals including MEK1, Ras, CyclinD1/Cdk4, CyclinE/Cdk2, CyclinA/Cdk1, CyclinB/Cdk1, and by inhibition of GSK3-α (Wierstra and Alves, 2007). One of the best documented molecular events in the generation of HNSCCs is that of CyclinD1 (CCND1) upregulation, which is frequently followed by whole gene amplification (Jares et al., 1994; Wang et al., 1995; Izzo et al., 1998). CyclinD1 exerts its proliferative effect by forming complexes with cyclin dependent kinases (CDKs), which phosphorylate and inactivate retinoblastoma (Rb) tumour suppressor protein, thereby allowing progression through G1 phase (Sherr and Roberts, 1999). Rb protein normally retains FOXM1 in an inactive form by direct binding to its central N-terminal repressor domain (NRD-C) (Major et al., 2004; Wierstra and Alves, 2006d) (see also **Chapter 1, section 1.4.5**). CyclinD1 upregulation can therefore augment FOXM1 activity in two distinct ways. First, it does so by releasing the NRD-C of FOXM1 from Rb, and second by further releasing the transactivation domain of FOXM1 from auto-repression by its own N-terminus (see also **Chapter 1, section 1.4.5.2**). Once released, FOXM1 is further subjected to post-translational modifications (mainly phosphorylation) by Cyclin/Cdk complexes that enhance its stability, as well as its transactivation and DNA binding activity (Major et al., 2004; Wierstra and Alves, 2006b) (discussed in more detail in **Chapter 1, section 1.4.5.1**). Prior to the onset of anaphase, the hyperphosporylated forms of FOXM1 rapidly decrease, and FOXM1 protein gets rapidly degraded by ubiquitin ligase complex APC/Cdh1 which can directly bind to the N-terminal domain of FOXM1 (Laoukili et al., 2008a; Park et al., 2008). Although no inactivating mutations have been reported for APC/C (or its co-activator Cdh1) in HNSCCs, many of its degradation targets/substrates are deregulated in human malignancies, including carcinomas of the head and neck (Lehman et al., 2007).

A more detailed comparison between different cell lines with defined genetic hits may help to further understand the mechanisms by which FOXM1 expression is upregulated. For example, the isolation and examination of the molecular background of cell lines which do not express high levels of FOXM1 (e.g. H357, BICR31, SCC4, PE/CA-PJ15) would be of great value. For example, it is possible to examine how the expression of FOXM1 is influenced by genetic modification that deregulates the mechanism of several candidate upstream regulators of FOXM1, such as the Rb/p16INK4a/CyclinD1 pathway of cell cycle control which reportedly is one of the most important detemrminants of FOXM1 expression and protein stability. Furthermore, pre-malignant lesion-derived and OSCC tumour-derived cells can be extremely useful in examining all of the aforementioned pathways which directly and indirectly influence the expression and protein levels of FOXM1, and are implicated in the *in vivo* tumourigenesis of oral squamous cell carcinoma. This would further help to elucidate the exact mechanism of why FOXM1 is upregulated both in early as well as in later stages of epithelial malignant transformation *in vitro*.

It was found it this study that FOXM1 expression and subsequent protein activity were significantly upregulated when oral keratinocytes were exposed to one of the major alkaloids found in tobacco, nicotine, at concentrations that are relevant to tobacco chewers (0.01 μM -100μM) (**Figure 3.8**). Importantly, this response remained intact in normal human oral keratinocytes, indicating that the expression FOXM1 can be directly induced by nicotine, even in a normal non-aberrant molecular background. This is surprising since nicotine is not perceived as being a carcinogen, and is therefore being used as a frontline measure for tobacco replacement. However, recent studies have also demonstrated the proliferative and angiogenic effects of nicotine in different cancer cell lines and established tumours *in vivo* (Heeschen et al., 2001; Heeschen et al., 2002; Dasgupta and Chellappan, 2006; Dasgupta et al., 2009). Interestingly, nicotine has been shown to mediate cell proliferation by down-regulating the activity of Rb protein and subsequent activation Cyclin/Cdks, E2F's 1, 2, and 3, and by activation of Cyclin D (Chu et al., 2005; Dasgupta et al., 2006). Perturbation of the G1 control has an immediate impact on FOXM1 expression and stability, and therefore nicotine treatment could have indirectly led to the dramatic upregulation of FOXM1 observed in oral

keratinocytes (**Figure 3.8**). Given that tobacco (both smoke and smokeless form) is a major risk factor contributing to the genesis of HNSCC, it is plausible to suggest that repeated and continuous exposure of the oral epithelium to nicotine, can potentially contribute to the overexpression of FOXM1 in early pre-malignant lesions. This, in combination with previously discussed mechanisms, may account for the high level overexpression of FOXM1 observed at later stages of these tumours. Although *in vitro* evidence from previous work done in our group, support the fact that FOXM1 and nicotine work synergistically to promote malignant transformation (Gemenetzidis et al., 2009), future studies are needed to delineate whether FOXM1 can be physiologically induced by nicotine *in vivo*, and whether this response is functionally related to HNSCC development.

The activity of FOXM1 depends on many different important cell cycle regulators. The fact that many of the latter are frequently deregulated in human malignancies, may explain why FOXM1 is one of the most commonly upregulated genes in human malignancies, including HNSCCs. The fact that FOXM1 can significantly contribute to, and promote, tumourigenesis (Kalinina et al., 2003; Kalinichenko et al., 2004; Kim et al., 2006; Liu et al., 2006; Dai et al., 2007; Wang et al., 2007; Wang et al., 2008a; Wang et al., 2008b; Gemenetzidis et al., 2009), suggests that its upregulation is an important step in the generation and progression of early pre-malignancies, which is also supported by the fact that its expression is significantly elevated in numerous human pre-cancerous lesions (Chan et al., 2008; Gemenetzidis et al., 2009).

Chapter 4

FOXM1B IS EXPRESSED AT MITOSIS AND INDUCES GENOMIC INSTABILITY IN HUMAN KERATINOCYTES

4 FOXM1B is Expressed at Mitosis and Induces Genomic Instability in Human Keratinocytes

4.1 Introduction

FOXM1 is a proliferation specific transcription factor, and as such, its expression is highly responsive to serum stimulation and cell cycle re-entry, possibly mediated by c-Myc/E2F dependent activation (Korver et al., 1997a; Laoukili et al., 2007; Blanco-Bose et al., 2008). Activation of FOXM1 occurs during late G1/S phase and reaches its peak at G2 phase and mitosis (Laoukili et al., 2008b). FOXM1 activation is also dependent on Ras/MEK/MAPK signalling (Major et al., 2004; Ma et al., 2005) and requires binding by cyclin E/A/Cdk2 complexes that facilitate its phosphorylation (Costa, 2005), and subsequent activation. In late G1, FOXM1 is also believed to regulate entry into the S-phase by promoting the degradation of key cell cycle inhibitors, $p21^{CIP1}$ and $p27^{KIP1}$ and by activation of CDC25A (Wang et al., 2002b; Costa, 2005).

FOXM1 is a major regulator of G2/M phase of the cell cycle, where a precise and controlled regulation of FOXM1 protein is required to ensure successful execution of the mitotic programme and the maintenance of chromosomal stability (Laoukili et al., 2005). Its downstream transcriptional targets comprise a variety of important G2/M regulatory proteins, including Plk1, Aurora B kinase, cyclin B, Cdc25B, Nek2 and CENP-F (Leung et al., 2001; Laoukili et al., 2005).

More recent studies have shown that expression and protein stability of FOXM1 is indeed tightly regulated by its N-terminal inhibitory domain, which can inhibit its transcriptional activity at the G1/S phase of the cell cycle, and also harbours specific APC/C recognition sites, that facilitate FOXM1 protein degradation following mitosis(Park et al., 2007; Laoukili et al., 2008a).

Here, a normal neonatal foreskin keratinocyte cell line immortalized by hTERT, N/TERT (Dickson et al., 2000), and a cervical cancer derived cell line, HeLa, were used to investigate the expression pattern of each of the three distinct FOXM1 isoforms during normal cell cycle. Furthermore, by using high efficiency retroviral mediated gene transfer, FOXM1B was stably introduced in N/TERT keratinocytes to investigate and define the cell cycle dependent distribution of FOXM1B protein.

It has been previously established that FOXM1 is critical for the regulation and maintenance of chromosomal stability (Laoukili et al., 2005). Given that genomic instability is a widespread feature of human tumours (Lengauer et al., 1998), and that FOXM1 is overexpressed in majority of human malignancies (Pilarsky et al., 2004), including OSCC as shown here (**Chapter 3**), and by work from our group (Gemenetzidis et al., 2009), this study set out to investigate the effect of FOXM1 overexpression in the maintenance of genomic stability. Due to the molecular and genetic aberrations present in many immortalised and/or tumour derived cell line systems, this study employed normal primary human epithelial keratinocytes derived from clinically normal epidermis and oral mucosa. To test this hypothesis, 10K SNP array was employed to investigate global genomic instability events.

4.2 Results

4.2.1 FOXM1 Isoform Expression Pattern during Cell Cycle

FOXM1 protein and mRNA levels vary during cell cycle progression. Its expression is activated at late G1/S and peaks at G2/M phase of the cell cycle, where it transactivates the vast majority of its downstream targets (Laoukili et al., 2008b). However, little is still known about the relative expression of FOXM1 specific isoforms throughout the cell cycle.

First, the endogenous expression patterns of FOXM1A, FOXM1B, and FOXM1C were investigated in N/TERT keratinocytes, using FOXM1 isoform specific qPCR. N/TERT cells were synchronized at the G1/S boundary by double thymidine block, and then released from cell cycle block. Cell cycle synchronization was confirmed by flow cytometry analysis (**Figure 4.1 A i, ii,**

iii). mRNA was extracted at regular time intervals and FOXM1A, FOXM1B, and FOXM1C mRNA copy numbers were independently quantified using qPCR. Surprisingly, only FOXM1B showed a significant (~2 fold) increase at 6 hours (corresponding to the time that cells pass through G2/M phase) after cell cycle was resumed (**Figure 4.1 Bi)**. FOXM1A and FOXM1C were fluctuating between 0.5-1 fold throughout the whole time course.

Due to the partial synchronization effect observed in N/TERT cells, HeLa cells that have been shown to be totally synchronized in culture following double thymidine block (Whitfield et al., 2002), were also used. FOXM1 isoform specific quantitation revealed that FOXM1B is again the only isoform being significantly expressed in response to cell cycle events (**Figure 4.1 Bii**). FOXM1 (all isoforms) induction started being evident at 4 hours (S phase entry), but only FOXM1B reached a maximum of 3.3-fold increase 6-8 hours after release, which correlates with the time at which HeLa cells undergo the first synchronous mitosis (Whitfield et al., 2002) (**Figure 4.1 Bii**). The higher fold increase in FOXM1B expression in HeLa cells, compared to N/TERT cells, could be attributed to the differences in the efficiency of synchronization between these two cell lines.

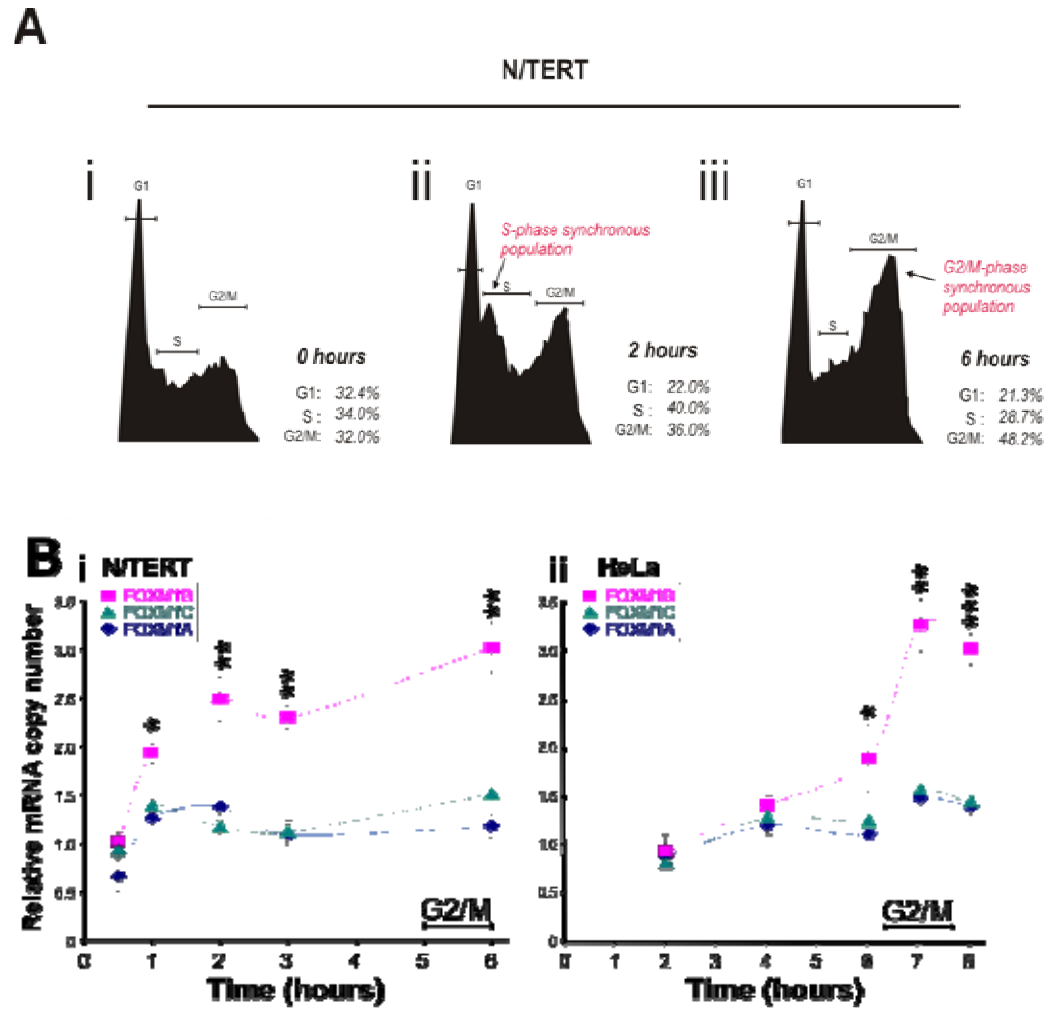

Figure 4.1: FOXM1B isoform expression is cell cycle dependent.

(A) N/TERT cells were released from double thymidine cell cycle block (G1/S synchronization) and were stained with propidium iodide, followed by flow cytometry analysis at 0hours **(i)**, 2hours **(ii)**, and 6hours **(iii)**. **(B) (i)** N/TERT cells were released from double thymidine cell cycle block (G1/S synchronization) and mRNA was harvested at regular time intervals. qPCR results indicated that FOXM1B was the only isoform that is significantly upregulated (*$P \leq 0.05$; **$P \leq 0.01$) during cell cycle re-entry. **(ii)** HeLa cells were released from double thymidine cell cycle block (G1/S) synchronization and mRNA was harvested at regular time intervals. FOXM1A and FOXM1C show an almost complete lack of induction throughout the cell cycle. FOXM1B shows a significant (**$P \leq 0.01$) increase (3.3 fold) at 6 hours and a 3 fold increase (***$P \leq 0.001$) at 8 hours after cell cycle re-entry.

4.2.2 Ectopic FOXM1B Expression Peaks at G2/M

A time-lapse video fluorescence microscopy was performed to visualize EGFP-FOXM1B protein expression during cell cycle. First, N/TERT keratinocytes were transduced with EGFP-FOXM1B retrovirus and allowed to express the transgene 72 hours prior to inducing growth arrest by growth factor deprivation for 18 hours. Next, cells were grown in normal growth

medium, and were subsequently observed at 20 minute intervals, using fluorescent time-lapse microscopy over a total time course of 72 hours. EGFP-FOXM1B expressing cells showed strong nuclear protein accumulation as evidenced by increased fluorescence beginning at 7 hours and reached maximum expression level (~3-fold, **Figure 4.2**) at 15-25 hours, subsequently fluorescence level returned to basal level at 48 hours. This result is consistent with endogenous FOXM1B mRNA expression levels in **Figure 4.1 Bi**. The delay in FOXM1B induction observed in **Figure 4.2**, was due to the fact that cells were synchronized at G0/G1 phase whereas cells in **Figure 4.1** were synchronized at G1/S boundary.

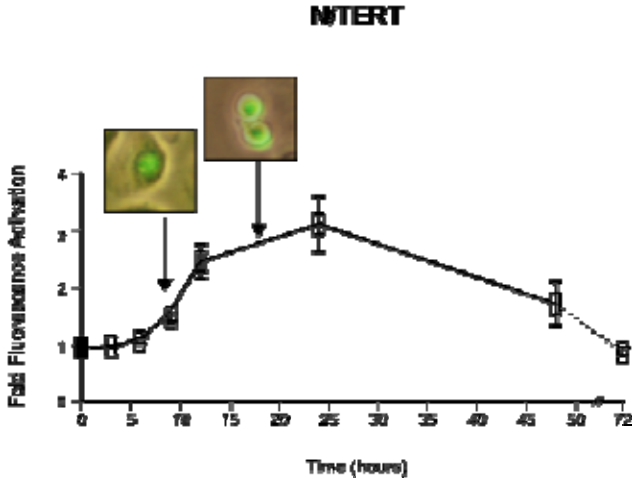

Figure 4.2: Exogenous FOXM1B protein expression is cell cycle dependent

Time-lapse fluorescent video microscopy of G0/G1 synchronized N/TERT keratinocytes. FOXM1B protein expression level (fluorescence intensity) was quantitated by digital densitometry. Graphical representation of FOXM1B expression pattern during cell cycle re-entry. Each point represents mean ± S.E.M. (n=6) fold fluorescence activation over control time 0 hour. Inset images show the cellular distribution of EGFP-FOXM1B protein at the indicated time points.

To further understand how FOXM1B protein is distributed throughout the cell cycle, N/TERT keratinocytes were stably transduced with EGFP-FOXM1B, and their cell cycle was examined by flow cytometry. Cells were stained with Hoechst-33342 and analyzed both for DNA content and green fluorescence (EGFP), which corresponds to exogenous EGFP-FOXM1B fusion protein. Populations of $EGFP^+$ and $EGFP^-$ cells were obtained by using wild type

N/TERT (wt) as a control cell line to acquire background levels of fluorescence. $EGFP^-$ cells profile exhibited a normal cell cycle distribution with a major peak at G1 (73.5%) and a minor peak at G2/M phase (16%) (**Figure 4.3 Ai**). $EGFP^+$ (EGFP-FOXM1B expressing) populations showed a significant ~3.3 fold increase in G2/M phase (52.7%) and a largely reduced G1 phase (33.8%) (**Figure 4.3 Aii**).

EGFP-FOXM1B expressing populations were then subdivided into low and high fluorescence intensity groups. Cells with low EGFP-FOXM1B expression show a relatively normal cell cycle (**Fig. 4.3 Bi**), whereas, 89% of cells expressing high levels of EGFP-FOXM1B were found to be exclusively in the G2/M phase of the cell cycle (**Fig. 4.3 Bii**). This clearly suggests a role for FOXM1B protein in late G1/S, but mainly in G2/M phases of human keratinocytes, and confirms that ectopic FOXM1B expression is regulated in a similar fashion to the endogenous one, as observed in normal N/TERT human keratinocytes.

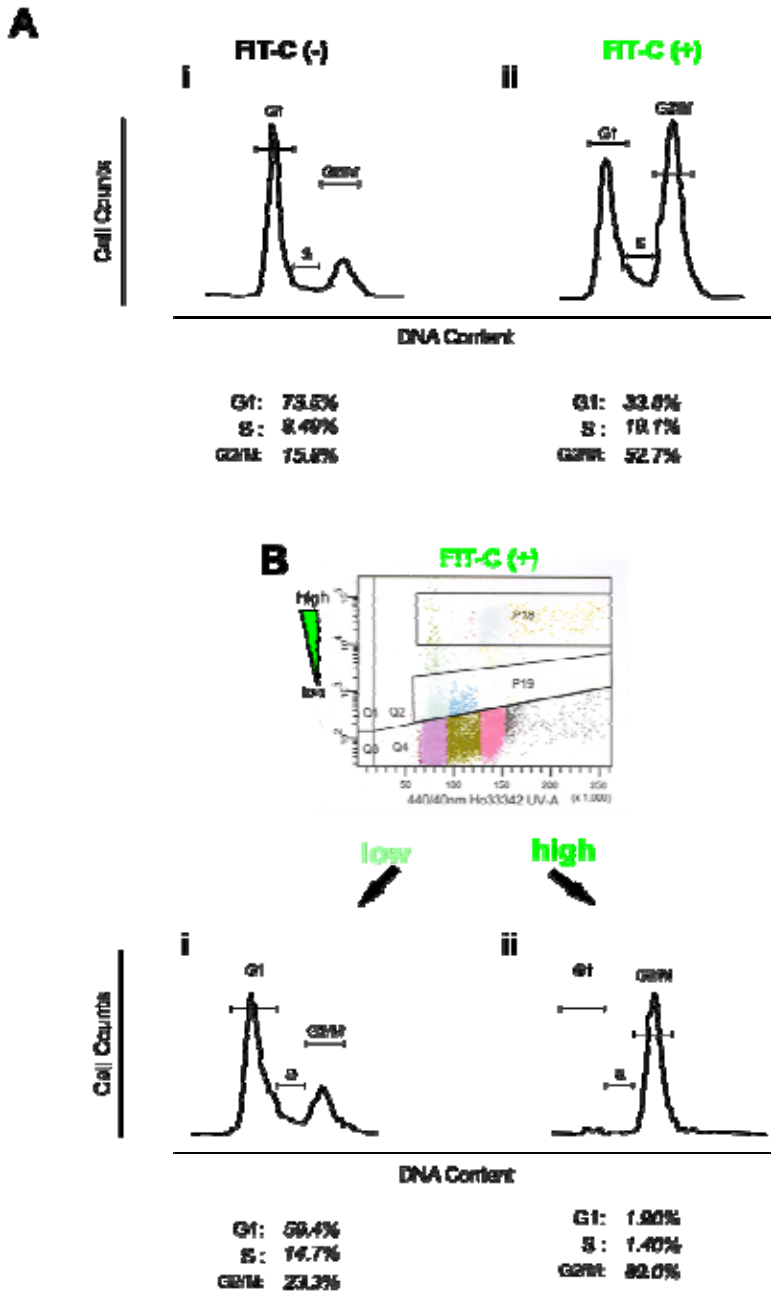

Figure 4.3: FOXM1B protein is present at G2/M phase of human keratinocytes.

(A) N/TERT human keratinocytes were transduced with EGFP-FOXM1B and stained with Hoechst 33342 prior to DNA content analysis using flow cytometry. EGFP (+) and EGFP (-) populations were discriminated and their cell cycles were obtained. The cell cycle distribution of EGFP-FOXM1B expressing cells is altered showing a significantly lower G1 phase and 3.4-fold increase at the G2/M phase of the cell cycle. **(B)** EGFP (+) cells were further sub-divided into two groups: low **(Bi)** and high **(Bii)** expression of EGFP-FOXM1B. Low expressing cells display a relatively normal cell cycle (Bi), while high EGFP expressing cells (Bii) were exclusively at the G2/M phase (89%).

4.2.3 Overexpression of FOXM1B induces Genomic Copy Number Alterations

It is well established that tumour progression requires sequential genomic alterations, and that FOXM1 has a role in the maintenance of genomic integrity. Since FOXM1 is strongly overexpressed in the majority of human malignancies, this study also investigated the effect of FOXM1 overexpression on the maintenance of genomic stability. Since only the B isoform of FOXM1 was preferentially expressed at mitosis (**Figure 4.1, 4.2, 4.3**), it was reasoned that this isoform may be predominantly involved in the execution of important mitotic processes, the deregulation of which could potentially affect the genomic stability epithelial keratinocytes.

Early passage primary normal human epidermal keratinocytes (NHEK) (P1) were either mock transduced (no transgene expression) or transduced with either EGFP control or EGFP-FOXM1B (over 95% gene delivery was observed), and were let to grow until confluent (96 hours), and gDNA was harvested for SNP array profiling (see also **Chapter 2, section 2.14**). SNP genotype profile from transduced cells were compared with the mock-transduced wild-type NHEK in order to obtain genomic instability data in the form of loss of heterozygosity (LOH) and copy number alterations (CNA) (**Figure 4.4**).

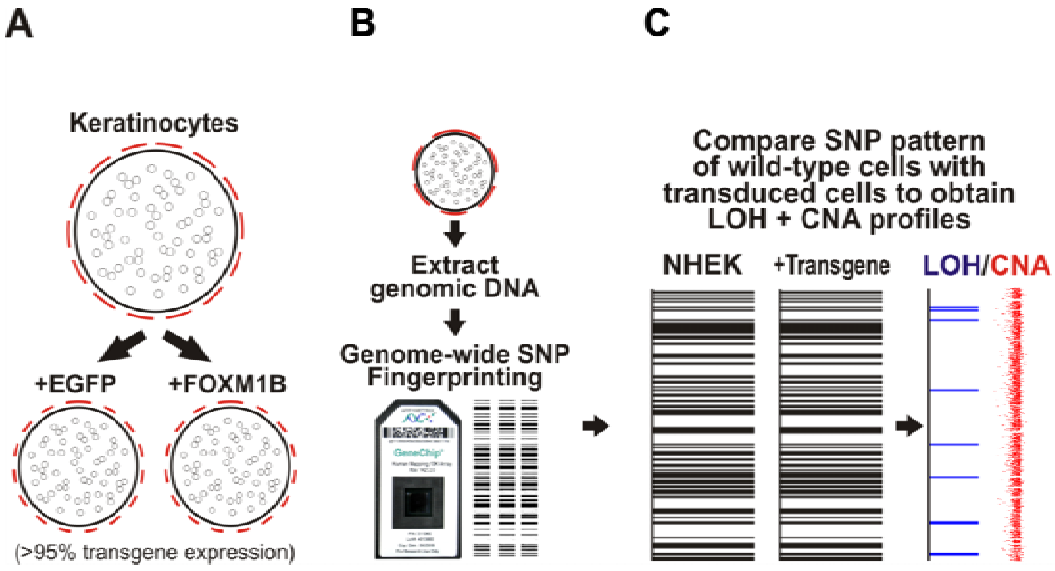

Figure 4.4: Detection of genomic instability events using 10K SNP array

(A) Early passage (P1) primary NHEK were either mock transduced, EGFP or FOXM1B transduced, left to grow for until confluent and **(B)** gDNA was harvested for SNP array analysis. **(C)** Loss of heterozygosity (LOH, blue lines) and copy number alterations (CNA, red dots) data were obtained by comparing test samples (EGFP or FOXM1B) with reference genome (mock transduced NHEK).

EGFP overexpression did not induce any detectable LOH or CNV in the wildtype control NHEK. In contrast, FOXM1B overexpression induced a low level but detectable genomic instability where a small number of SNPs had undergone LOH (**Figure 4.5 A, blue lines**). Interestingly, using Affymetrix Copy Number Analysis Tool (CNAT) algorithm to determine the likelihood of LOH (Huang et al., 2004), FOXM1B-expressing cells showed marked increase (at least 2-fold) in LOH likelihood compared to EGFP-expressing cells (**Fig 4.5 A, grey lines**). The increase in LOH likelihood and CNA in FOXM1B-expressing cells is not due to the decrease in SNP call rate because all 'No Call' SNPs were excluded from analyses. Four days of FOXM1B expression in primary NHEK may not have sufficient time to accrue definitive LOH/CNA loci, which may explain the low number of SNPs acquiring LOH in the FOXM1B expressing cells. Nevertheless, this experiment shows that acute FOXM1B, but not EGFP, expression can induce genomic instability. Although FOXM1B did not significantly alter genome ploidy status, CNA (compare red-dot plots in **Figure 4.5 A** with **B**) appear to have more fluctuations (instability) in FOXM1B (genome ploidy ± sd: 1.999 ± 0.208; SNP Call: 97.27%) compared to EGFP (genome ploidy: 2.000 ± 0.122; SNP Call: 98.24%) expressing cells. In agreement, when examining the copy number of

individual SNPs, FOXM1B expressing cells showed ~10-fold increased in CNA (534 losses and 160 gains) compared to EGFP expressing cells showed almost negligible CNA (65 loss and 0 gain). Similar results were obtained from two further independent SNP array experiments with primary NHEK from 2 different normal skin tissues of healthy volunteers (**Figure 4.5 B**). The differing degree of FOXM1B-induced genomic instability of the three normal patients is likely due to individual's variations in intrinsic cellular susceptibility to oncogene expression. Overall on average, FOXM1B significantly (6.60-fold, *P<0.05, n=3; **Figure 4.5 C**) induced genomic instability in primary normal human keratinocytes. EGFP overexpression did not induce significant genomic instability. Consistently, FOXM1B overexpression produced the same effect in primary human oral keratinocytes (**Figure 4.5 E**) (Gemenetzidis et al., 2009).

Next, it was investigated whether the acute genomic instability induced by FOXM1B overexpression, was transient or stable. In a separate experiment, SNP array mapping was performed in NHEK transduced with either EGFP or FOXM1B at three consecutive passages (P1, P2 and P3; **Figure 4.5 D**). The SNP data showed that the genomic instability induced by FOXM1B was maintained and accumulated with increasing passage number. EGFP-expressing cells did not show accumulation of genomic instability with increasing passage number. At passage 3, the total number of SNP copy number instability accumulated in FOXM1B-expressing cells (112 losses and 272 gains; total: 384 CNA) was substantially (42.7-fold) higher than in EGFP-expressing cells (0 losses and 9 gains).

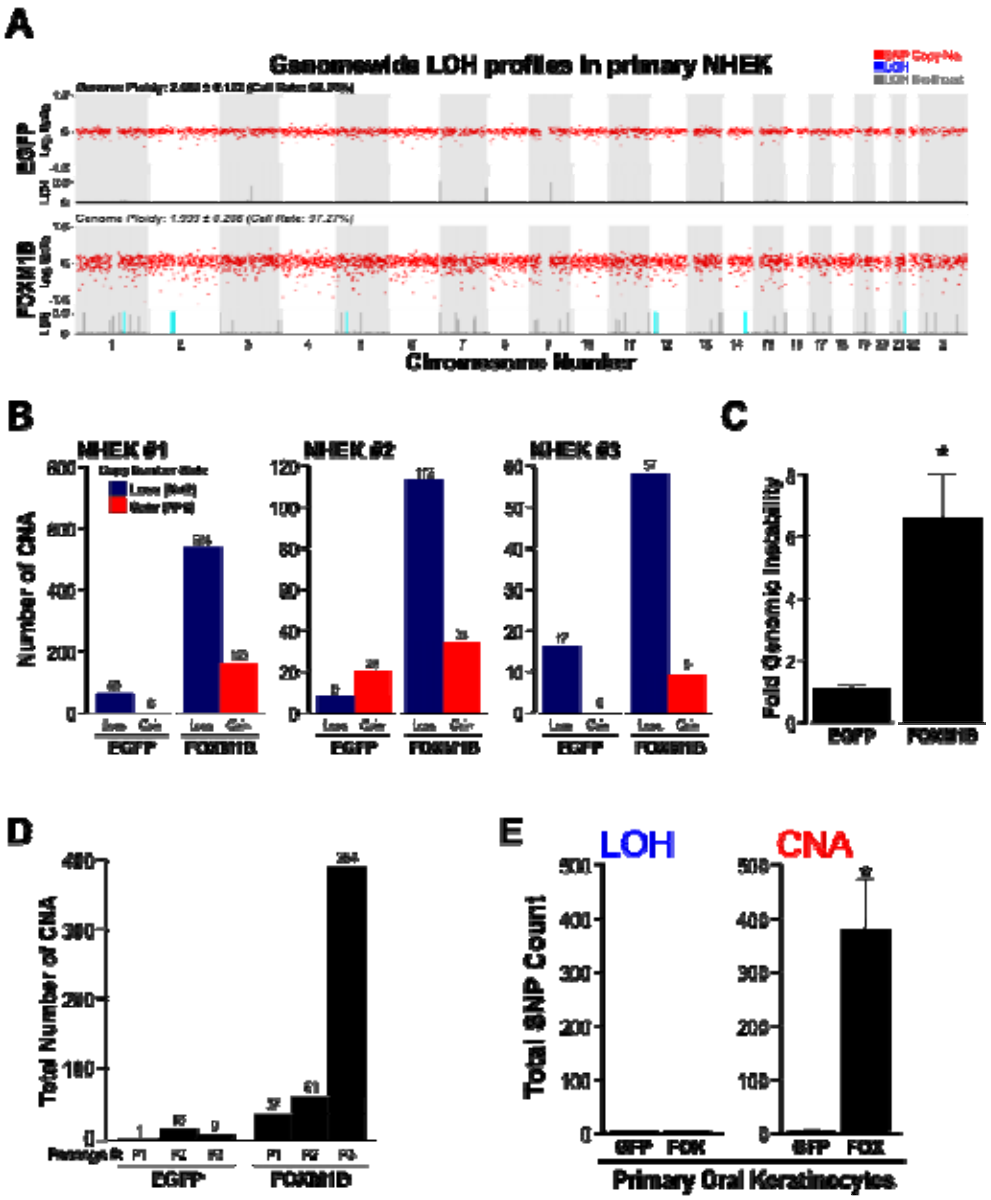

Figure 4.5: Acute overexpression of FOXM1B induces genomic instability in primary NHEK

(A) CNA (Log 2 ratio, red dots), LOH (blue lines) and LOH likelihood (grey lines) plots for EGFP or FOXM1B expressing cells. LOH likelihood was calculated based on Affymetrix GTYPE algorithm. **(B)** Three normal healthy primary keratinocytes (NHEK#1-3) SNP copy number analysis showing CAN as losses (N<2) or gains (N>2) in EGFP and FOXM1B overexpressing NHEK, respectively. **(C)** Average fold-increase in CNA of the tree normal primary NHEK cells in (C). *(P<0.05) indicates significant increase in FOXM1B-induced CNA. **(D)** FOXM1B-induced CNA (total SNP undergoing CNA as indicated above each bar) showed gradual accumulation during primary NHEK culture (3 passages, P1, P2 and P3). **(E)**Total number of SNPs that show copy number alterations (CNA), as observed in primary human oral keratinocytes overexpressing either EGFP or FOXM1B. Bars represent the mean ± S.E.M. of duplicate samples. *$P \leq 0.0.5$*

4.2.4 Genotoxic Stress Cooperates with FOXM1B to Promote Genomic Instability

The finding that FOXM1B expression induces genomic instability led to the hypothesis that upregulation of FOXM1B may predispose cells to oncogenesis by synergistically potentiating genomic instability induced by DNA damaging agents such as UVB. To test this hypothesis, the levels of genomic instability were quantified following UVB exposure on primary NHEK cells expressing either EGFP or FOXM1B. Unfortunately, following UVB, primary NHEK (both EGFP and FOXM1B expressing cells) undergo terminal differentiation and cell death which did not allow the clonal expansion of UVB resistant cells hence precluding further experiments. Instead, this experiment was performed using the immortalised N/TERT cells whereby UVB was used to induce >95% cell death and ~5% of surviving cells were allowed to proliferate (~50 days in culture) and gDNA was harvested for SNP array analyses. In agreement with the above hypothesis, following UVB exposure, cells overexpressing FOXM1B, but not EGFP, showed dramatic genomic instability especially in chromosome 6 and 7 as illustrated in **Figure 4.6**. EGFP-expressing cells showed low levels of random CNA throughout the genome and no LOH was detected. In contrast, FOXM1B-expressing cells showed specific genomic instability in two chromosomes (6 and 7) where a high number of CNA was observed in groups of no less than 16 adjacent SNPs each. LOH as a result of copy number loss was detected at 6q25.1-6q25.3 (SNP location: 149761596 to 160783097), whereas, copy number gain was detected in most of chromosome 7 (7p21.3-7q36.3). The copy number gain in chromosome 7 did not amount to LOH status. This could be reflecting a mix population of cells bearing either without or with CNA in chromosome 7. It was hypothesised that given a longer proliferation time after UVB exposure, cells bearing copy number gain in chromosome 7 would be positively selected and resulted in an LOH status detectable by the SNP array. This also indicates that LOH/CNA at 6q represents an earlier genomic instability event preceding CNA of chromosome 7 in the FOXM1B-expressing cells following UVB exposure.

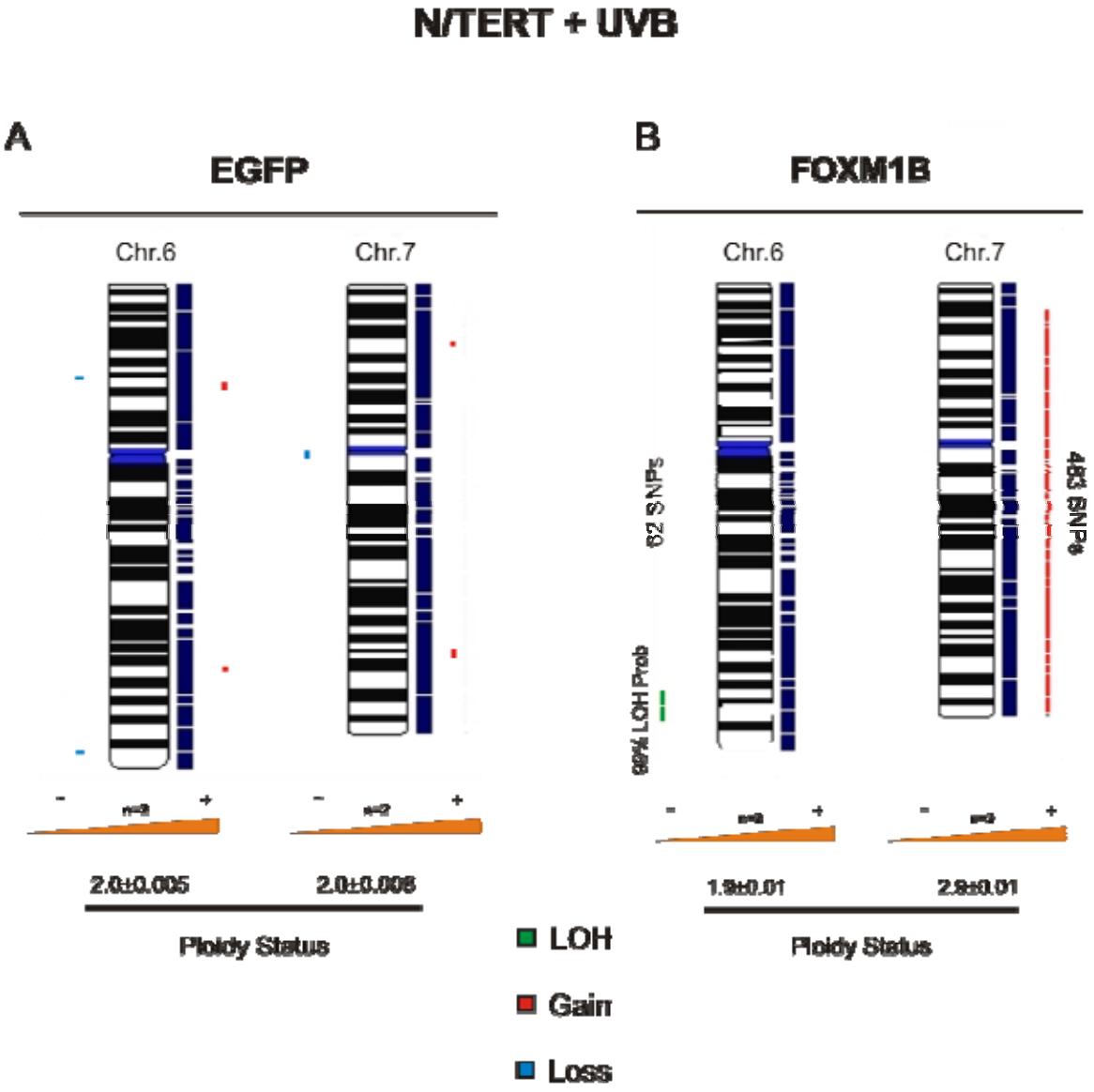

Figure 4.6: FOXM1B, but not EGFP, enhances LOH and CNA formation in N/TERT cells that survived UVB insult.

N/TERT cells were transduced with either **(A)** EGFP or **(B)** EGFP-FOXM1B and were UVB irradiated with 10mJ/cm^2. Cells were allowed to expand during a period of 4 weeks and gDNA was extracted. LOH and CNA analysis revealed gross chromosomal abnormalities in EGFP-FOXM1B expressing cells but not in EGFP expressing cells. LOH, copy number gains and copy number losses are shown as indicated. EGFP expressing N/TERT cells show random CNA compared to EGFP-FOXM1B where there is an almost complete chromosome gain on Chr.7 and a large region that had undergone LOH on Chr. 6q25.1-6q25.3. LOH Prob=LOH Probability as calculated by Affymetrix GTYPE Software.

4.3 Discussion

4.3.1 Cell Cycle Dependent Expression of FOXM1

Previous studies have investigated the expression pattern of FOXM1 during the cell cycle of mammalian cells (Korver et al., 1997a; Major et al., 2004; Ma et al., 2005; Laoukili et al., 2008b; Park et al., 2008). FOXM1 transcription factor is induced at both the mRNA and protein levels, when cells are stimulated to re-enter the cycle, and is further subjected to post-translational modifications, which result in the stabilization and further activation of the protein, when cells are entering G2/M phase. However, the role of each of the three FOXM1 isoforms in cell cycle remains unclear. Since there is evidence (**Figure 3.6, 3.7**) that FOXM1 isoforms can be differentially expressed in normal and tumour derived keratinocytes, this study aimed to investigate how each of the three isoforms is regulated during the cell cycle of human cells.

By using synchronous cultures of N/TERT human keratinocytes and HeLa cells, it was confirmed that while all FOXM1 isoforms are slightly induced upon cell cycle re-entry, only the expression of FOXM1B was significantly induced during G2/M. The time of the strongest FOXM1B induction is consistent with the time during which N/TERT (**Figure 4.1**) and HeLa cells go through the first synchronous mitosis (Whitfield et al., 2002). The lack of induction in the other two FOXM1 isoforms agrees with the fact that (**a)** FOXM1A is a transcriptionally inactive isoform (Ye et al., 1997) and (**b)** FOXM1C, although active, its mRNA remains similar between asynchronous, G1, S, or G2 synchronized 3T3 and BJ1 fibroblasts (Ma et al., 2005). FOXM1C is the most abundantly expressed isoform in human cell lines and various mouse tissues (Teh et al., 2002; Ma et al., 2005), while FOXM1B is expressed at low levels (Teh et al., 2002) and thus previous studies using semi-quantitative approaches have failed to detect FOXM1B mRNA expression, in either asynchronous, or synchronized *in vitro* cell systems (Ma et al., 2005). The absolute qPCR used in this study revealed the relative levels of FOXM1 isoform expression in human cells. This is the first experiment demonstrating a differential expression pattern of FOXM1 isoforms and that FOXM1B exhibits the most prominent cell-cycle dependent expression pattern during cell cycle.

Given that downstream target transactivation requires active proteins to be present, FOXM1B mRNA transcripts may be needed for the continuous supply of translated protein during late S and G2/M phases of the cell cycle. To examine the relationship between FOXM1B mRNA expression and protein translation, ectopic EGFP-FOXM1B was introduced in N/TERT keratinocytes. EGFP-FOXM1B protein was directly visualized by fluorescence microscopy in live human keratinocytes during a period of three days, which provided evidence for rapid protein turnover in cycling cells with no detectable cytoplasmic distribution. EGFP-FOXM1B fluorescence was highly restricted to the nuclei of dividing cells. Consistently, flow cytometry analysis revealed that FOXM1B protein was upregulated partly at the G1/S phase boundary, but its peak expression was mainly found at G2 phase and mitosis, following exactly the same cell cycle dependent distribution as predicted from mRNA expression analysis. This indicates that mRNA and protein levels of FOXM1B are tightly linked during cell cycle.

However, other studies have reported a different expression pattern of FOXM1, which is contradictory to the results presented here. In synchronized osteosarcoma U2OS cells, there was no evidence of a cell cycle dependent expression of neither FOXM1B isoform (Major et al., 2004) nor FOXM1 protein as a whole (all isoforms) (Laoukili et al., 2008b). This however is inconsistent with the fact that FOXM1 protein is rapidly degraded upon exit from mitosis (Laoukili et al., 2008a; Park et al., 2008), and therefore subsequent mitotic entry would require *de novo* synthesis of FOXM1 protein, unavoidably resulting in fluctuating protein levels throughout a normal cell cycle. This effect could be attributed to a specific property of the U2OS human osteosarcoma cell line, which may allow aberrant expression or abnormal stability of FOXM1, and therefore abolishing the intrinsic mechanism of FOXM1 regulation present in other cell line systems.

In contrast, the evidence presented here and in previous studies, in synchronous cultures of N/TERT, HeLa cells, Rat-1 fibroblasts, and BJ-1 human fibroblasts, showed that FOXM1 protein follows a cell cycle dependent distribution, with highest levels being observed always at G2/M (Korver et al., 1997a; Ma et al., 2005; Park et al., 2008), which is consistent with the fact that the downstream targets of FOXM1 are not induced until entry to G2/M (Leung et al., 2001; Laoukili

et al., 2005; Laoukili et al., 2008b).

Taken together, these data suggest that FOXM1B mRNA expression, protein translation and subsequent nuclear accumulation must occur very rapidly. This isoform expression pattern is also consistent with the fact that FOXM1 protein becomes detectable in late S and remains stable throughout G2 phase and mitosis in HeLa cells (Leung et al., 2001; Park et al., 2008). At least for FOXM1B isoform, this may be the predominant mechanism for its cell cycle dependent expression and activation, as opposed to FOXM1C, which responds to cell cycle events by translocation from the cytoplasm to the nucleus, which is sufficient for DNA binding activity during G2/M (Ma et al., 2005).

4.3.2 FOXM1 and Genomic Instability

It is now well accepted that the manifestation of a human tumour requires sequential genomic alterations (Vogelstein and Kinzler, 1998). The accumulation of such events is thought to be driven by an underlying genomic instability during the process of tumourigenesis, and although it appears to be a widespread feature of human malignancies (Lengauer et al., 1998), the originating stage of such genomic instability is not clearly defined. Evidence suggests that genetic instability appears at the early stages of human malignancy, slowly driving the clonal expansion of tumourigenic progenies. In human colorectal tumourigenesis, allelic imbalances have been observed in early adenomas, by using chromosome specific SNP markers (Shih et al., 2001). Similar genomic alterations have also been reported in metaplastic lesions of gastric carcinoma (Kobayashi et al., 2000), ulcerative colitis (UC) - associated neoplasia (Willenbucher et al., 1999), intraepithelial neoplasia of the vulva (Pinto et al., 2000), in dysplastic epithelium of Barrett's oesophagus (Galipeau et al., 1999), and in pre-neoplastic lesions of the breast epithelium (O'Connell et al., 1998; Gong et al., 2001).

This study has therefore focused in the genome-wide effects of FOXM1, aiming to provide a link between the established role of FOXM1 in the maintenance of genomic integrity (Laoukili et al., 2005), and the fact that it is overexpressed in early pre-malignant epithelial lesions (**Chapter 3**)

(Gemenetzidis et al., 2009). The evidence presented here are the first to show that constitutive and acute (4 days) expression of FOXM1B alone, is sufficient to induce LOH and CNA in primary human epidermal and oral keratinocytes. Furthermore, FOXM1B-induced genomic alterations were accumulated and amplified when these cells were passaged in culture (genomic instability). It is important to stress the fact that a SNP copy number loss, or gain at this stage, does not necessarily correspond to the loss or gain of gene loci that are important in cellular processes. These SNPs often comprise large segments of genomic DNA that may, or may not, contain genes with important regulatory functions. Therefore, the initial effects of FOXM1B on genome stability may not be readily assimilated to a genetic instability signature present in tumours. The latter is the culmination of many years of development, as a result of the positive selection and clonal expansion of populations with beneficial genomic alterations. The former, however, is suggesting that excessive accumulation of FOXM1B protein at mitosis (**section 4.2.2**; ectopic FOXM1B protein accumulates at G2/M phase of keratinocytes) is sufficient to disturb the genomic stability of human primary keratinocytes. Consistent with this notion, data obtained from genome-wide SNP analysis, across four individual primary keratinocyte cell lines overexpressing FOXM1B, did not show any trend of consensus genomic alterations. This leads to the anticipated conclusion that early genomic instability events introduced by overexpression of FOXM1B occur at random.

4.3.3 Clonal Expansion of Genetically Unstable Cells

The effect of FOXM1B occurred independently of any other stimuli, which suggests that its overexpression can generate a predisposition for the accumulation of genomic instability. Although FOXM1B overexpression alone is not sufficient to induce pathologically relevant genetic aberrations in this setting, it may trigger and facilitate the accumulation of subsequent oncogenic events required for malignant conversion. This is supported by recent studies showing that FOXM1 is linked to the progression of genomic instability in human cancer (Carter et al., 2006), and second that it can cooperate with environmental (i.e. UVB or carcinogens) stress to promote genomic instability (Gemenetzidis et al., 2009; Teh et al., 2010). The clonal

expansion of cells with beneficial genomic alterations can be expedited by selective killing of normal surrounding cells. It was therefore plausible to think, that if FOXM1B overexpression can promote genomic instability, a genotoxic insult would serve as a selection pressure for the clonal expansion of progenies that have acquired beneficial genomic alterations. Indeed, results presented here show that the genetic profile of UVB irradiated N/TERT keratinocytes expressing FOXM1B, showed gross chromosomal CNA and LOH following UVB exposure. Interestingly, numerous genes (including MAP3K7IP2, SUMO4, p34/ZC3H12D, LATS1, RAET1 cluster, ULBP cluster, AKAP12, ESR1, MYCT1, VIP, TIAM2, SOD2, WTAP, MAS1, SLC22A cluster, IGF2R, etc.) found within the FOXM1B-induced LOH at 6q25.1-6q25.3, have been previously linked to oncogenesis of various human cancers (Rabin et al., 1987; Chiu et al., 1999; Qiu et al., 2003; Jiang et al., 2006; Rong et al., 2006; Cao et al., 2007; Valdehita et al., 2007; Yildirim et al., 2007; Yoon et al., 2007; Jin et al., 2008; Kotsinas et al., 2008; Martinez-Galan et al., 2008; Wheatley-Price et al., 2008). Furthermore, genes including EGFR and IGFB1-3 found within the FOXM1-induced CNA gain in chromosome 7p12-22 were previously reported to be amplified in early stages of HNSCC (Patmore et al., 2005).

These observations suggest that overexpression of FOXM1B can render cells susceptible to the acquisition of additional genetic alterations, an effect that was largely accelerated by additional genotoxic stress. This is further supported by the established role of environmental DNA damaging insults in the genesis of tumours. Importantly, BCC tumours are strongly associated with skin exposure to UVB irradiation, and further to that, they exhibit both FOXM1B overexpression and genomic instability (Teh et al., 2002; Teh et al., 2005). However, with the exception of distinct LOH events, BCC tumours are generally characterized by genetic homogeneity (Teh et al., 2005) and it is therefore thought that the extent of genomic instability present in those skin tumours is appreciably lower when compared to that of other human malignancies. This is consistent with the lack of aggression seen in BCCs (Wong et al., 2003), and further suggests that additional oncogenic hits may be necessary for the manifestation of widespread genomic instability events,

contrarily to OSCC tumours which display extensive genomic alterations comparable to a genetic instability signature present in other human tumours (**Chapter 1**; reviewed in Hunter et al, 2005). The effects of FOXM1B on genomic stability were present in epithelial keratinocytes from both the epidermis and the oral mucosa, indicating that the effect of FOXM1 is not tissue specific. Further experiments are required to understand the mechanisms underlying this observation, and to establish whether the FOXM1B-induced genomic instability is responsible for generating oncogenic LOH and CNA relevant to human malignant transformation. Nevertheless, evidence from work in our group suggest that FOXM1B indeed cooperates with environmental stress, to direct a program of genomic instability that drives malignant transformation (Gemenetzidis et al., 2009; Teh et al., 2010).

4.3.4 Mechanisms of Genomic Instability

A possible reason for the immediate impact of FOXM1 in genomic integrity is that the list comprising its downstream targets contains many genes associated with centrosome function and chromosome segregation (reviewed in Wierstra & Alves, 2007). The relative abundance of each of these genes' products during mitosis is tightly regulated, since any deviations from their physiological critical concentrations may cause defects (Carter et al., 2006). Numerous studies have demonstrated that proteins which are important in the maintenance of genomic stability are often found amplified in human cancers, with centrosome amplification being a well characterized mechanism contributing to genomic instability (D'Assoro et al., 2002a; D'Assoro et al., 2002b; Gisselsson et al., 2002; Lingle et al., 2002; Pihan et al., 2003; Fukasawa, 2005; Jefford and Irminger-Finger, 2006). CENP-F overexpression has been linked to the generation of chromosomal instability in breast cancer patients, while NEK2 is consistently overexpressed in a variety of human tumours contributing to genomic instability (Hayward and Fry, 2006; O'Brien et al., 2007). Overexpression of Aurora centrosome kinase is also invariably associated to genomic instability in primary non-small cell lung carcinomas, breast carcinomas, and ovarian cancer derived cell lines (Li et al., 2004b; Hu et al., 2005; Smith et al., 2005), two of which (breast and lung) are reported to express high levels of FOXM1 (Wonsey and Follettie, 2005; Kim et al., 2006;

Madureira et al., 2006; Bektas et al., 2008; Francis et al., 2009). Specifically, Aurora kinase B (AURKB), a direct downstream target of FOXM1, is a marker of tumours with extensive allelic imbalances (Smith et al., 2005). Given the important role of FOXM1 in the regulation of downstream targets involved in normal chromosome segregation and cell division, it would be interesting to investigate the effect of FOXM1B overexpression on the mitotic processes of primary human keratinocytes.

4.3.5 Contrasting Effects of FOXM1

The evidence shown here supports the view that FOXM1B overexpression can disturb the mitotic process, thereby leading to genomic instability. That said, it is also known that lack of FOXM1 protein during mitosis, can impair cell division and lead to mitotic failure and endoreduplication, thereby leading to genomic instability (Laoukili et al., 2005; Wonsey and Follettie, 2005). An important observation however, is that the effects of FOXM1B overexpression observed here, are largely permissive for cell cycle and cell division, as opposed to the mitotic break-down and cell cycle arrest caused by FOXM1 depletion. This was particularly demonstrated when keratinocytes overexpressing FOXM1B, could be serially passaged in culture while accumulating further genomic aberrations (**see Figure 4.5 D**). It therefore follows, that although both lack and overexpression of FOXM1 may produce overlapping effects, only the latter can allow cell cycle progression and concomitant genomic aberrations. This can also explain why tumours exhibit both elevated levels of FOXM1, and genomic instability, and is in keeping with a recent study supporting a strong requirement for both in human malignancy (Carter et al., 2006). Recently, Carter et al. (Carter et al., 2006) have attempted to characterize the levels of aneuploidy, as a result of genomic instability in human tumours, based on a specific gene expression pattern. Each sample was given a total functional aneuploidy (tFA) 'score', based on its functional aneuploid features. A chromosomal instability score for a wide array of genes was therefore derived, by combining the level of correlation of each gene to tFA, from diverse types of human malignancies. The results of this study are highly relevant to the evidence presented here, since FOXM1 was found to be the third highest ranked, and thus overexpressed, gene with an

expression pattern that was consistently associated with genomic instability (Carter et al., 2006). The same study showed that FOXM1 downstream target genes, including CCNB1, AURKB, NEK2, and the novel target of FOXM1 reported here, CEP55, were amongst the top 70 highest ranked genes (Carter et al., 2006). Another study has also shown that the expression of FOXM1B is also invariably associated with genomic instability in hepatocellular carcinomas (Calvisi et al., 2009).

4.3.5.1 Implication of FOXM1 in DNA Repair

A recent study by Tan et al. (2007) provided evidence that depletion of FOXM1 leads to the generation DNA strand breaks and cell cycle arrest mediated by the induction of *TP53* and $p21^{WAF-1/CIP1}$ genes (Tan et al., 2007). More importantly, the same study showed that FOXM1 is stabilized by Chk2 mediated phosphorylation during DNA damage, and suggested a role for FOXM1 in DNA repair, by regulating the expression of DNA repair associated genes, BRCA2 and XRCC1. Based on these findings, the authors concluded that FOXM1 depletion renders cells susceptible to mutations and chromosomal aberrations, which they associated with the high tumour incidence in aged populations where FOXM1 expression is diminished (Tan et al., 2007). Since FOXM1 can lead to the induction of DNA repair pathways, it would then be expected that its loss will inevitably lead to increased susceptibility to oncogenesis given the increased rate of spontaneous mutations and DNA breaks, which was indeed evidenced in FOXM1 depleted MEFs (Tan et al., 2007). In fact, DNA repair genes are among the most susceptible genes to be targeted by inactivating mutations in human malignancies (Negrini et al., 2010).

However, in light of the observations from models of carcinogenesis in mice it is difficult to comprehend how loss of FOXM1 may contribute to oncogenesis as suggested by Tan et al. (Tan et al., 2007). Studies, many of which were conduced by the same group, have clearly shown that the loss of FOXM1 is efficiently protecting mice from chemically induced carcinogenesis (Kim et al., 2006; Gusarova et al., 2007; Wang et al., 2009), while its overexpression is

tumour promoting (Kalinina et al., 2003; Kalinichenko et al., 2004; Kalin et al., 2006; Kim et al., 2006; Yoshida et al., 2007; Wang et al., 2008b). It is known that the chemicals used to induce carcinogenesis can cause extensive DNA damage, and according to the DNA repair hypothesis, loss of FOXM1 would be expected to lead to the accumulation DNA adducts, and therefore to an increased susceptibility to oncogenesis. However, this is not seen *in vivo*, as mice develop very few tumours in the absence of FOXM1, supposedly due to the proliferative block caused by lack of FOXM1 protein. Therefore, even if FOXM1 has a role in repairing DNA damage, this effect is likely to be abolished due to the lack of proliferation in the absence of FOXM1.

In the alternative scenario of overexpression, it is shown that FOXM1 confers a proliferative advantage to pre-malignant and tumour cells, leading to development of more proliferative and aggressive tumours *in vivo*, while it enhances the tumourigenic potential of already transformed cell lines *in vitro* **(see Chapter 1, section 1.4.6)**. This of course fits with the established fact that most human tumours are characterized by overexpression, rather than suppression of FOXM1. But how could the expression of a DNA repair associated gene be tumourigenic? One explanation is that DNA repair genes also have functions other than DNA repair. For example, it was shown that BRCA2 overexpression in a small subset of breast tumours correlated with increased tumour proliferation rates (Bieche et al., 1999). There is also evidence suggesting that the re-acquisition of wild type function of DNA repair genes is responsible for the resistance to chemotherapy, by repairing DNA adducts and allowing cell survival of already malignant cells (Sakai et al., 2008). This certainly fits well with a role for FOXM1 as a DNA repair associated gene, since Kwok et al. (2010) provided conclusive data that expression of ΔN-FOXM1 in MCF-7 breast carcinoma cells can confer resistance to cisplatin (Kwok et al., 2010). Even though depletion of FOXM1 did not result in the reduction of BRCA2 and XRCC1, the resistant breast cancer cell line MCF-7CIS^{R} was still sensitised to cisplatin. This suggests that either FOXM1 is either regulating DNA repair through other genes or that it is regulating the DNA damage response and recognition differently.

Nevertheless, this provides insight into the mechanism by which FOXM1 may be involved in DNA repair in already established tumour cells where DNA repair may be needed to maintain a more stable genotype as suggested previously (Cahill et al., 1999), or to confer resistance to genotoxic insults (i.e. chemotherapy). However FOXM1 is also upregulated early in cancer, prior to malignant conversion. At least in the cases of early lesions of cervical intraepithelial hyperplasia (Chan et al., 2008), ductal breast hyperplasia, Barrett's metaplasia, uterine fibroid, transitional cell carcinoma without CIS, and OSCC mild dysplasias, FOXM1 appears to be significantly overexpressed (Gemenetzidis et al., 2009) (also **Chapter 3**), and almost certainly not as a result of gene mutation, since only one missense mutation with a yet unidentified phenotypic effect has been reported for FOXM1, and was found in malignant melanoma cells targeting the protein's C-terminus (source: Sanger; COSMIC- catalogue of somatic mutations in cancer). Since numerous pre-neoplastic epithelial lesions exhibit signs of DNAds breaks (Bartkova et al., 2005; Gorgoulis et al., 2005) , it appears that there is also the need for DNA repair in early stages of human malignancy. Some pre-malignant epithelial lesions show constitutive activation of ATM-CHK2-p53 pathway which is suggested to function as an anti-cancer barrier, triggered by the presence DNA breaks, which occur as a result of sustained oncogenic stimulation (Bartkova et al., 2005; Gorgoulis et al., 2005). Since CHK2 is shown to phosphorylate FOXM1, leading to protein stabilisation and activation, it is possible that FOXM1 is part of this tumour anti-cancer response that is triggered by DNA damage. The other alternative, which is also supported by the findings in this study, suggests that aberrant activation of FOXM1 can induce copy number alterations at multiple genomic loci and thereby could also explain both its overexpression (Chan et al., 2008; Gemenetzidis et al., 2009) and the presence of such alterations in early pre-malignant lesions (Lengauer et al., 1998; O'Connell et al., 1998; Vogelstein and Kinzler, 1998; Willenbucher et al., 1999; Kobayashi et al., 2000; Pinto et al., 2000; Gong et al., 2001; Shih et al., 2001; Bartkova et al., 2005; Gorgoulis et al., 2005; Negrini et al., 2010). Whether FOXM1 upregulation is observed because it is necessary to repair damaged DNA in pre-neoplastic lesions, or whether it is the cause of such genome de-stabilising events, remains unclear.

Its primary role in important mitotic processes favours the latter, while its suggested role in the regulation of DNA repair favours the former. The findings herein that FOXM1 could be activated by genotoxic agents (e.g., UVB and nicotine) and that ectopic FOXM1B expression causes genomic instability favour the view that the upregulation of this transcription factor is contributing the genomic instability seen in human malignancies. However, the possibility that FOXM1-induced overexpression of DNA repair genes can trigger genomic instability and DNA repair, to an extent that will allow tumour cell survival, could also grant further consideration.

Human carcinogenesis is a multistep process driven by the selection of cells with an acquired survival advantage. During this process cells need to overcome numerous anti-cancer barriers (Stevenson and Volsky, 1986; Hahn and Weinberg, 2002). The data presented here indicate that aberrant upregulation of FOXM1B may serve as a 'first hit' where cells acquire a susceptibility to genomic instability. This can predispose cells to a 'second hit', presumably mediated by extrinsic factors (i.e. UVB irradiation), whereby a DNA-damage/proliferative stress checkpoint response is abolished, to allow uncontrolled proliferation and the accumulation of genetic aberrations/mutations required for human cancer initiation.

Chapter 5

FOXM1 MODULATES HUMAN KERATINOCYTE PROGENITOR DIFFERENTIATION

5 FOXM1 Modulates Human Keratinocyte Progenitor Differentiation

5.1 Introduction

Many epithelial malignancies, including HNSCC, are heterogeneous in nature and arise from a common premalignant progenitor, followed by the outgrowth of clonal populations, which are usually subjected to cumulative genetic alterations that lead to invasive malignancy (Hunter et al., 2005). Endogenous FOXM1 protein is normally expressed at low levels within the basal and suprabasal layers of human oral mucosa (**Chapter 3**) and skin epithelium (Teh et al., 2002). The finding that FOXM1 expression precedes oral (**Chapter 3**), esophagus, lung, breast, kidney, bladder and uterus malignancies, predicts a vital role for this transcription factor in the early stages of human neoplasia (Gemenetzidis et al., 2009).

The superior proliferative potential and capacity for self-renewal are two attributes that render stem cells potential targets of epithelial tumour initiation. Being the long term residents of epithelial tissues, stem cells have the ability to accumulate the number of genetic hits necessary for tumour formation (Owens and Watt, 2003). Given that FOXM1 is upregulated in the majority of human cancers, it was hypothesized that aberrant FOXM1 expression may play a pivotal role in cancer initiation by modulating the balance between epithelial stem cell proliferation and differentiation. It is therefore essential to investigate how FOXM1 is regulated in epithelial stem cell populations, with an aim to understand how its upregulation may contribute to the initiation of epithelial malignancies.

To date, studies of *FOXM1* as a cancer causing gene have been performed in the context of transformed and/or immortalized cell lines, undoubtedly providing invaluable insight into the molecular mechanisms mediated by FOXM1. However, due to the aberrant molecular background already present in most cell line systems, the role of FOXM1 in the earliest stage of neoplasia

could not be delineated and it is not fully understood. Therefore the regulation and the effect of FOXM1 (isoform B) proto-oncogene overexpression, was examined in normal primary human epithelial cells as they represent the main target population of human malignancies.

5.2 Results

5.2.1 Expression Pattern of FOXM1 in Normal Human Oral Epithelium

During epithelial regeneration, the slow cycling immature basal populations give rise to rapidly proliferating keratinocytes, which migrate upwards to finally give rise to terminally differentiating squames. In order to investigate the functional significance of FOXM1 in the initiation of epithelial tumours, it is important to first understand how its expression is regulated under normal homeostatic conditions in the epithelial tissue. Therefore, normal human oral mucosa epithelium was examined by means of immunohistochemistry using high power confocal imaging, to visualize the relative expression patterns of both FOXM1, and a previously characterized oral keratinocyte stem cell marker, p75NTR (Nakamura et al., 2007).

The immunoreactivity of p75NTR was strictly localised to the basal layer, with regions of intense p75NTR positivity at the tips of tissue papillae, whereas p75NTR staining was notably less intense in deep rete ridges (**Fig. 5.1 C, i**). Unlike the epidermis, proliferative activity in the oral epithelium is present in both the basal and parabasal epithelial layers (2-3 layers above the basal layer). Reportedly, Cyclin D1 and CENP-F, an established FOXM1 target (Laoukili et al., 2005), are predominantly expressed in mitotic cells of the parabasal layers of oral mucosa epithelium (Liu et al., 2007). In line with these observations, FOXM1 was found to be mainly expressed in the proliferative parabasal layers of oral epithelium, while it was also detected in isolated cells within the basal layer (**Figure 5.1**). Nuclear FOXM1 immunostaining was also infrequently found in the suprabasal layers, possibly marking early differentiating cells, undergoing the last stages of cell division prior to terminal differentiation. Importantly, the expressions of p75NTR and FOXM1 were mutually exclusive in within the oral epithelium. Specifically, in areas of intense p75NTR (**see Fig. 5.1 A, magnified in B**), FOXM1 is mainly expressed in cells above the basal layer with no significant co-localisation with p75NTR. In deep rete ridges, both proteins show a higher degree of co-expression (**Fig. 5.1 A magnified in C, and D**). The presence of isolated basal keratinocytes co-expressing p75NTR and FOXM1 could represent either early

progenitor TA keratinocytes, or the rarely dividing oral keratinocyte 'stem cell' population.

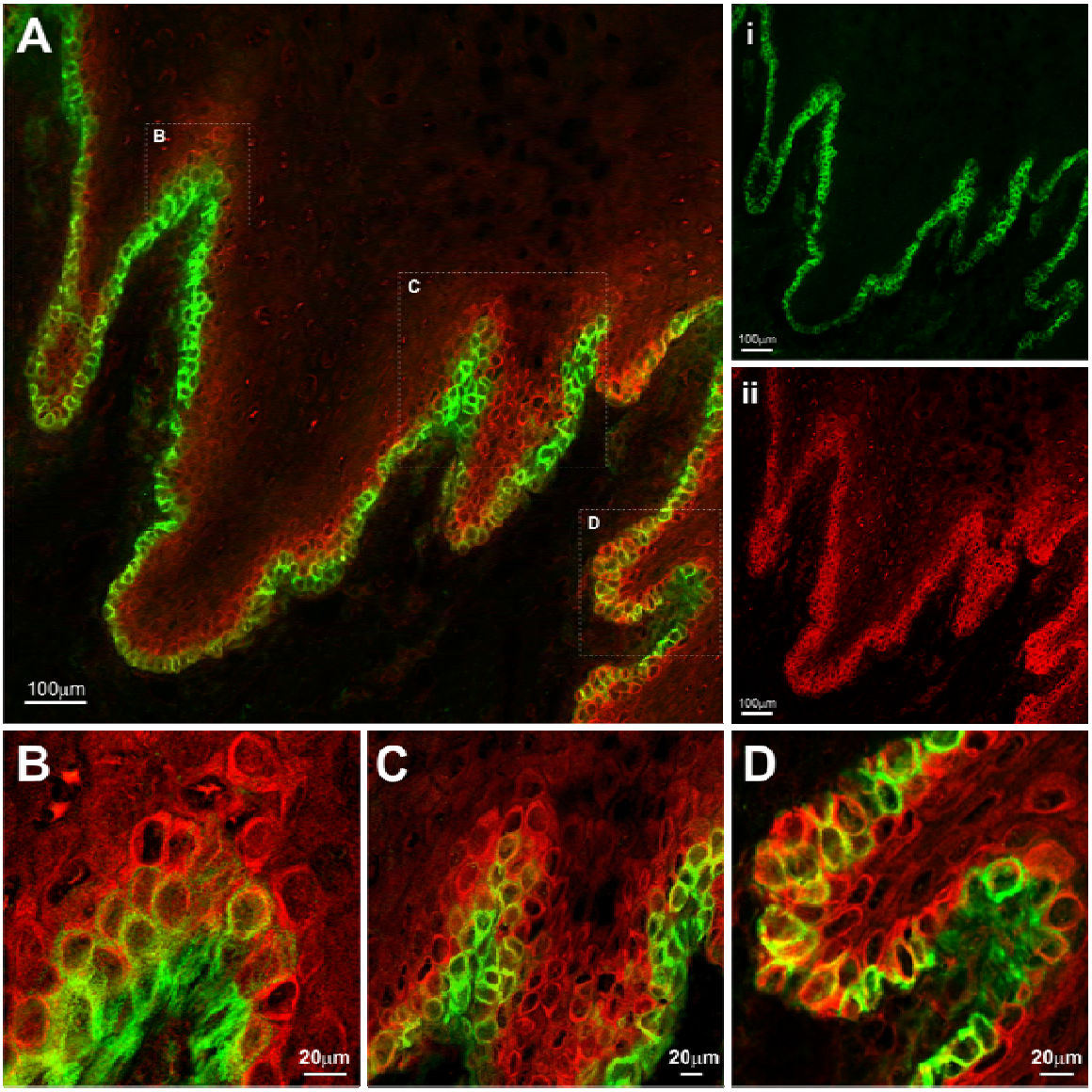

Figure 5.1: Mutually exclusive expression pattern of FOXM1 and p75NTR in normal human oral epithelium

(A) Immunohistochemistry of p75NTR (green) **(i)**, and FOXM1 (red) **(ii)** in normal human oral mucosa epithelium. **(B) (C)** and **(D)** High magnification of sections in **C** showing co-expression (yellow) of p75NTR and FOXM1 protein within discrete cells within the basal cell layer above the connective tissue papillae.

5.2.2 Oral Keratinocyte Stem Cell Isolation and Validation

To further understand how FOXM1 expression is regulated during keratinocyte stem cell expansion, this study aimed to directly isolate putative oral keratinocyte stem cells. This would allow keratinocyte stem cell

population expansion *in vitro* in a controlled environment, where FOXM1 expression could be directly assessed.

Enrichment of keratinocyte stem cells has been previously demonstrated *in vitro*, based on the differential expression of cell surface markers. Immature populations of basal epidermal keratinocytes have been identified by differential expression of β1 integrins. Integrin β1-positive fluorescence activated cell sorting (FACS) sorted fractions of epidermal keratinocytes that adhere rapidly to extracellular matrices (Collagen IV and Fibronectin), possess greater regenerative and proliferative capacity *in vitro* (Watt, 1998). Whereas, human oesophageal and oral mucosal keratinocyte stem cells have been previously shown to express high levels of the low affinity nerve growth factor receptor, p75NTR (Okumura et al., 2003; Nakamura et al., 2007).

In order to investigate the regulation of FOXM1 in oral keratinocyte stem cells (OKSCs), fluorescence activated cell sorting (FACS) was used to isolate specific population subsets that express either integrin β1 or p75NTR or both (**Fig. 5.2A**). Secondary cultures of normal human oral keratinocytes (population doublings, PD 6-9) were used for fluorescence activated cell sorting (FACS) and equal numbers from each sorted population were seeded diretly onto mitomycin C-treated 3T3 feeder layers, and *in vitro* clonogenic assays were performed, to examine their proliferative potential. To verify the FACS procedure integrin $\beta1^{+\ bright}$/$p75NTR^{-}$ (represented on **Fig. 5.2A** as fraction P3) and integrin $\beta1^{+\ bright}$ /$p75NTR^{+}$ (represented on **Fig. 5.2A** as fraction P4) populations were examined under fluorescence microscopy immediately after plating (**Fig. 5.2B**).

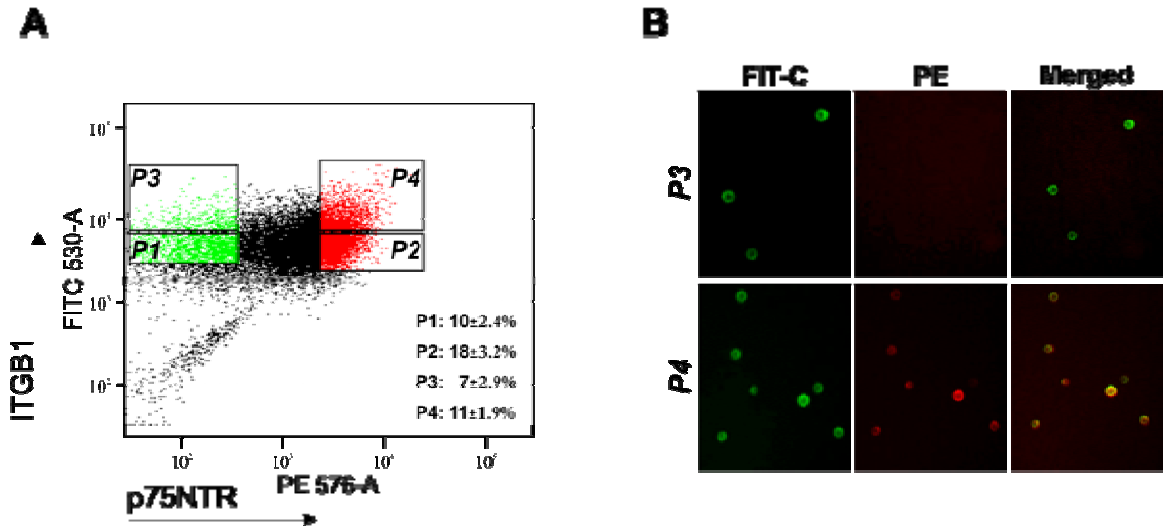

Figure 5.2: Oral keratinocyte stem cell isolation.

(A) FACS staining profile of primary human oral keratinocytes stained with anti-integrin β1 (CD29) and anti-p75NTR (CD271) antibodies. Populations marked as P1, P2, P3 and P4 were used for combined cell sorting analysis. The relative abundance of each population is derived from experiments performed on oral keratinocytes derived from three different donors and were carried out in triplicates. **(B)** Fluorescence microscopy on oral keratinocyte populations immediately after flow sorting to demonstrate successful discrimination between the indicated populations.

In line with previous observations, $p75NTR^+$ cells possessed a superior clonogenic capacity compared to $p75NTR^-$ (**Figure 5.3A i, ii**, and **Figure 5.3 B**) cells when examined 12 days after flow sorting. Although $p75NTR^-$ cells gave rise to some large colonies, many of them were highly irregular and displayed characteristics of terminal differentiation (**Figure 5.3 Aii**). The $p75NTR^+$ cells gave rise mostly to large colonies with a smooth perimeter (**Figure 5.3 Aii**). The latter colony morphology signifies that such populations originate from the cells of a holoclone, which contains cells of high self-renewal and proliferative capacity (Barrandon and Green, 1987).

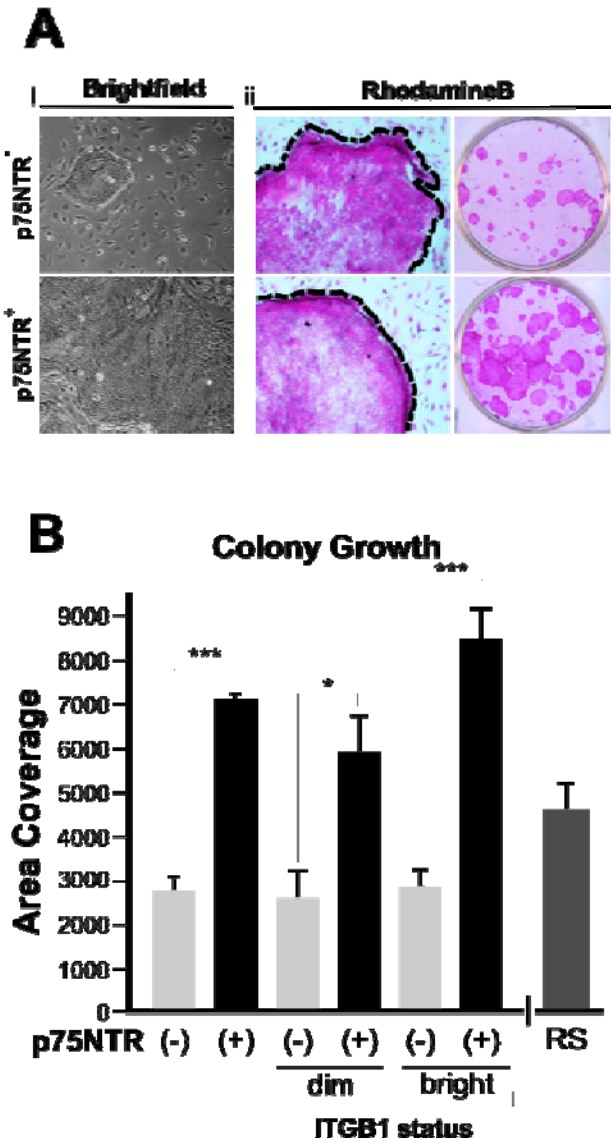

Figure 5.3: Oral Keratinocytes sorted for p75NTR display high clonogenic capacity

(A) Oral keratinocytes sorted for p75NTR$^-$ or p75NTR$^+$ were allowed to grow for 12 days. Keratinocyte colonies were examined under bright field microscopy (i) and were later stained with Rhodamine B (ii) for quantification of the clonogenic potential of each separate keratinocyte population. **(B)** Colony growth values for each different keratinocyte population were obtained by means of area coverage (pixels) as described in materials and methods. Clonogenic assays were carried out in 6 replicate wells for each sample. **RS** stands for random sorted control cells. Integrin β1 positive keratinocytes were further discriminated according to p75NTR positivity. p75NTR expression determined the clonogenic potential of integrin β1 (+) keratinocytes. Values represent the fold difference from p75NTR$^-$ control samples ±SEM for each average values. **P≤0.05, **P≤0.01, ***P≤0.001*

Keratinocytes with the highest integrin β1 expression levels, were observed mainly in the p75NTR$^+$ subset (represented as fraction P4 in **Figure 5.1 A**), which is consistent with the fact that β1 integrins are highly expressed in the stem cell containing basal layers of human epidermis (Watt, 1998). However,

integrin β1 positivity conferred an advantage only when combined with p75NTR positivity, since only integrin $\beta1^{+\ bright}$ / $p75NTR^{+}$ (**Figure 5.2 A** fraction P4) cells showed high levels (comparable to integrin $\beta1^{+\ dim}$ / $p75NTR^{+}$ (P3) or $p75NTR^{+}$ alone) of clonogenic potential (**Figure 5.3 B**, and **Appendix 4**), colony forming efficiency % (CFE), population doublings (PD) (**Figure 5.4 B**) and total cell output (**Figure 5.4 A**). As expected, all random sorted (RS; double stained keratinocytes randomly sorted from the same pool of cells) population showed intermediate levels between the (-) and (+) populations, indicating a mixed population.

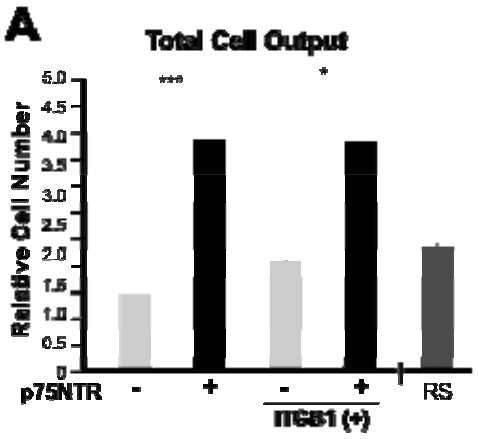

B

		Clonogenicity (%)	PD
ITGB1 status: dim	P1 (-)	3.6±0.2	7.6
	P2 (+)	5.1±0.3	9.9
ITGB1 status: bright	P3 (-)	4.1±0.2	8.9
	P4 (+)	5.3±0.2	10.9
p75NTR status	(-)	3.7±0.2	7.6
	(+)	5.9±0.4	10.4
	RS	4.2±0.3	8.7

Figure 5.4: Proliferative potential of distinct keratinocyte subsets

(A) Total cell output values were calculated as mentioned in materials and methods section after 12 days of culture. **RS** stands for random sorted control cells. Values are representative of two independent experiments carried out in duplicates. Bars represent the average fold difference from $p75NTR^{-}$ control samples ±SEM. *$P\leq0.05$, **$P\leq0.005$, ***$P\leq0.001$. **(B)** Clonogenicity % and population doublings (PD) measurements of all sorted oral keratinocytes after 12 days in culture. RS stands for random sorted populations. Values are representative of three independent experiments carried out in duplicate wells, ±SEM for each average value**.**

Next, the molecular profile of putative human OKSC ($p75NTR^{+}$ cells) was investigated by qPCR. The mRNA expression levels of p75NTR were significantly elevated (~3.5 fold), in the $p75NTR^{+}$ subsets proving successful FACS sorting (**Figure 5.5 Ai, ii**). Confluent cultures of lethally treated 3T3 feeders were also included in expression analysis to control for possible contamination during cDNA preparations. Although 3T3 feeders were routinely removed prior to experiments, there is a possibility that a small amount of 3T3 cells may interfere with expression analysis. However, qPCR

results confirmed that lethally treated 3T3 feeders did not express detectable mRNA levels of either gene (see **Figures 5.5 A, 5.6 A and 5.7)**

By examining the levels of a well established keratinocyte stem cell marker, ΔNp63α (Pellegrini et al., 2001), shortly after cell sorting, it was found that ΔNp63α protein was slightly more abundant in both the $p75NTR^{+}$ and integrin $\beta1^{+\ bright}$ / $p75NTR^{+}$) compared to the $p75NTR^{-}$ population (**Figure 5.5 Bi**). As expected, random sorted (RS) control cells retained intermediate levels of ΔNp63α protein (**Figure 5.5 Bi**). The differences in ΔNp63α protein levels became much more pronounced after 12 days in culture, indicating the long term ability of OKSC derived populations to maintain the expression of stem cell associated markers (**Figure 5.5 Bii**). This comes in agreement with the first report identifying ΔNp63α as a keratinocyte stem cell marker, which showed that it was still present in holoclone (but not in meroclone or paraclone) derived populations of limbal and epidermal keratinocytes, after 11-12 days in culture (Pellegrini et al., 2001).

Further qPCR expression analysis of freshly isolated $p75NTR^{+}$ oral keratinocytes, revealed significantly higher expression levels of two other putative stem cell genes NESTIN and NUMB, when compared to non-stem cell fractions (**Figure 5.5 C**). NESTIN has been shown to be neuronal stem cell marker (Lendahl et al., 1990) while NUMB was reported as a maker of asymmetric division in mouse epidermal keratinocytes *in vivo* (Clayton et al., 2007) and mouse satellite muscle progenitor cells *in vitro* (Shinin et al., 2006). The expression of cytokeratin 4 which is a marker specific for differentiating oral epithelia (Moharamzadeh et al., 2007) was also reduced in the stem cell enriched fractions of oral keratinocytes (**see Appendix 5A**). Collectively, these experiments validate the use of p75NTR as a stem cell marker for isolating human oral keratinocyte stem cells which are undifferentiated, highly clonogenic and proliferative.

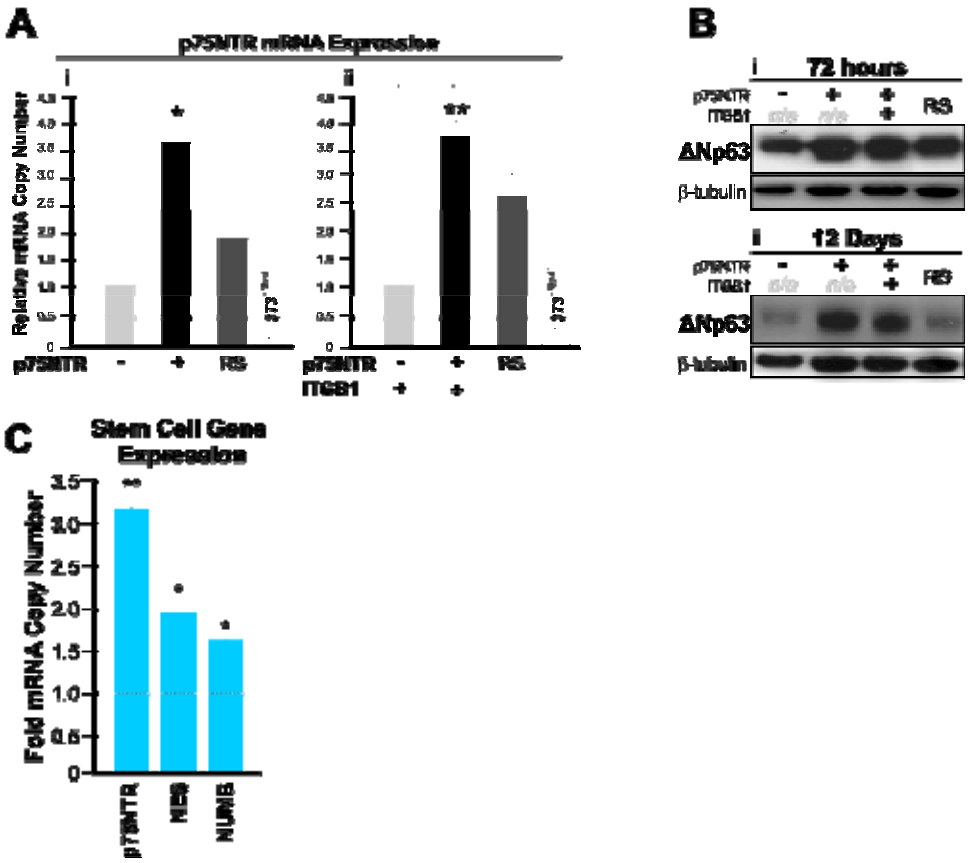

Figure 5.5: Molecular profile of putative oral keratinocyte stem cells

(A) Absolute qPCR analysis of p75NTR expression levels in sorted oral keratinocytes three days after flow sorting. All values are representative of three independent experiments. Graphs show single (p75NTR) **(i)** or double-sorted (p75NTR/initegrin β1) cells **(ii)**. Bars represent the average fold difference from $p75NTR^-$ (arbitrary value of 1) control samples ±SEM.*$P \leq 0.05$, **$P \leq 0.005$, ***$P \leq 0.001$. **(B)** OKSCs retain high levels of ΔNp63α protein after short and long term culture. Oral keratinocyte sorted populations were harvested for total protein at 72 hours **(i)** and 12 days **(ii)** and immunoblotted with anti-p63 antibody recognizing human ΔNp63 isoforms, and β-tubulin as protein loading control. **(C)** Absolute qPCR analysis of p75NTR, NESTIN, and NUMB in $p75NTR^+$ oral keratinocytes. All values are fold expression relative to $p75NTR^-$ cells (arbitrary value of 1). Each bar represents the mean ± SEM of two independent experiments performed in duplicates. .*$P \leq 0.05$, **$P \leq 0.005$, ***$P \leq 0.001$.

5.2.3 FOXM1B Is tightly Regulated in OKSC

The slow cycling nature of putative epithelial stem cells is well supported, from *in vivo* labelling experiments, *in vitro* cultured cells and observations made from organotypic reconstructs of human epidermis (Barrandon and Green, 1987; Morris and Potten, 1994; Morris, 2000; Muffler et al., 2008). In order to investigate the endogenous expression level of proliferation specific transcription factor, FOXM1, in freshly isolated OKSCs, sorted cells were

allowed to settle and grow for 72 hours (to generate sufficient cell number) prior to experiments. In these early p75NTR^{+} fractions of OKSCs, FOXM1B was significantly reduced at both mRNA (**Figure 5.6 Ai, ii**) and protein (**Figure 5.6 Bi**) when compared to p75NTR^{-} fractions. However, when the expression patterns of these cells were examined after 12 days in culture, FOXM1 protein was exclusively upregulated in the stem cell enriched fractions (**Figure 5.6 Bii**) compared to the p75NTR^{-} fraction. Furthermore, the upward shift of FOXM1 protein band in the p75NTR^{+} and RS cells compared to p75NTR^{-} cells indicates that FOXM1 protein remained in its active phosphorylated form in the OKSCs (**Figure 5.6 Bii**).

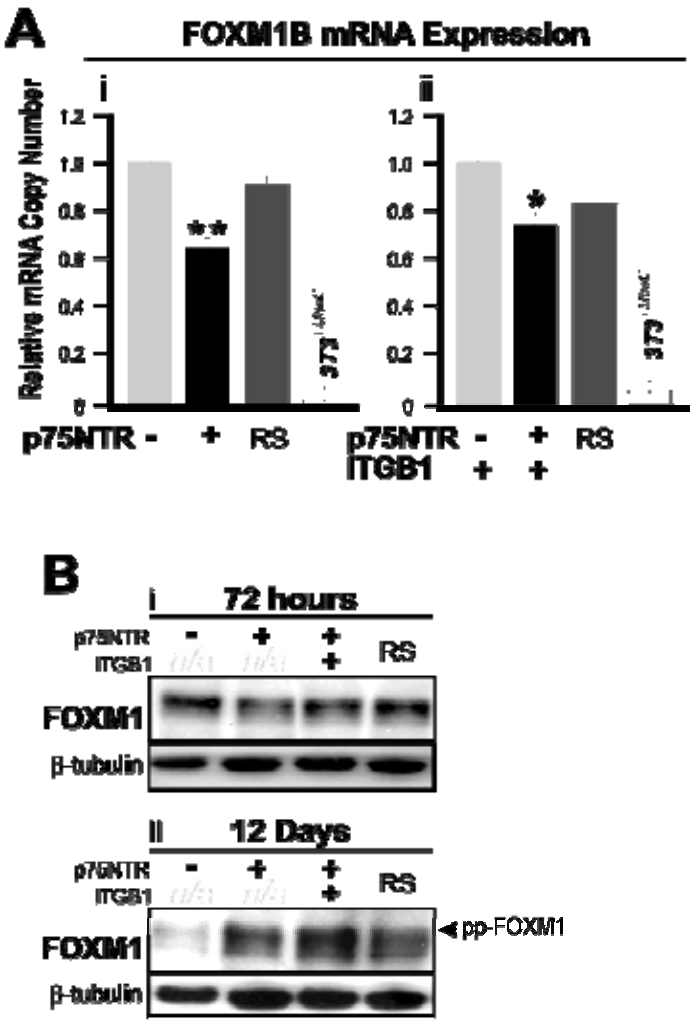

Figure 5.6: FOXM1 expression in OKSC.

(A) Absolute qPCR analysis of FOXM1B expression levels in single p75NTR **(i)** and double integrin β1/p75NTR **(ii)** sorted oral keratinocytes three days after flow sorting. *RS* stands for random sorted populations. All values are representative of three independent experiments and graphs show the relative FOXM1B mRNA copy number against $p75NTR^-$ **(i)** or integrin β1 (+) $p75NTR^-$ **(ii)** samples. Bars represent the mean ± SEM of three replicate samples.**P≤0.05, **P≤0.005, ***P≤0.001.* **(B)** FOXM1 protein expression pattern in OKSC. Oral keratinocyte sorted populations were harvested for total protein at 72 hours **(i)** and 12 days **(ii)** and immunoblotted with anti-FOXM1 (C20) antibody and β-tubulin as protein loading control.

The downregulation of FOXM1 protein in the remaining cell populations after long term culture suggests that FOXM1 is switched off during terminal differentiation of oral keratinocytes. In support, FOXM1 protein levels are diminished after a 12-day period in the p75NTR$^-$ fraction (**Figure 5.6 Bii**). Additionally, FOXM1 and involucrin protein levels were inversely correlated during prolonged culture of p75NTR$^-$ oral keratinocytes (**see Appendix 5 B**).

As decribed earlier in **Chapter 4**, the mRNA expression pattern of FOXM1B isoform, but not isoforms A or C, oscillates during cell cycle whereby its peak expression coincides with the G2/M phases of the cell cycle (**Figure 4.1**). Consistent with the observation that FOXM1C was not induced during cell cycle progression, there was no differential expression for this isoform between p75NTR$^-$ and p75NTR$^+$ enriched populations (**Figure 5.7**). It is worth mentioning that the antibody used to detect FOXM1 does not discriminate between all different isoforms, and hence, the reduction of FOXM1B protein levels in OKSC derived keratinocytes, could be potentially underestimated.

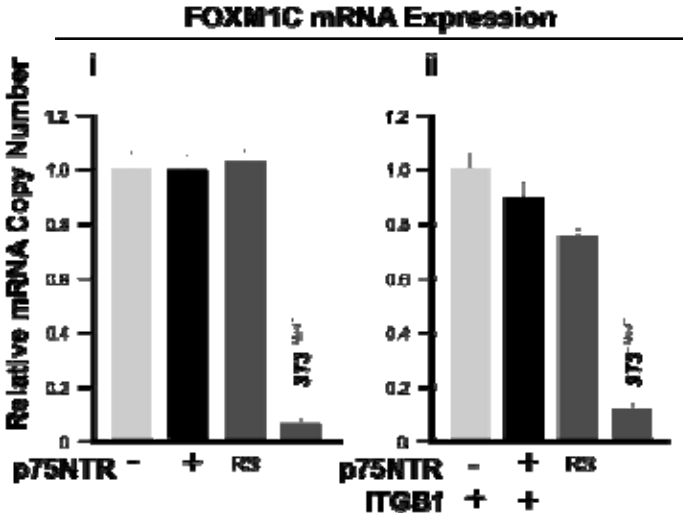

Figure 5.7: FOXM1C isoform is not differentially expressed in OKSCs.

Oral keratinocytes were either single (i) or double (ii) sorted as indicated. FOXM1C mRNA copy number was quantified using absolute qPCR. *RS* stands for random sorted populations. All values are fold expression relative to p75NTR$^-$ (i) or integrin $\beta1^+$ p75NTR$^+$ cells (ii). Each bar represents the mean ± SEM of two independent experiments performed in triplicates.

5.2.4 FOXM1B Modulates Primary OKSC Expansion

The elevation of FOXM1 in the majority of human solid cancers raises the possibility its overexpression may be an initiating event required for oncigenesis possibly by targeting the long lived residents of epithelial tissues resulting in persistent expression of FOXM1 in cancers. Given that FOXM1 was found to be an early event in the progression of OSCC (**Chapter 3**) (Gemenetzidis et al., 2009), I sought to investigate the effect of FOXM1B overexpression on OKSCs, since sustained overexpression of this oncogenic transcription factor could constitute an initiating event whereby cells acquire a proliferative advantage. Consistent with its proliferation specific role, FOXM1 was only found to be transiently expressed during OKSC expansion (**Figure 5.6**), while its expression was strongly suppressed in terminally differentiated keratinocytes. In order to gain a better understanding of how the deregulation of this expression pattern contributes to the initiation of oncogenesis, FOXM1B was ectopically expressed in distinct subsets of normal primary human keratinocytes, distinguished by their degree of 'stemness', by using the expression levels of p75NTR as an indicator. Due to the heterogeneity of human primary keratinocytes (see also **Chapter 1, section 1.2**), it was hypothesized that diverse populations may respond differently to FOXM1B overexpression.

Primary oral keratinocytes FACS sorted into $p75NTR^+$ and $p75NTR^-$ populations representing OKSCs and lineage committed differentiating/differentitated keratinocytes respectively. Sorted keratinocytes were then transduced with either empty (MCS) or EGFP control retroviruses, or with EGFP-FOXM1B retrovirus (diagrammatic representation of the experimental procedure is shown in **Appendix 6**). Three days following transduction, keratinocytes were plated at low densities (500 cells /8cm^2) in the presence of 3T3 feeder layers. Total protein lysates were also prepared, in order to assess the relative expression levels of FOXM1B in the $p75NTR^+$ fraction (**Figure 5.8B**). In a separate experiment conducted to acquire sufficient numbers of transduced $p75NTR^-$ keratinocytes, it was confirmed that even ectopically expressed FOXM1B protein levels are still down-regulated in OKSC (**Figure 5.8 C**), suggesting that FOXM1 proteins are also

regulated at the protein level in putative OKSC populations. It is important to mention that the downregulation of FOXM1 in $p75NTR^{+}$ populations is much more evident at the level of ectopic FOXM1B protein when compared to FOXM1 protein as a whole which represents all three FOXM1 isoforms. Given that FOXM1B, but not FOXM1C, transcription is also significantly downregulated (**Figure 5.6A, 5.7**), it is possible that this mechanism is specific for the B isoform of FOXM1 both at mRNA and protein levels.

Although $p75NTR^{-}$ keratinocytes failed to grow extensively after transduction with either construct, it was noteworthy that individual keratinocyte $p75NTR^{+}$ stem cell colonies expressing EGFP-FOXM1B ($p75NTR^{+FOXM1B}$) showed an altered phenotype in that they contained cells with a higher nuclear to cytoplasmic ratio, and were highly cohesive. A representative image on **Figure 5.8A v, and vi** shows the relative size of a keratinocyte colony expressing EGFP-FOXM1B compared to an un-transduced keratinocyte colony. Overall, approximately 87% of clonogenic keratinocytes were efficiently transduced, as judged by quantification of EGFP-positive keratinocyte colonies.

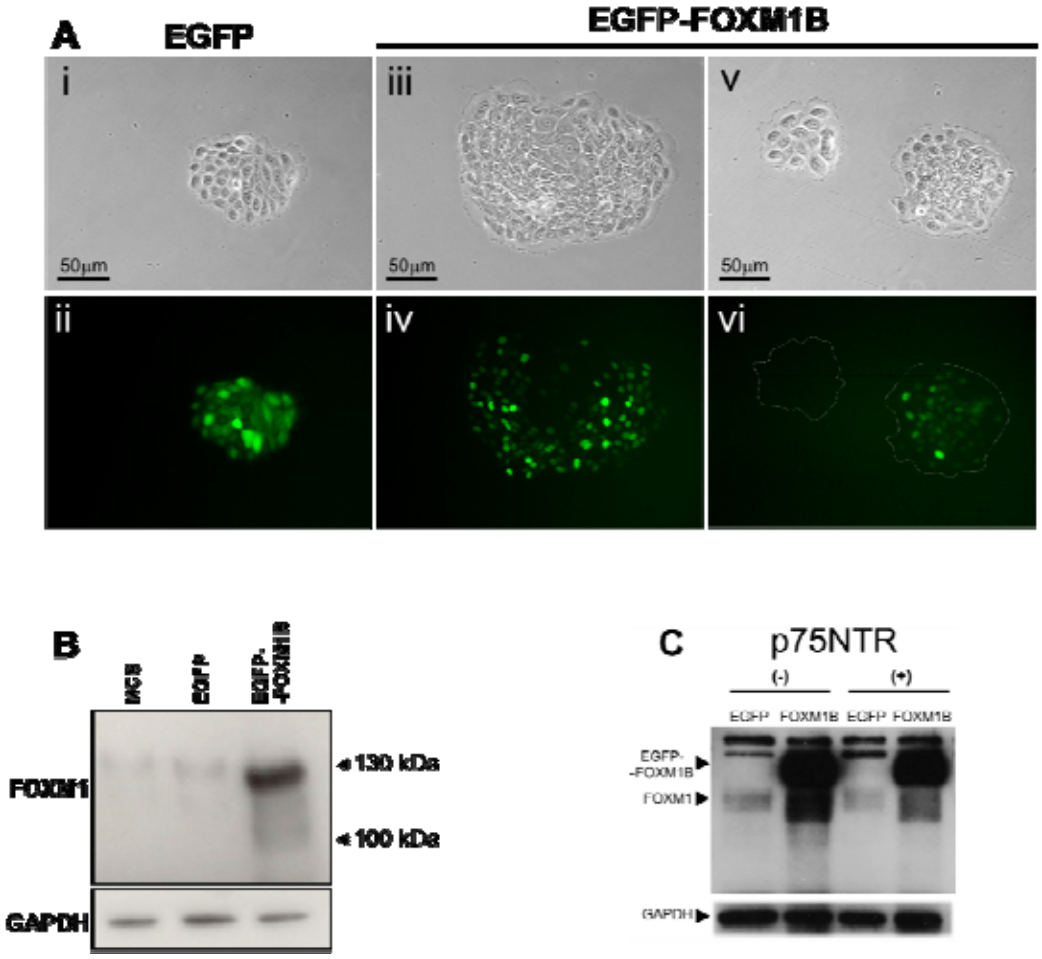

Figure 5.8: FOXM1B expressing keratinocyte stem cell colonies

(A) Primary human oral keratinocyte stem cells ($p5NTR^+$) were transduced with either **(i)** pSINEGFP or **(ii)** pSINEGFP-FOXM1B and individual keratinocyte colonies were examined under bright and fluorescence (FfIT-C) microscopy following 3T3 feeder removal. Figures **(v), (vi)** depict two keratinocyte stem cell colonies the size of which correlates with the level of FOXM1B expression as evidenced by green fluorescence intensity. **(B)** Keratinocytes were harvested and total protein was immunoblotted against anti-FOXM1 antibody. Anti-GAPDH antibody was used to confirm equal protein loading. **(C)** Oral keratinocytes were sorted in $p75NTR^+$ and $p75NTR^-$ fractions and were transduced with pSINEGFP or pSINEGFP-FOXM1B. Cells were allowed to grow for 5 days prior to harvesting to assess the relative expression levels of FOXM1. Proteins were immunoblotted against anti-FOXM1 antibody and anti-GAPDH antibody as a protein loading control. Cells overexpressing FOXM1B also show massive increase in the levels of FOXM1 endogenous protein suggesting a positive feedback loop, whereby exogenous FOXM1B could in turn promote the expression of FOXM1 gene. The excessive levels of FOXM1 proteins are significantly reduced in the stem cell fraction of oral keratinocytes ($p75NTR^+$).

Twelve days after clonal plating, keratinocyte colonies were stained with Rhodamine B and the total number and surface areas (mm^2) of colonies from each population were measured as described in **Chapter 2**, **section 2.4**. The more committed progeny of oral keratinocytes ($p75NTR^-$) failed to show any significant differences in colony growth, following transduction with MCS, EGFP, or FOXM1B. However, within the $p75NTR^+$ transductants, the average area of colonies founded by $p75NTR^{+FOXM1B}$ was significantly increased compared to both MCS and EGFP-expressing control cells (**Figure 5.9**).

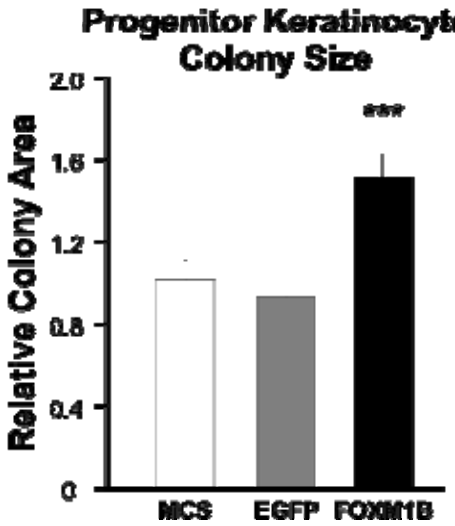

Figure 5.9: FOXM1B expression induces progenitor keratinocyte colony growth

$p75NTR^+$ oral human keratinocytes were infected with pSINMCS, EGFP, or FOXM1B and were plated at clonal densities. Cells were allowed to grow for 12 days prior to counting colony number and size. >100 colonies were measured for each construct. The bars represent the mean relative fold difference in colony area value, against MCS control (arbitrary value of 1) ±S.E.M for replicate samples (n=6) *$***P\leq0.001$*.

When plating human keratinocytes at low densities, morphologically distinct types of colonies become apparent after 12-14 days of culture (Barrandon and Green, 1987; Jones and Watt, 1993). The larger keratinocyte colonies (10-30mm^2), which are thought to be founded by putative stem cells, and consist of a mixture of transit amplifying and differentiated keratinocytes, as well the smaller keratinocyte colonies (<5mm^2) which are thought to consist primarily of transit amplifying and terminally differentiated keratinocytes (Barrandon and Green, 1987). Based on these features, we found that the progeny of $p75NTR^{+FOXM1B}$ showed a ~2.6 fold increase (compared to $p75NTR^{+MCS}$ or

p75NTR^{+EGFP}) in the percentage of large keratinocyte colonies (>10mm^2), and a concomitant reduction in the percentage of smaller/abortive colonies (<5mm^2) after 12 days in culture (**Figure 5.10**). This evidence suggests that elevation of FOXM1B expression confers a proliferative advantage in OKSC (p75NTR$^+$), but not in committed keratinocytes (p75NTR$^-$), thereby increasing their intrinsic capacity to clonally expand *in vitro*. This indicates that FOXM1B overexpression can either directly promote the maintenance of the stem cell population, or oppose/delay the terminal differentiation of their immediate progeny (TA keratinocytes).

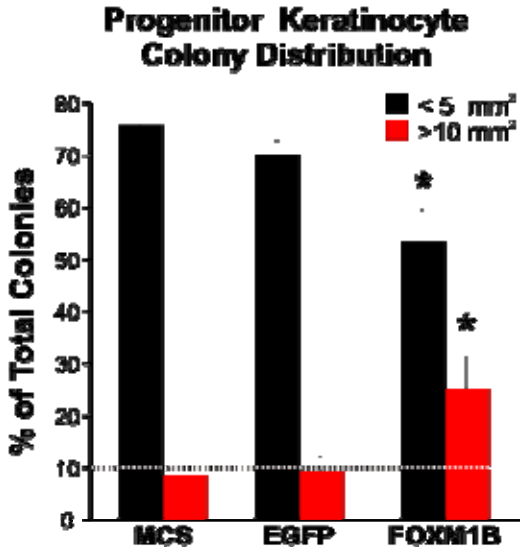

Figure 5.10: FOXM1B induces expansion of p75NTR$^+$ OKSC colonies

p75NTR$^+$ oral human keratinocytes were infected with pSINMCS, EGFP, or FOXM1B and were plated at clonal densities. Cells were allowed to grow for 12 days prior to counting colony number and size. >100 colonies were measured for each construct. The bars represent the mean percentage of colonies >10mm^2 (red) or <5mm^2 (black) ±S.E.M for replicate samples (n=6) *$P \leq 0.05$*

In order to gain a better understanding of how aberrant expression FOXM1B contributes to stem cell colony expansion, the function of keratinocyte stem cell differentiation was studied using a well-established 3D organotypical epithelium regeneration model system using primary human oral keratinocytes (Moharamzadeh et al., 2007; Teh et al., 2007). Oral keratinocytes were transduced with either pSINEGFP (the empty vector pSINMCS produces

identical results in keratinocyte colony growth assays; **Figures 5.9, 5.10**) or pSINEGFP-FOXM1B and were cultured on de-epidermalised dermis (DED) for 15 days with the support of normal human oral fibroblasts as described previously in **Chapter 2**. EGFP-FOXM1B overexpressing organotypic cultures showed a hyper-proliferative phenotype producing thicker spinous cell layers than the control EGFP expressing organotypic culture (compare **Figures 5.11 A and B**). Consistent with its expression pattern in normal oral mucosa, FOXM1 (**Figure 5.1**) was expressed at low levels in the basal epithelial layers of the control (pSINEGFP) organotypic DED culture (**Figure 5.11 C**). Importantly, FOXM1 protein localization is mainly nuclear in dividing keratinocytes within the basal layer. Similar to normal oral mucosa tissue, low levels of FOXM1 protein were detected in the basal layers of the control organotypic DED culture

In contrast to control DED, high levels of FOXM1 protein were detected in both the basal and suprabasal layers of the DED culture derived from FOXM1B overexpressing oral keratinocytes (compare **Figures 5.11 C and D**). The keratinocytes in the spinous and granular layers of FOXM1B derived reconstructs retain ectopic FOXM1B, which also correlated with increased Ki-67 immunoreactivity throughout these layers (**Figure 5.11 F, H**). On the other hand, Ki-67 immunoreactivity was strictly confined to basal proliferative layer of the control DED (**Figure 5.11 E**). This was not an artefact due to increased tissue thickness, since the same pattern and extent of Ki-67 immunoreactivity was observed even in thickness-matched areas of EGFP and EGFP-FOXM1B derived DEDs (**Figure 5.11 G and H**). In agreement with previous FOXM1 and Ki-67 immunohistochemical staining patterns in basal cell carcinoma (Teh et al., 2002), only a subset of FOXM1 expressing cells are also Ki-67 positive. The expansion of keratinocyte populations seen in organotypic reconstructs, is highly consistent with the expansion of $p75NTR^{+FOXM1B}$ keratinocytes after the same period of time in monolayer cultures (**Figures 5.9, 5.10**). The patterns of keratinocyte proliferation seen in the organotypics suggest that FOXM1B overexpression did not increase the proliferative rate of basal keratinocytes, but instead, it resulted in sustained proliferation of the more mature spinous keratinocytes. This suggests that FOXM1B alone does not have an immediate

proliferative effect on OKSC, but it leads to the defective terminal differentiation of their immediate progeny (TA keratinocytes). In addition, staining with integrin β1, a marker for basal keratinocytes, revealed the presence of intact basement membranes with no breaks, or any other abnormalities between EGFP and EGFP-FOXM1B (**Figure 5.11 I, K**).

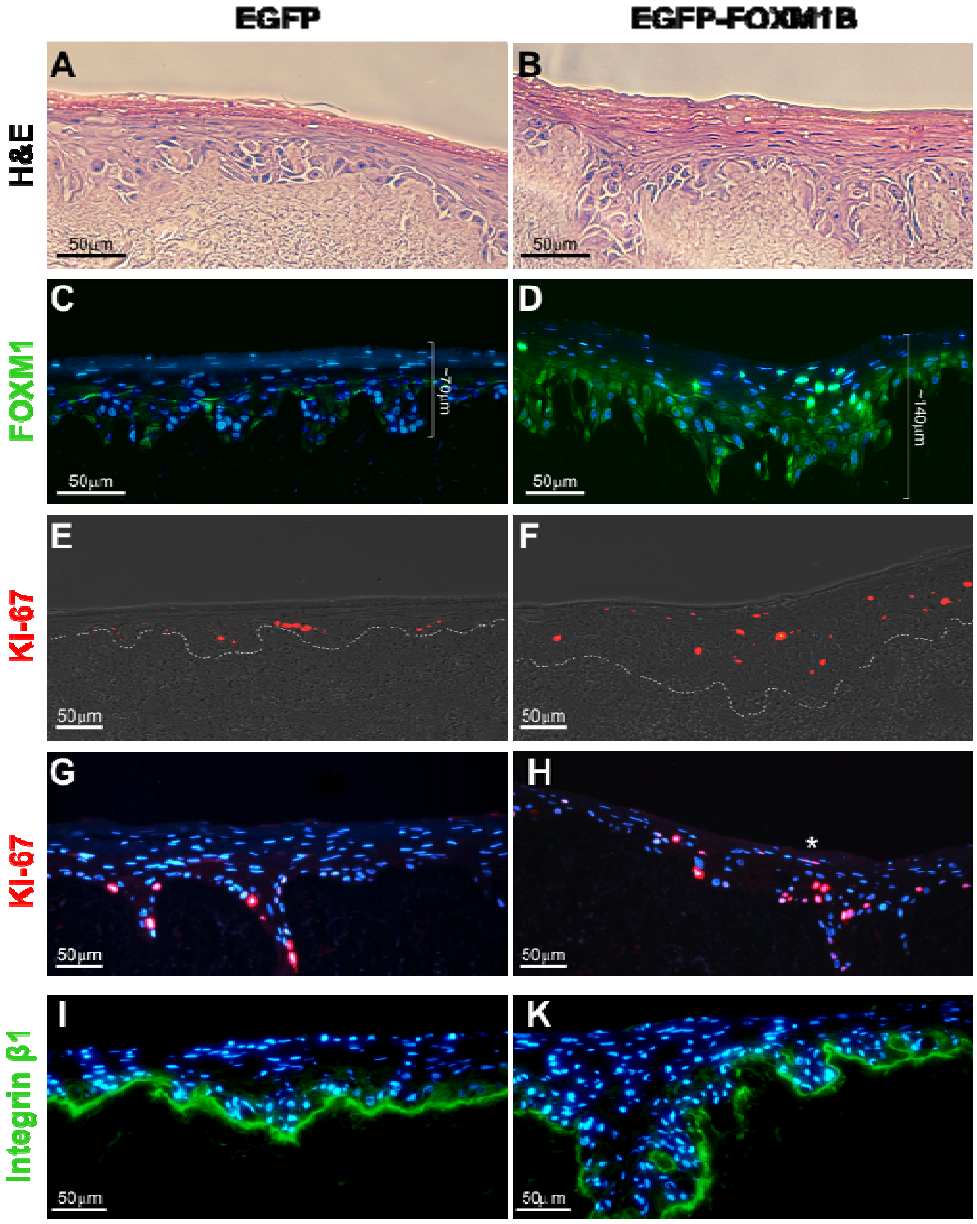

Figure 5.11: FOXM1B induces hyper-proliferation phenotype in oral mucosa organotypical culture model.

Representative images taken from haematoxylin and eosin stained 3D organotypic cultures of human oral mucosa, derived from DEDs from **(A)** pSINEGFP or **(B)** pSINEGFP-FOXM1B transduced oral keratinocytes. DED tissues were stained with anti-FOXM1 (green) **(C, D)**, Ki-67 (red) **(E, F, G, H),** and anti-integrin β1 **(I, K)**. DED sections were counterstained with DAPI for nuclear DNA visualization (blue).

To further investigate the effect of aberrant FOXM1B overexpression during epithelial regeneration, I looked for the expression of cytokeratin 16, which is a marker of the regenerating epithelium and is induced prior to, or during, hyper-proliferative conditions such as wound healing (Tyner and Fuchs, 1986), and trans-glutaminase 1 (TGA-1), which is specifically expressed in the

granular and cornified layers of the oral epithelium (Ta et al., 1990), but is also a maker of the upper spinous layers of the organotypic epithelium (Tsunenaga et al., 1994). Both cytokeratin 16 and TGA were significantly upregulated in FOXM1B derived DED cultures (**Figure 5.12 A, B, C, D**), compared to control DED cultures. Overexpression of Cytokeratin 16 has been reported in hyperproliferative disorders of human epidermis (Stoler et al., 1988), and its increased abundance in FOXM1B derived DED tissues, indirectly indicates sustained keratinocyte expansion. This along with the inappropriate mitotic activity in the suprabasal layers suggested that the expanding FOXM1B expressing keratinocyte population is not immature, and it has probably acquired a defective terminal differentiation programme.

Following up on this hypothesis, I performed immunostaining using keratinocyte terminal differentiation markers, cytokeratin 13 and filaggrin. Control EGFP DED cultures showed specific cytokeratin 13 (**Figure 5.12 E**) and Filaggrin (**Figure 5.12 G**) expression within the granular and cornified layers. In contrast, FOXM1B-derived DED cultures showed complete absence of immunoreactivity of these late differentiation markers (**Figure 5.12 F, H**). This effect was not only restricted to areas of increased thickness in FOXM1B derived DEDs, but was also notable across the whole sections of FOXM1B reconstructed tissues.

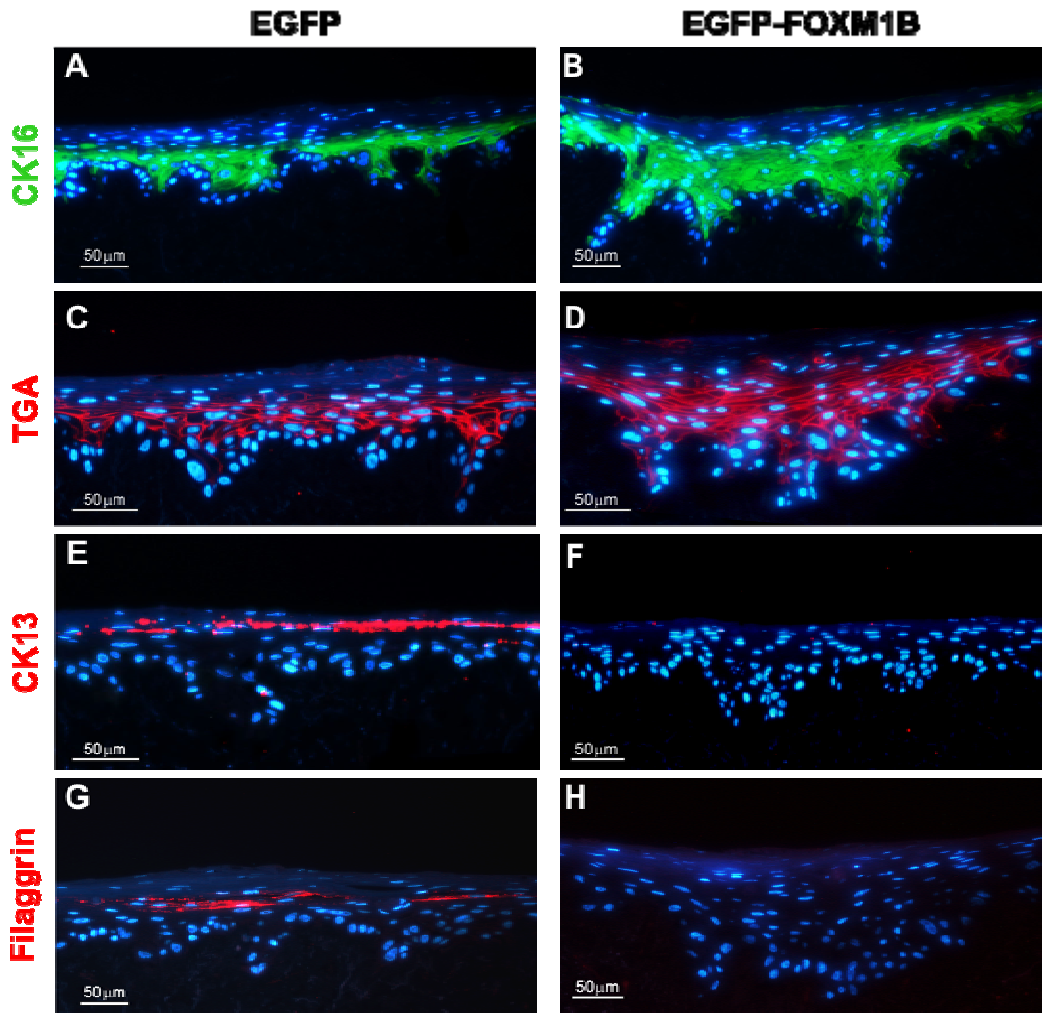

Figure 5.12: Abnormal differentiation characteristics of FOXM1B organotypic reconstructs.

DED tissues were stained with anti-cytokeratin 16 (CK16) (**A, B**), transglutaminase-1 (TGA-1) **(C, D)** anti-cytokeratin 13 **(E, F)** or anti-Filaggrin **(G, H).** Note the complete absence of cytokeratin 13 and filaggrin from FOXM1B organotypic tissues **(F, H)**. DED sections were counterstained with DAPI for nuclear DNA visualization (blue).

5.3 Discussion

The aberrant upregulation of FOXM1 in the majority of human epithelial cancers indicates a key role of FOXM1 in oncogenesis. The finding that FOXM1 expression precedes human epithelial malignancy (**Chapter 3**) (Gemenetzidis et al., 2009) led to the hypothesis that excessive FOXM1 serves as an oncogenic 1st hit rendering cells susceptible to subsequent hits required for cancer initiation. The epithelial tissue undergoes continuous renewal, under a strictly organised system that is governed by a hierarchy of cells with

differing capacities for proliferation. The gene expression profile across the hierarchy of cells within the epithelial tissue provides valuable insight into normal tissue homeostatic control mechanisms, which are frequently perturbed in human neoplasia. It is generally thought that a stem cell, owing to its longer lifespan within the tissue, serves as a host which allows long-term accumulation of oncogenic mutations giving rise to premalignant and malignant cells (Morris, 2000).

5.3.1 Oral Keratinocyte Stem Cell Properties

The localisation of p75NTR positive keratinocytes presented herein is in agreement with that of previous studies and is consistent with putative location of oral epithelial stem cells (Watt, 1998; Seery and Watt, 2000; Watt, 2001; Nakamura et al., 2007). Consistent with previous reports (Okumura et al., 2003; Nakamura et al., 2007), it was observed that human primary oral keratinocytes that express high levels of p75NTR, represent a population of OKSC which fulfils many *in vitro* stem cell characteristics (Barrandon and Green, 1987; Jones and Watt, 1993; Morris and Potten, 1994; Morris, 2000), whereby they showed enhanced holoclone-type colony formation, proliferative potential and life span in culture compared to $p75NTR^-$ cells**.** Furthermore, $p75NTR^+$ cells exhibited basal-like undifferentiated morphology, and low or suppressed expression of keratinocyte differentiation-specific marker cytokeratin 4. Contrarily to previous observations, suggesting that integrin β1 can also be used for the enrichment for human OKSC (Jensen et al., 2008), there were no significant differences between integrin $\beta1^+$ and integrin $\beta1^-$ populations examined here. The reason for this apparent disparity could be that the enrichment protocols used here, did not include rapid adhesion to extracellular matrix proteins, or further enrichment based on cell size, as previously suggested (Jones and Watt, 1993). Nevertheless, the results presented here show that inclusion of integrin β1 as an additional marker for OKSC enrichment did not provide significant advantage. Although integrin β1 is a well demonstrated marker of epidermal stem cells, it is yet unclear whether its expression pattern in other epithelia correlates with a stem cell status. For example in human oesophangeal epithelia integrin β1 correlates with a decreased clonogenic capaicy of keratinocytes *in vitro* (Seery and Watt,

2000). It is also demonstrated that highly proliferative populations of p75NTR$^+$ keratinocytes display, among other stem cell related markers (NESTIN and NUMB (Lendahl et al., 1990; Clayton et al., 2007)), elevated levels of ΔNp63α protein, which is also preferentially expressed in holoclone-derived populations of epidermal and limbal keratinocytes (Pellegrini et al., 2001). This suggests that ΔNp63α may also serve as a potential *in vitro* stem cell marker for keratinocytes of the oral epithelium. In support, there is significant overlap between the localization of p75NTR and p63 in normal oral and oesophageal epithelium (Hatakeyama et al., 2007; Huang et al., 2009).

5.3.2 The Regulation of FOXM1 in OKSC

The expression pattern of FOXM1 in normal oral epithelium *in vivo* is consistent with that of a proliferation associated protein as it is predominantly expressed in the parabasal, most proliferative, layers of the oral epithelium. Its expression was not seen in areas of intense p75NTR expression suggesting that FOXM1 is possibly down-regulated in the more immature populations of oral keratinocytes. This hypothesis was confirmed after analysis of the molecular gene expression profile of putative OKSC *in vitro.*

When keratinocyte populations are expanded *in vitro* under optimized conditions, they are expected to contain the slow cycling immature population, the more rapidly proliferating transit amplifying keratinocytes as well as terminally differentiated keratinocytes. This heterogeneity was previously shown to exist in *ex vivo* human epidermal keratinocyte cultures (Eisinger et al., 1979). By isolating each separate population, it is therefore expected that putative keratinocyte stem cells will display features of quiescence.

The evidence presented here, as well as in previous studies, demonstrate that the expression and activity of FOXM1 is mainly restricted to the G2/M phases of the cell cycle (Leung et al., 2001; Laoukili et al., 2008b). Therefore, it is possible that the suppression of FOXM1 in OKSC is a requirement for the maintenance of their slow cycling status. Others have found that the majority of isolated p75NTR$^+$ human oesophageal keratinocytes, are mainly in a G0/G1 state, and are characterized by a slow cell cycle profile *in vitro* (Okumura et

al., 2003). Expression analysis of human epidermal keratinocyte stem cells *in vitro* revealed that the maintenance of their quiescent state is partly attributed to a negative regulator of c-MYC, namely LRIG1 (Jensen and Watt, 2006). As there is evidence that c-MYC transactivates FOXM1 (Blanco-Bose et al., 2008), it is possible, that LRIG1-induced suppression of c-MYC, indirectly contributed to the observed repression of FOXM1, in OKSC populations. It should be noted however, that while this may be a possible mechanism in normal physiological conditions, it is not necessarily applicable in cases of pathological activation of FOXM1. For example, FOXM1B is highly overexpressed in basal cell carcinomas (BCCs), despite the fact that these tumours exhibit reduced levels of c-MYC protein (Bonifas et al., 2001).

Although keratinocyte stem cells are slow cycling, they are capable of sustained proliferation and are solely responsible for the expansion and replenishment of the keratinocyte population. This can explain the finding that after prolonged culture, FOXM1 protein was present only in the originally isolated p75NTR^{+} cells. Given that FOXM1 promotes cellular proliferation by regulating the expression of G1/S and G2/M transition specific genes (Wierstra and Alves, 2007), its expression pattern represents the expansion of OKSCs, which give rise to the more rapidly dividing transit amplifying keratinocytes.

During the course of the experiments, it was observed that the initial expression levels of FOXM1 in freshly isolated primary keratinocytes, positively correlated with their clonogenic and proliferative potential in culture (personal observation). FOXM1 is broadly expressed in all embryonic tissues, while in adult organs its expression is restricted to tissues of a high proliferative index (e.g. testis, thymus and bone marrow), where it is important for replenishing the post-mitotic differentiated cells and for tissue expansion in response to injury (Ye et al., 1997). Hepatic deletion of Foxm1b in mice can result in diminution of mitotic entry during liver regeneration, while ectopic Foxm1b is alone sufficient to re-establish proliferation of aged mouse hepatocytes, following partial hepatectomy (Wang et al., 2002b). More recently, Foxm1 was shown to be critical for the maintenance and expansion

of pancreatic β-cell mass and pancreatic-wide deletion of Foxm1 resulted in impaired glucose tolerance and diabetes in mice (Zhang et al., 2006). In the context of epithelial carcinogenesis, a recent report provided *in vivo* evidence, suggesting that the presence of Foxm1 is essential for the successful expansion of tumourigenic progenies in chemically induced carcinogenesis in mice (Wang et al., 2009). Overall, these observations led to the hypothesis that the initial expression levels of FOXM1 in the keratinocyte stem cell pool may be an important determinant of their total proliferative output, and the successful expansion of their progeny. This is further supported by data presented here, where specific overexpression of FOXM1B in putative OKSC ($p75NTR^{+}$), increased the ability of keratinocytes for clonal expansion.

The suppression of FOXM1 following prolonged culture of $p75NTR^{-}$ cells, suggests that FOXM1 is down-regulated in the progeny of keratinocytes undergoing terminal differentiation. This is consistent with the finding that FOXM1 protein and mRNA expression levels decline during confluence-induced differentiation of a human epithelial colon carcinoma cell line (Caco-2) toward the enterocyte cell lineage (Ye et al., 1997). Although the onset of replicative senescence could also contribute to a the downregulation of FOXM1 in primary normal oral keratinocytes, FOXM1 expression levels were diminished in differentiating keratinocytes, well before they entered a state of replicative senescence, which became evident at approximately PD~23-28. Furthermore, FOXM1 protein is absent from the differentiated layers of normal oral epithelium (**Figures 3.1, 5.1**). The down-modulation of the proliferative effects of FOXM1 may allow exit from the cell cycle and signify the onset of keratinocyte terminal differentiation. The $p75NTR^{-}$ population consists of a good model of *in vitro* keratinocyte differentiation, in that it is a committed keratinocyte progeny with an early passage history, which allows a clear demonstration of the differentiation programme, devoid of the 'contaminating' effects of replicative senescence.

5.3.3 The Impact of FOXM1B Overexpression in OKSC

Given the fact that FOXM1B is upregulated in early epithelial pre-malignancies (Gemenetzidis et al., 2009), it was reasoned that its overexpression may constitute an initiating proliferative stimulus, possibly targeting the immature basal populations of the human epithelium.

Since FOXM1 expression is mainly detected during the expansion of OKSCs *in vitro*, and is localised in proliferative expanding parabasal layers of oral epithelium *in vivo*, it was possible that overexpression of this transcription factor could in turn promote keratinocyte population expansion and consequently, prematurely forcing the exit of keratinocytes from the stem cell compartment. However, this was not the case as ectopic expression of FOXM1B was maintained in OKSCs with no loss or premature differentiation of keratinocyte stem cells. Genomic DNA copy number of EGFP-FOXM1B viral transgene remained similar between day 3 and day 10 in culture indicating that there was no loss of viral transgene in prolonged culture (see **Appendix 7**). FOXM1B expressing OKSCs showed evidence of increased clonal expansion and were also able to efficiently support epithelial reconstruction *in vitro*, indicating that overexpression of FOXM1B did not deplete the stem cell population. This observation could be contradictory if one considers that forced overexpression of the downstream target of FOXM1, c-Myc, has been shown to deplete the stem cell population of human epidermal keratinocytes by forcing them to commit to premature differentiation (Gandarillas and Watt, 1997). However, ectopic expression of a constitutively active, non-degradable form of β-catenin (ΔNβ-catenin), an upstream regulator of c-Myc, not only did not lead to premature differentiation, but instead it was shown to increase the proliferative capacity of human epidermal keratinocytes (Zhu and Watt, 1999). These studies indicate that the mechanism of stem cell exit and differentiation is complex and dependent upon the nature of the stimuli.

The overexpression of FOXM1B resulted in increased population expansion, only when it was specifically targeted to the $p75NTR^{+}$ populations, but had no effect when directed to the committed progeny of $p75NTR^{-}$ keratinocytes.

p75NTR$^+$ cells strictly represent the basal oral keratinocyte population, which apart from putative OKSCs also includes the early TA keratinocytes (see also **Chapter 1, section 1.2.1**). The evidence provided herein as well as in previous reports suggest that this p75NTR expression signature is largely maintained *in vitro* (Okumura et al., 2003; Nakamura et al., 2007). Therefore, FOXM1B overexpression in both the OKSC and/or early TA (p75NTR$^+$) compartment could have produced the observed effect. In the case of the latter, the oncogenic event should occur immediately after a cell exits the stem cell compartment (still at p75NTR$^+$ state), since it will only be proliferative for a brief period of time prior to initiation of terminal differentiation (enters a p75NTR$^-$ state).

It is known that FOXM1B protein is subject to extensive post-translational modifications. As such, its nuclear translocation and subsequent activation requires mitogenic signalling (Ye et al., 1999; Ma et al., 2005), while it is also shown that it can mainly transactivate its downstream targets upon entry in G2/M phase, at which time it is heavily phosphorylated (Leung et al., 2001; Laoukili et al., 2005; Laoukili et al., 2008b). Hence, this oncogenic insult can only be effective during normal OKSC expansion, when cells engage in limited but rapid cycles of cell division, and in support of our findings, it could not theoretically have any effect on late differentiating/differentiated keratinocytes where mitogenic signalling is normally completely lost (Barrandon and Green, 1987; Fuchs, 1993). Therefore, consistent with the notion that stem cells are hosts of oncogenic events (Morris, 2000; Morris et al., 2000) (see also **Chapter 1, section 1.2.4**), the most conceivable explanation is that a 'successful' FOXM1B 'hit' would have to be present in OKSC prior to their expansion. The inability of TA cells to subsequently suppress levels of excessive FOXM1B proteins can induce sustained proliferation, at the expense of terminal differentiation, as seen in the organotypic epithelial reconstructs. As discussed above, we have found that OKSCs (early passage immature p75NTR$^+$ cells) are able to retain the FOXM1B transgene without causing stem cell exit, presumably through a yet unknown intrinsic mechanism that prevents FOXM1B-induced cell cycle entry and mains a slow cycling status of OKSCs, whereas, OKSCs committed to

differentiation ($p75NTR^-$ cells) were not able to suppress FOXM1B transgene expression. In a similar fashion, human FOXM1B was shown to exert a strong proliferative advantage in the livers of transgenic mice, only following partial liver hepatectomy, which is known to induce liver regeneration, at which time mitogenic signalling is abundant (Ye et al., 1999). The availability of additional markers, to discriminate between early TA keratinocytes and OKSCs, would allow more extensive characterisation of the target population of FOXM1B oncogenic insults.

5.3.4 FOXM1B Overexpression Perturbs Normal Epithelial Differentiation

In a functional differentiation 3D model of human epithelium, FOXM1B induced a hyperproliferative phenotype leading enhanced development of multiple proliferative spinous cell layers. As keratinocyte proliferation is a main characteristic of transit amplifying cells before undergoing permanent cell cycle arrest and commitment to terminal differentiation (Watt, 1998), excessive proliferation detected in the suprabasal layer is perceived to be pathological. It is therefore possible that FOXM1B-induced keratinocyte expansion may interfere with the normal keratinocyte differentiation program by rendering keratinocytes refractory to growth arrest and terminal differentiation.

In this respect, the expansion of Cytokeratin 16 positive layers, as observed in FOXM1B organotypics, has been suggested to be a marker of suprabasal epithelial keratinocytes in a transient state, during which they maintain their proliferative capacity while being resilient to terminal differentiation (Bernot et al., 2002). The upregulation of cytokeratin 16, along with the inappropriate mitotic activity detected in the spinous layers of FOXM1B organotypics, suggest the presence of a defective or perturbed differentiation program within the progenitor TA cells that have acquired/inherited ectopic FOXM1B. This hypothesis is further supported by the complete inhibition of two terminal differentiation markers, cytokeratin 13 and filaggrin, in FOXM1B-derived organotypics. The mechanism behind this is yet unclear, since FOXM1B could be directly suppressing keratinocyte differentiation, or the latter could be a

result of sustained proliferation of progenitor (TA) keratinocytes. Both are equally possible, and require further investigation to fully understand the underlying mechanisms involved, since they can provide additional insight to the early oncogenic effects mediated by FOXM1B.

In summary, it is demonstrated for the first time that FOXM1B is involved in epithelial stem cell expansion and that ectopic expression of FOXM1B in this population of cells resulted in hyper-proliferation and concomitant suppression of keratinocyte terminal differentiation. It is therefore proposed that aberrant upregulation of FOXM1B in oral keratinocyte stem cell cells may constitute an early event in OSCC development, which may explain why upregulation of FOXM1 precedes epithelial malignancy.

Chapter 6

GENERAL DISCUSSION

6 General Discussion

The present study investigated the role of FOXM1, a cell-cycle dependent transcription factor, in human oral squamous cell carcinoma (OSCC). Despite the fact that FOXM1 is overexpressed in the majority of human malignancies (Pilarsky et al., 2004), its expression had not yet been investigated in the case of human oral SCCs. This study showed that FOXM1 is significantly upregulated at both protein and mRNA levels in early pre-malignant lesions of human oral mucosa, as well as in more advanced stages of oral cancer such as CIS, invasive malignancy and lymph node metastases. This expression pattern was also maintained *in vitro*, as observed from expression analysis of cultured neoplastic and pre-neoplastic human oral keratinocytes. In addition, it was demonstrated that neoplastic oral keratinocytes retain high levels of active, phosphorylated FOXM1 protein and consistently, they exhibit enhanced expression of established FOXM1 downstream target genes including CENPA, CENPF, CCNB1, and NEK2, which agrees with a FOXM1-dependent expression signature. The fact that FOXM1 upregulation is evident in mildly dysplastic oral epithelia suggests a role for this gene in the early stages of epithelial carcinogenesis. This is also consistent with the fact that FOXM1 has been found to promote cellular proliferation in pre-neoplastic lesions of mouse liver epithelium (Kalinina et al., 2003). Hence, it is proposed that its expression might be a marker of heightened proliferation in such lesions. As many pre-malignant lesions of the oral mucosa do not progress to form SCCs later on, it is currently unknown whether the levels of FOXM1 expression in such lesions show any correlation with an advanced risk for malignant transformation. Certainly, other studies have shown that FOXM1 expression is an indicator of tumour stage and poor prognosis in other human tumours (Kalin et al., 2006; Liu et al., 2006; Chandran et al., 2007; Bektas et al., 2008; Chan et al., 2008; Martin et al., 2008; Yang et al., 2009), and as such, it would be very important to study the relationship between its expression in pre-neoplastic lesions and the incidence of tumour development in the oral epithelium since the failure in early diagnosis is one of the most important caveats in the management of OSCCs.

FOXM1 mRNA expression and protein transcriptional activation were found to be enhanced by exposing human oral epithelial keratinocytes to nicotine, which represents one of the main constituents of tobacco. Surprisingly, this response was present in both pre-malignant and normal human primary oral keratinocytes. It is known that the fate of oral epithelial pre-malignancies such as leukoplakias is largely dependent upon exposure to tobacco smoke. Taken together, these observations suggest that exposure of human oral epithelium to nicotine can activate the expression and transactivation ability of FOXM1, explaining its presence in oral pre-malignancies and SCCs. Given the fact that many leukoplakias regress after smoking cessation, it would be interesting to investigate the levels of FOXM1 expression in leukoplakias. By screening the expression patterns of candidate genes downstream of FOXM1, it was found that centrosome associated protein, CEP55, is a direct transcriptional target of FOXM1 and further that it is significantly overexpressed in pre-malignant and malignant oral keratinocytes *in vitro*. In addition, lymphoid-specific helicase (HELLS) was also found to be significantly upregulated in pre-malignant and OSCC derived keratinocytes, and together with CEP55 they represent novel targets whose expressions are regulated by FOXM1, and could therefore be useful markers in the pathogenesis of OSCC.

The fact that early pre-malignant oral lesions display features of genetic aberrations, further implies that progression to OSCC is largely dependent upon oncogenic stimulation which is thought to initiate, and promote genomic instability (Negrini et al., 2010). Consistent with this hypothesis, thie present study shows that FOXM1B overexpression compromises the genomic integrity of primary human epidermal and oral keratinocytes. By allowing primary human epidermal keratinocytes to grow in the presence of ectopic FOXM1B protein levels, these cells were able to undergo sequential population expansions while accumulating genomic CNV consistent with a pattern of genomic instability. Following genotoxic stress (UVB), human N/TERT keratinocytes overexpressing FOXM1B showed gross genomic abnormalities mainly characterised by long stretches of contiguous copy number losses and/or gains leading to whole chromosome 7 amplification and

extensive LOH at chromosome 6. Since it was shown here that both the endogenous, as well as exogenous FOXM1B, are exclusively expressed at G2/M phase of human keratinocytes, it is proposed that the observed effects may result from the excessive accumulation of FOXM1B proteins at mitosis. FOXM1 is known to have multiple roles in mitotic progression, which is also evidenced by the fact that the list comprising it downstream targets includes many genes that regulate chromosome segregation, the assembly of the spindle checkpoint, chromosome alignment and attachment to kinetochores, all of which are important processes, and their deregulation can affect genomic stability (D'Assoro et al., 2002a; D'Assoro et al., 2002b; Gisselsson et al., 2002; Lingle et al., 2002; Li et al., 2004b; Hu et al., 2005; Smith et al., 2005; Hayward and Fry, 2006). The fact that depletion of FOXM1 can lead to mitotic catastrophe, genomic instability and apoptosis, further highlights its critical importance in mitotic division. The finding that FOXM1B overexpression can cause genomic instability while being permissive for normal cell cycle is consistent with the fact that both FOXM1 and genomic instability occur in parallel in many human malignancies (Carter et al., 2006).

The appearance of a human epithelial malignancy, such as OSCC, is the culmination of many years of development. Epithelial tumours are thought to arise from common pre-malignant progenitors, which are slowly subjected to cumulative genetic aberrations that ultimately lead to invasive malignancy. Owing to their self-renewal capacity, epithelial stem cells have been long proposed as being the hosts for initiating mutations (Morris, 2000). In this respect, this study examined the effect of FOXM1B overexpression in the immature basal epithelial stem cell population of the oral mucosa (OKSC), in the attempt to create an oncogenic 'first hit' in OKSC. It is shown that FOXM1 expression is normally kept at low levels in human OKSC both *in vivo* and *in vitro*. Consistent with the enhanced proliferation of TA keratinocytes, FOXM1 levels were increased upon keratinocyte population expansion, but were subsequently diminished upon terminal keratinocyte differentiation. Aiming to understand its potential role in tumour initiation, FOXM1B was ectopically expressed in human OKSCs. OKSCs overexpressing FOXM1B show enhanced population expansion *in vitro,* while

TA keratinocytes failed to show any responses to FOXM1B overexpression. In addition, FOXM1B overexpressing keratinocytes show abnormal patterns of proliferation and epithelial differentiation in organotypic 3D models of human oral musocal epithelium. The phenotype and the pattern of differentiation marker expression of FOXM1B organotypics was reminiscent of that observed in early hyperplastic lesions of oral mucosa, which are the earliest detectable alteration in the progression of OSCC. These results led to my subsequent proposal of a mechanistic model of how FOXM1 induce cancer formation.

6.1 A Model of Oncogenic Activity for FOXM1

This study has provided several lines of evidence that support the notion that FOXM1 is a gene that can affect various biological processes relevant to human malignancy. By combining and translating the results that were obtained from *in vivo* observations and the manipulation of primary human epithelial keratinocytes *in vitro*, the deduction of a model for the oncogenic activity of FOXM1 is proposed.

This study proposes that oral epithelial keratinocyte stem cells are a good candidate cell population to host a genetic hit resulting in the activation of FOXM1 expression. This event could be randomly introduced either through a stochastic somatic mutation that directly affects the transcriptional regulation or FOXM1 or, as proposed from *in vitro* observations, through the sustained exposure of oral mucosal keratinocytes to one of the main constituents of tobacco, nicotine. This fits well with the notion that epithelial stem cells are the main target population of carcinogens in exposed epithelium (Morris, 2000). Exploiting the normal process of epithelial renewal, FOXM1 overexpression is later established in the expanding population of epithelial keratinocytes, resulting in increased proliferation and subsequent suppression of epithelial differentiation. Since FOXM1 overexpression in primary human keratinocytes leads to the generation of genetically unstable progenies as shown herein, it is further suggested that epithelial population expansion occurs parallel to the acquisition of genetic aberrations.

This proposed model is in keeping with the general consensus regarding oral epithelial carcinogenesis, suggesting that a common pre-malignant progenitor, in this case an oral epithelial stem cell overexpressing FOXM1B, undergoes rounds of clonal expansion due to an acquired deficiency in epithelial differentiation, leading to the propagation of genetically unstable progenies. Although this is a proposed model by which FOXM1 could possibly contribute or mediate the early transition from a normal to a potentially pre-malignant clone, the conversion to invasive malignancy would further require sequential molecular and genetic alterations. The proposed model can further

provide a reasonable explanation for the observed upregulation of FOXM1 in pre-malignant as well as in invasive neoplastic keratinocytes both *in vivo* and *in vitro*.

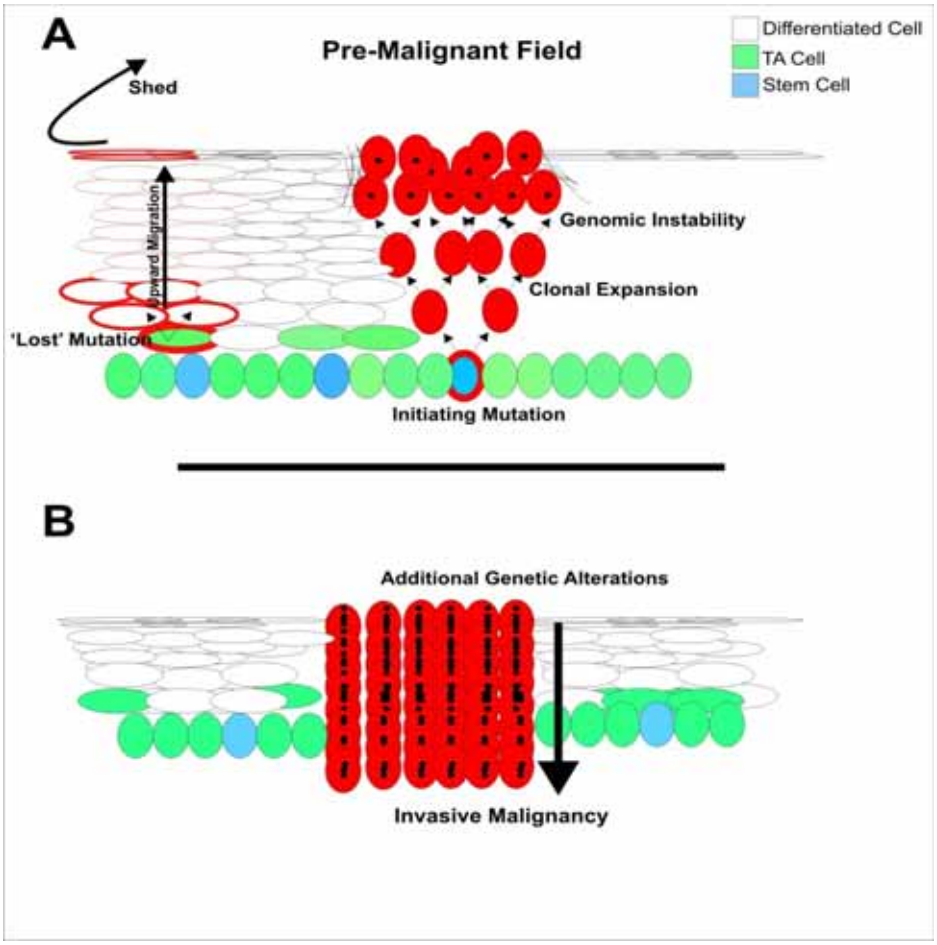

Figure 6.1: A model of oncogenic activity for FOXM1

(A) An initiating mutation in oral epithelial stem cells can result in the clonal expansion of pre-malignant epithelial progenies due to acquired defect in epithelial differentiation. Aberrant activation of FOXM1 leads to the acquisistion of genomic instability which can potentially give rise to a pre-malignant 'field'.Contrarily, a mutation targeted in more commited transit amplifying (TA) progenitor cells would be lost through the process of epithelial renewal. **(B)** Following further genetic hits which may result in the activation of oncogenes and/or suppression of tumour suppressor genes, can later enable the malignant conversion of epithelial keratinocytes, leading to invasive malignancy.

List of References

Aebersold DM, Burri P, Beer KT, Laissue J, Djonov V, Greiner RH et al (2001). Expression of hypoxia-inducible factor-1alpha: a novel predictive and prognostic parameter in the radiotherapy of oropharyngeal cancer. *Cancer Res* **61:** 2911-6.

Amati B, Alevizopoulos K, Vlach J (1998). Myc and the cell cycle. *Front Biosci* **3:** d250-68.

Bailleul B, Surani MA, White S, Barton SC, Brown K, Blessing M et al (1990). Skin hyperkeratosis and papilloma formation in transgenic mice expressing a ras oncogene from a suprabasal keratin promoter. *Cell* **62:** 697-708.

Barrandon Y, Green H (1985). Cell size as a determinant of the clone-forming ability of human keratinocytes. *Proc Natl Acad Sci U S A* **82:** 5390-4.

Barrandon Y, Green H (1987). Three clonal types of keratinocyte with different capacities for multiplication. *Proc Natl Acad Sci U S A* **84:** 2302-6.

Barsotti AM, Prives C (2009). Pro-proliferative FoxM1 is a target of p53-mediated repression. *Oncogene*.

Bartkova J, Horejsi Z, Koed K, Kramer A, Tort F, Zieger K et al (2005). DNA damage response as a candidate anti-cancer barrier in early human tumorigenesis. *Nature* **434:** 864-70.

Beasley NJ, Leek R, Alam M, Turley H, Cox GJ, Gatter K et al (2002). Hypoxia-inducible factors HIF-1alpha and HIF-2alpha in head and neck cancer: relationship to tumor biology and treatment outcome in surgically resected patients. *Cancer Res* **62:** 2493-7.

Bedi GC, Westra WH, Gabrielson E, Koch W, Sidransky D (1996). Multiple head and neck tumors: evidence for a common clonal origin. *Cancer Res* **56:** 2484-7.

Bektas N, Haaf A, Veeck J, Wild PJ, Luscher-Firzlaff J, Hartmann A et al (2008). Tight correlation between expression of the Forkhead transcription factor FOXM1 and HER2 in human breast cancer. *BMC Cancer* **8:** 42.

Bernot KM, Coulombe PA, McGowan KM (2002). Keratin 16 expression defines a subset of epithelial cells during skin morphogenesis and the hair cycle. *J Invest Dermatol* **119:** 1137-49.

Bhat UG, Halasi M, Gartel AL (2009). Thiazole antibiotics target FoxM1 and induce apoptosis in human cancer cells. *PLoS One* **4:** e5592.

Bickenbach JR (1981). Identification and behavior of label-retaining cells in oral mucosa and skin. *J Dent Res* **60 Spec No C:** 1611-20.

Bickenbach JR, Chism E (1998). Selection and extended growth of murine epidermal stem cells in culture. *Exp Cell Res* **244:** 184-95.

Bickenbach JR, Holbrook KA (1987). Label-retaining cells in human embryonic and fetal epidermis. *J Invest Dermatol* **88:** 42-6.

Bieche I, Nogues C, Lidereau R (1999). Overexpression of BRCA2 gene in sporadic breast tumours. *Oncogene* **18:** 5232-8.

Blanco-Bose WE, Murphy MJ, Ehninger A, Offner S, Dubey C, Huang W et al (2008). C-Myc and its target FoxM1 are critical downstream effectors of constitutive androstane receptor (CAR) mediated direct liver hyperplasia. *Hepatology* **48:** 1302-11.

Blanpain C, Fuchs E (2006). Epidermal stem cells of the skin. *Annu Rev Cell Dev Biol* **22:** 339-73.

Blanpain C, Horsley V, Fuchs E (2007). Epithelial stem cells: turning over new leaves. *Cell* **128:** 445-58.

Blaydon DC, Ishii Y, O'Toole EA, Unsworth HC, Teh MT, Ruschendorf F et al (2006). The gene encoding R-spondin 4 (RSPO4), a secreted protein implicated in Wnt signaling, is mutated in inherited anonychia. *Nat Genet* **38:** 1245-7.

Bockmuhl U, Wolf G, Schmidt S, Schwendel A, Jahnke V, Dietel M et al (1998). Genomic alterations associated with malignancy in head and neck cancer. *Head Neck* **20:** 145-51.

Bonifas JM, Pennypacker S, Chuang PT, McMahon AP, Williams M, Rosenthal A et al (2001). Activation of expression of hedgehog target genes in basal cell carcinomas. *J Invest Dermatol* **116:** 739-42.

Bouquot JE, Weiland LH, Kurland LT (1988). Leukoplakia and carcinoma in situ synchronously associated with invasive oral/oropharyngeal carcinoma in Rochester, Minn., 1935-1984. *Oral Surg Oral Med Oral Pathol* **65:** 199-207.

Boutwell RK (1974). The function and mechanism of promoters of carcinogenesis. *CRC Crit Rev Toxicol* **2:** 419-43.

Boyle JO, Hakim J, Koch W, van der Riet P, Hruban RH, Roa RA et al (1993). The incidence of p53 mutations increases with progression of head and neck cancer. *Cancer Res* **53:** 4477-80.

Brown K, Strathdee D, Bryson S, Lambie W, Balmain A (1998). The malignant capacity of skin tumours induced by expression of a mutant H-ras transgene depends on the cell type targeted. *Curr Biol* **8:** 516-24.

Burgeson RE, Christiano AM (1997). The dermal-epidermal junction. *Curr Opin Cell Biol* **9:** 651-8.

Cahill DP, Kinzler KW, Vogelstein B, Lengauer C (1999). Genetic instability and darwinian selection in tumours. *Trends Cell Biol* **9:** M57-60.

Califano J, Leong PL, Koch WM, Eisenberger CF, Sidransky D, Westra WH (1999). Second esophageal tumors in patients with head and neck squamous cell carcinoma: an assessment of clonal relationships. *Clin Cancer Res* **5:** 1862-7.

Califano J, van der Riet P, Westra W, Nawroz H, Clayman G, Piantadosi S et al (1996). Genetic progression model for head and neck cancer: implications for field cancerization. *Cancer Res* **56:** 2488-92.

Califano J, Westra WH, Meininger G, Corio R, Koch WM, Sidransky D (2000). Genetic progression and clonal relationship of recurrent premalignant head and neck lesions. *Clin Cancer Res* **6:** 347-52.

Calvisi DF, Pinna F, Ladu S, Pellegrino R, Simile MM, Frau M et al (2009). Forkhead box M1B is a determinant of rat susceptibility to hepatocarcinogenesis and sustains ERK activity in human HCC. *Gut* **58:** 679-87.

Candi E, Schmidt R, Melino G (2005). The cornified envelope: a model of cell death in the skin. *Nat Rev Mol Cell Biol* **6:** 328-40.

Cao W, Xi X, Hao Z, Li W, Kong Y, Cui L et al (2007). RAET1E2, a soluble isoform of the UL16-binding protein RAET1E produced by tumor cells, inhibits NKG2D-mediated NK cytotoxicity. *J Biol Chem* **282:** 18922-8.

Carter SL, Eklund AC, Kohane IS, Harris LN, Szallasi Z (2006). A signature of chromosomal instability inferred from gene expression profiles predicts clinical outcome in multiple human cancers. *Nat Genet* **38:** 1043-8.

Carvalho AL, Nishimoto IN, Califano JA, Kowalski LP (2005). Trends in incidence and prognosis for head and neck cancer in the United States: a site-specific analysis of the SEER database. *Int J Cancer* **114:** 806-16.

Chan DW, Yu SY, Chiu PM, Yao KM, Liu VW, Cheung AN et al (2008). Over-expression of FOXM1 transcription factor is associated with cervical cancer progression and pathogenesis. *J Pathol* **215:** 245-52.

Chandran UR, Ma C, Dhir R, Bisceglia M, Lyons-Weiler M, Liang W et al (2007). Gene expression profiles of prostate cancer reveal involvement of multiple molecular pathways in the metastatic process. *BMC Cancer* **7:** 64.

Chang SE, Foster S, Betts D, Marnock WE (1992). DOK, a cell line established from human dysplastic oral mucosa, shows a partially transformed non-malignant phenotype. *Int J Cancer* **52:** 896-902.

Charles RL, Rammohan T, Jos JPN, Isaac Van Der W, Gordon BS. (1994). *Vol. 73*, pp 187-190.

Chen CH, Chien CY, Huang CC, Hwang CF, Chuang HC, Fang FM et al (2009a). Expression of FLJ10540 is correlated with aggressiveness of oral cavity squamous cell carcinoma by stimulating cell migration and invasion through increased FOXM1 and MMP-2 activity. *Oncogene* **28:** 2723-37.

Chen CH, Lai JM, Chou TY, Chen CY, Su LJ, Lee YC et al (2009b). VEGFA upregulates FLJ10540 and modulates migration and invasion of lung cancer via PI3K/AKT pathway. *PLoS One* **4:** e5052.

Chen CH, Lu PJ, Chen YC, Fu SL, Wu KJ, Tsou AP et al (2007). FLJ10540-elicited cell transformation is through the activation of PI3-kinase/AKT pathway. *Oncogene* **26:** 4272-83.

Chiu CY, Leng S, Martin KA, Kim E, Gorman S, Duhl DM (1999). Cloning and characterization of T-cell lymphoma invasion and metastasis 2 (TIAM2), a novel guanine nucleotide exchange factor related to TIAM1. *Genomics* **61:** 66-73.

Chu M, Guo J, Chen CY (2005). Long-term exposure to nicotine, via ras pathway, induces cyclin D1 to stimulate G1 cell cycle transition. *J Biol Chem* **280:** 6369-79.

Chu TY, Shen CY, Lee HS, Liu HS (1999). Monoclonality and surface lesion-specific microsatellite alterations in premalignant and malignant neoplasia of uterine cervix: a local field effect of genomic instability and clonal evolution. *Genes Chromosomes Cancer* **24:** 127-34.

Chung KY, Mukhopadhyay T, Kim J, Casson A, Ro JY, Goepfert H et al (1993). Discordant p53 gene mutations in primary head and neck cancers and corresponding second primary cancers of the upper aerodigestive tract. *Cancer Res* **53:** 1676-83.

Clausen OP, Kirkhus B, Thorud E, Schjolberg A, Moen E, Cromarty A (1986). Evidence of mouse epidermal subpopulations with different cell cycle times. *J Invest Dermatol* **86:** 266-70.

Clausen OP, Potten CS (1990). Heterogeneity of keratinocytes in the epidermal basal cell layer. *J Cutan Pathol* **17:** 129-43.

Clayton E, Doupe DP, Klein AM, Winton DJ, Simons BD, Jones PH (2007). A single type of progenitor cell maintains normal epidermis. *Nature* **446:** 185-9.

Collins LM, Dawes C (1987). The surface area of the adult human mouth and thickness of the salivary film covering the teeth and oral mucosa. *J Dent Res* **66:** 1300-2.

Costa RH (2005). FoxM1 dances with mitosis. *Nat Cell Biol* **7:** 108-10.

Cotsarelis G, Sun TT, Lavker RM (1990). Label-retaining cells reside in the bulge area of pilosebaceous unit: implications for follicular stem cells, hair cycle, and skin carcinogenesis. *Cell* **61:** 1329-37.

D'Assoro AB, Barrett SL, Folk C, Negron VC, Boeneman K, Busby R et al (2002a). Amplified centrosomes in breast cancer: a potential indicator of tumor aggressiveness. *Breast Cancer Res Treat* **75:** 25-34.

D'Assoro AB, Lingle WL, Salisbury JL (2002b). Centrosome amplification and the development of cancer. *Oncogene* **21:** 6146-53.

Dahl E, Kristiansen G, Gottlob K, Klaman I, Ebner E, Hinzmann B et al (2006). Molecular profiling of laser-microdissected matched tumor and normal breast tissue identifies karyopherin alpha2 as a potential novel prognostic marker in breast cancer. *Clin Cancer Res* **12:** 3950-60.

Dahl E, Sadr-Nabavi A, Klopocki E, Betz B, Grube S, Kreutzfeld R et al (2005). Systematic identification and molecular characterization of genes differentially expressed in breast and ovarian cancer. *J Pathol* **205:** 21-8.

Dai B, Kang SH, Gong W, Liu M, Aldape KD, Sawaya R et al (2007). Aberrant FoxM1B expression increases matrix metalloproteinase-2 transcription and enhances the invasion of glioma cells. *Oncogene* **26:** 6212-9.

Dale BA, Salonen J, Jones AH (1990). New approaches and concepts in the study of differentiation of oral epithelia. *Crit Rev Oral Biol Med* **1:** 167-90.

Dasgupta P, Chellappan SP (2006). Nicotine-mediated cell proliferation and angiogenesis: new twists to an old story. *Cell Cycle* **5:** 2324-8.

Dasgupta P, Rastogi S, Pillai S, Ordonez-Ercan D, Morris M, Haura E et al (2006). Nicotine induces cell proliferation by beta-arrestin-mediated activation of Src and Rb-Raf-1 pathways. *J Clin Invest* **116:** 2208-2217.

Dasgupta P, Rizwani W, Pillai S, Kinkade R, Kovacs M, Rastogi S et al (2009). Nicotine induces cell proliferation, invasion and epithelial-mesenchymal transition in a variety of human cancer cell lines. *Int J Cancer* **124:** 36-45.

de la Guardia C, Casiano CA, Trinidad-Pinedo J, Baez A (2001). CENP-F gene amplification and overexpression in head and neck squamous cell carcinomas. *Head Neck* **23:** 104-12.

De Strooper B, Van der Schueren B, Jaspers M, Saison M, Spaepen M, Van Leuven F et al (1989). Distribution of the beta 1 subgroup of the integrins in human cells and tissues. *J Histochem Cytochem* **37:** 299-307.

Deng H, Lin Q, Khavari PA (1997). Sustainable cutaneous gene delivery. *Nat Biotechnol* **15:** 1388-91.

Dennis K, Fan T, Geiman T, Yan Q, Muegge K (2001). Lsh, a member of the SNF2 family, is required for genome-wide methylation. *Genes Dev* **15:** 2940-4.

Dickson MA, Hahn WC, Ino Y, Ronfard V, Wu JY, Weinberg RA et al (2000). Human keratinocytes that express hTERT and also bypass a p16(INK4a)-enforced

mechanism that limits life span become immortal yet retain normal growth and differentiation characteristics. *Mol Cell Biol* **20:** 1436-47.

DiGiovanni J (1992). Multistage carcinogenesis in mouse skin. *Pharmacol Ther* **54:** 63-128.

Dole J, zcaron, el, Bartoscaron J, Voglmayr H, Greilhuber J. (2003). *Vol. 51A*, pp 127-128.

Dong SM, Sun DI, Benoit NE, Kuzmin I, Lerman MI, Sidransky D (2003). Epigenetic inactivation of RASSF1A in head and neck cancer. *Clin Cancer Res* **9:** 3635-40.

Dover R, Potten CS (1983). Cell cycle kinetics of cultured human epidermal keratinocytes. *J Invest Dermatol* **80:** 423-9.

Einbond LS, Su T, Wu HA, Friedman R, Wang X, Jiang B et al (2007). Gene expression analysis of the mechanisms whereby black cohosh inhibits human breast cancer cell growth. *Anticancer Res* **27:** 697-712.

Eisinger M, Lee JS, Hefton JM, Darzynkiewicz Z, Chiao JW, de Harven E (1979). Human epidermal cell cultures: growth and differentiation in the absence of differentiation in the absence of dermal components or medium supplements. *Proc Natl Acad Sci U S A* **76:** 5340-4.

Engelbert D, Schnerch D, Baumgarten A, Wasch R (2008). The ubiquitin ligase APC(Cdh1) is required to maintain genome integrity in primary human cells. *Oncogene* **27:** 907-17.

Eversole LR, Sapp JP (1993). c-myc oncoprotein expression in oral precancerous and early cancerous lesions. *Eur J Cancer B Oral Oncol* **29B:** 131-5.

Fabbro M, Zhou BB, Takahashi M, Sarcevic B, Lal P, Graham ME et al (2005). Cdk1/Erk2- and Plk1-dependent phosphorylation of a centrosome protein, Cep55, is required for its recruitment to midbody and cytokinesis. *Dev Cell* **9:** 477-88.

Faragher AJ, Fry AM (2003). Nek2A kinase stimulates centrosome disjunction and is required for formation of bipolar mitotic spindles. *Mol Biol Cell* **14:** 2876-89.

Fernandez PC, Frank SR, Wang L, Schroeder M, Liu S, Greene J et al (2003). Genomic targets of the human c-Myc protein. *Genes Dev* **17:** 1115-29.

Filipowicz W, Bhattacharyya SN, Sonenberg N (2008). Mechanisms of post-transcriptional regulation by microRNAs: are the answers in sight? *Nat Rev Genet* **9:** 102-14.

Ford AC, Grandis JR (2003). Targeting epidermal growth factor receptor in head and neck cancer. *Head Neck* **25:** 67-73.

Forsti A, Louhelainen J, Soderberg M, Wijkstrom H, Hemminki K (2001). Loss of heterozygosity in tumour-adjacent normal tissue of breast and bladder cancer. *Eur J Cancer* **37:** 1372-80.

Francis RE, Myatt SS, Krol J, Hartman J, Peck B, McGovern UB et al (2009). FoxM1 is a downstream target and marker of HER2 overexpression in breast cancer. *Int J Oncol* **35:** 57-68.

Franklin WA, Gazdar AF, Haney J, Wistuba, II, La Rosa FG, Kennedy T et al (1997). Widely dispersed p53 mutation in respiratory epithelium. A novel mechanism for field carcinogenesis. *J Clin Invest* **100:** 2133-7.

Fuchs E (1990). Epidermal differentiation: the bare essentials. *J Cell Biol* **111:** 2807-14.

Fuchs E (1993). Epidermal differentiation and keratin gene expression. *J Cell Sci Suppl* **17:** 197-208.

Fuchs E (2008). Skin stem cells: rising to the surface. *J Cell Biol* **180:** 273-84.

Fujii H, Marsh C, Cairns P, Sidransky D, Gabrielson E (1996). Genetic divergence in the clonal evolution of breast cancer. *Cancer Res* **56:** 1493-7.

Fujiki H, Suganuma M, Yoshizawa S, Kanazawa H, Sugimura T, Manam S et al (1989). Codon 61 mutations in the c-Harvey-ras gene in mouse skin tumors induced by 7,12-dimethylbenz[a]anthracene plus okadaic acid class tumor promoters. *Mol Carcinog* **2:** 184-7.

Fukasawa K (2005). Centrosome amplification, chromosome instability and cancer development. *Cancer Lett* **230:** 6-19.

Galipeau PC, Prevo LJ, Sanchez CA, Longton GM, Reid BJ (1999). Clonal expansion and loss of heterozygosity at chromosomes 9p and 17p in premalignant esophageal (Barrett's) tissue. *J Natl Cancer Inst* **91:** 2087-95.

Gandarillas A, Watt FM (1997). c-Myc promotes differentiation of human epidermal stem cells. *Genes Dev* **11:** 2869-82.

Garant PR (2003). *Oral Cells and Tissues* Quintessence Pub Co.

Garrod DR (1993). Desmosomes and hemidesmosomes. *Curr Opin Cell Biol* **5:** 30-40.

Geiman TM, Durum SK, Muegge K (1998). Characterization of gene expression, genomic structure, and chromosomal localization of Hells (Lsh). *Genomics* **54:** 477-83.

Gemenetzidis E, Bose A, Riaz AM, Chaplin T, Young BD, Ali M et al (2009). FOXM1 upregulation is an early event in human squamous cell carcinoma and it is enhanced by nicotine during malignant transformation. *PLoS ONE* **4:** e4849.

Gibbs S, Ponec M (2000). Intrinsic regulation of differentiation markers in human epidermis, hard palate and buccal mucosa. *Arch Oral Biol* **45:** 149-58.

Giese A, Bjerkvig R, Berens ME, Westphal M (2003). Cost of migration: invasion of malignant gliomas and implications for treatment. *J Clin Oncol* **21:** 1624-36.

Gisselsson D, Jonson T, Yu C, Martins C, Mandahl N, Wiegant J et al (2002). Centrosomal abnormalities, multipolar mitoses, and chromosomal instability in head and neck tumours with dysfunctional telomeres. *Br J Cancer* **87:** 202-7.

Goessel G, Quante M, Hahn WC, Harada H, Heeg S, Suliman Y et al (2005). Creating oral squamous cancer cells: a cellular model of oral-esophageal carcinogenesis. *Proc Natl Acad Sci U S A* **102:** 15599-604.

Gong G, DeVries S, Chew KL, Cha I, Ljung BM, Waldman FM (2001). Genetic changes in paired atypical and usual ductal hyperplasia of the breast by comparative genomic hybridization. *Clin Cancer Res* **7:** 2410-4.

Gorgoulis VG, Vassiliou LV, Karakaidos P, Zacharatos P, Kotsinas A, Liloglou T et al (2005). Activation of the DNA damage checkpoint and genomic instability in human precancerous lesions. *Nature* **434:** 907-13.

Gorunova L, Hoglund M, Andren-Sandberg A, Dawiskiba S, Jin Y, Mitelman F et al (1998). Cytogenetic analysis of pancreatic carcinomas: intratumor heterogeneity and nonrandom pattern of chromosome aberrations. *Genes Chromosomes Cancer* **23:** 81-99.

Grandis JR, Tweardy DJ (1993). Elevated levels of transforming growth factor alpha and epidermal growth factor receptor messenger RNA are early markers of carcinogenesis in head and neck cancer. *Cancer Res* **53:** 3579-84.

Greenhalgh DA, Rothnagel JA, Quintanilla MI, Orengo CC, Gagne TA, Bundman DS et al (1993). Induction of epidermal hyperplasia, hyperkeratosis, and papillomas in transgenic mice by a targeted v-Ha-ras oncogene. *Mol Carcinog* **7:** 99-110.

Guhaniyogi J, Brewer G (2001). Regulation of mRNA stability in mammalian cells. *Gene* **265:** 11-23.

Gusarova GA, Wang IC, Major ML, Kalinichenko VV, Ackerson T, Petrovic V et al (2007). A cell-penetrating ARF peptide inhibitor of FoxM1 in mouse hepatocellular carcinoma treatment. *J Clin Invest* **117:** 99-111.

Ha PK, Benoit NE, Yochem R, Sciubba J, Zahurak M, Sidransky D et al (2003). A transcriptional progression model for head and neck cancer. *Clin Cancer Res* **9:** 3058-64.

Hahn WC, Counter CM, Lundberg AS, Beijersbergen RL, Brooks MW, Weinberg RA (1999). Creation of human tumour cells with defined genetic elements. *Nature* **400:** 464-8.

Hahn WC, Weinberg RA (2002). Rules for making human tumor cells. *N Engl J Med* **347:** 1593-603.

Hamilton AI, Blackwood HJ (1974). Cell renewal of oral mucosal epithelium of the rat. *J Anat* **117:** 313-27.

Harbour JW, Dean DC (2000). The Rb/E2F pathway: expanding roles and emerging paradigms. *Genes Dev* **14:** 2393-409.

Harper LJ, Piper K, Common J, Fortune F, Mackenzie IC (2007). Stem cell patterns in cell lines derived from head and neck squamous cell carcinoma. *J Oral Pathol Med* **36:** 594-603.

Hatakeyama S, Yaegashi T, Takeda Y, Kunimatsu K (2007). Localization of bromodeoxyuridine-incorporating, p63- and p75(NGFR)- expressing cells in the human gingival epithelium. *J Oral Sci* **49:** 287-91.

Haughey BH, von Hoff DD, Windle BE, Wahl GM, Mock PM (1992). c-myc oncogene copy number in squamous carcinoma of the head and neck. *Am J Otolaryngol* **13:** 168-71.

Hayward DG, Fry AM (2006). Nek2 kinase in chromosome instability and cancer. *Cancer Lett* **237:** 155-66.

Heeschen C, Jang JJ, Weis M, Pathak A, Kaji S, Hu RS et al (2001). Nicotine stimulates angiogenesis and promotes tumor growth and atherosclerosis. *Nat Med* **7:** 833-9.

Heeschen C, Weis M, Aicher A, Dimmeler S, Cooke JP (2002). A novel angiogenic pathway mediated by non-neuronal nicotinic acetylcholine receptors. *J Clin Invest* **110:** 527-36.

Heim S, Teixeira MR, Dietrich CU, Pandis N (1997). Cytogenetic polyclonality in tumors of the breast. *Cancer Genet Cytogenet* **95:** 16-9.

Ho T, Wei Q, Sturgis EM (2007). Epidemiology of carcinogen metabolism genes and risk of squamous cell carcinoma of the head and neck. *Head Neck* **29:** 682-99.

Hogewind WF, van der Waal I, van der Kwast WA, Snow GB (1989). The association of white lesions with oral squamous cell carcinoma. A retrospective study of 212 patients. *Int J Oral Maxillofac Surg* **18:** 163-4.

Hogg RP, Honorio S, Martinez A, Agathanggelou A, Dallol A, Fullwood P et al (2002). Frequent 3p allele loss and epigenetic inactivation of the RASSF1A tumour suppressor gene from region 3p21.3 in head and neck squamous cell carcinoma. *Eur J Cancer* **38:** 1585-92.

Howman EV, Fowler KJ, Newson AJ, Redward S, MacDonald AC, Kalitsis P et al (2000). Early disruption of centromeric chromatin organization in centromere protein A (Cenpa) null mice. *Proc Natl Acad Sci U S A* **97:** 1148-53.

Hu W, Kavanagh JJ, Deaver M, Johnston DA, Freedman RS, Verschraegen CF et al (2005). Frequent overexpression of STK15/Aurora-A/BTAK and chromosomal instability in tumorigenic cell cultures derived from human ovarian cancer. *Oncol Res* **15:** 49-57.

Huang J, Wei W, Zhang J, Liu G, Bignell GR, Stratton MR et al (2004). Whole genome DNA copy number changes identified by high density oligonucleotide arrays. *Hum Genomics* **1:** 287-99.

Huang SD, Yuan Y, Liu XH, Gong DJ, Bai CG, Wang F et al (2009). Self-renewal and chemotherapy resistance of p75NTR positive cells in esophageal squamous cell carcinomas. *BMC Cancer* **9:** 9.

Hunter KD, Parkinson EK, Harrison PR (2005). Profiling early head and neck cancer. *Nat Rev Cancer* **5:** 127-35.

Hynes RO (1992). Integrins: versatility, modulation, and signaling in cell adhesion. *Cell* **69:** 11-25.

Ishida S, Huang E, Zuzan H, Spang R, Leone G, West M et al (2001). Role for E2F in control of both DNA replication and mitotic functions as revealed from DNA microarray analysis. *Mol Cell Biol* **21:** 4684-99.

Izumi K, Tobita T, Feinberg SE (2007). Isolation of human oral keratinocyte progenitor/stem cells. *J Dent Res* **86:** 341-6.

Izzo JG, Papadimitrakopoulou VA, Li XQ, Ibarguen H, Lee JS, Ro JY et al (1998). Dysregulated cyclin D1 expression early in head and neck tumorigenesis: in vivo evidence for an association with subsequent gene amplification. *Oncogene* **17:** 2313-22.

Jang SJ, Chiba I, Hirai A, Hong WK, Mao L (2001). Multiple oral squamous epithelial lesions: are they genetically related? *Oncogene* **20:** 2235-42.

Jares P, Fernandez PL, Campo E, Nadal A, Bosch F, Aiza G et al (1994). PRAD-1/cyclin D1 gene amplification correlates with messenger RNA overexpression and tumor progression in human laryngeal carcinomas. *Cancer Res* **54:** 4813-7.

Jefford CE, Irminger-Finger I (2006). Mechanisms of chromosome instability in cancers. *Crit Rev Oncol Hematol* **59:** 1-14.

Jensen KB, Jones J, Watt FM (2008). A stem cell gene expression profile of human squamous cell carcinomas. *Cancer Lett* **272:** 23-31.

Jensen KB, Watt FM (2006). Single-cell expression profiling of human epidermal stem and transit-amplifying cells: Lrig1 is a regulator of stem cell quiescence. *Proc Natl Acad Sci U S A* **103:** 11958-63.

Jensen UB, Lowell S, Watt FM (1999). The spatial relationship between stem cells and their progeny in the basal layer of human epidermis: a new view based on whole-mount labelling and lineage analysis. *Development* **126:** 2409-18.

Jiang Z, Li X, Hu J, Zhou W, Jiang Y, Li G et al (2006). Promoter hypermethylation-mediated down-regulation of LATS1 and LATS2 in human astrocytoma. *Neurosci Res* **56:** 450-8.

Jin C, Jin Y, Wennerberg J, Dictor M, Mertens F (2000). Nonrandom pattern of cytogenetic abnormalities in squamous cell carcinoma of the larynx. *Genes Chromosomes Cancer* **28:** 66-76.

Jin Z, Hamilton JP, Yang J, Mori Y, Olaru A, Sato F et al (2008). Hypermethylation of the AKAP12 promoter is a biomarker of Barrett's-associated esophageal neoplastic progression. *Cancer Epidemiol Biomarkers Prev* **17:** 111-7.

Jonason AS, Kunala S, Price GJ, Restifo RJ, Spinelli HM, Persing JA et al (1996). Frequent clones of p53-mutated keratinocytes in normal human skin. *Proc Natl Acad Sci U S A* **93:** 14025-9.

Jones PH, Harper S, Watt FM (1995). Stem cell patterning and fate in human epidermis. *Cell* **80:** 83-93.

Jones PH, Simons BD, Watt FM (2007). Sic transit gloria: farewell to the epidermal transit amplifying cell? *Cell Stem Cell* **1:** 371-81.

Jones PH, Watt FM (1993). Separation of human epidermal stem cells from transit amplifying cells on the basis of differences in integrin function and expression. *Cell* **73:** 713-24.

Jothy S, Slesak B, Harlozinska A, Lapinska J, Adamiak J, Rabczynski J (1996). Field effect of human colon carcinoma on normal mucosa: relevance of carcinoembryonic antigen expression. *Tumour Biol* **17:** 58-64.

Kalin TV, Wang IC, Ackerson TJ, Major ML, Detrisac CJ, Kalinichenko VV et al (2006). Increased levels of the FoxM1 transcription factor accelerate development and progression of prostate carcinomas in both TRAMP and LADY transgenic mice. *Cancer Res* **66:** 1712-20.

Kalinichenko VV, Major ML, Wang X, Petrovic V, Kuechle J, Yoder HM et al (2004). Foxm1b transcription factor is essential for development of hepatocellular carcinomas and is negatively regulated by the p19ARF tumor suppressor. *Genes Dev* **18:** 830-50.

Kalinina OA, Kalinin SA, Polack EW, Mikaelian I, Panda S, Costa RH et al (2003). Sustained hepatic expression of FoxM1B in transgenic mice has minimal effects on

hepatocellular carcinoma development but increases cell proliferation rates in preneoplastic and early neoplastic lesions. *Oncogene* **22:** 6266-76.

Katoh M, Katoh M (2004). Human FOX gene family (Review). *Int J Oncol* **25:** 1495-500.

Kelsell DP, Norgett EE, Unsworth H, Teh MT, Cullup T, Mein CA et al (2005). Mutations in ABCA12 underlie the severe congenital skin disease harlequin ichthyosis. *Am J Hum Genet* **76:** 794-803.

Kennedy GC, Matsuzaki H, Dong S, Liu WM, Huang J, Liu G et al (2003). Large-scale genotyping of complex DNA. *Nat Biotechnol* **21:** 1233-7.

Kim IM, Ackerson T, Ramakrishna S, Tretiakova M, Wang IC, Kalin TV et al (2006). The Forkhead Box m1 transcription factor stimulates the proliferation of tumor cells during development of lung cancer. *Cancer Res* **66:** 2153-61.

Kim IM, Ramakrishna S, Gusarova GA, Yoder HM, Costa RH, Kalinichenko VV (2005). The forkhead box m1 transcription factor is essential for embryonic development of pulmonary vasculature. *J Biol Chem* **280:** 22278-86.

Kirkhus B, Clausen OP (1990). Cell kinetics in mouse epidermis studied by bivariate DNA/bromodeoxyuridine and DNA/keratin flow cytometry. *Cytometry* **11:** 253-60.

Kobayashi K, Okamoto T, Takayama S, Akiyama M, Ohno T, Yamada H (2000). Genetic instability in intestinal metaplasia is a frequent event leading to well-differentiated early adenocarcinoma of the stomach. *Eur J Cancer* **36:** 1113-9.

Korver W, Roose J, Clevers H (1997a). The winged-helix transcription factor Trident is expressed in cycling cells. *Nucleic Acids Res* **25:** 1715-9.

Korver W, Roose J, Wilson A, Clevers H (1997b). The winged-helix transcription factor Trident is expressed in actively dividing lymphocytes. *Immunobiology* **198:** 157-61.

Korver W, Schilham MW, Moerer P, van den Hoff MJ, Dam K, Lamers WH et al (1998). Uncoupling of S phase and mitosis in cardiomyocytes and hepatocytes lacking the winged-helix transcription factor Trident. *Curr Biol* **8:** 1327-30.

Kose O, Lalli A, Kutulola AO, Odell EW, Waseem A (2007). Changes in the expression of stem cell markers in oral lichen planus and hyperkeratotic lesions. *J Oral Sci* **49:** 133-9.

Kotsinas A, Evangelou K, Sideridou M, Kotzamanis G, Constantinides C, Zavras AI et al (2008). The 3' UTR IGF2R-A2/B2 variant is associated with increased tumor growth and advanced stages in non-small cell lung cancer. *Cancer Lett* **259:** 177-85.

Kramer RH, Shen X, Zhou H (2005). Tumor cell invasion and survival in head and neck cancer. *Cancer Metastasis Rev* **24:** 35-45.

Krupczak-Hollis K, Wang X, Kalinichenko VV, Gusarova GA, Wang IC, Dennewitz MB et al (2004). The mouse Forkhead Box m1 transcription factor is essential for hepatoblast mitosis and development of intrahepatic bile ducts and vessels during liver morphogenesis. *Dev Biol* **276:** 74-88.

Kulasekara KK, Lukandu OM, Neppelberg E, Vintermyr OK, Johannessen AC, Costea DE (2009). Cancer progression is associated with increased expression of basement membrane proteins in three-dimensional in vitro models of human oral cancer. *Arch Oral Biol* **54:** 924-31.

Kulkarni PS, Sundqvist K, Betsholtz C, Hoglund P, Wiman KG, Zhivotovsky B et al (1995). Characterization of human buccal epithelial cells transfected with the simian virus 40 T-antigen gene. *Carcinogenesis* **16:** 2515-21.

Kwok JM, Peck B, Monteiro LJ, Schwenen HD, Millour J, Coombes RC et al (2010). FOXM1 confers acquired cisplatin resistance in breast cancer cells. *Mol Cancer Res* **8:** 24-34.

Lajtha LG (1979). Stem cell concepts. *Differentiation* **14:** 23-34.

Laoukili J, Alvarez-Fernandez M, Stahl M, Medema RH (2008a). FoxM1 is degraded at mitotic exit in a Cdh1-dependent manner. *Cell Cycle* **7:** 2720-6.

Laoukili J, Alvarez M, Meijer LA, Stahl M, Mohammed S, Kleij L et al (2008b). Activation of FoxM1 during G2 requires CyclinA/Cdk-dependent relief of auto-repression by the FoxM1 N-terminal domain. *Mol Cell Biol*.

Laoukili J, Kooistra MR, Bras A, Kauw J, Kerkhoven RM, Morrison A et al (2005). FoxM1 is required for execution of the mitotic programme and chromosome stability. *Nat Cell Biol* **7:** 126-36.

Laoukili J, Stahl M, Medema RH (2007). FoxM1: at the crossroads of ageing and cancer. *Biochim Biophys Acta* **1775:** 92-102.

Lavker RM, Sun TT (1982). Heterogeneity in epidermal basal keratinocytes: morphological and functional correlations. *Science* **215:** 1239-41.

Lavker RM, Sun TT (2000). Epidermal stem cells: properties, markers, and location. *Proc Natl Acad Sci U S A* **97:** 13473-5.

Lazarov M, Kubo Y, Cai T, Dajee M, Tarutani M, Lin Q et al (2002). CDK4 coexpression with Ras generates malignant human epidermal tumorigenesis. *Nat Med* **8:** 1105-14.

Lee DW, Zhang K, Ning ZQ, Raabe EH, Tintner S, Wieland R et al (2000). Proliferation-associated SNF2-like gene (PASG): a SNF2 family member altered in leukemia. *Cancer Res* **60:** 3612-22.

Lehman NL, Tibshirani R, Hsu JY, Natkunam Y, Harris BT, West RB et al (2007). Oncogenic regulators and substrates of the anaphase promoting complex/cyclosome are frequently overexpressed in malignant tumors. *Am J Pathol* **170:** 1793-805.

Lendahl U, Zimmerman LB, McKay RD (1990). CNS stem cells express a new class of intermediate filament protein. *Cell* **60:** 585-95.

Lengauer C, Kinzler KW, Vogelstein B (1998). Genetic instabilities in human cancers. *Nature* **396:** 643-9.

Leung TW, Lin SS, Tsang AC, Tong CS, Ching JC, Leung WY et al (2001). Over-expression of FoxM1 stimulates cyclin B1 expression. *FEBS Lett* **507:** 59-66.

Li A, Pouliot N, Redvers R, Kaur P (2004a). Extensive tissue-regenerative capacity of neonatal human keratinocyte stem cells and their progeny. *J Clin Invest* **113:** 390-400.

Li A, Simmons PJ, Kaur P (1998). Identification and isolation of candidate human keratinocyte stem cells based on cell surface phenotype. *Proc Natl Acad Sci U S A* **95:** 3902-7.

Li JJ, Weroha SJ, Lingle WL, Papa D, Salisbury JL, Li SA (2004b). Estrogen mediates Aurora-A overexpression, centrosome amplification, chromosomal instability, and breast cancer in female ACI rats. *Proc Natl Acad Sci U S A* **101:** 18123-8.

Li M, Zhang P (2009). The function of APC/CCdh1 in cell cycle and beyond. *Cell Div* **4:** 2.

Lingle WL, Barrett SL, Negron VC, D'Assoro AB, Boeneman K, Liu W et al (2002). Centrosome amplification drives chromosomal instability in breast tumor development. *Proc Natl Acad Sci U S A* **99:** 1978-83.

Liu M, Dai B, Kang SH, Ban K, Huang FJ, Lang FF et al (2006). FoxM1B is overexpressed in human glioblastomas and critically regulates the tumorigenicity of glioma cells. *Cancer Res* **66:** 3593-602.

Liu SC, Sauter ER, Clapper ML, Feldman RS, Levin L, Chen SY et al (1998). Markers of cell proliferation in normal epithelia and dysplastic leukoplakias of the oral cavity. *Cancer Epidemiol Biomarkers Prev* **7:** 597-603.

Liu VC, Wong LY, Jang T, Shah AH, Park I, Yang X et al (2007). Tumor evasion of the immune system by converting CD4+CD25- T cells into CD4+CD25+ T regulatory cells: role of tumor-derived TGF-beta. *J Immunol* **178:** 2883-92.

Liu WM, Di X, Yang G, Matsuzaki H, Huang J, Mei R et al (2003). Algorithms for large-scale genotyping microarrays. *Bioinformatics* **19:** 2397-403.

Loeffler M, Potten CS, Wichmann HE (1987). Epidermal cell proliferation. II. A comprehensive mathematical model of cell proliferation and migration in the basal

layer predicts some unusual properties of epidermal stem cells. *Virchows Arch B Cell Pathol Incl Mol Pathol* **53:** 286-300.

Loughran O, Clark LJ, Bond J, Baker A, Berry IJ, Edington KG et al (1997). Evidence for the inactivation of multiple replicative lifespan genes in immortal human squamous cell carcinoma keratinocytes. *Oncogene* **14:** 1955-64.

Luscher-Firzlaff JM, Westendorf JM, Zwicker J, Burkhardt H, Henriksson M, Muller R et al (1999). Interaction of the fork head domain transcription factor MPP2 with the human papilloma virus 16 E7 protein: enhancement of transformation and transactivation. *Oncogene* **18:** 5620-30.

Ma RY, Tong TH, Cheung AM, Tsang AC, Leung WY, Yao KM (2005). Raf/MEK/MAPK signaling stimulates the nuclear translocation and transactivating activity of FOXM1c. *J Cell Sci* **118:** 795-806.

Macintosh CA, Stower M, Reid N, Maitland NJ (1998). Precise microdissection of human prostate cancers reveals genotypic heterogeneity. *Cancer Res* **58:** 23-8.

Mackenzie IC (1970). Relationship between mitosis and the ordered structure of the stratum corneum in mouse epidermis. *Nature* **226:** 653-5.

Mackenzie IC (1997). Retroviral transduction of murine epidermal stem cells demonstrates clonal units of epidermal structure. *J Invest Dermatol* **109:** 377-83.

Mackenzie IC (2004). Growth of malignant oral epithelial stem cells after seeding into organotypical cultures of normal mucosa. *J Oral Pathol Med* **33:** 71-8.

Madureira PA, Varshochi R, Constantinidou D, Francis RE, Coombes RC, Yao KM et al (2006). The Forkhead box M1 protein regulates the transcription of the estrogen receptor alpha in breast cancer cells. *J Biol Chem* **281:** 25167-76.

Mahlapuu M, Enerback S, Carlsson P (2001). Haploinsufficiency of the forkhead gene Foxf1, a target for sonic hedgehog signaling, causes lung and foregut malformations. *Development* **128:** 2397-406.

Major ML, Lepe R, Costa RH (2004). Forkhead box M1B transcriptional activity requires binding of Cdk-cyclin complexes for phosphorylation-dependent recruitment of p300/CBP coactivators. *Mol Cell Biol* **24:** 2649-61.

Mao L, Lee JS, Fan YH, Ro JY, Batsakis JG, Lippman S et al (1996). Frequent microsatellite alterations at chromosomes 9p21 and 3p14 in oral premalignant lesions and their value in cancer risk assessment. *Nat Med* **2:** 682-5.

Martin KJ, Patrick DR, Bissell MJ, Fournier MV (2008). Prognostic breast cancer signature identified from 3D culture model accurately predicts clinical outcome across independent datasets. *PLoS One* **3:** e2994.

Martinez-Galan J, Torres B, Del Moral R, Munoz-Gamez JA, Martin-Oliva D, Villalobos M et al (2008). Quantitative detection of methylated ESR1 and 14-3-3-

sigma gene promoters in serum as candidate biomarkers for diagnosis of breast cancer and evaluation of treatment efficacy. *Cancer Biol Ther* **7:** 958-65.

Mashberg A (1977). Erythroplasia vs. leukoplasia in the diagnosis of early asymptomatic oral squamous carcinoma. *N Engl J Med* **297:** 109-10.

Mashberg A, Morrissey JB, Garfinkel L (1973). A study of the appearance of early asymptomatic oral squamous cell carcinoma. *Cancer* **32:** 1436-45.

McGregor F, Muntoni A, Fleming J, Brown J, Felix DH, MacDonald DG et al (2002). Molecular changes associated with oral dysplasia progression and acquisition of immortality: potential for its reversal by 5-azacytidine. *Cancer Res* **62:** 4757-66.

Meraldi P, Honda R, Nigg EA (2004). Aurora kinases link chromosome segregation and cell division to cancer susceptibility. *Curr Opin Genet Dev* **14:** 29-36.

Meredith SD, Levine PA, Burns JA, Gaffey MJ, Boyd JC, Weiss LM et al (1995). Chromosome 11q13 amplification in head and neck squamous cell carcinoma. Association with poor prognosis. *Arch Otolaryngol Head Neck Surg* **121:** 790-4.

Mertens F, Johansson B, Hoglund M, Mitelman F (1997). Chromosomal imbalance maps of malignant solid tumors: a cytogenetic survey of 3185 neoplasms. *Cancer Res* **57:** 2765-80.

Millour J, Constantinidou D, Stavropoulou AV, Wilson MS, Myatt SS, Kwok JM et al (2010). FOXM1 is a transcriptional target of ERalpha and has a critical role in breast cancer endocrine sensitivity and resistance. *Oncogene*.

Mirchandani D, Zheng J, Miller GJ, Ghosh AK, Shibata DK, Cote RJ et al (1995). Heterogeneity in intratumor distribution of p53 mutations in human prostate cancer. *Am J Pathol* **147:** 92-101.

Moharamzadeh K, Brook IM, Van Noort R, Scutt AM, Thornhill MH (2007). Tissue-engineered oral mucosa: a review of the scientific literature. *J Dent Res* **86:** 115-24.

Moles JP, Watt FM (1997). The epidermal stem cell compartment: variation in expression levels of E-cadherin and catenins within the basal layer of human epidermis. *J Histochem Cytochem* **45:** 867-74.

Mori Y, Okumura T, Tsunoda S, Sakai Y, Shimada Y (2006). Gli-1 expression is associated with lymph node metastasis and tumor progression in esophageal squamous cell carcinoma. *Oncology* **70:** 378-89.

Morris RJ (2000). Keratinocyte stem cells: targets for cutaneous carcinogens. *J Clin Invest* **106:** 3-8.

Morris RJ, Coulter K, Tryson K, Steinberg SR (1997). Evidence that cutaneous carcinogen-initiated epithelial cells from mice are quiescent rather than actively cycling. *Cancer Res* **57:** 3436-43.

Morris RJ, Fischer SM, Slaga TJ (1986). Evidence that a slowly cycling subpopulation of adult murine epidermal cells retains carcinogen. *Cancer Res* **46:** 3061-6.

Morris RJ, Potten CS (1994). Slowly cycling (label-retaining) epidermal cells behave like clonogenic stem cells in vitro. *Cell Prolif* **27:** 279-89.

Morris RJ, Potten CS (1999). Highly persistent label-retaining cells in the hair follicles of mice and their fate following induction of anagen. *J Invest Dermatol* **112:** 470-5.

Morris RJ, Tryson KA, Wu KQ (2000). Evidence that the epidermal targets of carcinogen action are found in the interfollicular epidermis of infundibulum as well as in the hair follicles. *Cancer Res* **60:** 226-9.

Muffler S, Stark HJ, Amoros M, Falkowska-Hansen B, Boehnke K, Buhring HJ et al (2008). A stable niche supports long-term maintenance of human epidermal stem cells in organotypic cultures. *Stem Cells* **26:** 2506-15.

Muller A, Holzmann K, Kestler HA (2007). Visualization of genomic aberrations using Affymetrix SNP arrays. *Bioinformatics* **23:** 496-7.

Muller S (2007). Oral Precancer. In: John W. Werning (ed.) Oral Cancer, diagnosis, management and rehabilitation. pp 8-17. Theme Medical Publishers.

Munger K, Howley PM (2002). Human papillomavirus immortalization and transformation functions. *Virus Res* **89:** 213-28.

Munro J, Stott FJ, Vousden KH, Peters G, Parkinson EK (1999). Role of the alternative INK4A proteins in human keratinocyte senescence: evidence for the specific inactivation of p16INK4A upon immortalization. *Cancer Res* **59:** 2516-21.

Nakamura T, Endo K, Kinoshita S (2007). Identification of human oral keratinocyte stem/progenitor cells by neurotrophin receptor p75 and the role of neurotrophin/p75 signaling. *Stem Cells* **25:** 628-38.

Nannya Y, Sanada M, Nakazaki K, Hosoya N, Wang L, Hangaishi A et al (2005). A robust algorithm for copy number detection using high-density oligonucleotide single nucleotide polymorphism genotyping arrays. *Cancer Res* **65:** 6071-9.

Negrini S, Gorgoulis VG, Halazonetis TD (2010). Genomic instability--an evolving hallmark of cancer. *Nat Rev Mol Cell Biol* **11:** 220-8.

Nievers MG, Schaapveld RQ, Sonnenberg A (1999). Biology and function of hemidesmosomes. *Matrix Biol* **18:** 5-17.

Nigg EA (2001). Mitotic kinases as regulators of cell division and its checkpoints. *Nat Rev Mol Cell Biol* **2:** 21-32.

O'Brien SL, Fagan A, Fox EJ, Millikan RC, Culhane AC, Brennan DJ et al (2007). CENP-F expression is associated with poor prognosis and chromosomal instability in patients with primary breast cancer. *Int J Cancer* **120:** 1434-43.

O'Connell P, Pekkel V, Fuqua SA, Osborne CK, Clark GM, Allred DC (1998). Analysis of loss of heterozygosity in 399 premalignant breast lesions at 15 genetic loci. *J Natl Cancer Inst* **90:** 697-703.

Okumura T, Shimada Y, Imamura M, Yasumoto S (2003). Neurotrophin receptor p75(NTR) characterizes human esophageal keratinocyte stem cells in vitro. *Oncogene* **22:** 4017-26.

Ophof R, van Rheden RE, Von den HJ, Schalkwijk J, Kuijpers-Jagtman AM (2002). Oral keratinocytes cultured on dermal matrices form a mucosa-like tissue. *Biomaterials* **23:** 3741-8.

Opitz OG, Suliman Y, Hahn WC, Harada H, Blum HE, Rustgi AK (2001). Cyclin D1 overexpression and p53 inactivation immortalize primary oral keratinocytes by a telomerase-independent mechanism. *J Clin Invest* **108:** 725-32.

Owens DM, Watt FM (2003). Contribution of stem cells and differentiated cells to epidermal tumours. *Nat Rev Cancer* **3:** 444-51.

Pandis N, Teixeira MR, Adeyinka A, Rizou H, Bardi G, Mertens F et al (1998). Cytogenetic comparison of primary tumors and lymph node metastases in breast cancer patients. *Genes Chromosomes Cancer* **22:** 122-9.

Pandit B, Halasi M, Gartel AL (2009). p53 negatively regulates expression of FoxM1. *Cell Cycle* **8:** 3425-7.

Park HJ, Costa RH, Lau LF, Tyner AL, Raychaudhuri P (2008). Anaphase-promoting complex/cyclosome-CDH1-mediated proteolysis of the forkhead box M1 transcription factor is critical for regulated entry into S phase. *Mol Cell Biol* **28:** 5162-71.

Park HJ, Wang Z, Costa RH, Tyner A, Lau LF, Raychaudhuri P (2007). An N-terminal inhibitory domain modulates activity of FoxM1 during cell cycle. *Oncogene*.

Parkin DM, Bray F, Ferlay J, Pisani P (2005). Global cancer statistics, 2002. *CA Cancer J Clin* **55:** 74-108.

Parkinson EK, Al-Yaman FM, Appleby MW (1987). The effect of donor age on the proliferative response of human and mouse keratinocytes to phorbol, 12-myristate, 13-acetate. *Carcinogenesis* **8:** 907-12.

Parkinson EK, Grabham P, Emmerson A (1983). A subpopulation of cultured human keratinocytes which is resistant to the induction of terminal differentiation-related changes by phorbol, 12-myristate, 13-acetate: evidence for an increase in the resistant population following transformation. *Carcinogenesis* **4:** 857-61.

Patel D, Incassati A, Wang N, McCance DJ (2004). Human papillomavirus type 16 E6 and E7 cause polyploidy in human keratinocytes and up-regulation of G2-M-phase proteins. *Cancer Res* **64:** 1299-306.

Patmore HS, Cawkwell L, Stafford ND, Greenman J (2005). Unraveling the chromosomal aberrations of head and neck squamous cell carcinoma: a review. *Ann Surg Oncol* **12:** 831-42.

Pellegrini G, Dellambra E, Golisano O, Martinelli E, Fantozzi I, Bondanza S et al (2001). p63 identifies keratinocyte stem cells. *Proc Natl Acad Sci U S A* **98:** 3156-61.

Peltonen J, Larjava H, Jaakkola S, Gralnick H, Akiyama SK, Yamada SS et al (1989). Localization of integrin receptors for fibronectin, collagen, and laminin in human skin. Variable expression in basal and squamous cell carcinomas. *J Clin Invest* **84:** 1916-23.

Penneys NS, Fulton JE, Jr., Weinstein GD, Frost P (1970). Location of proliferating cells in human epidermis. *Arch Dermatol* **101:** 323-7.

Perez-Ordonez B, Beauchemin M, Jordan RC (2006). Molecular biology of squamous cell carcinoma of the head and neck. *J Clin Pathol* **59:** 445-53.

Perez de Castro I, de Carcer G, Malumbres M (2007). A census of mitotic cancer genes: new insights into tumor cell biology and cancer therapy. *Carcinogenesis* **28:** 899-912.

Pihan GA, Wallace J, Zhou Y, Doxsey SJ (2003). Centrosome abnormalities and chromosome instability occur together in pre-invasive carcinomas. *Cancer Res* **63:** 1398-404.

Pilarsky C, Wenzig M, Specht T, Saeger HD, Grutzmann R (2004). Identification and validation of commonly overexpressed genes in solid tumors by comparison of microarray data. *Neoplasia* **6:** 744-50.

Pindborg J, Reichart P, Smith C, Van der Waal I (1997). World Health Organization: histological typing of cancer and precancer of the oral mucosa. *Berlin: Springer-Verlag,1997*.

Pines J (1995). Cyclins and cyclin-dependent kinases: a biochemical view. *Biochem J* **308 (Pt 3):** 697-711.

Pinto AP, Lin MC, Sheets EE, Muto MG, Sun D, Crum CP (2000). Allelic imbalance in lichen sclerosus, hyperplasia, and intraepithelial neoplasia of the vulva. *Gynecol Oncol* **77:** 171-6.

Porter MJ, Field JK, Leung SF, Lo D, Lee JC, Spandidos DA et al (1994). The detection of the c-myc and ras oncogenes in nasopharyngeal carcinoma by immunohistochemistry. *Acta Otolaryngol* **114:** 105-9.

Potten CS (1974). The epidermal proliferative unit: the possible role of the central basal cell. *Cell Tissue Kinet* **7:** 77-88.

Potten CS, Booth C (2002). Keratinocyte stem cells: a commentary. *J Invest Dermatol* **119:** 888-99.

Potten CS, Hendry JH (1973). Letter: Clonogenic cells and stem cells in epidermis. *Int J Radiat Biol Relat Stud Phys Chem Med* **24:** 537-40.

Potten CS, Morris RJ (1988). Epithelial stem cells in vivo. *J Cell Sci Suppl* **10:** 45-62.

Potten CS, Owen G, Booth D (2002). Intestinal stem cells protect their genome by selective segregation of template DNA strands. *J Cell Sci* **115:** 2381-8.

Potten CS, Wichmann HE, Loeffler M, Dobek K, Major D (1982). Evidence for discrete cell kinetic subpopulations in mouse epidermis based on mathematical analysis. *Cell Tissue Kinet* **15:** 305-29.

Presland RB, Dale BA (2000). Epithelial structural proteins of the skin and oral cavity: function in health and disease. *Crit Rev Oral Biol Med* **11:** 383-408.

Prevo LJ, Sanchez CA, Galipeau PC, Reid BJ (1999). p53-mutant clones and field effects in Barrett's esophagus. *Cancer Res* **59:** 4784-7.

Prime SS, Nixon SV, Crane IJ, Stone A, Matthews JB, Maitland NJ et al (1990). The behaviour of human oral squamous cell carcinoma in cell culture. *J Pathol* **160:** 259-69.

Qiu GB, Gong LG, Hao DM, Zhen ZH, Sun KL (2003). Expression of MTLC gene in gastric carcinoma. *World J Gastroenterol* **9:** 2160-3.

Rabin M, Birnbaum D, Young D, Birchmeier C, Wigler M, Ruddle FH (1987). Human ros1 and mas1 oncogenes located in regions of chromosome 6 associated with tumor-specific rearrangements. *Oncogene Res* **1:** 169-78.

Rao PH, Sreekantaiah C, Schantz SP, Chaganti RS (1994). Cytogenetic analysis of 11 squamous cell carcinomas of the head and neck. *Cancer Genet Cytogenet* **77:** 60-4.

Regl G, Neill GW, Eichberger T, Kasper M, Ikram MS, Koller J et al (2002). Human GLI2 and GLI1 are part of a positive feedback mechanism in Basal Cell Carcinoma. *Oncogene* **21:** 5529-39.

Renstrup G (1963). Studies in Oral Leukoplakias. Iv. Mitotic Activity in Oral Leukoplakias. a Preliminary Report. *Acta Odontol Scand* **21:** 333-40.

Rheinwald JG (1980). Serial cultivation of normal human epidermal keratinocytes. *Methods Cell Biol* **21A:** 229-54.

Rheinwald JG, Beckett MA (1981). Tumorigenic keratinocyte lines requiring anchorage and fibroblast support cultures from human squamous cell carcinomas. *Cancer Res* **41:** 1657-63.

Rheinwald JG, Hahn WC, Ramsey MR, Wu JY, Guo Z, Tsao H et al (2002). A two-stage, p16(INK4A)- and p53-dependent keratinocyte senescence mechanism that limits replicative potential independent of telomere status. *Mol Cell Biol* **22:** 5157-72.

Robbins PB, Lin Q, Goodnough JB, Tian H, Chen X, Khavari PA (2001). In vivo restoration of laminin 5 beta 3 expression and function in junctional epidermolysis bullosa. *Proc Natl Acad Sci U S A* **98:** 5193-8.

Rodriguez S, Khabir A, Keryer C, Perrot C, Drira M, Ghorbel A et al (2005). Conventional and array-based comparative genomic hybridization analysis of nasopharyngeal carcinomas from the Mediterranean area. *Cancer Genet Cytogenet* **157:** 140-7.

Rong Y, Cheng L, Ning H, Zou J, Zhang Y, Xu F et al (2006). Wilms' tumor 1 and signal transducers and activators of transcription 3 synergistically promote cell proliferation: a possible mechanism in sporadic Wilms' tumor. *Cancer Res* **66:** 8049-57.

Rosenthal AN, Ryan A, Hopster D, Jacobs IJ (2002). Molecular evidence of a common clonal origin and subsequent divergent clonal evolution in vulval intraepithelial neoplasia, vulval squamous cell carcinoma and lymph node metastases. *Int J Cancer* **99:** 549-54.

Rosin MP, Cheng X, Poh C, Lam WL, Huang Y, Lovas J et al (2000). Use of allelic loss to predict malignant risk for low-grade oral epithelial dysplasia. *Clin Cancer Res* **6:** 357-62.

Ross J (1995). mRNA stability in mammalian cells. *Microbiol Rev* **59:** 423-50.

Rousseau A, Lim MS, Lin Z, Jordan RC (2001). Frequent cyclin D1 gene amplification and protein overexpression in oral epithelial dysplasias. *Oral Oncol* **37:** 268-75.

Roz L, Wu CL, Porter S, Scully C, Speight P, Read A et al (1996). Allelic imbalance on chromosome 3p in oral dysplastic lesions: an early event in oral carcinogenesis. *Cancer Res* **56:** 1228-31.

Ryu B, Kim DS, Deluca AM, Alani RM (2007). Comprehensive expression profiling of tumor cell lines identifies molecular signatures of melanoma progression. *PLoS One* **2:** e594.

Sakai W, Swisher EM, Karlan BY, Agarwal MK, Higgins J, Friedman C et al (2008). Secondary mutations as a mechanism of cisplatin resistance in BRCA2-mutated cancers. *Nature* **451:** 1116-20.

Sanburn N, Cornetta K (1999). Rapid titer determination using quantitative real-time PCR. *Gene Ther* **6:** 1340-5.

Schneider TE, Barland C, Alex AM, Mancianti ML, Lu Y, Cleaver JE et al (2003). Measuring stem cell frequency in epidermis: a quantitative in vivo functional assay for long-term repopulating cells. *Proc Natl Acad Sci U S A* **100:** 11412-7.

Scholes AG, Woolgar JA, Boyle MA, Brown JS, Vaughan ED, Hart CA et al (1998). Synchronous oral carcinomas: independent or common clonal origin? *Cancer Res* **58:** 2003-6.

Scribner JD, Suss R (1978). Tumor initiation and promotion. *Int Rev Exp Pathol* **18:** 137-98.

Seery JP, Watt FM (2000). Asymmetric stem-cell divisions define the architecture of human oesophageal epithelium. *Curr Biol* **10:** 1447-50.

Shahnavaz SA, Bradley G, Regezi JA, Thakker N, Gao L, Hogg D et al (2001). Patterns of CDKN2A gene loss in sequential oral epithelial dysplasias and carcinomas. *Cancer Res* **61:** 2371-5.

Shahnavaz SA, Regezi JA, Bradley G, Dube ID, Jordan RC (2000). p53 gene mutations in sequential oral epithelial dysplasias and squamous cell carcinomas. *J Pathol* **190:** 417-22.

Sherr CJ, Roberts JM (1999). CDK inhibitors: positive and negative regulators of G1-phase progression. *Genes Dev* **13:** 1501-12.

Shih IM, Zhou W, Goodman SN, Lengauer C, Kinzler KW, Vogelstein B (2001). Evidence that genetic instability occurs at an early stage of colorectal tumorigenesis. *Cancer Res* **61:** 818-22.

Shinin V, Gayraud-Morel B, Gomes D, Tajbakhsh S (2006). Asymmetric division and cosegregation of template DNA strands in adult muscle satellite cells. *Nat Cell Biol* **8:** 677-87.

Singh B, Gogineni SK, Sacks PG, Shaha AR, Shah JP, Stoffel A et al (2001). Molecular cytogenetic characterization of head and neck squamous cell carcinoma and refinement of 3q amplification. *Cancer Res* **61:** 4506-13.

Slack JM (2000). Stem cells in epithelial tissues. *Science* **287:** 1431-3.

Slamon DJ, Clark GM, Wong SG, Levin WJ, Ullrich A, McGuire WL (1987). Human breast cancer: correlation of relapse and survival with amplification of the HER-2/neu oncogene. *Science* **235:** 177-82.

Slamon DJ, Godolphin W, Jones LA, Holt JA, Wong SG, Keith DE et al (1989). Studies of the HER-2/neu proto-oncogene in human breast and ovarian cancer. *Science* **244:** 707-12.

Slaughter DP, Southwick HW, Smejkal W (1953). Field cancerization in oral stratified squamous epithelium; clinical implications of multicentric origin. *Cancer* **6:** 963-8.

Smith SA, Dale BA (1986). Immunologic localization of filaggrin in human oral epithelia and correlation with keratinization. *J Invest Dermatol* **86:** 168-72.

Smith SL, Bowers NL, Betticher DC, Gautschi O, Ratschiller D, Hoban PR et al (2005). Overexpression of aurora B kinase (AURKB) in primary non-small cell lung carcinoma is frequent, generally driven from one allele, and correlates with the level of genetic instability. *Br J Cancer* **93:** 719-29.

Snijders AM, Huey B, Connelly ST, Roy R, Jordan RC, Schmidt BL et al (2009). Stromal control of oncogenic traits expressed in response to the overexpression of GLI2, a pleiotropic oncogene. *Oncogene* **28:** 625-37.

Somers KD, Merrick MA, Lopez ME, Incognito LS, Schechter GL, Casey G (1992). Frequent p53 mutations in head and neck cancer. *Cancer Res* **52:** 5997-6000.

Sommer S, Fuqua SA (2001). Estrogen receptor and breast cancer. *Semin Cancer Biol* **11:** 339-52.

Sondell B, Thornell LE, Stigbrand T, Egelrud T (1994). Immunolocalization of stratum corneum chymotryptic enzyme in human skin and oral epithelium with monoclonal antibodies: evidence of a proteinase specifically expressed in keratinizing squamous epithelia. *J Histochem Cytochem* **42:** 459-65.

Spirin KS, Simpson JF, Takeuchi S, Kawamata N, Miller CW, Koeffler HP (1996). p27/Kip1 mutation found in breast cancer. *Cancer Res* **56:** 2400-4.

Squier CA, Hill MW (1989). *Oral Mucosa In Ten Cate AR : Oral Histology, development, structure, and function*. CV Mosby: St. Louis (MO).

Squier CA, Kremer MJ (2001). Biology of oral mucosa and esophagus. *J Natl Cancer Inst Monogr***:** 7-15.

Sreekantaiah C, Rao PH, Xu L, Sacks PG, Schantz SP, Chaganti RS (1994). Consistent chromosomal losses in head and neck squamous cell carcinoma cell lines. *Genes Chromosomes Cancer* **11:** 29-39.

Staiano-Coico L, Higgins PJ, Darzynkiewicz Z, Kimmel M, Gottlieb AB, Pagan-Charry I et al (1986). Human keratinocyte culture. Identification and staging of epidermal cell subpopulations. *J Clin Invest* **77:** 396-404.

Stern RS, Bolshakov S, Nataraj AJ, Ananthaswamy HN (2002). p53 mutation in nonmelanoma skin cancers occurring in psoralen ultraviolet a-treated patients: evidence for heterogeneity and field cancerization. *J Invest Dermatol* **119:** 522-6.

Steven AC, Steinert PM (1994). Protein composition of cornified cell envelopes of epidermal keratinocytes. *J Cell Sci* **107 (Pt 2):** 693-700.

Stevenson M, Volsky DJ (1986). Activated v-myc and v-ras oncogenes do not transform normal human lymphocytes. *Mol Cell Biol* **6:** 3410-7.

Stoler A, Kopan R, Duvic M, Fuchs E (1988). Use of monospecific antisera and cRNA probes to localize the major changes in keratin expression during normal and abnormal epidermal differentiation. *J Cell Biol* **107:** 427-46.

Storchova Z, Kuffer C (2008). The consequences of tetraploidy and aneuploidy. *J Cell Sci* **121:** 3859-66.

Sturgis EM, Wei Q (2007). Epidemiology of Oral Cancer In: John W. Werning (ed.) Oral Cancer, diagnosis, management and rehabilitation. pp 8-17. Theme Medical Publishers

Sudo T, Ota Y, Kotani S, Nakao M, Takami Y, Takeda S et al (2001). Activation of Cdh1-dependent APC is required for G1 cell cycle arrest and DNA damage-induced G2 checkpoint in vertebrate cells. *EMBO J* **20:** 6499-508.

Sugerman PB, Savage NW (1999). Current concepts in oral cancer. *Aust Dent J* **44:** 147-56.

Ta BM, Gallagher GT, Chakravarty R, Rice RH (1990). Keratinocyte transglutaminase in human skin and oral mucosa: cytoplasmic localization and uncoupling of differentiation markers. *J Cell Sci* **95 (Pt 4):** 631-8.

Tabor MP, Brakenhoff RH, Ruijter-Schippers HJ, Van Der Wal JE, Snow GB, Leemans CR et al (2002). Multiple head and neck tumors frequently originate from a single preneoplastic lesion. *Am J Pathol* **161:** 1051-60.

Tabor MP, Brakenhoff RH, van Houten VM, Kummer JA, Snel MH, Snijders PJ et al (2001). Persistence of genetically altered fields in head and neck cancer patients: biological and clinical implications. *Clin Cancer Res* **7:** 1523-32.

Takahashi T, Habuchi T, Kakehi Y, Mitsumori K, Akao T, Terachi T et al (1998). Clonal and chronological genetic analysis of multifocal cancers of the bladder and upper urinary tract. *Cancer Res* **58:** 5835-41.

Tan Y, Raychaudhuri P, Costa RH (2007). Chk2 mediates stabilization of the FoxM1 transcription factor to stimulate expression of DNA repair genes. *Mol Cell Biol* **27:** 1007-16.

Teh MT, Blaydon D, Chaplin T, Foot NJ, Skoulakis S, Raghavan M et al (2005). Genomewide single nucleotide polymorphism microarray mapping in basal cell carcinomas unveils uniparental disomy as a key somatic event. *Cancer Res* **65:** 8597-603.

Teh MT, Blaydon D, Ghali LR, Briggs V, Edmunds S, Pantazi E et al (2007). Role for WNT16B in human epidermal keratinocyte proliferation and differentiation. *J Cell Sci* **120:** 330-9.

Teh MT, Gemenetzidis E, Chaplin T, Young BD, Philpott MP (2010). Upregulation of FOXM1 induces genomic instability in human epidermal keratinocytes. *Mol Cancer* **9:** 45.

Teh MT, Wong ST, Neill GW, Ghali LR, Philpott MP, Quinn AG (2002). FOXM1 is a downstream target of Gli1 in basal cell carcinomas. *Cancer Res* **62:** 4773-80.

Tomonaga T, Matsushita K, Yamaguchi S, Oohashi T, Shimada H, Ochiai T et al (2003). Overexpression and mistargeting of centromere protein-A in human primary colorectal cancer. *Cancer Res* **63:** 3511-6.

Torske KR (2007). Malignant Lesions of the Oral Cavity. In: John W. Werning (ed.) Oral Cancer, diagnosis, management and rehabilitation. pp 18-30. Theme Medical Publishers

Tsunenaga M, Kohno Y, Horii I, Yasumoto S, Huh NH, Tachikawa T et al (1994). Growth and differentiation properties of normal and transformed human keratinocytes in organotypic culture. *Jpn J Cancer Res* **85:** 238-44.

Tyner AL, Fuchs E (1986). Evidence for posttranscriptional regulation of the keratins expressed during hyperproliferation and malignant transformation in human epidermis. *J Cell Biol* **103:** 1945-55.

Valdehita A, Carmena MJ, Collado B, Prieto JC, Bajo AM (2007). Vasoactive intestinal peptide (VIP) increases vascular endothelial growth factor (VEGF) expression and secretion in human breast cancer cells. *Regul Pept* **144:** 101-8.

van den Boom J, Wolter M, Kuick R, Misek DE, Youkilis AS, Wechsler DS et al (2003). Characterization of gene expression profiles associated with glioma progression using oligonucleotide-based microarray analysis and real-time reverse transcription-polymerase chain reaction. *Am J Pathol* **163:** 1033-43.

van der Flier A, Sonnenberg A (2001). Function and interactions of integrins. *Cell Tissue Res* **305:** 285-98.

van Neste D, Staquet MJ, Viac J, Lachapelle JM, Thivolet J (1983). A new way to evaluate the germinative compartment in human epidermis, using [3H]thymidine incorporation and immunoperoxidase staining of 67 K polypeptide. *Br J Dermatol* **108:** 433-9.

van Oijen MG, Leppers Vd Straat FG, Tilanus MG, Slootweg PJ (2000). The origins of multiple squamous cell carcinomas in the aerodigestive tract. *Cancer* **88:** 884-93.

Vandesompele J, De Preter K, Pattyn F, Poppe B, Van Roy N, De Paepe A et al (2002). Accurate normalization of real-time quantitative RT-PCR data by geometric averaging of multiple internal control genes. *Genome Biol* **3:** RESEARCH0034.

Vogelstein B, Kinzler KW (1998). *Colorectal Cancer. In: Bert Vogelstein and Kinzler K. W. (eds). The Genetic Basis of Human Cancer, : 565-587*. McGraw-Hill New York.

Wain HM, Bruford EA, Lovering RC, Lush MJ, Wright MW, Povey S (2002). Guidelines for human gene nomenclature. *Genomics* **79:** 464-70.

Wang IC, Chen YJ, Hughes D, Petrovic V, Major ML, Park HJ et al (2005). Forkhead box M1 regulates the transcriptional network of genes essential for mitotic progression and genes encoding the SCF (Skp2-Cks1) ubiquitin ligase. *Mol Cell Biol* **25:** 10875-94.

Wang IC, Chen YJ, Hughes DE, Ackerson T, Major ML, Kalinichenko VV et al (2008a). FoxM1 regulates transcription of JNK1 to promote the G1/S transition and tumor cell invasiveness. *J Biol Chem* **283:** 20770-8.

Wang IC, Meliton L, Ren X, Zhang Y, Balli D, Snyder J et al (2009). Deletion of Forkhead Box M1 transcription factor from respiratory epithelial cells inhibits pulmonary tumorigenesis. *PLoS One* **4:** e6609.

Wang IC, Meliton L, Tretiakova M, Costa RH, Kalinichenko VV, Kalin TV (2008b). Transgenic expression of the forkhead box M1 transcription factor induces formation of lung tumors. *Oncogene* **27:** 4137-49.

Wang X, Kiyokawa H, Dennewitz MB, Costa RH (2002a). The Forkhead Box m1b transcription factor is essential for hepatocyte DNA replication and mitosis during mouse liver regeneration. *Proc Natl Acad Sci U S A* **99:** 16881-6.

Wang X, Krupczak-Hollis K, Tan Y, Dennewitz MB, Adami GR, Costa RH (2002b). Increased hepatic Forkhead Box M1B (FoxM1B) levels in old-aged mice stimulated liver regeneration through diminished p27Kip1 protein levels and increased Cdc25B expression. *J Biol Chem* **277:** 44310-6.

Wang X, Pavelic ZP, Li YQ, Wang L, Gleich L, Radack K et al (1995). Amplification and overexpression of the cyclin D1 gene in head and neck squamous cell carcinoma. *Clin Mol Pathol* **48:** M256-M259.

Wang X, Quail E, Hung NJ, Tan Y, Ye H, Costa RH (2001). Increased levels of forkhead box M1B transcription factor in transgenic mouse hepatocytes prevent age-related proliferation defects in regenerating liver. *Proc Natl Acad Sci U S A* **98:** 11468-73.

Wang Z, Banerjee S, Kong D, Li Y, Sarkar FH (2007). Down-regulation of Forkhead Box M1 transcription factor leads to the inhibition of invasion and angiogenesis of pancreatic cancer cells. *Cancer Res* **67:** 8293-300.

Warnakulasuriya S, Reibel J, Bouquot J, Dabelsteen E (2008). Oral epithelial dysplasia classification systems: predictive value, utility, weaknesses and scope for improvement. *J Oral Pathol Med* **37:** 127-33.

Watt FM (1998). Epidermal stem cells: markers, patterning and the control of stem cell fate. *Philos Trans R Soc Lond B Biol Sci* **353:** 831-7.

Watt FM (2001). Stem cell fate and patterning in mammalian epidermis. *Curr Opin Genet Dev* **11:** 410-7.

Watt FM (2002). Role of integrins in regulating epidermal adhesion, growth and differentiation. *EMBO J* **21:** 3919-26.

Weaver BA, Cleveland DW (2006). Does aneuploidy cause cancer? *Curr Opin Cell Biol* **18:** 658-67.

Westendorf JM, Rao PN, Gerace L (1994). Cloning of cDNAs for M-phase phosphoproteins recognized by the MPM2 monoclonal antibody and determination of the phosphorylated epitope. *Proc Natl Acad Sci U S A* **91:** 714-8.

Wheatley-Price P, Asomaning K, Reid A, Zhai R, Su L, Zhou W et al (2008). Myeloperoxidase and superoxide dismutase polymorphisms are associated with an increased risk of developing pancreatic adenocarcinoma. *Cancer* **112:** 1037-42.

Whitfield ML, Sherlock G, Saldanha AJ, Murray JI, Ball CA, Alexander KE et al (2002). Identification of genes periodically expressed in the human cell cycle and their expression in tumors. *Mol Biol Cell* **13:** 1977-2000.

Wierstra I, Alves J (2006a). Despite its strong transactivation domain, transcription factor FOXM1c is kept almost inactive by two different inhibitory domains. *Biol Chem* **387:** 963-76.

Wierstra I, Alves J (2006b). FOXM1c is activated by cyclin E/Cdk2, cyclin A/Cdk2, and cyclin A/Cdk1, but repressed by GSK-3alpha. *Biochem Biophys Res Commun* **348:** 99-108.

Wierstra I, Alves J (2006c). FOXM1c transactivates the human c-myc promoter directly via the two TATA boxes P1 and P2. *Febs J* **273:** 4645-67.

Wierstra I, Alves J (2006d). Transcription factor FOXM1c is repressed by RB and activated by cyclin D1/Cdk4. *Biol Chem* **387:** 949-62.

Wierstra I, Alves J (2007). FOXM1, a typical proliferation-associated transcription factor. *Biol Chem* **388:** 1257-74.

Willenbucher RF, Aust DE, Chang CG, Zelman SJ, Ferrell LD, Moore DH, 2nd et al (1999). Genomic instability is an early event during the progression pathway of ulcerative-colitis-related neoplasia. *Am J Pathol* **154:** 1825-30.

Withers HR (1967). Recovery and repopulation in vivo by mouse skin epithelial cells during fractionated irradiation. *Radiat Res* **32:** 227-39.

Wong CS, Strange RC, Lear JT (2003). Basal cell carcinoma. *Bmj* **327:** 794-8.

Wonsey DR, Follettie MT (2005). Loss of the forkhead transcription factor FoxM1 causes centrosome amplification and mitotic catastrophe. *Cancer Res* **65:** 5181-9.

Xia LM, Huang WJ, Wang B, Liu M, Zhang Q, Yan W et al (2009). Transcriptional up-regulation of FoxM1 in response to hypoxia is mediated by HIF-1. *J Cell Biochem* **106:** 247-56.

Yang DK, Son CH, Lee SK, Choi PJ, Lee KE, Roh MS (2009). Forkhead box M1 expression in pulmonary squamous cell carcinoma: correlation with clinicopathologic features and its prognostic significance. *Hum Pathol* **40:** 464-70.

Yano M, Ouchida M, Shigematsu H, Tanaka N, Ichimura K, Kobayashi K et al (2004). Tumor-specific exon creation of the HELLS/SMARCA6 gene in non-small cell lung cancer. *Int J Cancer* **112:** 8-13.

Ye H, Holterman AX, Yoo KW, Franks RR, Costa RH (1999). Premature expression of the winged helix transcription factor HFH-11B in regenerating mouse liver accelerates hepatocyte entry into S phase. *Mol Cell Biol* **19:** 8570-80.

Ye H, Kelly TF, Samadani U, Lim L, Rubio S, Overdier DG et al (1997). Hepatocyte nuclear factor 3/fork head homolog 11 is expressed in proliferating epithelial and mesenchymal cells of embryonic and adult tissues. *Mol Cell Biol* **17:** 1626-41.

Yildirim M, Paydas S, Tanriverdi K, Seydaoglu G, Disel U, Yavuz S (2007). Gravin gene expression in acute leukaemias: clinical importance and review of the literature. *Leuk Lymphoma* **48:** 1167-72.

Yoon DK, Jeong CH, Jun HO, Chun KH, Cha JH, Seo JH et al (2007). AKAP12 induces apoptotic cell death in human fibrosarcoma cells by regulating CDKI-cyclin D1 and caspase-3 activity. *Cancer Lett* **254:** 111-8.

Yoshida Y, Wang IC, Yoder HM, Davidson NO, Costa RH (2007). The forkhead box M1 transcription factor contributes to the development and growth of mouse colorectal cancer. *Gastroenterology* **132:** 1420-31.

Yuspa SH, Ben T, Hennings H, Lichti U (1980). Phorbol ester tumor promoters induce epidermal transglutaminase activity. *Biochem Biophys Res Commun* **97:** 700-8.

Yuspa SH, Ben T, Hennings H, Lichti U (1982). Divergent responses in epidermal basal cells exposed to the tumor promoter 12-O-tetradecanoylphorbol-13-acetate. *Cancer Res* **42:** 2344-9.

Yuspa SH, Hennings H, Saffiotti U (1976). Cutaneous chemical carcinogenesis: past, present, and future. *J Invest Dermatol* **67:** 199-208.

Zeng J, Wang L, Li Q, Li W, Bjorkholm M, Jia J et al (2009). FoxM1 is up-regulated in gastric cancer and its inhibition leads to cellular senescence, partially dependent on p27 kip1. *J Pathol* **218:** 419-27.

Zhang H, Ackermann AM, Gusarova GA, Lowe D, Feng X, Kopsombut UG et al (2006). The FoxM1 transcription factor is required to maintain pancreatic beta-cell mass. *Mol Endocrinol* **20:** 1853-66.

Zhou R, Han L, Li G, Tong T (2009). Senescence delay and repression of p16INK4a by Lsh via recruitment of histone deacetylases in human diploid fibroblasts. *Nucleic Acids Res* **37:** 5183-96.

Zhu AJ, Watt FM (1999). beta-catenin signalling modulates proliferative potential of human epidermal keratinocytes independently of intercellular adhesion. *Development* **126:** 2285-98.

APPENDIX

Appendix 1

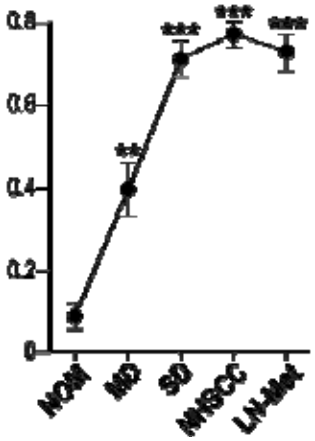

Digital pixel densitometry for FOXM1 protein immunoreactivity in a panel of 25 oral tissues (n = 5 in each group) as shown in **Chapter 3 Figure 3.1**. ***(P≤0.01) and ***(P≤0.001)* indicate statistically significant elevation of FOXM1 protein levels when compared to NOM tissues.

Appendix 2

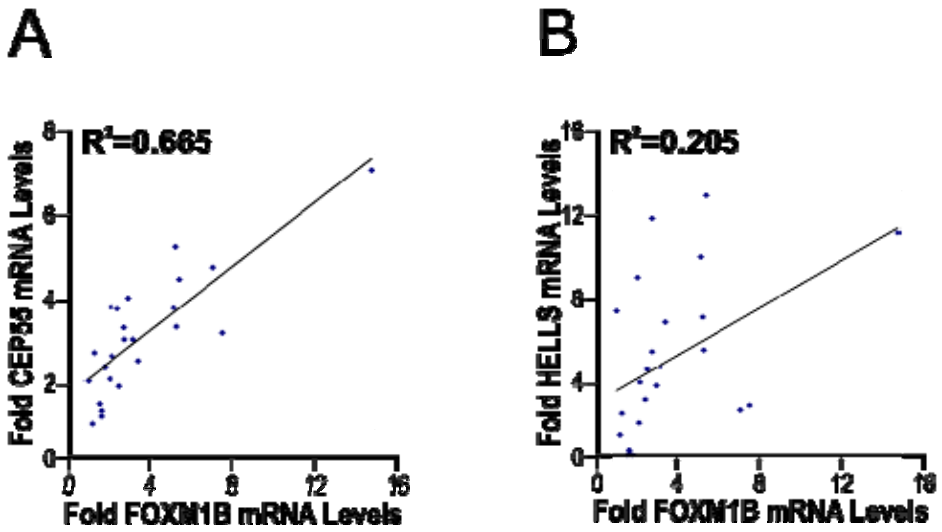

(A) Linear regression analysis between FOXM1B and CEP55 expression in the panel of cell lines used in **Figures 3.6 and 3.7**. **(B)** Linear regression analysis between FOXM1B and HELLS expression in the panel of cell lines used in **Figures 3.6 and 3.7.**

Appendix 3

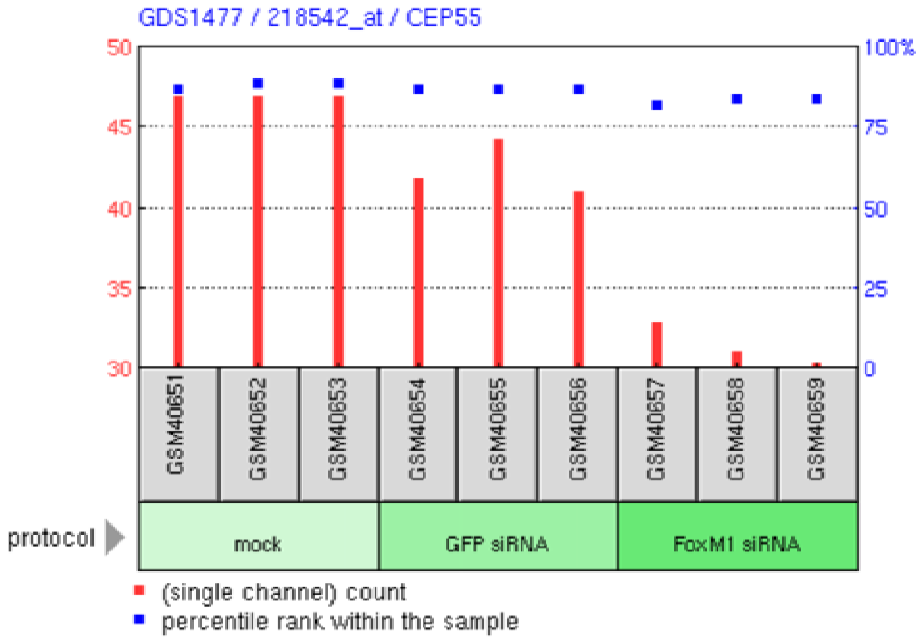

Bioinformatics analysis of CEP55 gene expression level from a published microarray dataset (GEO accession: GDS1477) comparing BT-20 breast cancer cells expressing either mock, siGFP or siFOXM1 at 48 h post-transfection (Wonsey and Follettie, 2005).

Appendix 4

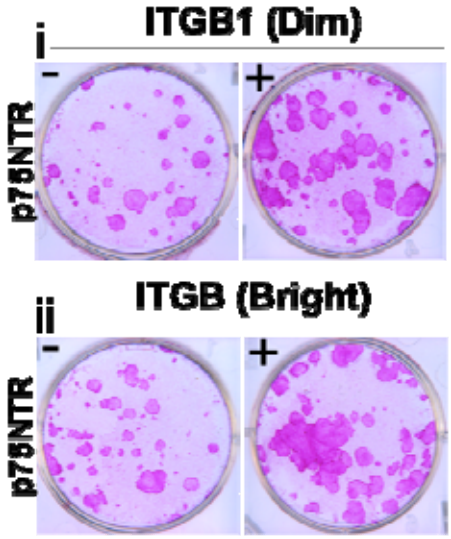

Oral keratinocytes sorted for p75NTR and Integrin β1 levels. After sorting each separate population as shown, cells were allowed to grow for 12 days in the presence of 3T3 feeders. Keratinocyte colonies were examined under bright field microscopy and were later stained with Rhodamine B for quantification of the clonogenic potential of each separate keratinocyte population

Appendix 5

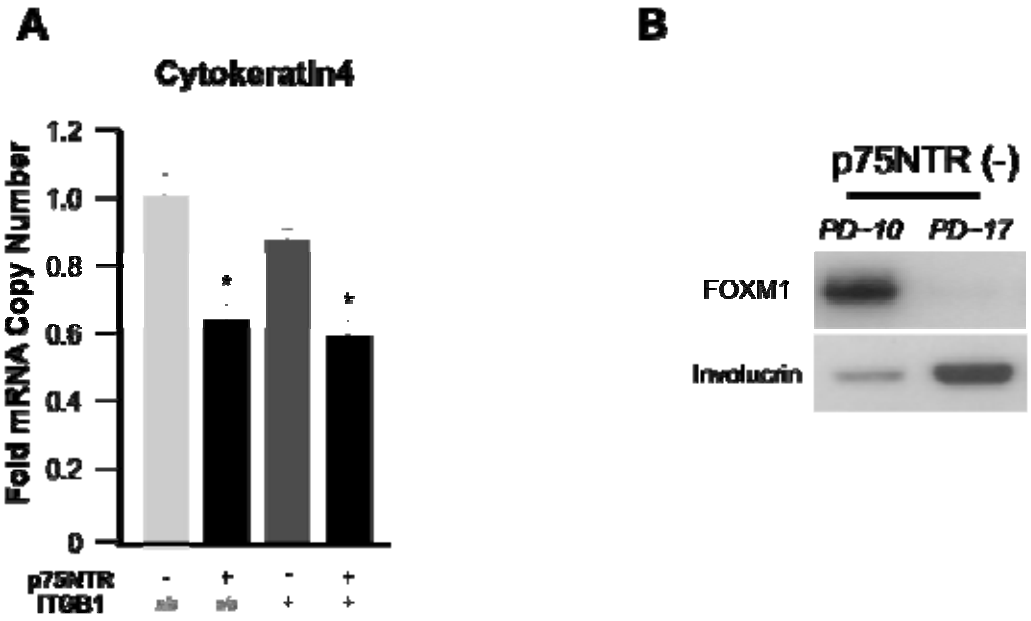

(A) Oral keratinocytes were sorted as described and were allowed to grow 5 days prior to harvesting for total RNA. The levels of differentiation specific Cytokeratin 4 were measured by qRT-PCR. Bars represent the average fold difference from $p75NTR^-$ control samples (arbitrary value 1) ±S.E.M. of three replicate samples for each type. *$P \leq 0.05$. **(B)** NHOK were FACS sorted (PD~10) and were allowed to grow for 12 days (PD~17). Protein extracts were prepared from the $p75NTR^-$ fraction and were immunoblotted against anti-FOXM1 and anti-Involucrin antibodies.

Appendix 6

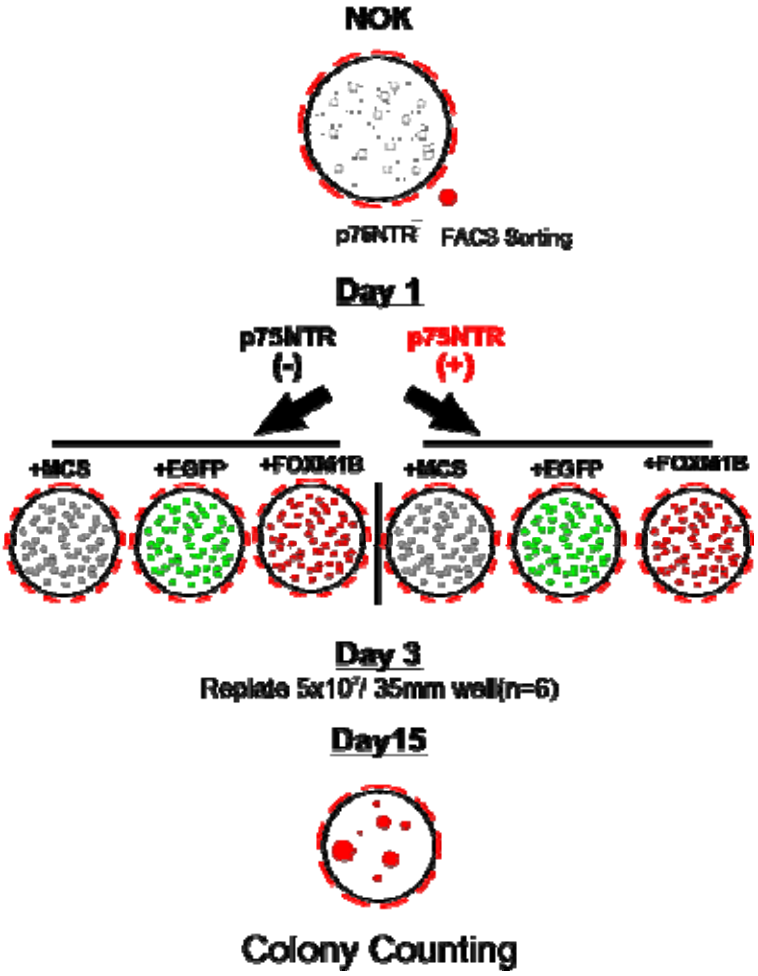

Early passage primary NOK were allowed to grow to 70% confluence prior to staining with anti-p75NTR-PE antibody. Stained keratinocytes were flow sorted into $p75NTR^{+}$ or $p75NTR^{-}$ populations. Each population was retrovirally transduced with pSINMCS, pSINEGFP, or pSINEGFP-FOXM1B. Transduced clones were allowed to grow for another 48hours prior to being plated at very low densities. After another 12 days, keratinocytes were fixed, stained and approximately 100 colonies from each construct, and their relative areas (mm^2) were measured

Appendix 7

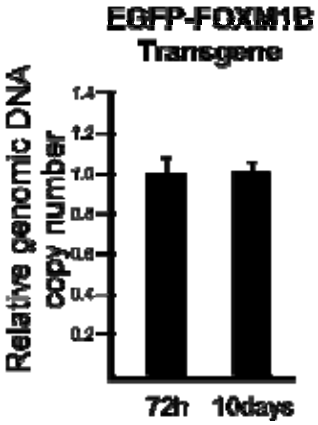

Transduced human keratinocytes were harvested either 72 hours, or 10 days after retroviral transduction. 10ng of genomic DNA (gDNA) were used for qRT-PCR analysis for the detection of EGFP transgene copy number (**see also Chapter 2, section 3.5).**